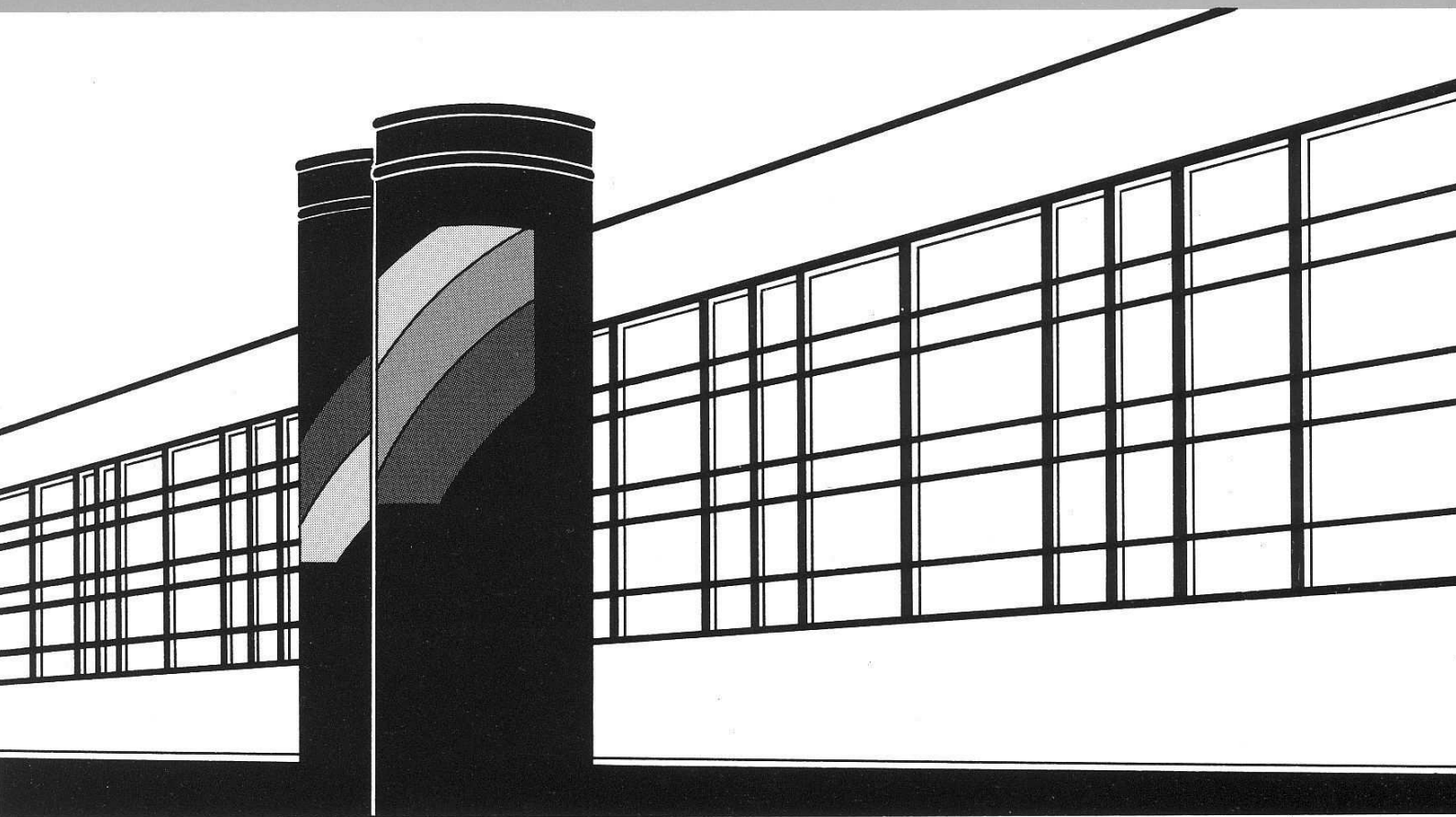


Institut für Wasserbau · Universität Stuttgart

# *Mitteilungen*



Heft 198    Shailesh Kumar Singh

**Robust Parameter Estimation in  
Gauged and Ungauged Basins**



# **Robust Parameter Estimation in Gauged and Ungauged Basins**

Von der Fakultät Bau- und Umweltingenieurwissenschaften der  
Universität Stuttgart zur Erlangung der Würde eines  
Doktor-Ingenieurs (Dr.-Ing.) genehmigte Abhandlung

Vorgelegt von  
**Shailesh Kumar Singh**  
aus Dhanbad, Indien

Hauptberichter: Prof. Dr. rer. nat. Dr.-Ing. habil. András Bárdossy  
Mitberichter: Prof. Dr. Thorsten Wagener, Ph. D.

Tag der mündlichen Prüfung: 25. Oktober 2010

Institut für Wasserbau der Universität Stuttgart  
2010



Heft 198    Robust Parameter Estimation  
in Gauged and Ungauged  
Basins

von  
Dr.-Ing.  
Shailesh Kumar Singh

**D93 Robust Parameter Estimation in Gauged and Ungauged Basins**

**Bibliografische Information der Deutschen Nationalbibliothek**

Die Deutsche Nationalbibliothek verzeichnet diese Publikation in der Deutschen Nationalbibliografie; detaillierte bibliografische Daten sind im Internet über <http://www.d-nb.de> abrufbar

Singh, Shailesh Kumar:

Robust Parameter Estimation in Gauged and Ungauged Basins / von Shailesh Kumar Singh. Institut für Wasserbau, Universität Stuttgart. - Stuttgart: Inst. für Wasserbau, 2010

(Mitteilungen / Institut für Wasserbau, Universität Stuttgart: H. 198)

Zugl.: Stuttgart, Univ., Diss., 2010

ISBN 978-3-942036-02-3

NE: Institut für Wasserbau <Stuttgart>: Mitteilungen

Gegen Vervielfältigung und Übersetzung bestehen keine Einwände, es wird lediglich um Quellenangabe gebeten.

Herausgegeben 2010 vom Eigenverlag des Instituts für Wasserbau  
Druck: Document Center S. Kästl, Ostfildern

# Acknowledgment

This research work was carried out under the supervision of Prof. Dr. Dr. András Bárdossy. I feel greatly honored for being one of his students, his prodigious expertise has unfailingly enlightened my path on this journey in the challenging territory of hydrology and statistics. I would like to express my deep gratitude to him for providing me this wonderful opportunity to work with him. I greatly appreciate his enthusiasm, guidance, and the many discussions and the criticism which he shared with me throughout this work. Above all, I will cherish his ever optimistic attitude which not only helped during this work but will be an asset for the future too. I would also like to express my sincere thanks to Prof. Dr. Thorsten Wagener for accepting to co-supervise this research work and for his valuable suggestions during research visit to The Pennsylvania State University and through out the work.

I sincerely acknowledge the ENWAT International Doctoral Program of the Universität Stuttgart for providing the academic framework for this research work. I am very much thankful to Dr.-Ing. Gabriele Hartmann for always being cooperative and helpful to me. I am greatly thankful to the financial support provided by IPSWaT Scholarship Program of the German Federal Ministry of Education and Research (BMBF).

I would like to extend my acknowledgments further to Dr. S. K. Jain, Dr. Jim Freer for helping me for their valuable suggestions in my work. Many many hearty thanks to Dr.-Ing. Pawan Kumar Thapa, Dr.-Ing. Sachin Patil, Dr.-Ing. Jens Götzinger, Dr.-Ing. Tapash Das, Dipl.-Ing. C. Ebert, Dipl.-Geoökol. Jan Bliefernicht, Dipl.-Ing. Thomas Pfaff, Dipl.-Ing. Ferdinand Beck, Dipl.-Ing. Alejandro Chamorro Chávez, Jhan Rodríguez-Fernández, Dr.-Ing. J. Brommundt and Dr.-Ing. Yi He for their cooperation and the troubleshooting they offered from time to time. My sincere thanks also go to Mrs. Krista Uhrmann for her assistance in the bureaucratic matters and for patiently informing me about the availability of Prof. Bárdossy every now and then.

I also remain indebted to all my friends at Stuttgart, who helped me in completing this work successfully.

Although there are no words to express my feeling for them, I would like to mention my deepest gratitude to my parents, my brother, his family and Deepika G. for their love and encouragements. Above all, I am thankful to God for granting me the resources and the strength to accomplish this research work.





# Contents

<b>List of Figures</b>	<b>ix</b>
<b>List of Tables</b>	<b>xiii</b>
<b>Abstract</b>	<b>xvii</b>
<b>Kurzfassung</b>	<b>xxi</b>
<b>1 Introduction</b>	<b>1</b>
1.1 Background and Motivation . . . . .	1
1.2 Problem Definition . . . . .	1
1.3 Objectives of the Research . . . . .	4
1.4 Organization of the Thesis . . . . .	5
<b>2 Parameter Estimation in Conceptual Hydrological Modeling</b>	<b>6</b>
2.1 Hydrological Model . . . . .	6
2.2 Parameter Estimation . . . . .	6
<b>3 Data Depth Function</b>	<b>9</b>
3.1 Definition . . . . .	9
3.1.1 Desirable properties of data depth function . . . . .	9
3.2 Type of Data Depth Function . . . . .	11
3.3 Use of Data Depth Function . . . . .	15
<b>4 Study Area and Hydrological Models</b>	<b>16</b>
4.1 Study Area . . . . .	16
4.1.1 Upper Neckar catchment . . . . .	16
4.1.2 United Kingdom catchments . . . . .	17
4.1.3 Indian catchments . . . . .	17
4.1.4 Rems catchment . . . . .	22
4.2 Models . . . . .	25
4.2.1 HBV . . . . .	25
4.2.2 HYMOD . . . . .	28
4.2.3 Three reservoirs model . . . . .	29
4.2.4 Water Flow Balance Simulation Model-WaSiM-ETH . . . . .	31

<b>5</b>	<b>Robust Estimation of Hydrological Model Parameters</b>	<b>33</b>
5.1	Introduction . . . . .	33
5.2	The Effect of Observation Errors . . . . .	33
5.3	Geometrical Structure of the Good Parameter Set . . . . .	36
5.3.1	Data depth of the good parameter set . . . . .	36
5.3.2	Transferability . . . . .	37
5.3.3	Sensitivity . . . . .	39
5.4	Robust Parameter Estimation ( <b>ROPE</b> ) . . . . .	40
5.5	Application of the ROPE Algorithm to Different Models and Different Catchments . . . . .	45
5.5.1	Result from HYMOD . . . . .	45
5.5.2	Result from three reservoirs model . . . . .	46
5.6	Modification of the ROPE Algorithm . . . . .	49
5.6.1	Sequential replacement of weak parameters ( <b>SRWP</b> ) . . . . .	49
5.7	Case Study . . . . .	50
5.7.1	Application of the SRWP algorithm on test functions . . . . .	50
5.8	Case Study Result from SRWP Algorithm . . . . .	52
5.8.1	Comparison with existing methods . . . . .	64
5.9	Conclusions . . . . .	66
<b>6</b>	<b>Impact of Objective Function on Mapping of Model Parameters During Cali- bration</b>	<b>67</b>
6.1	Introduction . . . . .	67
6.2	Methodology . . . . .	67
6.2.1	Objective functions . . . . .	68
6.2.2	Parameter space for model calibration . . . . .	69
6.2.3	Intersection of parameter space . . . . .	73
6.2.4	Hierarchical optimization . . . . .	77
6.3	Application and Results . . . . .	80
6.4	Conclusions . . . . .	84
<b>7</b>	<b>Calibration of Hydrological Models on Hydrologically Unusual Events</b>	<b>86</b>
7.1	Introduction . . . . .	86
7.2	Methodology . . . . .	87
7.2.1	Identification of critical time period using data depth function . . . . .	88
7.2.2	Identification of Critical Events ( <b>ICE</b> algorithm) . . . . .	90
7.3	Application and Results . . . . .	90
7.4	Extension to Ungauged Catchments . . . . .	94
7.4.1	Practical application: start measuring important events . . . . .	94
7.5	Applications of the ICE Algorithm . . . . .	96
7.5.1	Result from physically based model . . . . .	96
7.5.2	Result from data driven model . . . . .	100
7.6	Case Study . . . . .	102
7.6.1	Artificial neural networks . . . . .	102

7.6.2	Data used in the study . . . . .	104
7.6.3	Different cases for the training of ANN . . . . .	105
7.6.4	Results from rating curve analysis . . . . .	106
7.7	Conclusions . . . . .	111
<b>8</b>	<b>Robust Dynamic Parameter Estimation for Hydrological Models</b>	<b>114</b>
8.1	Introduction . . . . .	114
8.2	Concept of Time Varying Parameters . . . . .	116
8.2.1	Robust dynamic parameter estimation ( <b>RDPE</b> ) <b>algorithm</b> . . .	116
8.2.2	Diagnosis of model . . . . .	117
8.2.3	Hydrological model prediction . . . . .	123
8.3	Conclusions . . . . .	125
<b>9</b>	<b>Regionalization of the Hydrological Model Parameters Using Data Depth</b>	<b>126</b>
9.1	Introduction . . . . .	126
9.2	Methodology . . . . .	127
9.2.1	Choice of catchment properties . . . . .	131
9.2.2	How to perform regionalization . . . . .	135
9.3	Case Study . . . . .	135
9.4	Application and Results . . . . .	136
9.4.1	Choice of catchment properties . . . . .	136
9.4.2	Regionalization . . . . .	136
9.5	Conclusions . . . . .	144
<b>10</b>	<b>Summary and Outlook</b>	<b>146</b>
10.1	Summary . . . . .	146
10.2	Outlook . . . . .	150



# List of Figures

3.1	<i>Example of convex hull</i>	10
3.2	<i>Circles represent the boundary points or low depth points</i>	10
3.3	<i>Schematic representation of a half-space calculation in two dimensions</i>	12
3.4	<i>Schematic representation of convex hull peeling in two dimensions</i>	14
4.1	<i>Study area: Upper Neckar catchment in South-West Germany</i>	16
4.2	<i>Study area: 28 catchments of England and Wales, UK</i>	18
4.3	<i>Index map of the Kolar basin</i>	21
4.4	<i>Rems catchment in southern Germany and its subcatchments (Thapa, 2009)</i>	22
4.5	<i>Monthly mean precipitation 1990-2005 for Rems catchments (stations with 100 % observation)</i>	23
4.6	<i>Annual average precipitation for Rems catchments (stations with 100 % observation)</i>	23
4.7	<i>Monthly average discharge (1900-2005) for Rems catchments</i>	24
4.8	<i>Annual average discharge for Rems catchments</i>	24
4.9	<i>Schematic representation of the HBV model</i>	27
4.10	<i>Schematic representation of the HYMOD model</i>	28
4.11	<i>Structure of the three reservoirs model (Jain, 1993)</i>	31
4.12	<i>Structure of WaSiM-ETH using TOPMODEL approach (Liang, 2010)</i>	32
5.1	<i>Scatter plot of the model parameters obtained by optimization using random discharge errors</i>	35
5.2	<i>The performance of the model using different depth</i>	38
5.3	<i>Construction of the points <math>C_1, C_2</math> and <math>C_3</math> in one dimension for sensitivity analysis of parameters</i>	40
5.4	<i>Systematic representation of the ROPE algorithm</i>	42
5.5	<i>Histograms of the model performances for the different iterations of the algorithm for the Süssen catchment</i>	42
5.6	<i>Parameter value vs. model performance for the sets obtained in iteration 2 (crosses) and iteration 4 (circles) for the Süssen catchment</i>	43
5.7	<i>Parameter value for the sets obtained in iteration 2 (crosses) and iteration 4 (circles) for the Tübingen catchment</i>	44
5.8	<i>Hydrograph with confidence interval for boundary points and inner points</i>	44
5.9	<i>Confidence band width of high depth Vs confidence band width of low depth</i>	45
5.10	<i>Observed and model hydrograph for calibration run</i>	47
5.11	<i>Observed and model hydrograph for validation</i>	49

5.12	<i>Schematic explanation of the sequential replacement of weak parameters algorithm</i>	51
5.13	<i>Giunta function</i>	53
5.14	<i>Contour Map for Giunta function and optimal region</i>	53
5.15	<i>Leon function</i>	54
5.16	<i>Contour Map for Leon function and optimal region</i>	54
5.17	<i>McCormick function</i>	55
5.18	<i>Contour Map for McCormick function and optimal region</i>	55
5.19	<i>Styblinski-Tang function</i>	56
5.20	<i>Contour Map for Styblinski-Tang function and optimal region</i>	56
5.21	<i>Levy function</i>	57
5.22	<i>Contour Map for Levy and optimal region</i>	57
5.23	<i>Rastrigin function</i>	58
5.24	<i>Contour Map for Rastrigin function and optimal region</i>	58
5.25	<i>Six-Hump Camelback function</i>	59
5.26	<i>Contour Map for Six-Hump Camelback function and optimal region</i>	59
5.27	<i>Improvement of performance by SRWP algorithm</i>	60
5.28	<i>Different parameter at different iteration</i>	62
5.29	<i>Plot matrix of parameter at initial iteration</i>	63
5.30	<i>Plot matrix of parameter at final iteration</i>	64
6.1	<i>Parameter values for different objective functions</i>	71
6.2	<i>Parameter values for the different Logarithmic objective functions</i>	72
6.3	<i>Decrease in volume of space by each objective functions</i>	72
6.4	<i>Initial parameters in the diffusion space (red colour represents higher performance)</i>	73
6.5	<i>Decrease in volume of space after third and fourth iteration of ROPE algorithm by different objective functions in diffusion space</i>	74
6.6	<i>Decrease in volume of space after first and second iteration of ROPE algorithm by different objective functions in diffusion space</i>	75
6.7	<i>Decrease in volume of space after fifth iteration of ROPE algorithm by different objective functions in diffusion space</i>	76
6.8	<i>Intersection of parameter space for different objective functions at different iterations of ROPE algorithm (the numbers specify the strength of intersection)</i>	78
6.9	<i>An ideal intersection of parameter space for different objective functions</i>	79
6.10	<i>Comparison of the performance from space <math>P_1</math>, <math>P_2</math> over all space</i>	79
6.11	<i>Hydrograph from different objective functions</i>	83
6.12	<i>Difference of 95 and 5 percent from different objective functions</i>	83
6.13	<i>Distribution of parameter (<math>C_{max}</math>) obtained by different objective functions</i>	84
7.1	<i>Histogram for slopes in all the three cases</i>	88
7.2	<i>Example of event selection from Neckar Catchment (Rottwiel)</i>	89

7.3	<i>The sequential addition of years to the calibration of HYMOD and validated over 10 years (1961-70)</i>	93
7.4	<i>The sequential addition of years to the calibration of HYMOD and validated over 10 years (1981-90)</i>	93
7.5	<i>Conditional depth with precipitation curve for measuring events</i>	95
7.6	<i>Critical events selected from year 1993 from Rems catchments</i>	97
7.7	<i>Distributions of parameters calibrated in both cases</i>	99
7.8	<i>Calibration and validation with 90 % confidence</i>	101
7.9	<i>Three-Layer, Feed Forward ANN structure</i>	106
7.10	<i>Observed and computed discharge by different cases for the Chester validation period</i>	108
7.11	<i>Observed and computed sediment concentration for each case for the Chester validation period</i>	108
7.12	<i>Observed and computed discharge by different cases for the Thebes validation period</i>	109
7.13	<i>Observed and computed sediment concentration by different cases for the Thebes validation period</i>	110
7.14	<i>Convex hull of the training and testing set</i>	111
7.15	<i>Residuals of the observed and computed discharge at each validation period for the Chester site</i>	112
7.16	<i>Residuals of the observed and computed sediment concentration at each validation period for the Chester site</i>	112
8.1	<i>Schematic outline of RDPE algorithm</i>	117
8.2	<i>Parameter Beta and Performance (NS) at low depth and at high depth</i>	118
8.3	<i>Typical time series of beta with window size</i>	119
8.4	<i>Active and inactive period for parameter beta</i>	120
8.5	<i>Active and inactive period for parameter DD</i>	120
8.6	<i>Example of parameters, which has more variation over time</i>	121
8.7	<i>Example of parameters, which has less variation over time</i>	122
9.1	<i>Schematic representation of inside catchment (blue star) and case of extrapolation (green circle)</i>	129
9.2	<i>The condition of step 7 of the algorithm for the case of one catchment property (red and black are two extreme catchments and blue is inbetween catchment)</i>	134
9.3	<i>The condition of step 7 of the algorithm for the case of two catchment properties (red, black and blue are the extreme catchments and green is inbetween catchment)</i>	135
9.4	<i>Observed and simulated hydrographs for catchment 17 using the convex estimator (using 4 boundary catchments only) and multiple linear regression with the deepest point</i>	140

9.5	<i>Observed and simulated hydrographs for catchment 17 using the convex estimator and multiple linear regression with the deepest point in case of extrapolation (negative weights allowed)</i> . . . . .	140
9.6	<i>The performance (<math>NS_p</math>) of the convex estimator for target catchment 5 using the possible 4 catchment combinations with the deepest (red crosses) and randomly selected parameters (black stars)</i> . . . . .	143
9.7	<i>The performance (<math>NS_p</math>) of the convex estimators for catchment number 20 using the deepest (red crosses) and lower depth (black stars). The estimators using the deepest parameter vectors including catchment 16 are marked with a green cross</i> . . . . .	144



# List of Tables

2.1	<i>The advantages and disadvantages of manual and automatic calibration</i>	7
4.1	<i>Summary of the size of the different subcatchments in Upper Neckar catchment</i>	17
4.2	<i>Possible catchments properties from UK catchments (Yadav et al., 2007)</i>	18
4.3	<i>Different UK catchments and their properties</i>	19
4.4	<i>Annual mean discharge and precipitation for all UK catchments</i>	20
4.5	<i>Summary of the basic characteristics of Rems catchment</i>	25
4.6	<i>Model parameters range for HBV model</i>	27
4.7	<i>Model parameters range for the HYMOD</i>	29
4.8	<i>The possible range of the three reservoirs model parameters</i>	29
4.9	<i>Input data for WaSiM-ETH model</i>	32
5.1	<i>Model performance for the observed series using optimal parameters obtained using 100 randomly perturbed discharge data sequences</i>	35
5.2	<i>Model performance for the observed series using optimal parameters obtained using 100 randomly perturbed temperature data sequences</i>	35
5.3	<i>Model parameters range for Rottweil (Neckar) catchment</i>	37
5.4	<i>Model performance for the <math>N = 10000</math> random parameter sets with respect to the data depth calculated on the basis of the points selected corresponding to the upper 10 % performance</i>	37
5.5	<i>Runoff characteristics for different time periods</i>	38
5.6	<i>Model performance for parameter vectors according to their depth corresponding to the time period 1961-1970</i>	39
5.7	<i>Model performance for the inner and the shifted boundary and deep points</i>	40
5.8	<i>Model performance for calibration time period 1961-1970 and validation for other time period for Rottweil</i>	46
5.9	<i>Model performance (NS) for calibration time period 1981-1985 and validation for the other time period for catchment 27 in the UK</i>	46
5.10	<i>Range of model parameters</i>	47
5.11	<i>Range of model parameters after calibration</i>	48
5.12	<i>Performance for calibration and validation</i>	48
5.13	<i>Model performance for calibration time period 1961-1970 and validation for other time period for Rottweil</i>	61
5.14	<i>Initial and final parameter range</i>	61

5.15	<i>Model performance for calibration time period 1961-1970 and validation for other time period for Rottweil using SCE-UA . . . . .</i>	65
5.16	<i>Initial and final Parameter Range in SA and SCE-UA . . . . .</i>	65
6.1	<i>Different objective functions and their notations . . . . .</i>	68
6.2	<i>Parameter range obtained by different objective functions after calibration . . . . .</i>	69
6.3	<i>Parameter range obtained by different log objective functions after calibration . . . . .</i>	70
6.4	<i>Optimized at different objective functions but all the performance criteria is calculated for each objective function . . . . .</i>	81
6.5	<i>Optimized by logarithm of different objective functions but all the performance criteria is calculated for each objective function . . . . .</i>	82
6.6	<i>Result from hierarchical calibration . . . . .</i>	82
7.1	<i>Calibration of HYMOD model at Rottweil over period 1961-70 . . . . .</i>	91
7.2	<i>Calibration of HBV model at Rottweil over period 1961-70 . . . . .</i>	91
7.3	<i>Validation of HYMOD model at Rottweil over period 1971-80 . . . . .</i>	92
7.4	<i>Validation of HBV model at Rottweil over period 1971-80. . . . .</i>	92
7.5	<i>Calibration of HYMOD for Rottweil for time period 1991-00; event selection is based on predicted precipitation and known precipitation . . . . .</i>	96
7.6	<i>Validation of HYMOD for Rottweil for time period 1981-90; event selection is based on predicted precipitation and known precipitation . . . . .</i>	96
7.7	<i>Statistics of the best 10 % parameter sets of WaSim-ETH, calibrated by ROPE algorithm . . . . .</i>	97
7.8	<i>Statistical entropy for different parameters of WaSim-ETH . . . . .</i>	98
7.9	<i>Statistics for calibration and validation of WaSim-ETH (best 10 % performance) . . . . .</i>	100
7.10	<i>RMSE, SSE and correlation coefficient from the ANN model for the training period of Chester site . . . . .</i>	107
7.11	<i>RMSE, SSE and correlation coefficient from the ANN model for the validation period of Chester site . . . . .</i>	107
7.12	<i>RMSE, SSE and correlation coefficient of the ANN model for training period of Thebes site . . . . .</i>	107
7.13	<i>RMSE, SSE and correlation coefficient of the ANN model for validation period of Thebes site . . . . .</i>	109
8.1	<i>Calibration of model by time invariant and with RPDE method . . . . .</i>	119
8.2	<i>Statistical entropy for different parameters of HBV model . . . . .</i>	123
8.3	<i>Validation using different parameter by each method for different time periods . . . . .</i>	125
9.1	<i>The catchments properties to be considered for regionalization (Yadav et al. (2007)) . . . . .</i>	136
9.2	<i>The numerical values of the considered catchment properties . . . . .</i>	137
9.3	<i>List of the boundary and the inside catchments . . . . .</i>	138

9.4	<i>A set of possible boundary catchments for catchment 20 and the corresponding weights . . . . .</i>	138
9.5	<i>The performance (<math>NS_p</math>) of the convex estimation (9.5) and the explicit multiple linear regression using the deepest and randomly selected parameter vectors for inside catchments . . . . .</i>	139
9.6	<i>Cross validated performance (<math>NS_p</math>) of the relaxed convex combination (negative weights allowed) and multiple linear regression using the deepest and randomly selected parameter vectors . . . . .</i>	142
9.7	<i>Number of possible combinations for the choice of 4 boundary catchments which include the properties of the given inside catchments . . . . .</i>	143



# Abstract

Hydrological modeling has become a widely accepted theoretical tool for water resources engineering and management. Rainfall-runoff models are used both for short and medium time management (for example flood forecasting) and long time design purposes. However, the application of hydrological models is limited due to several reasons. One important limitation is imposed by the availability of data and parameter estimation. Discharges are only measured at a few selected river cross sections, leading to a small number of catchments for which the runoff calculated from the models might be verified. Further, the high spatial and temporal variability of the meteorological input (such as precipitation, temperature or wind) cannot fully be captured by the usually small number of meteorological stations. Radar measurement of precipitation can provide a more detailed space time information on precipitation but unfortunately the reliability of the data is at present still low. Other influencing factors such as soil properties also vary considerably in space and even to some extent in time (for example macropores in soils). These problems among others make models which are based on physical principles only infeasible for many practical applications. Models which to some extent use analogous concepts can partly smoothen out the effects of variability and thus can often be successfully used for practical purposes. The limitation of these models lies in the fact that some of their parameters are not directly related to physically measurable quantities. Therefore those have to be estimated from observations using calibration techniques.

This research work was aimed at developing an efficient, practical and robust methodology for parameter estimation (calibration) for a reliable hydrological modeling at gauged and ungauged basin.

The estimation of hydrological model parameters is a challenging task. With increasing capacity of computational power several complex optimization algorithms have emerged, but none of the algorithms give a unique and *very best* parameter vector. The parameters of fitted hydrological models depend upon the input data. The quality of input data cannot be assured as there may be measurement errors for both input and state variables. In this research a methodology has been developed to find a set of robust parameter vectors for a hydrological model. To see the effect of observational error on parameters, stochastically generated synthetic measurement errors were applied to observed discharge and temperature data. With this modified data, the model was calibrated and the effect of measurement errors on parameters was analysed. It was found that the measurement errors have a significant effect on the best performing parameter vector. The erroneous data led to very different optimal parameter vectors. To overcome this problem and to find a set of robust parameter vectors, a geometrical approach based on Tukey's half-space depth was used. The depth of the set of  $N$  randomly generated parameters

## *Abstract*

was calculated with respect to the set with the best model performance (Nash-Sutcliffe efficiency was used for this research) for each parameter vector. Based on the depth of parameter vectors, one can find a set of robust parameter vectors. The results show that the parameters chosen according to the above criteria have low sensitivity and perform well when transferred to a different time period. The method is firstly demonstrated on the Upper Neckar catchment in Germany. The conceptual HBV model was used to develop the methodology. The algorithm developed based on the data depth function is termed as robust parameter estimation (ROPE) algorithm.

The ROPE algorithm was tested on different models such as HYMOD and Three Reservoir, in various catchments in England and Indian, where these catchments have very diverse characteristic and have different data availability. The result shows ROPE algorithm has perform well on these catchments and models, which makes the ROPE algorithm more of a general purpose tool for model calibration. In further extension to ROPE algorithm, a very simple and effective optimization algorithm called Sequential Replacement of Weak Parameter (SRWP), is introduced for automatic calibration of hydrological model. In SRWP algorithm, weak parameter set is sequentially replaced with another deeper and better parameter set. SRWP is tested on several test functions as well as with hydrological models. SRWP results are compared with the generally used global optimization shuffled complex evolution (SCE-UA) algorithm. The results show SRWP easily over comes the local minima and converge to optimal region. SRWP does not converges to a single optima, instead it gives a convex hull of optimal region. The methodology was demonstrated using HYMOD conceptual model on the Upper Neckar Catchments of South-West Germany. The results show that the parameters estimated by this stepwise calibration are robust.

Hydrological models are used for different purposes. Hence, one model can have several goals; this leads us to having different objective functions for model calibration. There are several objective functions, but not a single objective function can describe all the components of a hydrograph. In this research an attempt has been taken to analysis the parameter space mapped by different objective functions during calibration of a hydrological model by ROPE algorithm. A conceptual hydrological model HYMOD was calibrated using ROPE algorithm with various objective functions, namely Nash-Sutcliff coefficient, root mean square error, volume error and peak error. Also with another objective function, logarithm Nash-Sutcliff coefficient, logarithm root mean square error, logarithm volume error and logarithm peak error. It has been found that the different objective function have mapped parameter spaces differently. Nash-Sutcliff coefficient and root mean square error have very similar parameter distributions. This is because formulation of both the objective function is very similar. There is no common intersection of parameter space obtained by various objective functions. The volume shrinkage of parameter space by different objective functions is very different, which indicates that the optimal parameter obtained by various objective functions is at different rate. The diagnosis of parameter space has lead us to develop a hierarchical calibration technique. It can overcome the problem of the single and multi-objective function. The result of this research will be helpful for robust parameterization of hydrological model.

The length of the observation period used for model calibration has a great influence on the identification of the parameters. So it is very necessary to know how much data is enough for model calibration. However, it is very difficult to say which data and what length of data is sufficient for the proper choice of calibration data to give proper identification of model parameters. The data that contains lots of hydrological variability may be the best choice for calibration data because it may contain most of information that is required for parameter identification (Gupta and Sorooshian, 1985). In this contribution model parameters are estimated from so-called unusual time periods. These are identified from discharge or precipitation observations series using the statistical concept of data depth. Depth functions are used to identify unusual events from four days lagged discharge or API (antecedent precipitation index) series. Data with low half-space depth are considered as unusual. The critical event selected by API and discharge are almost at the same time period in a series. Model calibration is only slightly worse than using all data if one uses the selected critical periods only. The transferability of the parameters for different time periods is for the rank based depth significantly better than using all data. Two different models (HBV and HYMOD) are used to demonstrate the methodology for the Neckar catchment in South-West Germany. The algorithm developed based on data depth for identification of critical time period is termed as ICE (Identification of Critical Events) algorithm. To make more general purpose, the ICE algorithm was further tested on complex physically based hydrological model like WaSim-ETH. It has been found that, models like WaSim-ETH can also be successfully calibrated using critical events. The result is as good as if we would have used whole available data set. ICE algorithm can also be very helpful in data driven modeling. So the ability of ICE algorithm was tested on Artificial Neural Networks (ANNs) modelling.

Artificial Neural Networks (ANNs) are classified as a data driven technique which implies that their learning improves as more and more training data are presented to it. This observation is based on the premise that longer time series of training samples will contain more events of different types and hence the generalization ability of the ANN will improve. However, longer time series of training samples need not necessarily contain more information. If there is considerable repetition of the same type of information, the ANN may not become *wiser* and one may be just wasting computational efforts and time. In this research, it has been assumed that there are segments in a long time series which contain large quantum of information. If an ANN is trained using these segments rather than the whole series, the training would be the same or better. Here, ICE algorithm was used as tool for identification of critical segments in a time series. Different ANN architectures were trained using the whole time series data and using the data of only critical segments. A comparison of the results shows that the performance of the ANNs is only slightly worse then using all data if one uses the selected critical periods only.

Due to the simplification of the complex natural processes and the limited availability of observations the parameters of the hydrological models cannot be identified perfectly. Usually, the parameters of the models are assumed to be time independent. However, some of the catchment properties are not stationary. Hence, some of the model parame-

## *Abstract*

ters corresponding to a certain natural process may vary with time. The purpose of this research is to develop a methodology which can investigate dynamic nature of parameters in a hydrological model. In this research a robust dynamic parameter (*RDPE*) estimation algorithm was developed. *RDPE* can be used for diagnosis of hydrological model as well as for improvement of model prediction using time varying nature of parameters. After identifying the range of time varying parameters using the *ROPE* algorithm, moving window approach and simulated annealing was used to optimized the parameters of HBV model for the each window size. The resulting time series of parameters is used for defining sensitive and insensitive periods in parameter time series. It has also been used for understanding the reason for parameter variation in time. To improve the prediction, from time series of parameter, a predictive parameter model was developed and it has been applied for future prediction. The methodology has been demonstrated on mezo-scale catchments in the Neckar basin in South-West Germany using the HBV model. Further, it is shown that the new methodology leads to more realistic confidence intervals for model simulations and model structure identification. A spatial and temporal transfer of hydrological model parameters from gauged to ungauged catchments is possible under the assumption that similar catchments produce similar hydrological processes. The relationships between catchment characteristics and model parameters are important prerequisites for predictions in ungauged basins and assessment of land use changes. The parameters of hydrological models with no or short discharge records can only be estimated using regional information. One can assume that catchments with similar characteristics show a similar hydrological behavior. Therefore a regionalization of hydrological model parameters on the basis of catchment characteristics is plausible. However, due to the non-uniqueness of the rainfall/runoff model parameters (equifinality), a procedure of a regional parameter estimation by model calibration and a subsequent fit of a regional function is not appropriate. In this research a different procedure based on the depth function and convex combinations of model parameters is introduced. Catchment characteristics to be used for regionalization can be identified by the same procedure. Regionalization is then performed using different approaches: multiple linear regression employing the deepest parameter sets and convex combinations. An example of 28 British catchments is used to illustrate the methodology. The HYMOD model was used for this research. The results show regionalization based on the depth function and convex combinations of model parameters is reasonable for prediction in ungauged basin.



# Kurzfassung

Die hydrologische Modellierung ist zu einem anerkannten theoretischen Hilfsmittel in der Wasserwirtschaft geworden. Niederschlagsabflussmodelle werden sowohl für kurz- und mittelfristige Fragestellungen (wie z.B. Hochwasservorhersage), als auch für langfristige Planungszwecke eingesetzt. Allerdings ist der Einsatz von hydrologischen Modellen aus verschiedenen Gründen beschränkt. Eine wesentliche Einschränkung für den Einsatz von hydrologischen Modellen ist die Datenverfügbarkeit und die Parameterabschätzung. Abflüsse werden nur an einzelnen ausgewählten Flussquerschnitten gemessen, weshalb es nur eine geringe Anzahl von Einzugsgebieten gibt, für die der berechnete Abfluss nachgeprüft werden kann. Des Weiteren kann die hohe räumliche und zeitliche Variabilität der meteorologischen Eingangsdaten wie Niederschlag, Temperatur oder Wind nicht vollständig von der in der Regel geringen Anzahl an Wetterstationen erfasst werden. Radarmessungen können eine detailliertere räumliche und zeitliche Auflösung des Niederschlags liefern, allerdings ist die Verlässlichkeit dieser Daten immer noch gering. Andere beeinflussende Faktoren, wie z.B. Bodeneigenschaften, variieren räumlich ebenfalls deutlich und in manchen Fällen sogar zeitlich (z.B. Makroporen im Boden). Durch diese und andere Probleme sind physikalisch-basierte Modelle für viele praktische Anwendungen nicht verwendbar. Verschiedene Modelle, die auf teilweise gleichen Konzepten basieren, können die Einflüsse der Variabilität herausfiltern und somit oft erfolgreich für praktische Aufgaben eingesetzt werden. Die Einschränkung bei solchen Modellen beruht darauf, dass einige ihrer Parameter nicht direkt mit physikalisch messbaren Größen zusammenhängen. Deshalb müssen solche Parameter durch Beobachtungen mit Hilfe von Kalibrierungsmethoden abgeschätzt werden.

Das Ziel dieser Forschungsarbeit war die Entwicklung von effektiven, praktischen und stabilen Methoden der Parameterabschätzung, welche für eine zuverlässige hydrologische Modellierung sowohl in beobachteten als auch in unbeobachteten Einzugsgebieten eingesetzt werden sollen.

Die Abschätzung von hydrologischen Modellparametern ist eine große Herausforderung. Mit zunehmenden Rechnerkapazitäten konnten in den letzten Jahren verschiedene komplexe Optimierungsalgorithmen entwickelt werden. Nach wie vor kann aber keiner dieser Algorithmen einen einheitlichen oder "besten" Parametersatz ausgeben. Die Parameter angepasster hydrologischer Modelle hängen von den Eingangsdaten der Modelle ab, deren Qualität aufgrund von Messfehlern allerdings nicht gewährleistet werden kann. In dieser Forschungsarbeit wurde eine Methode zur Bestimmung eines stabilen Parametersatzes für ein hydrologisches Modell entwickelt. Um die Auswirkungen von Messfehlern zu erkennen, wurden Versuche mit synthetisch generierten stochastischen Messfehler bei beobachteten Abfluss- und Temperaturdaten durchgeführt. Mit so veränderten Daten wurde das Modell kalibriert, womit die Auswirkungen der Messfehler auf die

## *Kurzfassung*

Parameter analysiert werden konnten. Dabei wurde festgestellt, dass Messfehler signifikante Auswirkungen auf die am besten ausführenden Parameter haben. Die fehlerhaften Daten führen zu sehr unterschiedlichen Parametersätzen. Um dieses Problem zu beseitigen und einen stabilen Parametersatz zu bestimmen, wurde ein geometrischer Ansatz basierend auf Tukey's Halbraumtiefe angewendet. Die Tiefe eines von  $N$  zufällig erzeugten Parametersatzes wurde hinsichtlich desjenigen Parametersatzes mit der besten Modelleistung (beurteilt anhand der Nash-Sutcliffe-Effizienz) berechnet. Die Ergebnisse zeigen zum einen, dass auf Grundlage der Parametertiefe ein stabiler Parametersatz bestimmt werden kann und zum andern, dass die ausgewählten Parameter bezüglich der oben genannten Kriterien eine geringe Sensitivität aufweisen und auch gut auf andere Zeitabschnitte übertragen werden können. Diese Methode wird zunächst am Beispiel des Einzugsgebietes des Oberen Neckars in Deutschland veranschaulicht. Für die Entwicklung dieser Methode wurde das konzeptionelle HBV-Modell verwendet. Der mit der "Data-Depth-Function" entwickelte Algorithmus wird als "Robust Parameter Estimation"-Algorithmus (ROPE) bezeichnet.

Der ROPE-Algorithmus wurde mit verschiedenen Modellen (z.B. HYMOD und "Three Reservoir") anhand verschiedener Einzugsgebiete mit sehr unterschiedlichen Eigenschaften und Datenverfügbarkeiten in England und Indien getestet. Die Ergebnisse zeigen, dass der ROPE-Algorithmus bei diesen Einzugsgebieten und Modellen gut funktioniert, was ihn zu einem grundsätzlich gut einsetzbaren Werkzeug für die Modellkalibrierung macht. Als Ergänzung zum ROPE-Algorithmus wurde ein einfacher und effektiver Algorithmus mit Namen "Sequential Replacement of Weak Parameter" (SRWP) zur automatischen Kalibrierung des hydrologischen Modells eingeführt. Beim SRWP-Algorithmus werden schwache Parametersätze fortlaufend mit besseren Parametersätzen ausgetauscht. SRWP wird mit verschiedenen Testfunktionen und auch anhand hydrologischer Modelle überprüft. Die mit dem SRWP-Algorithmus erzielten Ergebnisse wurden mit den Ergebnissen des normalerweise benutzten "Global Optimization Shuffled Complex Evolution"-Algorithmus (SCE-UA) verglichen. Der Vergleich zeigt, dass SRWP die lokalen Minima beseitigt und sich an den optimalen Bereich annähert. Der SRWP-Algorithmus nähert sich nicht einem einzelnen Optimum an, sondern gibt eine konvexe Hülle des optimalen Bereichs aus. Diese Methode wurde mithilfe des Modells HYMOD am Oberen Neckareinzugsgebiet getestet. Die Ergebnisse zeigen, dass die so bestimmten Parameter bei dieser schrittweisen Kalibrierung stabil sind.

Hydrologische Modelle werden für verschiedene Zielsetzungen genutzt. Mit einem Modell können deshalb verschiedene Ziele verfolgt werden, indem verschiedene Zielfunktionen für die Modellkalibrierung verwendet werden. Eine einzelne Zielfunktion kann nie alle Teile einer Abflussganglinie beschreiben. In dieser Forschungsarbeit wurde versucht, den durch unterschiedliche Zielfunktionen dargestellten Parameterraum während der Modellkalibrierung mit dem ROPE-Algorithmus zu analysieren. Das hydrologische Modell HYMOD wurde unter Verwendung verschiedener Zielfunktionen (Nash-Sutcliffe-Koeffizient, "Root Mean Square Error", "Volume Error" und "Peak Error") mit dem ROPE-Algorithmus kalibriert. Außerdem wurden die oben genannten Zielfunktionen logarithmiert und untersucht. Die verschiedenen Zielfunktionen ergaben unterschiedliche

Parameterbereiche, wobei der Nash-Sutcliffe-Koeffizient und der "Root Mean Square Error" sehr ähnliche Parameterverteilungen aufweisen. Dies lässt sich durch die ähnlichen Formeln der beiden Zielfunktionen begründen. Es lassen sich keine gemeinsamen Schnittmengen der Parameterbereiche der unterschiedlichen Zielfunktionen beobachten. Der Volumenschwund der Parameterbereiche durch die verschiedenen Zielfunktionen ist sehr unterschiedlich, was zeigt, dass der erhaltene optimale Parameter bei verschiedenen Zielfunktionen unterschiedlich bemessen wird. Die Auswertung der Parameterbereiche führte zur Entwicklung einer hierarchischen Kalibrierungstechnik. Dadurch wird das Problem der Einzel- und Mehrfachzielfunktion gelöst. Die Ergebnisse dieser Untersuchung werden für eine stabile Parametrisierung von hydrologischen Modellen hilfreich sein.

Die Dauer des Beobachtungszeitraumes, die für die Modellkalibrierung benutzt wird, hat einen großen Einfluss auf die Parameterbestimmung. Daher ist es notwendig herauszufinden, wie viele Daten für die Modellkalibrierung genügen. Schwer zu sagen ist allerdings, welche Daten und Dauer für eine Kalibrierung und Parameterbestimmung ausreichend sind. Daten, die eine hohe hydrologische Variabilität aufweisen, sind die beste Wahl für die Kalibrierung, da sie die meisten Informationen beinhalten, die für die Parameterbestimmung notwendig sind (Gupta and Sorooshian, 1985). Bei dieser Anwendung wurden die Modellparameter aus sogenannten ungewöhnlichen Zeitintervallen abgeschätzt. Diese wurden aus Beobachtungszeitreihen von Abfluss oder Niederschlag mit Hilfe des statistischen Verfahrens der Datentiefe bestimmt. Zielfunktionen werden verwendet, um aus API-Reihen (Antecedent Precipitation Index) oder dem Abfluss der vergangenen vier Tage ungewöhnliche Ereignisse zu ermitteln. Daten mit geringer Halbraumtiefe werden als ungewöhnlich angenommen. Die kritischen Ereignisse, welche durch den API oder Abfluss bestimmt wurden, sind etwa im gleichen Zeitraum in einer Zeitreihe. Die Verwendung der ausgewählten kritischen Ereignisse für die Modellkalibrierung ist nur geringfügig schlechter als die Verwendung aller Daten. Die Übertragbarkeit der Parameter für andere Zeitintervalle mit der klassifizierten Tiefe ist sogar signifikant besser als bei der Verwendung aller Daten. Anhand zweier verschiedener Modelle (HBV und HYMOD) wird diese Methodik am Einzugsgebiet des Oberen Neckars gezeigt. Der entwickelte Algorithmus für die Bestimmung der kritischen Zeitintervalle, welcher auf der Datentiefe basiert, wurde ICE-Algorithmus (Identification of Critical Events) genannt. Um mit dem ICE-Algorithmus auch allgemeinere Zwecke verfolgen zu können, wurde dieser an komplexen physikalisch-basierten hydrologischen Modellen, wie WaSim-ETH, getestet. Es hat sich gezeigt, dass Modelle wie WaSim-ETH sich erfolgreich unter Verwendung kritischer Ereignisse kalibrieren lassen. Die Ergebnisse sind genauso gut wie die Ergebnisse mit dem gesamten verfügbaren Datensatz. Der ICE-Algorithmus kann auch bei der datenbasierten Modellierung nutzbringend eingesetzt werden. Die Leistungsfähigkeit des ICE-Algorithmus wurde daher bei der Modellierung von sogenannten "Artificial Neural Networks" (ANNs) getestet.

ANNs sind als ein datengesteuertes Verfahren klassifiziert, was bedeutet, dass das "Lernen" der ANNs durch mehr und mehr zu Verfügung gestellte Trainingsdaten verbessert wird. Das liegt daran, dass längere Zeitreihen von Trainingsdaten mehr unterschiedliche

## *Kurzfassung*

Ereignisse beinhalten und somit die allgemeine Anwendbarkeit von ANNs verbessert. Allerdings bedeuten längere Zeitreihen von Trainingsdaten nicht zwingend mehr Information. Gibt es eine deutliche Wiederkehr derselben Information, werden die ANNs nicht "klüger" und es kostet unnötige Rechnerleistung und Zeit. In dieser Untersuchung wurde angenommen, dass es Abschnitte in langen Zeitreihen gibt, die einen hohen Informationsgehalt besitzen. Werden die ANNs nur für diese Bereiche geschult, anstatt für die gesamte Zeitreihe, liefert das Training die gleichen oder sogar bessere Ergebnisse. Hier wurde der ICE-Algorithmus für die Bestimmung der kritischen Bereiche angewendet. Verschiedene Formen von ANNs wurden zuerst für die gesamten Zeitreihen und dann nur auf Daten der kritischen Bereiche angewandt. Der Vergleich der Ergebnisse zeigt, dass die Güte der Ergebnisse, die mit den kritischen Bereichen berechnet wurden, geringfügig schlechter als die der mit allen Daten berechneten ist.

Weil komplexe natürliche Prozesse in einer Modellierung immer vereinfacht werden müssen und wegen der begrenzten Verfügbarkeit von Messungen können die Parameter für die hydrologischen Modelle nicht vollkommen bestimmt werden. Im Allgemeinen werden die Modellparameter als zeitunabhängig angenommen. Da die Einzugsgebietseigenschaften jedoch teilweise instationär sind, können einige Modellparameter wie die durch sie repräsentierten natürlichen Prozesse mit der Zeit variieren. Ein weiteres Ziel dieser Forschungsarbeit ist daher die Entwicklung einer Methode, welche die Dynamik von Parametern in hydrologischen Modellen untersucht. Zu diesem Zweck wurde ein "Robust Dynamic Parameter Estimation"-Algorithmus (RDPE) entwickelt. RDPE kann für die Diagnose von hydrologischen Modellen und zur Verbesserung von Modellvorhersagen unter Verwendung zeitvariabler Parameter angewendet werden. Nachdem der Bereich der zeitvariablen Parameter mit dem ROPE-Algorithmus bestimmt wurde, wurde der "Moving Window Approach" und "Simulated Annealing" angewendet, um die Parameter des HBV-Modells für jede Fenstergröße zu optimieren. Die daraus gewonnenen Zeitreihen der Parameter werden für die Bestimmung der sensitiven und insensitiven Perioden in den Parameterzeitreihen verwendet. Die Ursachen der zeitlichen Variabilität können damit ebenfalls erklärt werden. Um die Vorhersage von Parameterzeitreihen zu verbessern, wurde ein Vorhersagemodell für Parameter entwickelt und angewendet. Diese Methode wurde unter Verwendung des HBV-Modells an mesoskaligen Einzugsgebieten am Neckar getestet. Es zeigt sich, dass die neue Methodik zu realistischeren Konfidenzintervallen für Modellsimulationen führt.

Die räumliche und zeitliche Übertragbarkeit hydrologischer Modellparameter von beobachteten zu unbeobachteten Einzugsgebieten ist möglich, wenn man annimmt, dass ähnliche Einzugsgebietscharakteristika auch ähnliche hydrologische Prozesse hervorrufen. Die Güte der Beziehungen zwischen Einzugsgebietscharakteristika und Modellparametern ist eine wichtige Voraussetzung für eine verlässliche Vorhersage in unbeobachteten Einzugsgebieten und bei der Bewertung von Landnutzungsveränderungen. Die Parameter von hydrologischen Modellen, die ohne oder nur mit sehr kurzen Abflussaufzeichnungen auskommen müssen, können nur mit Hilfe regionaler Informationen abgeschätzt werden. Man könnte dabei annehmen, dass Einzugsgebiete mit ähnlichen Eigenschaften auch ein ähnliches hydrologisches Verhalten zeigen. Daher scheint die Regionalisierung von

hydrologischen Modellparametern auf der Basis von Einzugsgebietscharakteristika plausibel. Wegen der Uneindeutigkeit von Parametern in Niederschlags-Abfluss-Modellen ist eine Parameterabschätzung aufgrund regionaler Gegebenheiten bei der Modellkalibrierung und der anschließenden Anpassung der regionalen Funktion trotzdem nicht geeignet. In dieser Forschungsarbeit wurde daher ein anderes Verfahren basierend auf der Tiefenfunktion und der konvexen Kombination von Modellparametern entwickelt. Einzugsgebietscharakteristika, die für die Regionalisierung eingesetzt werden sollen, können so mit dem gleichen Verfahren bestimmt werden. Die Regionalisierung wird unter der Verwendung verschiedener Annäherungen durchgeführt: Die multiple lineare Regression unter Verwendung der Parametersätze mit der größten Tiefe und von konvexen Kombinationen. Am Beispiel von 28 Einzugsgebieten in Großbritannien wird diese Methode vorgestellt. Für diese Untersuchung wurde das Modell HYMOD verwendet. Die Ergebnisse zeigen, dass die Regionalisierung mit der Tiefenfunktion und konvexen Kombinationen der Modellparameter für die Vorhersage von unbeobachteten Einzugsgebieten sinnvoll ist.



# 1 Introduction

## 1.1 Background and Motivation

The hydrological model is a mathematical tool to represent a very complex and nonlinear natural phenomenon (hydrological process) in simple ways. The hydrological model has been in use for several decades for several purposes (flood forecasting, watershed management etc). Even so, hydrological science is not complete in itself because we have limitation in understanding some complex and nonlinear natural processes. Several decades of research have been devoted to make a simple hydrological model for every case study, but with limited success. A common generalization is that the complex model can represent hydrological processes in a better way, but several authors ([Michaud and Sorooshian, 1994](#); [Refsgaard and Knudsen, 1996](#); [Perrin et al., 2001, 2003](#); [van der Linden and Woo, 2003](#)) have proved that the complex hydrological model need not be the best, a simple model can also represent better. However, there is no fixed framework for building a model that is simple in a certain sense.

Even though the twentieth century has witnessed an enormous growth in hydrological process understanding, numerous challenges still remain ([Jakeman and Hornberger, 1993](#); [Blöschl and Sivapalan, 1995](#); [Bergström and Graham, 1998](#); [Singh and Woolhiser, 2002](#); [Moradkhani et al., 2005](#)). Among the challenges that remain, the dominating ones are: (1) Representation of dynamic hydrological process by static model; (2) Complexity in hydrological model; (3) Accuracy in measurement; (4) Gap between model and real world; (5) Scale problem; (6) Parameterization of model; (7) Hydrological process in the soil micro pores; (8) Preferential flow at large scale, and many more.

The study of hydrological models are two-fold: models for understanding physical processes and models for prediction. In the former, we try to represent the very complex and nonlinear process by some mathematical equation and try to learn at the small scale. In the latter, modelers attempt to predict the stream flow at some future time when given knowledge of the current state of the system and model parameters. In this respect, good estimates of the parameters and state variables are needed to enable the model to generate accurate forecasts ([Moradkhani et al., 2005](#)).

## 1.2 Problem Definition

The parameter estimation of hydrological model parameters is a difficult task. Reasons for this are the highly nonlinear nature of hydrological processes and the fact that different parameter vectors driving models describing the physical processes might have the same effect on the discharge. This means that changes of some parameters might be

## 1 Introduction

compensated by others. Unfortunately, traditional manual calibration of models with reasonable parameter values often leads to weak results. Hence, nowadays, automatic procedures based on numerical methods are used.

Many different optimization routines have been developed to find optimum parameter vectors. A variety of objective functions that measure model performance, including multi-objective approaches, have been tried to define optimality in this context. Non-linearity of the hydrological models and of the objective functions lead to very complex optimization problems. [Beven and Freer \(2001\)](#) argue that there are no optimum parameters; in fact there is a large set of parameter vectors which all perform reasonably and one cannot easily distinguish between them. They call this an *equifinality* problem which leads to high uncertainties in the model predictions. Frequently shown *dotty plots* give the impression that the set of good parameter vectors can be found anywhere in the space, but no clear convergence to a best single value can be observed. [Bárdossy \(2007\)](#) investigated the geometrical properties of a parameter vector with good performance for a two-dimensional case and found that the set of good parameters was well structured. Unfortunately in higher dimensional spaces one can not *see* these sets, thus it is not clear whether they are scattered or have some clear structure. The high scatter observed in the good individual parameters is very disturbing since it does not enable a classical identification of a single vector within corresponding confidence limits.

The GLUE procedure ([Beven and Binley, 1992](#)) has widely been applied for uncertainty assessment and discussed in the scientific literature, although alternative procedures using parametric approaches to obtain *best* solutions have also been suggested. These approaches are optimal under certain assumptions, however, they are often selected purely for mathematical convenience and not necessarily based on experience with data. In [Kavetski et al. \(2006a\)](#) and [Kavetski et al. \(2006b\)](#), it was noted that the performance metric of hydrological models is a *bumpy* function of the model parameters. They suggest different numerical procedures to *smoothen* parameter surfaces and to obtain optimal parameter vectors.

From the forthcoming discussion it is very clear that in the field of parameterization of hydrological model there is clearly a need for some kind of robust parameter estimation technique for the hydrological model.

In the parameterization problem of the hydrological model, the selection of a objective function plays a vital role in parameter estimation. Several authors advocated that there is no universal measure which can define all aspects of the hydrograph ([Moussa and Chahinian, 2009](#); [Krause et al., 2005](#); [Madsen, 2000](#)). Hence it is important to know how these objective functions map the parameter space and the parameter space changes from one objective to other.

The technique of simultaneously identifying parameters and their uncertainties is a recent development in the field of parameter estimation in hydrology ([Kuczera, 1983a,b](#); [Beven and Binley, 1992](#); [Uhlenbrook et al., 1999](#); [Thiemann et al., 2002](#); [Vrugt et al., 2002](#); [Wagener et al., 2003](#)). We required a measure of fit to evaluate the performance of every simulation. Hence these measures of goodness play a great role in deciding the uncertainty associated with parameters sets. This is simply because one parameter set is



maybe more qualified for one objective function but is relatively weak for another. This leads us to having different uncertainty quantifications for same parameter set. Hence, there is a need to have a very robust objective function which can overcome the problem mentioned above.

The available past observations of discharge and weather (temperature, precipitation, etc.) are used for calibration purposes. The observation period might contain floods, droughts and normal flow periods. It can be assumed that the calibration can only be successful if the observation period is representative for the hydrological behavior of the catchment. The information contained in the observations with respect to the parameters is not uniformly distributed along the series. Certain time periods might be useful for the identification of specific parameters while others might be useless. For example, summer observations are of no use to identify snow melt related parameters. In a study, [Wagener et al. \(2003\)](#) showed that the information contained in a data series is inhomogeneous. Only certain time periods of the observation series truly represented the hydrological behavior of the catchments.

The length and information content of a time series play a vital role in model parameter identification. Several authors have investigated the data requirement for identification of stable parameters ([Gupta and Sorooshian, 1985](#); [Harlin, 1991](#); [Yapo et al., 1996](#); [Xia et al., 2004](#); [Perrin et al., 2007](#); [Seibert and Beven, 2009](#)). Even so, it is very difficult to say precisely what length of data is enough to perfectly identify the model parameters. A rule of thumb is that a data length of one year to 8 years is sufficient to obtain robust parameters. However, it is not good to generalize because different models have different levels of complexity. Moreover, the information content of data is generally not known. Hence, we always use the whole data series so that a model can get correct information to identify its parameters. There are several cases where the time series are still not complete, meaning that there is need of some method which can identify the critical time period in a given time series and in which it contained most of the information to identify model parameters.

Proper choice of calibration data may play a great role in parameter identification of hydrological model. It is very difficult to say which data and what length of data is sufficient for the proper choice of calibration data which will give proper identification of model parameters. The data that contains lots of hydrological variability may be the best choice for calibration data because it may contain most of information that is required for parameter identification ([Gupta and Sorooshian, 1985](#)). Hence it is very necessary to test a similar hypothesis, assuming that unusual events in a given series may represent most of the hydrological variability.

Due to the simplification of the complex natural process and the limited availability of observations, the parameters of the hydrological model cannot be identified perfectly. Some of the catchment properties are not static in nature e.g. land use, catchment storage and soil properties. So dynamics inherent in hydrological processes can not be described by static parameters of the hydrological model. Generally we calibrate our model assuming that the parameters are static; this limits predictability. It is necessary to know, therefore, how static parameters limit predictability in hydrology.

## 1 Introduction

A spatial and temporal transfer of hydrological model parameters from gauged to ungauged catchments is possible under the assumption that similar catchments produce similar hydrological processes. The relationships between catchment characteristics and model parameters are important prerequisites for predictions in ungauged basins and assessment of land use changes.

Due to tremendous spatiotemporal heterogeneity of climatic, landscape (surface and subsurface), and land cover properties, the extrapolation of information or knowledge from gauged to ungauged basins remains a challenging task, with considerable difficulties and uncertainties, especially in light of our limited understanding of what flow path water takes to the stream. A main bottleneck to modeling ungauged basins is the complexity of the problem. In many previous studies, this has taken either a linear or a nonlinear regression form. However, such an approach has met with limited success. As mentioned in the previous section, model calibration results in only one realization among many other possible parameter sets that lead to a similar model performance. The relationships established between such a set of model parameters and the catchment characteristics are therefore likely to be weak or *random*. [Fernandez et al. \(2000\)](#) implemented a different approach that would take care of the problem cited above. Instead of following the two-step procedure implemented in the previous studies, they treated them concurrently. A very recent work on regionalization of parameter of HBV-IWS model indicates that the calibration of coefficients of a transfer function simultaneously for all catchments under consideration is a promising approach to determine the transfer function ([Hundecha and Bárdossy, 2004](#); [Göttinger and Bárdossy, 2007](#)). The following research work will tackle the issue of establishing a unique relationship between parameters of a conceptual model and hydrological variables by statistical manner, so that reliable estimates of model parameters for an ungauged catchment, merely based on a few measurable hydrological variables of the catchment, can be realized.

### 1.3 Objectives of the Research

The broad scope of this research is to make a reliable hydrological modeling at gauged and ungauged basins. The main focus of this research is to bring more insight into the process of parameter estimation techniques in hydrological modeling. The other objective of this research work is to develop a methodology that enables regional estimation of parameters of a conceptual continuous water balance model based on physical catchment descriptor, which includes the land use, soil type, stream network, elongation and topographic attributes of the catchment. It aims at improving the weakness inherent in the traditional two-step regionalization approach in estimating the relationship between the model parameters and the physical catchment descriptor. The specific objectives of the research is to answer some basic question as listed below:

- How can we estimate hydrologically reliable parameters for modeling?
- How do different objective functions map parameter space during calibration?

- Can we calibrate a hydrological model using carefully selected critical events?
- Can we improve prediction and model diagnosis by including dynamic variability in parameters?
- How can we extend hydrologically reliable parameters from gauged to ungauged basins?

## 1.4 Organization of the Thesis

This thesis is organized as follows: The theoretical background of hydrological model and parameter estimation is briefly reviewed in Chapter 2. In Chapter 3, the mathematical definitions of the depth function and its main properties are briefly described. The details of the study area and model used in this thesis is described in Chapter 4. In Chapter 5, the development of a new technique of robust parameter estimation for hydrological model is described and its application to different models and different catchments is tested to generalize the methodology. Chapter 6 presents the inference of the objective function on mapping of the parameter estimation. Chapter 7 deals with the length of data series for calibration. In this chapter, a novel method of identification of critical event is presented in detail. This also provides the use of the method for different studies. Chapter 8 describes the robust dynamic parameter estimation technique. The application of the data depth to prediction in an ungauged basin is given in Chapter 9. At the end of this thesis, a summary of the study and an outlook of the future steps are outlined.

## 2 Parameter Estimation in Conceptual Hydrological Modeling

This chapter provides a brief review of the problem associated with parameter estimation of the hydrological model.

### 2.1 Hydrological Model

Hydrological models are used for different purposes such as water resources management or watershed development. The art of hydrological modeling has been in practice for several decades, yet there is no universal hydrological model which can be used everywhere in this world. Broadly there are three types of hydrological models: empirical, conceptual and physically based (Wagener et al., 2004). At this advanced stage of hydrology, irrespective of the empirical, conceptual or physical type, a hydrological model cannot describe the precise nature of rainfall-runoff processes. This is mainly due to the lack of very clear and sound understanding of physics behind rainfall-runoff process and in adequate representation of the available process knowledge (Patil, 2008). A great deal of research has taken place in the past decades to improve our basic understanding of hydrological processes and implementing the knowledge in hydrological modeling, which in turn has resulted in increased model complexity (Blasone, 2007). The vast complex nature cannot be represented by present knowledge. The current state of knowledge does not allow for complex interaction among various hydrological variables and presently employed formulations to be characterized in the model structure (Sivapalan et al., 2003). Although, we cannot understand the very complex nature of rainfall-runoff process precisely, hydrological models are still of great use for any water resources developmental activity. Any model before its real use needs to be calibrated to obtain its parameters. This makes parameterization an important problem and has to be investigated in detail.

### 2.2 Parameter Estimation

The last few decades several other hydrological models have emerged to represent the hydrological process, though conceptual hydrological models are in great use as they are very simple. All the hydrological models have a certain number of parameters; some of them have physical meaning, while others does not. The only problem with these models is, that they need to estimate their parameters using observed data before the model can be used for practical purposes. This is because the predictability of the model will be very much depend on parameters. The typical way to estimate the parameters

is trying and adjusting the parameters values by various means so that precipitation-runoff behavior of the model approximate as closely and consistently as possible to the observed response of the catchments over some period of time for which precipitation, stream flow and other relevant catchments characteristic measured data are available. This process of parameter estimation is called model calibration (Gupta et al., 2003). Several techniques have been developed in different corners of the world to estimate parameters of a hydrological model. Generally, there are two types of model calibration. One constitutes the manual calibration, which completely relies on the expertise and judgment of the hydrologist. The other method is automatic calibration, which employs the power, ability to follow systematic programmed rules, speed and capability of the computer (Gupta et al., 2003; Hendrickson et al., 1988).

In manual calibration, the evaluation of the agreement between simulated and observed hydrograph is subjective and based on visual inspection. The parameters are tuned based on the expert guesses. For the automatic calibration, a different single or multi-objective function for the parameter adjustments and different criteria can be used for evaluation of goodness of fit between observed and modeled hydrograph. Even so, the non-uniqueness of the parameters makes parametrization a challenging task. There are several local and global optimization algorithms available. Some of the algorithm's results depend on the initial guesses and can be trapped in local minima or maxima. So to overcome such type of problem, global optimization algorithms like SCE-UA, Simulated Annealing, Genetic Algorithm etc. have emerged (Kavetski et al., 2006b). The advantages and disadvantage of manual and automatic calibration are given in Table 2.1 as given by Gupta et al. (2003).

Manual Calibration	Automatic Calibration
User knowledge and expertise is valuable	Speed and computational power of computer
Very subjective	Based on objective function
Labor intensive	Computational intensive
Time consuming	Time saving
Excellent result	Good result; some time result not acceptable
Not suitable for long time period of calibration	Can calibrate using long time period

**Table 2.1:** *The advantages and disadvantages of manual and automatic calibration*

There are several problems associated with parameter estimation. The major problems were described by Jackson and Aron (1971):

- Which method is best suited for analysis?
- Criteria used for
  - evaluating the parameters
  - comparison of model result with observed data (goodness of fit)
- Several kind of errors associated with observed data
- Problem associated with structure of the model

## 2 Parameter Estimation in Conceptual Hydrological Modeling

- Integration and combination of the above problems
- Uncertainty associated at various level of parameter estimation
- Availability of data
- Initial and boundary condition

Irrespective of this, all model calibrations and their subsequent predictions will be subjected to uncertainty (Beven, 2000) due to above problem associated with parameter estimation. In the process of model calibration, we have to obtain our model parameter from feasible space of parameter using some kind of objective function. But it is often very complex and difficult to find the response surface in the parameter space (Beven, 2000; Beven and Freer, 2001). Certain extend we can overcome these difficulties with a simple model with small number of parameters. This can have a smoother parameter response surface, but in reality it is very difficult to archive in hydrological modeling Beven (2000).

Beside these problems of parameter estimation in gauged catchments, the most important problem is the parameter estimation in ungauged catchments where we have poorly observed data or no data at all. Hence, parameter estimation for the hydrological model in ungauged catchments is even more difficult than in gauged catchments. Regionalisation of model parameter is the only solution for ungauged catchments. Regionalisation of model parameters means transferring parameters from gauged catchments to similar ungauged catchments. These similarities are defined based on the available catchments characteristics. Here, uncertainly associated with parameters is very high.

Parameter estimation for hydrological models has received increased attention from the hydrology and land surface modeling community (Sorooshian et al., 1993; Kuczera, 1997; Gupta et al., 1998; Andréassian et al., 2001; Beven and Freer, 2001; Vrugt et al., 2002; Gupta et al., 2003; Wagener et al., 2003; Samaniego and Bárdossy, 2005; Beven., 2006; Kavetski et al., 2006a,b; Bárdossy, 2007; Bárdossy and Singh, 2008). Following the same trend, this current research is also devoted to solving and understanding some of the problems associated in the parameter estimation of the hydrological model.

In this research, concepts of geometry and multivariate statistics are used to address the problem of parameter estimation. Specifically, convex sets along with the depth function defined in Tukey (1975) are used as the main tools. The details about data depth are given in the following chapter.

## 3 Data Depth Function

This chapter does not provide a rigorous mathematical exposition of the concept of data depth function. Instead, a few basic definitions and properties that are used in this thesis are recalled. Further details about the concept of data depth can be found in [Tukey \(1975\)](#), [Rousseeuw and Struyf \(1998\)](#), [Liu et al. \(1999\)](#) and [Zuo and Serfling \(2000\)](#).

### 3.1 Definition

Data depth is nothing but a quantitative measurement of how central a point is with respect to a multivariate data cloud or a distribution. This gives us the central outward ordering of a data points in a multivariate sample. This center-outward ordering of the multivariate data provides a foundation for various multivariate estimation and inference methods. Depth functions were first introduced by [Tukey \(1975\)](#) to identify the center (a kind of generalized median) of a multivariate dataset. Several generalizations of this concept have been defined in [Rousseeuw and Struyf \(1998\)](#), [Liu et al. \(1999\)](#) and [Zuo and Serfling \(2000\)](#), [Liu \(1990\)](#), [Donoho and Gasko \(1992\)](#). In higher dimensions, the calculations of depth functions is quite computationally intensive. The points with high depth are the points which lye in the interior of the data cloud while those with low depth lye near the side of the convex hull. A formal example of convex hull is given in Figure 3.1. The convex hull of a set of points  $S$  is the smallest area polygon which encloses  $S$ . An example of a convex hull in practical case is given in Figure 3.2. The  $X$  axis is one parameter of a model and  $Y$  axis is another parameter. The points that lye outside of the convex hull have depth  $\leq 4$ . All the points that lye inside the convex hull have higher depth.

#### 3.1.1 Desirable properties of data depth function

There are certain properties of data depth functions which makes them very powerful tools in providing a center-outward ordering of points in a multivariate dataset. It should satisfy following basic properties ([Zuo and Serfling, 2000](#)):

- *Affine invariance*: The depth of a point  $X \in \mathcal{R}^d$  should not depend on the underlying coordinate system or, in particular, on the scales of the underlying measurements.
- *Maximality at center*: For a distribution having a uniquely defined center (e.g., the point of symmetry with respect to some notion of symmetry), the depth function should attain maximum value at this center.

### 3 Data Depth Function

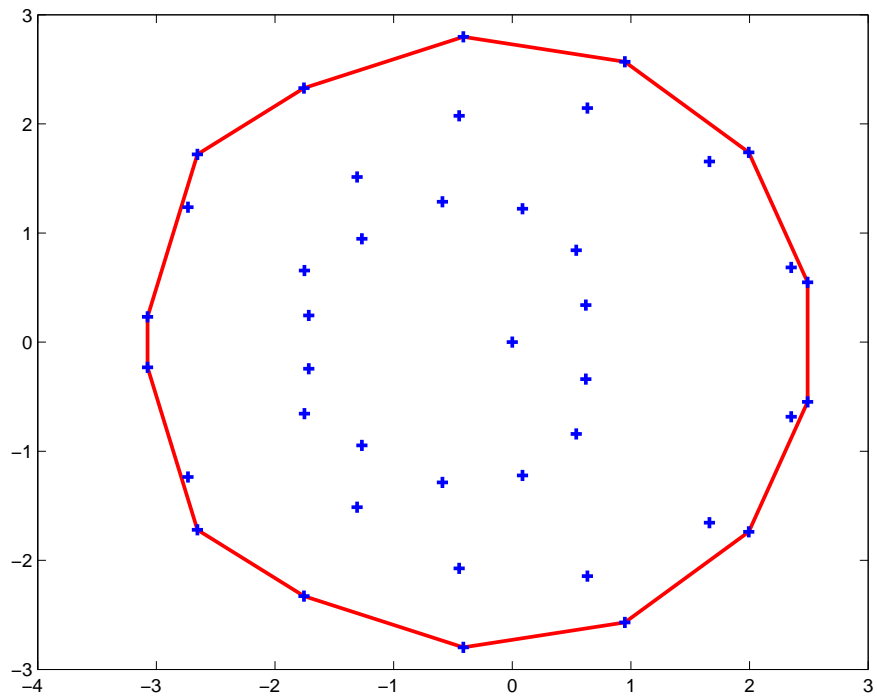


**Figure 3.1:** *Example of convex hull*

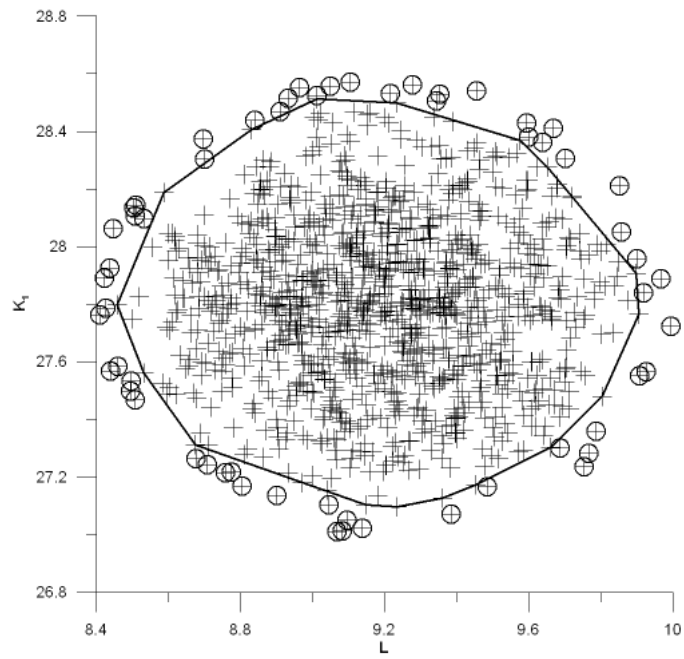


**Figure 3.2:** *Circles represent the boundary points or low depth points*



- *Monotonicity relative to deepest point:* As a point  $X \in \mathfrak{R}^d$  moves away from the deepest point (the point at which the depth function attains maximum value; in particular, for a symmetric distribution, the center) along any fixed ray through the center, the depth at  $X$  should decrease monotonically.
- *Vanishing at infinity:* The depth of a point  $X$  should approach zero as  $X$  approaches infinity.

## 3.2 Type of Data Depth Function

There are several types of data depth function available. Some of them are described in the following section.

### Half-space depth function

*Definition:* The half-space depth of a point  $p$  with respect to the finite set  $X$  in the  $d$  dimensional space  $\mathfrak{R}^d$  is defined as the minimum number of points of the set  $X$  lying on one side of a hyperplane through the point  $p$ . The minimum is calculated over all possible hyperplanes.

Formally the half-space depth of the point  $p$  with respect to set  $X$  is:

$$D_X(p) = \min_{n_h} (\min(|\{x \in X \langle n_h, x - p \rangle > 0\}|), (|\{x \in X \langle n_h, x - p \rangle < 0\}|)) \quad (3.1)$$

Here  $\langle x, y \rangle$  is the scalar product of the  $d$  dimensional vectors, and  $n_h$  is an arbitrary unit vector in the  $d$  dimensional space representing the normal vector of a selected hyperplane. If the point  $p$  is outside the convex hull of  $X$  then its depth is 0. Points on and near the boundary have low depth while points *deeply* inside have high depth. To illustrate the concept of half-space data depth let us consider a two dimensional data set. Figure 3.3 sets out the systematic calculation of depth in a two dimensional data set. The first parameter corresponds to the  $x$  axis and the second to the  $y$  axis. Let's assume that we want to have depth of the rectangular point in space of circular points. A hyperplane was drawn passing through the rectangular point as shown in figure (3.3a). The number of points are then counted at each side of the hyperplane. The hyperplane was rotated clockwise for all 360 degree (figure 3.3b-d). For each increment, the number of points lying either side is counted and the minimum of either side is recorded. Now the depth of the rectangular point becomes the minimum of all these minimum number of points. In this case the minimum of minimum is 4. So depth of this point is 4. The half-space depth function satisfied all the properties of depth function as mentioned above and stated in [Zuo and Serfling \(2000\)](#). The major advantage of this depth function is that it is invariant to affine transformations of the space.

### 3 Data Depth Function

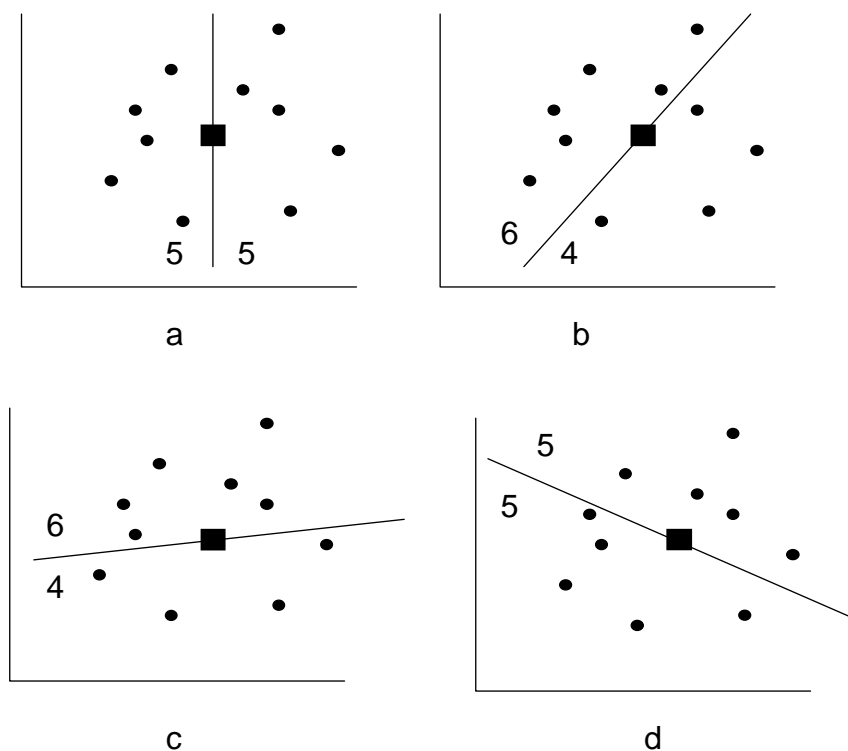


**Figure 3.3:** Schematic representation of a half-space calculation in two dimensions

#### $L_1$ Depth Function

According to [Hugg et al. \(2006\)](#) the  $L_1$  depth of a point  $X$  with respect to a data set  $S = X_1, \dots, X_n$  in  $R_d$  is one minus the average of the unit vectors from  $X$  to all observations in  $S$ . The formal definition from [Vardi and Zhang \(2000\)](#) is:

$$L_1 D(S, x) = 1 - \|\bar{e}(x)\| \quad (3.2)$$

$$\text{where } e_i(x) = \frac{x - X_i}{\|x - X_i\|}$$

$$\bar{e}(x) = \frac{\sum_{i=1}^n \eta_i \cdot e_i(x)}{\sum \eta_j}$$

$\eta_i$  is a weight assigned to observation  $X_i$  (and is 1 if all observations are unique), and  $\|x - X_i\|$  is the Euclidean distance between  $x$  and  $X_i$ . The  $L_1$  depth ranges between 0 and 1. It is computationally easy and fast.  $L_1$  median in calculation sense have the minimum sum of the euclidean distance to all points in the cloud. In a practical sense

$L_1$  median answers the question how much does the cloud need to be skewed before the points become the  $L_1$  median (Hugg et al., 2006).

### Mahalanobis depth

As described by Mahalanobis (1936) and several others (Liu, 1990, 1995; Hamurkaroglu et al., 2004; Chebana and Ouarda, 2008; Mahalanobis, 1936), the Mahalanobis depth can be defined as follows: Let  $X$  denote a random vector having distribution function  $F$  in  $R^p$ . Then the Mahalanobis measure of depth for any point  $x$  (a  $p \times 1$ -dimensional vector) in  $R^p$  with respect to the distribution  $F$  is as follows:

$$MD(F; x) = \frac{1}{[1 + (x - \mu F) \Sigma^{-1} (x - \mu F)]} \quad (3.3)$$

In equation 3.3,  $\mu F$  and  $\Sigma F$  are the mean vector and covariance matrix of the distribution function  $F$ , respectively. Hence,  $MD(F; x)$  is a measure showing how 'deep' or 'central'  $x$  is with respect to the distribution  $F$ . When  $F$  is unknown and a sample taken from distribution  $F$  is given, then the definition of Mahalanobis depth is:

$$MD(F_m; x) = \frac{1}{[1 + (x - \bar{X}) S^{-1} (x - \bar{X})]} \quad (3.4)$$

In 3.4,  $\bar{X}$  is a  $(p \times 1)$  sample mean vector and  $S$  a  $(p \times p)$  sample covariance matrix. The depth function  $MD(F_m; x)$  is a depth function satisfying all of the above properties (Liu, 1990, 1995).

### Oja median

Oja (1983) proposed that form a simplex with  $X$  for every subset of  $n$  points from the data set and summine together the volumes of each such simplex, the Oja simplex median is then any point  $X^*$  in  $R_n$  for which this sum is minimum. The formal definition given by Liu et al. (1999) is Oja median at  $x$  with respect to  $F$ :

$$OD(F; x) = \frac{1}{1 + E_f \{volume(S[x, X_1, X_2, \dots, X_d])\}} \quad (3.5)$$

where  $S[x, X_1, \dots, X_d]$  is the closed simplex with vertices  $x$ , and  $d$  random observations  $X_1, \dots, X_d$  from  $F$ . As volume in one dimension is just the length, the Oja median reduces to the standard univariate median. The Oja median need not be unique. It is affine invariant and it has been found to have a 0 breakdown point.

### Convex hull peeling

The formal definition of convex hull peeling depth given by Liu et al. (1999) and Barnett (1976) is, the convex hull peeling depth  $CD$ , at the sample point  $X_k$  with respect to the data set  $(X_1, \dots, X_n)$ , is simply the level of the convex layer  $X_k$  that belongs to

### 3 Data Depth Function

it. A convex layer can be defined as follows: Construct the smallest convex hull which encloses all sample points  $(X_1, \dots, X_n)$ . Then, the sample points on the perimeter are designated as the first convex layer and removed. The convex hull of the remaining points is constructed; these points on the perimeter are the second convex layer. The process is repeated, and a sequence of nested convex layers is formed. The higher layer point belongs to, the deeper the point is within the data cloud. The schematic representation of convex hull peeling in two dimensions is given in Figure 3.4. Here we can see that the depth at inner most convex hull has a depth of 3 and as we go out, the depth at the second convex hull is 2 and so on. Hence given a number of points, we can compute a convex hull and depth of the points that are on outer convex hull will be 1 and it will increase as we go to next convex hull. Convex hull peeling depth is relatively simple to compute. However it is not robust in the presence of outliers [Hugg et al. \(2006\)](#).

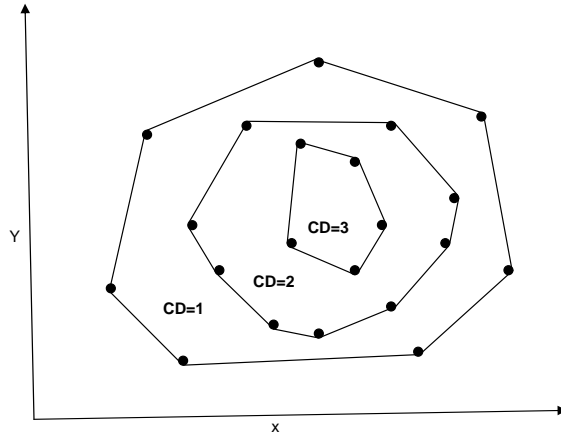


**Figure 3.4:** Schematic representation of convex hull peeling in two dimensions

#### Simplicial median

[Liu \(1990\)](#) and [Liu et al. \(1999\)](#) defined the Simplicial median as the simplicial depth **SD** at  $x$  with respect to  $F$ :

$$SD(F; x) = P_F \{x \in S [X_1, \dots, X_{d+1}]\} \quad (3.6)$$

Where  $S(X_1, \dots, X_d)$  is a closed simplex formed by  $(d + 1)$  random observations from  $F$ . The sample version of  $SD(F; x)$  is obtained by replacing  $F$  in  $SD(F; x)$  by  $F_n$ .

### 3.3 Use of Data Depth Function

The concept of data depth has received much attention from [Donoho and Gasko \(1992\)](#), [Rousseeuw and Struyf \(1998\)](#), [Rousseeuw and Ruts \(1998\)](#), [Liu et al. \(1999\)](#), [Zuo and Serfling \(2000\)](#), [Miller et al. \(2003\)](#) and [Lin and Chen \(2006\)](#). It has been used for the investigation of large data sets. The application of depth function has been seen in several fields. [Serfling \(2002\)](#) used the depth function for nonparametric multivariate analysis. [Cheng et al. \(2000\)](#) had used data depth function for monitoring multivariate aviation safety data for control charts. They were also applied in quality control by [Liu \(1995\)](#) and [Hamurkaroğlu et al. \(2004\)](#). [Liu and Singh \(1993\)](#) used data depth function for preparing a Quality Index. The hydrological applications found so far are to be found in [Chebana and Ouarda \(2008\)](#); the data depth was used to define weights for the regional estimation of hydrological extremes. Also in [Bárdossy and Singh \(2008\)](#), a half-space depth function was used to identify robust parameter for a hydrological model.

Due to the robust properties of the data depth function, convex sets (geometrical properties of parameter space) and the depth function defined in [Tukey \(1975\)](#) can be used to identify a set of good parameters. One advantage of this depth function is that, it is invariant to affine transformations of space. This means that the different ranges of the parameters have no influence on their depth. This makes it suitable for using the depth function for different applications in hydrological science. It is especially useful for identifying parameter space of any hydrological model, because each parameter of hydrological model has different scale and range.

Even after several experimental studies; it is still a mystery which depth measure is to be applied to which data sets, as one depth measure performs beautifully in two dimensions quickly becomes impractical as the dimensionality increases ([Hugg et al., 2006](#)). This is because computational demand can increase exponentially with increase in dimension. The half space depth function is more robust and computationally not expensive as shown by many authors, for example [Zuo and Serfling \(2000\)](#). It satisfies all the desired properties of the data depth function. Hence, in this research a half space depth function was used as a tool for different purposes, such as to identifying a set of good parameters and critical events and in the regionalization of model parameters.

The calculation of the half-space depth is computationally very expensive if the number of points in convex hull  $X$  is large or the dimension is high. Efficient algorithms are available for  $d = 2$  from [Miller et al. \(2003\)](#). In this research the approximate calculation suggested in [Rousseeuw and Struyf \(1998\)](#) was used.

## 4 Study Area and Hydrological Models

In hydrological modeling, it is very important to validate the developed methodology on different climatic conditions and catchment properties for generalization of the methodology. Therefore, four different regions - two in Germany, the United Kingdom and an Indian catchments were chosen for this research. The overview of the areas and models used in this research are presented in this chapter.

### 4.1 Study Area

#### 4.1.1 Upper Neckar catchment

The Upper Neckar basin is located in South-West Germany in the state of Baden-Württemberg. The region is flat, undulating in the east and north. The Black Forest and Swabian Alb are in the west and south. The 4000  $km^2$  large Upper Neckar basin was subdivided into 13 subcatchments (Figure 4.1).

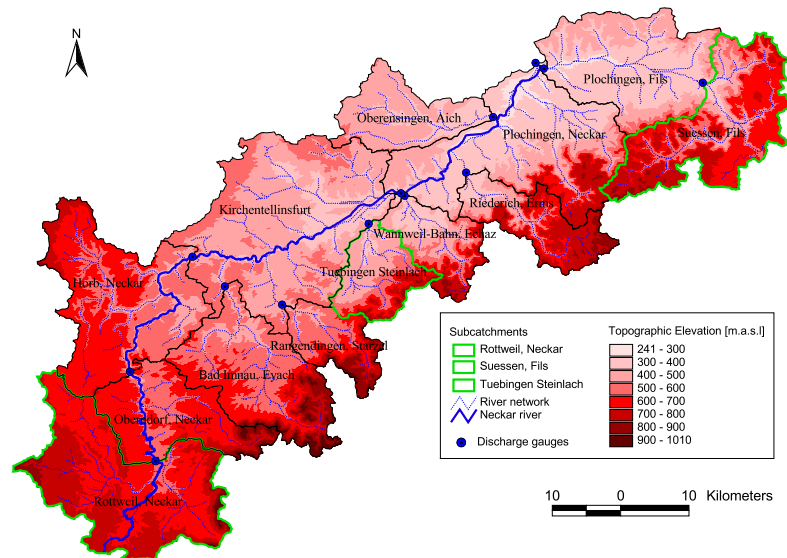


Figure 4.1: Study area: Upper Neckar catchment in South-West Germany

The study area elevation range is from 238 m a.s.l. to 1010 m a.s.l. The data set used in this research includes measurements of daily precipitation from 151 gauges and daily air temperature at 74 climatic stations. The meteorological input required for the

	Sub-catchment	Sub-catchment size ( $km^2$ )	Elevation ( $m$ )	Slope ( $degree$ )	Mean Dis-charge ( $m^3/s$ )	Annual Precipitation ( $mm$ )
1	Rottweil ( <i>Neckar</i> )	454.65	555-1010	0-34.2	5.1	968.16
2	Tübingen ( <i>Steinlach</i> )	140.21	340-880	0-38.8	1.7	849.84
3	Süssen ( <i>Fils</i> )	345.74	360-860	0-49.3	5.9	1003.45

**Table 4.1:** Summary of the size of the different subcatchments in Upper Neckar catchment

hydrological model was interpolated from the observations with External Drift Kriging (Ahmed and de Marsily, 1987) using topographical elevation as external drift. The mean annual precipitation is 908 mm/year. Land use is mainly agricultural in the lowlands and forested in the medium elevation ranges. Hydrological characteristics of the three selected subcatchments, which are used in this research, are given in table 4.1. For further details please refer to Samaniego (2003), Bárdossy et al. (2005), Hartmann (2007) and Singh (2010).

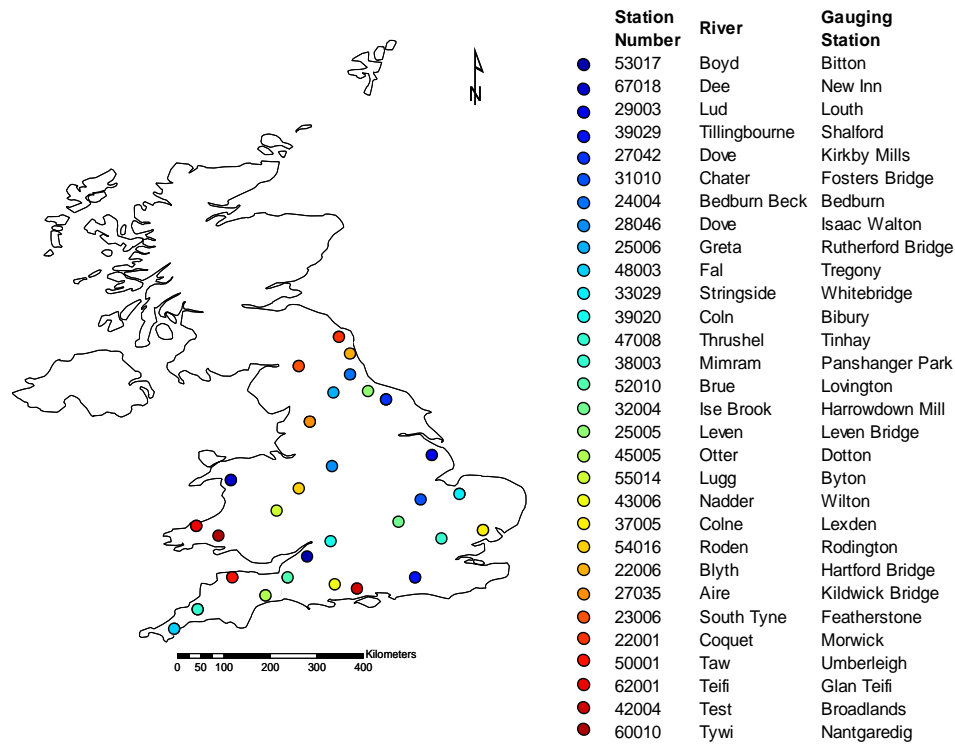
#### 4.1.2 United Kingdom catchments

The second study area for this research is located in the United Kingdom (UK). The eleven years (1980-1990) of data from 28 small to medium sized watersheds (50 to 1100  $km^2$ ) (Figure 4.2) are available for this research. The watersheds are located throughout England and Wales. Discharge and precipitation data were obtained from the Top-Down Working Group website (<http://www.tdwg.catchment.org/datasets.html>). The temperature data were provided by the British Atmospheric Data Center (<http://badc.nerc.ac.uk/home/index.html>). The overview of discharge precipitation and temperature for all the catchments is given in Table 4.4. The physical characteristics came from the National River Flow Archive (<http://www.nwl.ac.uk/ih/nrfa>) and the data CD of the Flood Estimation Handbook. Some of the catchments properties available and used in this research is given in Tables 4.2 and 4.3 An overview of the catchment can be found in (Yadav et al., 2007).

#### 4.1.3 Indian catchments

The third study area is located at the Kolar sub-basin of Narmada River in India. Temporal distribution of rainfall is highly skewed in in this catchments. Some rivers, particularly on the Indian peninsular are non-perennial and due to this, stream gauging is usually limited to the monsoon season only. The catchment has elevation varying from

#### 4 Study Area and Hydrological Models



Ref: Maitreya et. al.(2007), <http://www.nwl.ac.uk/ih/nrfa>

**Figure 4.2:** Study area: 28 catchments of England and Wales, UK

Characteristic	Unit	Description
AREA	km <sup>2</sup>	Watershed drainage area
BFIHOST		Base-flow index derived using HOST classification
DPSBAR	m/km	Index of watershed steepness
APSBAR		Index representing the dominant aspect of watershed slopes
APSVAR		Index representing the invariability of aspect of watershed slopes
RMED-1H	mm	Median annual maximum 1-hour precipitation
MED PERM		Percentage soil within watershed with medium/mixed permeability
LOW PERM		Percentage soil within watershed with low permeability

**Table 4.2:** Possible catchments properties from UK catchments (Yadav et al., 2007)



#### 4.1 Study Area

Cat. Nr.	AREA	BFIHOST	DPSBAR	APSBAR	APSVAR	RMED-1H	MOD PERM	LOW PERM
1	569.8	0.49	112.10	109.8	0.19	9.1	16.4	26.2
2	269.4	0.46	32.83	93.2	0.25	0.4	0.0	0.0
3	321.9	0.33	125.70	12.3	0.20	10.7	0.0	0.0
4	74.9	0.46	109.67	94.7	0.34	10.0	0.0	0.0
5	196.3	0.43	75.96	300.6	0.24	10.1	0.0	87.4
6	86.1	0.21	67.67	55.6	0.31	10.7	0.0	0.0
7	282.3	0.37	101.84	169.8	0.13	10.5	28.3	1.1
8	59.2	0.60	147.69	173.7	0.24	10.1	0.0	46.7
9	83.0	0.78	144.58	185.4	0.09	10.2	21.0	0.0
10	55.2	0.90	61.13	69.3	0.24	10.6	0.0	0.0
11	68.9	0.51	62.65	108.6	0.17	12.2	0.0	71.1
12	194.0	0.55	40.79	97.0	0.16	12.6	0.0	44.5
13	98.8	0.86	13.50	203.0	0.18	11.1	0.0	7.7
14	238.2	0.53	30.98	121.3	0.15	11.0	0.0	73.3
15	106.7	0.94	78.39	147.7	0.18	10.6	0.0	12.4
16	1040.0	0.90	50.10	176.0	0.15	10.6	0.1	3.1
17	220.6	0.81	80.13	125.0	0.15	10.9	25.5	13.2
18	202.5	0.54	85.00	195.0	0.11	11.4	31.7	40.6
19	112.7	0.39	91.19	227.2	0.17	12.0	0.0	100.0
20	87.0	0.69	80.74	242.4	0.15	11.8	0.0	76.9
21	826.2	0.42	106.94	219.9	0.07	11.9	2.3	95.4
22	135.2	0.47	72.51	218.3	0.17	10.7	12.8	44.3
23	47.9	0.46	64.00	270.1	0.24	10.8	4.3	84.1
24	259.0	0.61	22.76	119.3	0.11	9.4	0.0	73.2
25	203.3	0.67	161.66	122.8	0.19	9.8	0.0	83.7
26	1090.4	0.48	157.20	214.0	0.09	11.3	0.1	99.2
27	893.6	0.53	112.35	285.7	0.10	11.0	0.0	100.0
28	53.9	0.27	152.19	89.3	0.17	11.2	0.0	100.0

**Table 4.3:** *Different UK catchments and their properties*

300 m to 600 m. The Kolar basin is located in the latitude range of 22°40' to 23°08' and longitude 77°01' to 77°29'. The data availability in the catchment area is poor. The data from period 1983 to 1988 was available for this research. The catchment area of 820 sq. km up to the Satrana gauge and discharge measurement site has been used for this research. The index map of the basin showing the locations of gauge discharge and raingauge stations is given in Figure 4.3. The Kolar sub-basin has two distinct topographic zones. The upper four fifth part is predominantly covered by deciduous forest. The soils are skeleton to shallow in depth except near channels where they are relatively deep. The outcrops of weathered rocks are visible at many places. Crops are grown in large pockets in the north western part and in small pockets elsewhere. The general response of this part of basin appears to be quick. The lower part of the basin consisting of flat bottomed narrowing valley is predominantly cultivated. Here soils are deep and ground slopes are flat. The rainfall-runoff response of this part appears to be slow (Jain, 1990). The rainfall data at four stations was used to get a weighted average

#### 4 Study Area and Hydrological Models

Catchment. Nr.	Precipitation (mm)	Discharge (mm)
1	883.86	473.34
2	719.80	257.44
3	1507.61	1098.26
4	887.67	535.81
5	710.09	303.15
6	1283.20	862.15
7	1212.52	790.57
8	970.08	592.57
9	1147.49	803.03
10	690.30	296.98
11	657.82	249.00
12	662.04	230.61
13	643.99	160.55
14	597.85	151.39
15	824.70	409.13
16	773.64	297.84
17	865.43	398.76
18	980.911	467.08
19	1229.49	700.63
20	1271.71	721.05
21	1252.98	732.16
22	849.79	429.36
23	823.57	394.54
24	710.85	240.30
25	1042.32	630.95
26	1931.41	1162.38
27	1414.83	1028.51
28	2200.67	1870.39

**Table 4.4:** Annual mean discharge and precipitation for all UK catchments

#### 4.1 Study Area

daily rainfall for the basin. As seen from the Figure 4.3, the coverage of the rainfall stations is not uniform; there is no station in the northern part of the basin. The daily gauge and discharge data for monsoon season only was available at Satrana. The pan evaporation data for a station located near the basin in agricultural area was used. An overview of the catchments can be found in Jain (1990, 1993) and Singh et al. (2009).

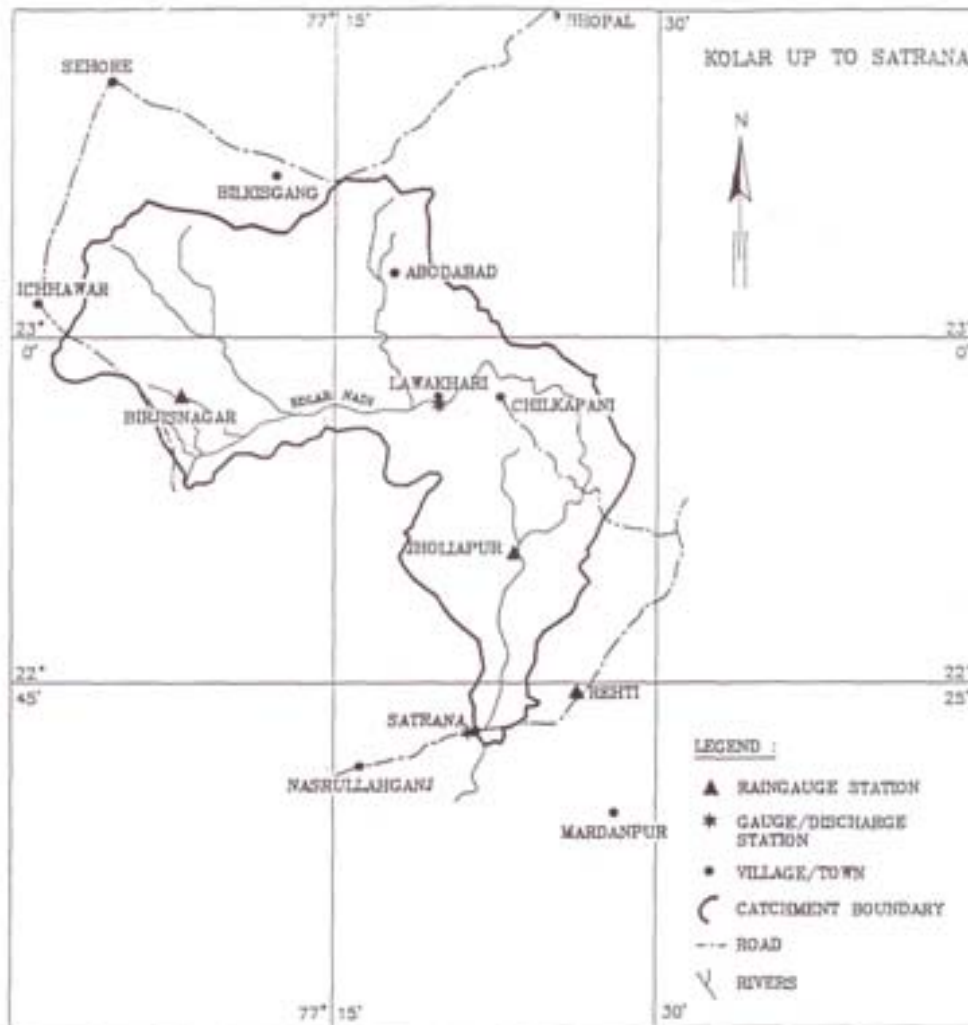
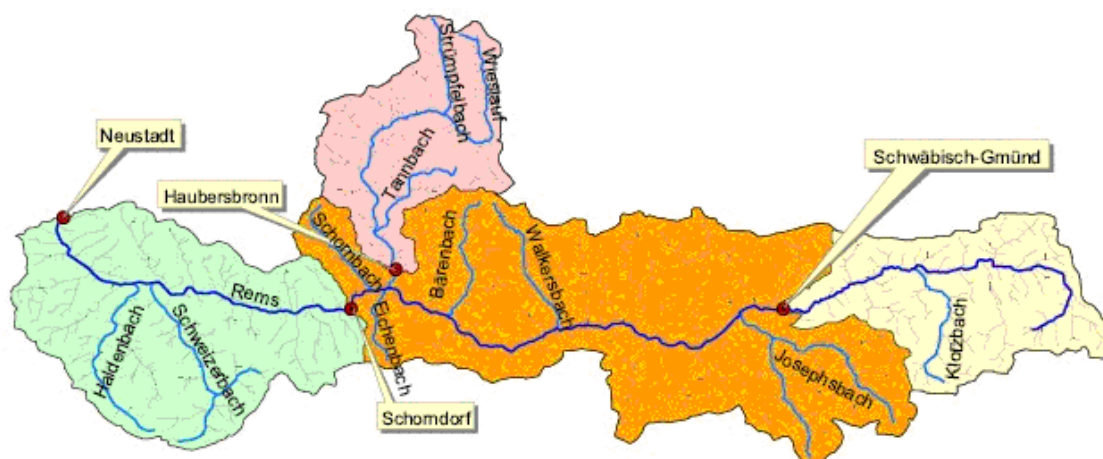


Figure 4.3: Index map of the Kolar basin

#### 4.1.4 Rems catchment

The fourth study area for this research is located in the south of Germany. The river Rems originates from Lutenburg near the city Aalen in Baden-Württemberg. It flows westwards to the river Neckar, of which it is the tributary. The catchment is about  $580 \text{ km}^2$ . The Rems catchment is composed of four subcatchments. Schwäbisch-Gmünd, Haubersbronn, Schorndorf and Neustadt (fig. 4.4). The data vaibility of this catchment is good. The hydrological and meteorological data series include discharges, precipitation, temperature, vapor pressure, humidity, wind speed, sunshine duration, snow depth, etc. The data was available in daily resolution for this research work.



**Figure 4.4:** Rems catchment in southern Germany and its subcatchments (Thapa, 2009)

Thapa (2009); Liang (2010); Liang et al. (2010) have done a simple assessment of the precipitation pattern in the Rems catchment by calculating the monthly and yearly average precipitation among the stations with 100 % observation from the period of 1990 to 2005. It is shown in figure 4.5 and 4.6. It can be seen that summer precipitation was generally higher than that of winter, July was observed to have the highest monthly precipitation while April the lowest. The yearly precipitation can differ from  $600 \text{ mm}$  to nearly  $1200 \text{ mm}$ . Similarly, the discharge pattern of the 4 subcatchments was analyzed in the same way. For the discharge gauge Schorndorf and Haubersbronn, the data of 1994 and 1995 were incomplete, and the yearly average was not calculated. So was in the case of Schwäbisch-Gmünd in 1995. The monthly average was considered within the years of full monthly data. Figure 4.7 and 4.8 shows the discharge characteristics of the Rems catchments. It can be observed that these four gauges perform similarly overall in the behavior of monthly average discharge. Higher monthly discharges occur in winter, from November to March, and the lowest appear in August and September. The yearly average discharges of Schwäbisch-Gmünd and Haubersbronn don't change much, even though with a similar fluctuation as the other 2 gauges. In the outlet of the whole catchment, Neustadt, the yearly average discharge can vary from  $4 \text{ m}^3/\text{s}$  to

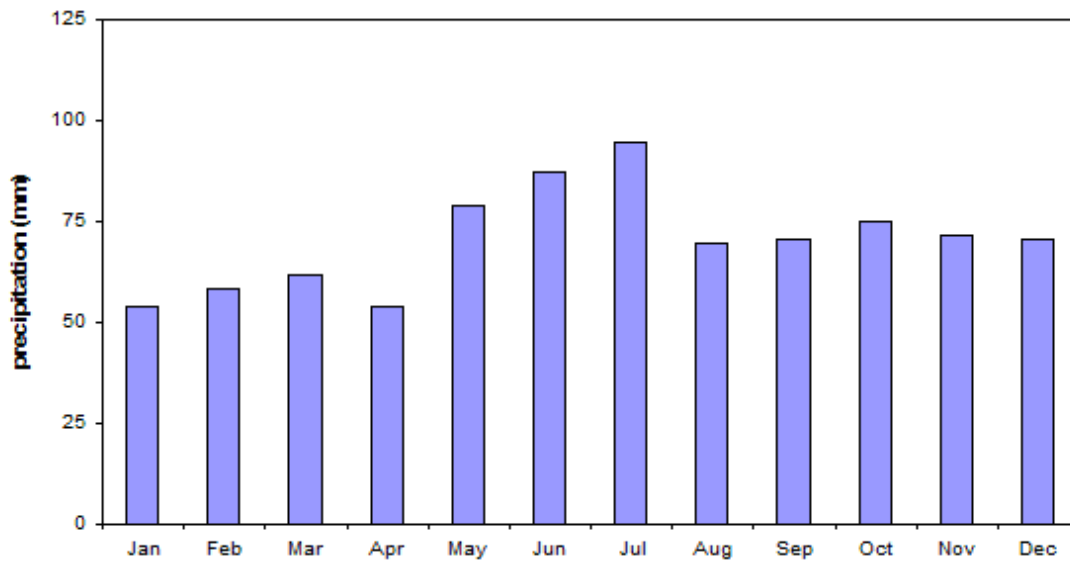


Figure 4.5: Monthly mean precipitation 1990-2005 for Rems catchments (stations with 100 % observation)

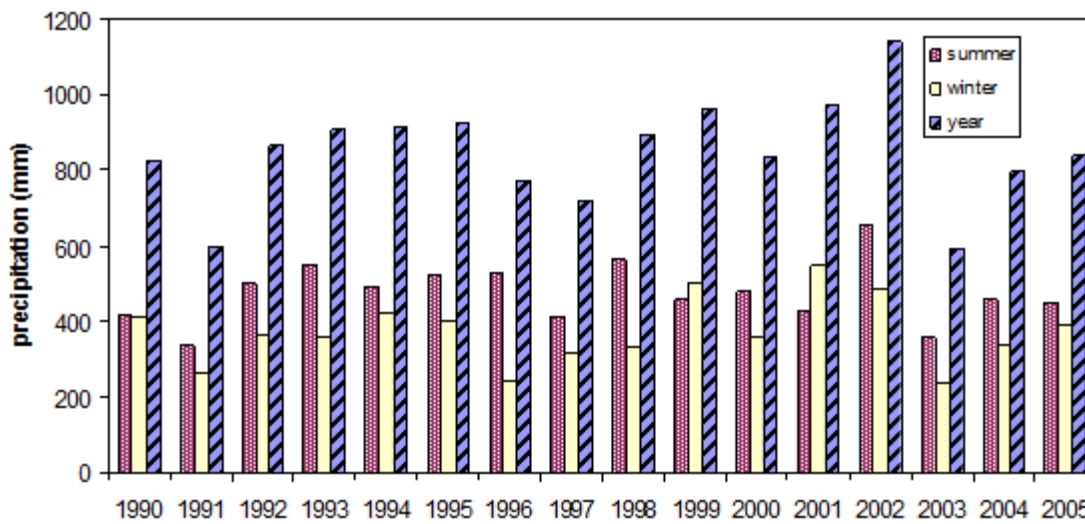


Figure 4.6: Annual average precipitation for Rems catchments (stations with 100 % observation)

4 Study Area and Hydrological Models

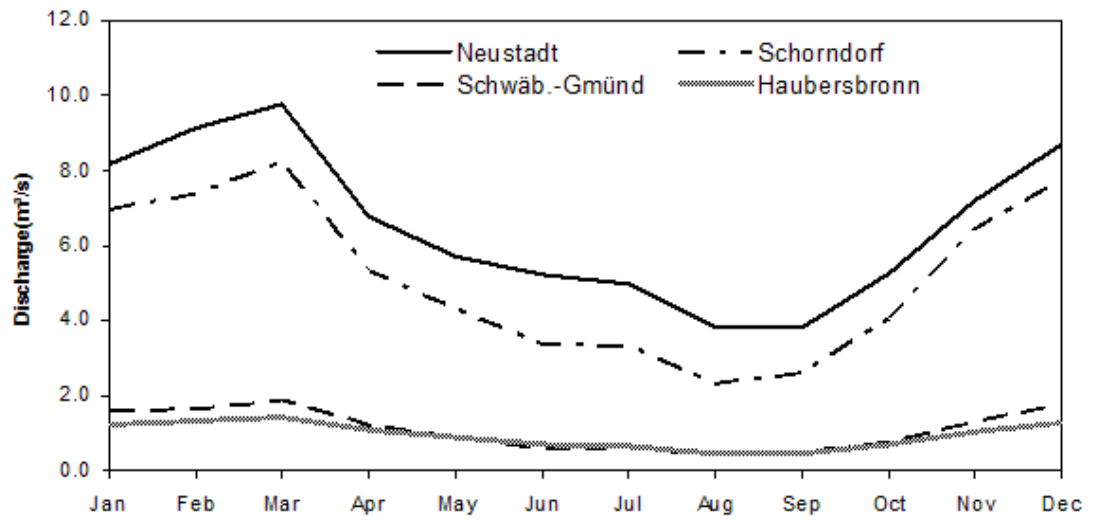


Figure 4.7: Monthly average discharge (1900-2005) for Rems catchments

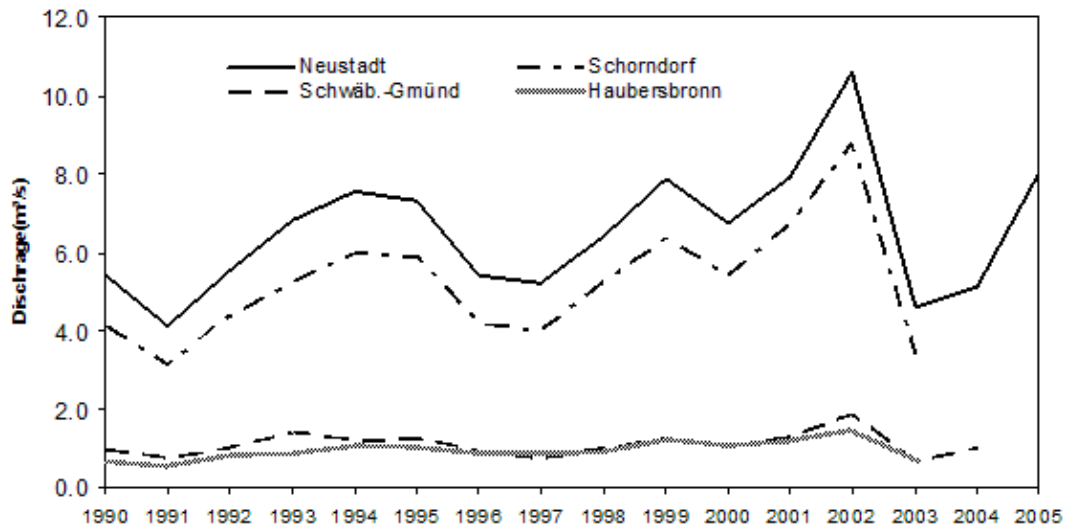


Figure 4.8: Annual average discharge for Rems catchments

11  $m^3/s$ . The overall hydrological characteristics of these subcatchments are shown in Table 4.5. Schwäbisch-Gmünd and Haubersbronn are gauges in the upper catchment, having a smaller drainage area, which corresponds to a much lower flow over whole year. Neustadt has the smallest slope and highest mean annual flow. For more details about the catchments, refer to [Thapa \(2009\)](#) and [Liang \(2010\)](#).

	Subcatchment size ( $km^2$ )	Elevation (m)	Slope ( <i>degree</i> )	Mean annual flow ( $m^3/s$ )	Mean annual precipitation (mm)	Mean annual temperature ( <i>degree C</i> )
Schwäbisch-Gmünd	92	331-768	0-31.34	1.15	1117.12	8.6
Haubersbronn	76	258-578	0-26.61	0.91	1050.23	9.3
Schorndorf	246	246-796	0-34.37	5.14	1076.11	9.4
Neustadt	149	231-531	0-24.56	6.54	913.10	10.2
Whole catchment	563	231-796	0-34.37	6.54	1036.03	9.5

**Table 4.5:** Summary of the basic characteristics of Rems catchment

## 4.2 Models

In this research, three conceptual and one physically based hydrological models were used. These models have different level of complexity in conceptualization and parameterization. These models have been used at different corners of the world.

### 4.2.1 HBV

The modified version of the conceptual HBV model was used for this research (Figure 4.9). The HBV model concept was developed by the Swedish Meteorological and Hydrological Institute (SMHI) in the early 1970's. It has been modified at the Institut für Wasserbau, Universität Stuttgart. It includes conceptual routines for calculating snow accumulation and melt, soil moisture and runoff generation, runoff concentration within the subcatchment, and flood routing of the discharge in the river network. The snow routine uses the degree-day approach as set out in Eq. 4.1 and Eq. 4.2. Soil moisture is calculated by balancing precipitation and evapotranspiration using field capacity and permanent wilting point as parameters, described by Eq. 4.3 to Eq. 4.5. The model structure is shown in Figure 4.9.

$$MELT = DD \cdot (T - T_{crit}); \text{ If } (T > T_{crit}) \quad (4.1)$$

$$DD = Dew + k \cdot P \quad (4.2)$$

#### 4 Study Area and Hydrological Models

$$P_{eff} = (SM/FC)^\beta \cdot P + MELT \quad (4.3)$$

Where  $P_{eff}$  is the effective precipitation,  $SM$  is the actual soil-moisture,  $FC$  is the maximum soil storage capacity,  $\beta$  is a model parameter (shape coefficient),  $P$  is the depth of daily precipitation,  $MELT$  is the amount of snow melt,  $DD$  is degree day factor,  $T$  is the mean daily air temperature,  $T_{crit}$  is threshold temperature,  $DD_0$  is degree day factor when there is no rainfall and  $k$  is a positive number.

$$PE_a = (1 + C \cdot (T - T_m)) \cdot PE_m \quad (4.4)$$

Where  $PE_a$  is the adjusted potential evapotranspiration,  $C$  is a model parameter,  $T$  is the mean daily air temperature,  $T_m$  is the long term mean monthly air temperature and  $PE_m$  is the long term mean monthly potential evapotranspiration.

$$E_a = (SM/PWP) \cdot PE_a \quad (4.5)$$

Where  $E_a$  is the actual evapotranspiration,  $SM$  is the actual soil-moisture and  $PWP$  is limiting soil-moisture at which potential evapotranspiration take place. Runoff generation is simulated by a non-linear function of the actual soil moisture and precipitation. The runoff concentration is modeled by two parallel nonlinear reservoirs representing the direct discharge and the groundwater response. Flood routing between the river network nodes uses the Muskingum method. Additional information about the HBV model in general can be found in [Hundecha and Bárdossy \(2004\)](#), and [Bergström \(1995\)](#). Direct runoff and percolation from each subcatchment are calculated using Eq. 4.6 to Eq. 4.10.

$$Q_0 = k_0 \cdot (S_1 - L) \quad (4.6)$$

$$Q_1 = k_1 \cdot S_1 \quad (4.7)$$

$$Q_{perc} = k_{perc} \cdot S_1 \quad (4.8)$$

$$Q_2 = k_2 \cdot S_2 \quad (4.9)$$

Here  $Q_0$  is near surface flow,  $Q_1$  is interflow,  $Q_{perc}$  is percolation,  $Q_2$  is baseflow,  $k_0$  is the near surface flow storage constant,  $k_1$  is the interflow storage constant,  $k_{perc}$  is the percolation storage constant,  $k_2$  is the baseflow storage constant,  $S_1$  is upper reservoir water level,  $S_2$  is lower reservoir water level,  $L$  is threshold water level for near surface flow. The total runoff is computed as the sum of the outflows from the upper and lower reservoirs. The total flow is then smoothed using a transformation function, consisting of a triangular weighing function with one free parameter, *MAXBAS*.

$$Q = g(t, MAXBAS) \cdot (Q_0 + Q_1 + Q_2) \quad (4.10)$$

Where  $Q$  is the current overall discharge and *MAXBAS* is the duration of the triangular weighting function (Unit Hydrograph). There are 15 parameters to describe the model, out of which 9 parameters are used for calibration in this research (table 4.6).



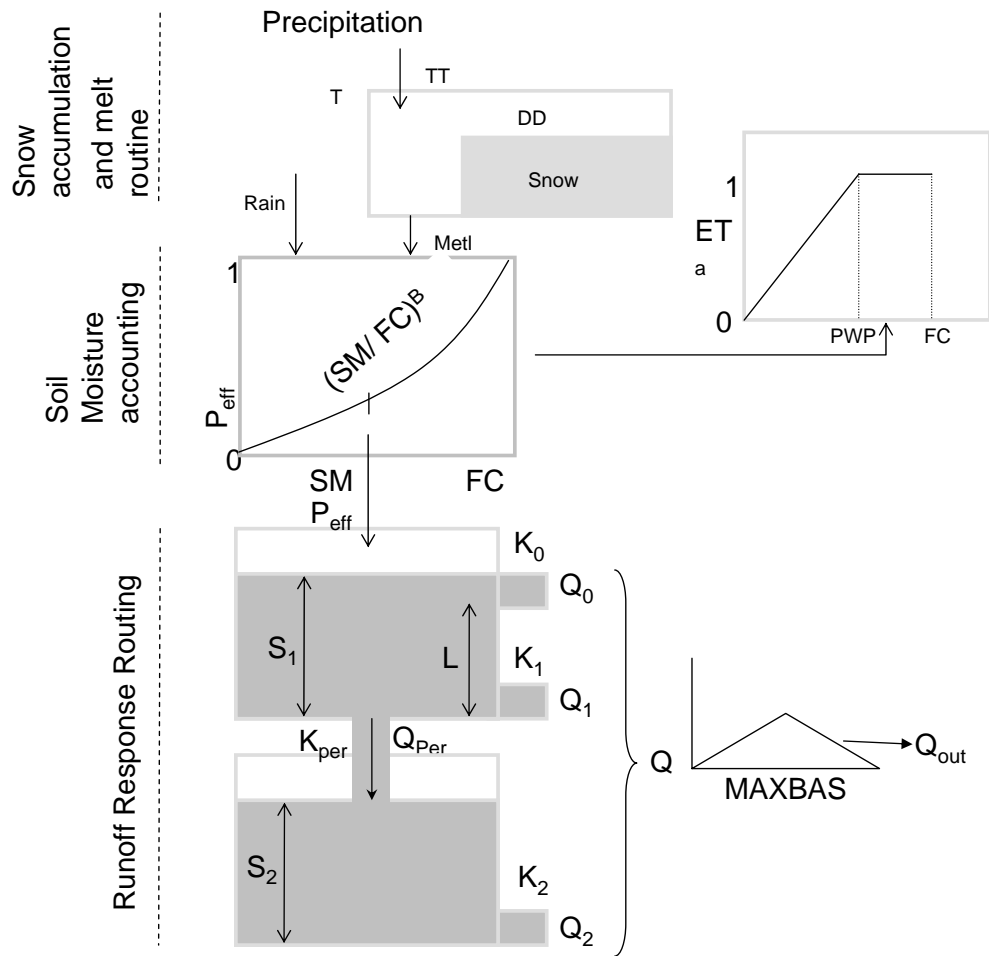


Figure 4.9: Schematic representation of the HBV model

Parameter	Description	Max	Min
$T_{crit}$	Threshold temperature for snow melt initiation	2	-2
$DD$	Degree-day factor	5	0.5
$Dew$	Precipitation/degree-day relation	2	0
$\beta$	Model parameter (shape coefficient)	6	1
$L$	Threshold water level for near surface flow	30	1
$k_0$	Near surface flow storage constant	20	0.5
$k_1$	Interflow storage constant	50	5
$k_{perc}$	Percolation storage constant	100	20
$k_2$	Baseflow storage constant	1000	10

Table 4.6: Model parameters range for HBV model

### 4.2.2 HYMOD

HYMOD is a simple conceptual model. This model has two main components, namely the rainfall excess (two parameters) and two series of linear reservoirs (three parameters, three identical quick and single for the slow response) in parallel as routing components. The model is based on the characteristics of the runoff production process at a point in a catchment and then a probability distribution which describes the spatial variation in the catchments is derived by algebraic expression (Moore, 1985). This model makes an assumption that the soil structure and texture, water storage capacity vary across the catchment, therefore, the distribution function of different storage capacity is described as

$$F(C) = 1 - (C/C_{max})^\beta \quad 0 \leq C \leq C_{max} \quad (4.11)$$

The model structure is shown in Figure 4.10. The five parameters of this model are: the maximum storage capacity in the catchment ( $C_{max}$ ), the degree of spatial variability of the soil moisture capacity within the catchment ( $\beta$ ), the factor distributing the flow between the two series of reservoirs ( $\alpha$ ), and the residence times of the linear reservoirs ( $R_q$ ) and ( $R_s$ ). Additional information about the HYMOD model in general can be found in Moore (1985), Boyle et al. (2001) and Wagener et al. (2001). In this research, the HYMOD model was modified by adding snow routing. The degree day method was used to calculate snow accumulation and snow melt. The range of parameters is given in Table 4.7.

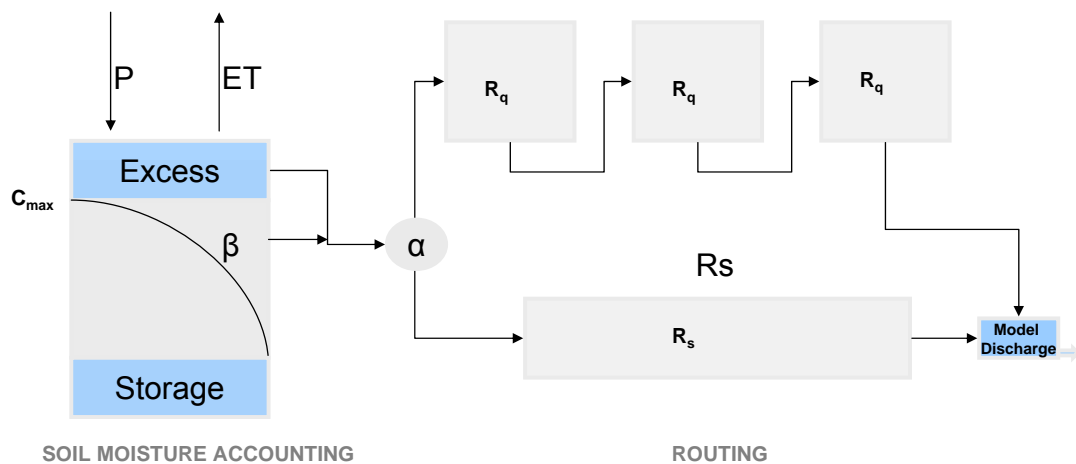


Figure 4.10: Schematic representation of the HYMOD model

Parameter	Description	Max	Min
$C_{max}$	Maximum storage capacity	600.000	150.000
Beta	Degree of spatial variability of the soil moisture capacity	8.000	3.000
Alpha	Flow distributing factor	0.800	0.200
$R_S$	Residence times of the slow reservoirs	0.200	0.010
$R_Q$	Residence times of the quick reservoirs	0.700	0.300
Th	Threshold temperature for snow melt initiation	1.500	-1.000
DD	Degree-day factor	3.000	1.000
Dew	Precipitation/degree-day relation	2.000	0.000

**Table 4.7:** Model parameters range for the HYMOD

### 4.2.3 Three reservoirs model

The conceptual three reservoirs model was developed by Jain (1993). The concept of the model described by Jain (1993) and Singh et al. (2009), is given here. In this model, rainfall-runoff process is conceptualized by three reservoirs. The catchment is represented with the help of three storages. The first storage, termed as surface storage, represents the water stored in the surface and top few centimeters of soil of the catchment. It has a maximum storage capacity given by  $S_{max}$ . The second storage represents the catchment soil moisture storage and has a maximum water holding capacity given by  $C_{max}$ . The third storage represents the ground water storage. The possible range of model parameters is given in Table 4.8.

Parameters	Description	Maximum	Minimum	Unit
$S_{max}$	Maximum storage capacity	500	5	mm
$C_{max}$	Maximum water holding capacity	1500	15	mm
F(C)	Threshold	0.90	0.1	-
$F_{inf}$	Factor	0.99	0.001	-
$C_{int}$	Coefficient	0.99	0.001	-

**Table 4.8:** The possible range of the three reservoirs model parameters

The rainfall is input to the surface storage. The water leaves this storage through evaporation, infiltration or overland flow. The moisture content of this storage at any time is denoted by SURF. So as long as  $SURF > E_p * dt$  ( $E_p$  is potential evaporation in mm/hr), the actual evapotranspiration (ET) is at the potential rate, else ET takes place at the lower storage at some lesser rate. If SURF = 0, the ET commences from the soil storage at a rate of  $E_a$  (mm/hr) given by

$$E_a = \frac{C_{soil}}{C_{max}} * E_p \quad (4.12)$$

#### 4 Study Area and Hydrological Models

$$C_{soil} = C_{soil} - E_p * dt$$

If  $SURF < E_p * dt$ , the actual ET is  $SURF + E_a * dt$  where  $E_a$  is calculated using Eq. 4.12 and  $dt$  is length of computation interval in hour. The maximum value of  $E_a$  is  $E_p$ . Infiltration of water from the surface storage to the soil storage takes place at the rate Infil:

$$Infil = \left(1 - \frac{C_{soil}}{C_{max}}\right) * F_{inf} \text{ if } SURF > 0 \quad (4.13)$$

$$= 0 \text{ otherwise}$$

$$C_{soil} = C_{soil} + Infil * dt$$

where  $F_{inf}$  is a factor (mm/hr) controlling the infiltration rate. If  $SURF > S_{max}$ , the excess water over  $S_{max}$  flows as overland flow (OF). The OF is routed through a linear reservoir LR1 with time constant  $K_1$ . Water infiltrating from the surface storage enters the soil storage from which outflow this storage can take place through evapotranspiration losses, interflow or recharge to the ground water zone.

If the contents of soil storage are greater than a threshold denoted by FC, moisture flows out of it as interflow and recharge to groundwater. The excess moisture available for these two is:

$$Exw = \left(\frac{C_{soil}}{C_{max}} - FC\right) * Ewf \text{ if } \frac{C_{soil}}{C_{max}} > FC \quad (4.14)$$

$$C_{soil} = C_{soil} - Exw * dt$$

where  $Ewf$  is a factor (mm/hr) controlling the volume of excess water. The interflow rate is given as :

$$IntF = Exw * C_{int} \quad (4.15)$$

and the rate of recharge to groundwater is

$$RR = Exw * (1 - C_{int}) \quad (4.16)$$

where  $C_{int}$  is a dimensionless coefficient which controls how much of the excess moisture goes as recharge and how much as interflow. The interflow is routed through a linear reservoir LR2 with time constant  $K_2$ . The ground water zone behaves as a linear reservoir whose time constant is KG. The moisture comes out of it as the baseflow (BF).

The flow coming out of the reservoirs LR1, LR2 and LR3 is combined and then routed through a linear reservoir, LR4, to yield the discharge from the catchment, denoted by Qt. The systematic representation of the model structure is given in Figure 4.11.

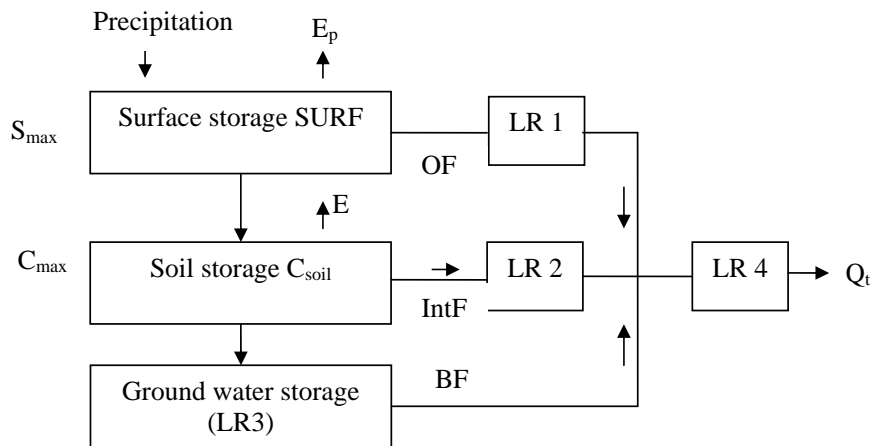


**Figure 4.11:** Structure of the three reservoirs model (Jain, 1993)

#### 4.2.4 Water Flow Balance Simulation Model-WaSiM-ETH

WaSiM-ETH is a physically grid-based and spatially distributed model. Spatial and temporal variability of hydrological process in a complex watershed can be represented by this model (Schulla and Jasper, 2007). This is kind of a physically-based model, where data requirement is low. It consists of several modules: For example, a module for correction and interpolation of meteorological data, evapotranspiration model, snow model, interception model, infiltration model, soil model, discharge routing model, groundwater model, irrigation model and transport model. To conceptualize some modules, several alternative are available. For instance, inverse-distance-weighting method or altitude dependent regression method can be chosen for interpolation of meteorological data. Similarly, for the calculation of potential evapotranspiration, Penman-Monteith approach, Wendling approach and Hamon approach can be chosen. WaSiM-ETH has two versions, namely TOPMODEL approach after Beven and Kirkby (1979) in the soil model, and secondly the RICHARDS equation for describing the water flow within the unsaturated soil. In this research the TOPMODEL approach is used. The model structure is shown in figure 4.12.

The basic input required in WaSiM-ETH is given in table 4.9, which includes both spatial and temporal data. Some of the input data needed to be preprocessed. There are several tools available e.g. TANALYS (Terrain Analysis). For more details about WaSiM-ETH, refer to Thapa (2009); Liang (2010) and Schulla and Jasper (2007).

4 Study Area and Hydrological Models

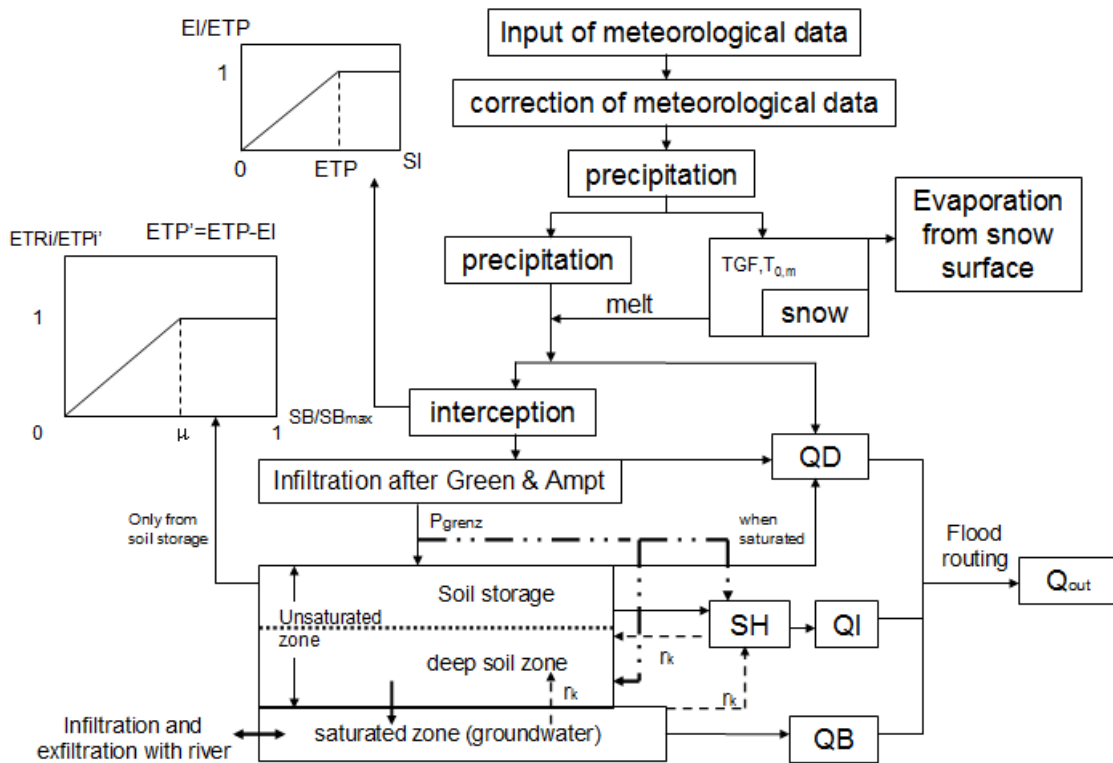


Figure 4.12: Structure of WaSiM-ETH using TOPMODEL approach (Liang, 2010)

	Categories	Subcategories
Spatial	DEM	Slope, watershed, flowtime, routing parameters, exposition . . .
	Land use	Albedo, leaf area index, vegetation, root depth
	Soil properties	Field capacity, saturated hydraulic conductivity, drainable porosity, soil topographic index, suction head
Temporal	Meteorological data	Precipitation, temperature, global radiation, relative sunshine duration, wind speed, humidity
	Hydrological data	Subcatchments runoff

Table 4.9: Input data for WaSiM-ETH model

# 5 Robust Estimation of Hydrological Model Parameters

## 5.1 Introduction

It is always a dream of a hydrologist to model the mystery of complex hydrological process in a precise way. A simple hydrological model can describe Nature in a simple way if it is parameterized correctly or perfectly. As we can see from Chapter 2, the parameter estimation of a hydrological model is a very difficult task.

The purpose of this chapter is to investigate the reasons that lead to very different near optimum parameter vectors and to investigate the properties of the set of good parameters in high dimensional spaces. The goal is not to find the parameter vectors which perform best for the calibration period but to find parameter vectors which:

1. Lead to good model performance over the selected time period
2. Lead to a hydrologically reasonable representation of the corresponding process
3. Are not sensitive: small changes of the parameters should not lead to very different results
4. Are transferable: they perform well for other time periods and might also perform well on other catchments (i.e they can be regionalized)

Concepts of computer geometry and multivariate statistics are used to identify the set of good parameters. Specifically, in this study convex sets and the depth function defined in chapter 3 were used.

## 5.2 The Effect of Observation Errors

In rainfall-runoff modeling, input errors play a crucial role but the problem of input errors is generally neglected by hydrologists (Paturel et al., 1995). Hydrological models use observation data for the identification of model parameters. Unfortunately, many of the hydrological observations contain partly systematic and partly random errors. Precipitation is measured at a few selected locations and typically interpolated for the catchment area. Thus, precipitation values used in the model can be wrong due to measurement (for example caused by evaporation or wind) and to interpolation errors. The impact due to error in precipitation has been investigated by Ibbitt (1972), Troutman

(1985), Paturel et al. (1995), Andréassian et al. (2001) and Oudin et al. (2006), who found that error in precipitation had significant influence on model performance.

The observed discharge was used as the main calibration quantity, thus their errors may have had significant influence on the model performance. In most cases water levels are observed and rating curves are used to transform them to discharges. This is an important source of partly systematic errors and, when combined with other errors, compromise the identification of the model parameters.

The parameter vectors obtained by model parameter optimization algorithms are optimal with respect to an erratic objective function. Measurement errors and errors due to model structure are mixed (Todini, 2007) and cannot be separated directly. The following examples illustrate the effect of observation uncertainty on parameter estimation.

Firstly, let us consider the observed meteorological variables and discharge. We assume that due to measurement errors the accuracy of the measured discharge  $Q_M(t)$  is  $q$  %. Thus, the real but unknown discharge  $Q_E(t)$  can be written as:

$$Q_E(t) = Q_M(t)(1 + \varepsilon_Q(t)) \quad (5.1)$$

with  $\varepsilon_Q(t)$  being a random error. This random error is due to uncertainties of the rating curve, non-uniqueness of the stage discharge relationship, changes of the cross section etc. Here we assume that the error follows a normal distribution  $N(0, \frac{q}{100})$ . This means we assume a constant relative random error and further, that the errors are independent (error dependence would increase the effect of observation uncertainty).

To quantify the effect of the flow error on model performance, a set of  $M = 100$  realizations of  $Q_E(t)$  was generated with  $q = 5$ . Note that the rating curve related errors are usually higher than this, especially in the case of extreme flows. Consequently the parameters of the hydrological model were estimated using simulated annealing by maximizing the Nash-Sutcliffe coefficient as if each parameter vector  $Q_E$  was the observed series. The model parameters obtained show a considerable scatter. For example in two dimensions, Figure 5.1 shows the scatter plot for the selected model parameters  $L$  and  $k_1$ , where  $M = 20$ .

The uncertainty of the estimated model parameters with respect to input error structure can also be investigated. With respect to temperature observations one can assume that the real but unknown temperature  $T_E(t)$  can be written as:

$$T_E(t) = T_I(t) + \varepsilon_T(t) \quad (5.2)$$

In this case an additive error of the catchment mean temperature was assumed. As in the previous case,  $M$  realizations were generated and model parameters were optimized for each of the series separately.

Tables 5.1 and 5.2 show the effect of observation error on the Nash-Sutcliffe coefficient for both discharge and temperature measurement errors, respectively. The uncertainty of model parameters with respect to precipitation uncertainty can be considerable, depending on the density of the observation network. This problem was investigated by Das (2006).



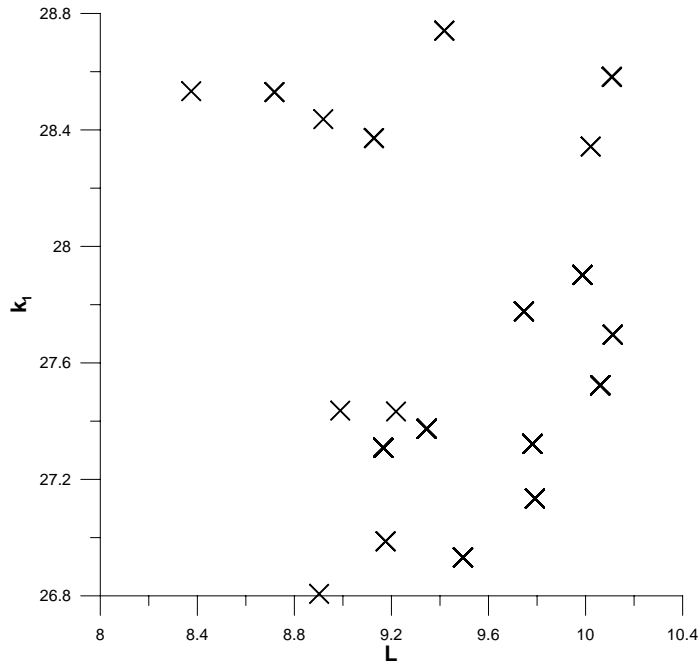


**Figure 5.1:** Scatter plot of the model parameters obtained by optimization using random discharge errors

Catchments	Mean NS	Median NS	Max NS	Min NS	Standard deviation
Rottweil	0.699	0.698	0.733	0.675	0.0123
Tübingen	0.716	0.716	0.733	0.703	0.0054
Süssen	0.751	0.751	0.775	0.733	0.0083

**Table 5.1:** Model performance for the observed series using optimal parameters obtained using 100 randomly perturbed discharge data sequences

Catchments	Mean NS	Median NS	Max NS	Min NS	Standard deviation
Rottweil	0.690	0.691	0.723	0.650	0.014
Tübingen	0.722	0.723	0.740	0.706	0.0062
Süssen	0.750	0.750	0.777	0.719	0.0121

**Table 5.2:** Model performance for the observed series using optimal parameters obtained using 100 randomly perturbed temperature data sequences

These examples show that model parameters and model performance are highly influenced by measurement errors. Two parameter vectors, with model performances differing in the range of the measurement error, caused fluctuations of the Nash-Sutcliffe value which cannot be distinguished from each other. Either of them might lead to a better description of the hydrological system. The parameters obtained by sophisticated optimization procedures might thus be suboptimal in reality. Thus, it is reasonable to investigate the set of parameters which gives similar performance as the numerical optimum. These parameters will be called *good parameters* in the subsequent sections.

### 5.3 Geometrical Structure of the Good Parameter Set

One of the major problems is that there is a large number of parameter vectors which perform nearly equally well. It is difficult then, to decide which of these should be taken for prediction. Scatter plots showing model performances as a function of individual parameters indicate that a wide range of parameter values can lead to good model performance. At present it seems impossible to know *a priori* if a fitted given parameter vector leads to good or bad performance when applied to a model. In Bárdossy (2007), the geometrical structure of the best performing parameters of the unit hydrograph (impulse response function) of the Nash cascade were investigated. It was shown that the set has a very clear geometrical structure. In this study, models with many more than two parameters are considered. It is difficult to visualise the subset of best parameters in higher dimensions; instead methods of computational geometry are used herein. In order to investigate the properties of the set of good parameter vectors, the concept of data depth was used.

#### 5.3.1 Data depth of the good parameter set

In order to explore the set of reasonably performing parameter vectors using the above introduced concept, nine parameters of the HBV model were considered. The parameter ranges used for the initial Monte Carlo simulation for the subcatchment Rottweil (Neckar) is given in Table 5.3.  $N$  random parameter vectors were generated in a rectangle bounded by reasonable limits in the  $d = 9$  dimensional space. For each of these parameter vectors the hydrological model was applied and the performance was calculated. This set of parameter vectors is denoted as  $X_N$ . A subset  $X_N^* \subset X_N$  of the best performing parameter vectors (in our case we chose the upper 10 %) were identified. The depth of each point in  $X_N$  with respect to  $X_N^*$  was calculated. Figure 5.2 shows the histogram of the performance of the hydrological model for the points  $\theta \in X_N$  with depth  $D(\theta) > L$ . One can see that all points with high depth (being in the geometrical interior of the set  $X_N$ ) lead to good model performance. The reason for this is that one assumes that the low depth points can be regarded as an iso-hypersurface corresponding to the selected level. If one assumes continuity of the objective function then higher values of the function are expected in the interior of the set.

In order to check this statement an independent second set  $Y_N$  of  $N$  random parameter

### 5.3 Geometrical Structure of the Good Parameter Set

Parameter	Description	Iteration 1		Iteration 4	
		Min	Max	Min	Max
$T_{crit}$	Threshold temperature for snow melt initiation	-1.50	2.50	-0.16	0.42
$DD$	Degree-day factor	0.12	2.12	1.30	2.11
$Dew$	Precipitation/degree-day relation	0.01	1.09	0.287	1.06
$\beta$	Model parameter (shape coefficient)	0.01	2.01	0.81	1.08
$L$	Threshold water level for near surface flow	8.30	10.29	8.419	10.28
$K_0$	Near surface flow storage constant	0.77	2.77	1.75	2.68
$K_1$	Interflow storage constant	26.80	28.81	26.82	28.62
$K_{per}$	Percolation storage constant	19.98	21.98	20.05	21.94
$K_2$	Baseflow storage constant	36.80	38.79	36.83	38.72

**Table 5.3:** Model parameters range for Rottweil (Neckar) catchment

vectors were generated. The depth of the points of  $Y_N$  with respect to  $X_N^*$  was calculated. For all parameters  $\theta \in Y_N$ , the hydrological model was run and the performances calculated. The results are evaluated for parameters such that  $D(\theta) \geq L$ , exemplified in Table 5.4 with the statistics of the performances. One can see that the randomly generated parameter vectors which possess high depth have good model performance. The standard deviation of the performance decreases with increasing depth, showing that in the *deep* interior of the set all parameter vectors perform similarly. These results show that for this case one can geometrically identify parameter vectors which are good. Note that even if the best performance is related to the deepest subset, this is not necessarily always the case, since the global optimum might itself correspond to a low depth.

Depth	Number of points	Mean NS	Standard deviation
-	10000	0.3132	0.6766
$\geq 1$	1743	0.6720	0.0198
$\geq 10$	893	0.6839	0.0135
$\geq 50$	182	0.6931	0.0090
$> 100$	33	0.6971	0.0069

**Table 5.4:** Model performance for the  $N = 10000$  random parameter sets with respect to the data depth calculated on the basis of the points selected corresponding to the upper 10 % performance

#### 5.3.2 Transferability

In order to investigate the transferability of the parameters with respect to their depth, two experiments were carried out.

As a first test the total observation period of 30 years was divided into three 10 year periods. The hydrologic characteristics of the three time periods are listed in Table 5.5.

## 5 Robust Estimation of Hydrological Model Parameters

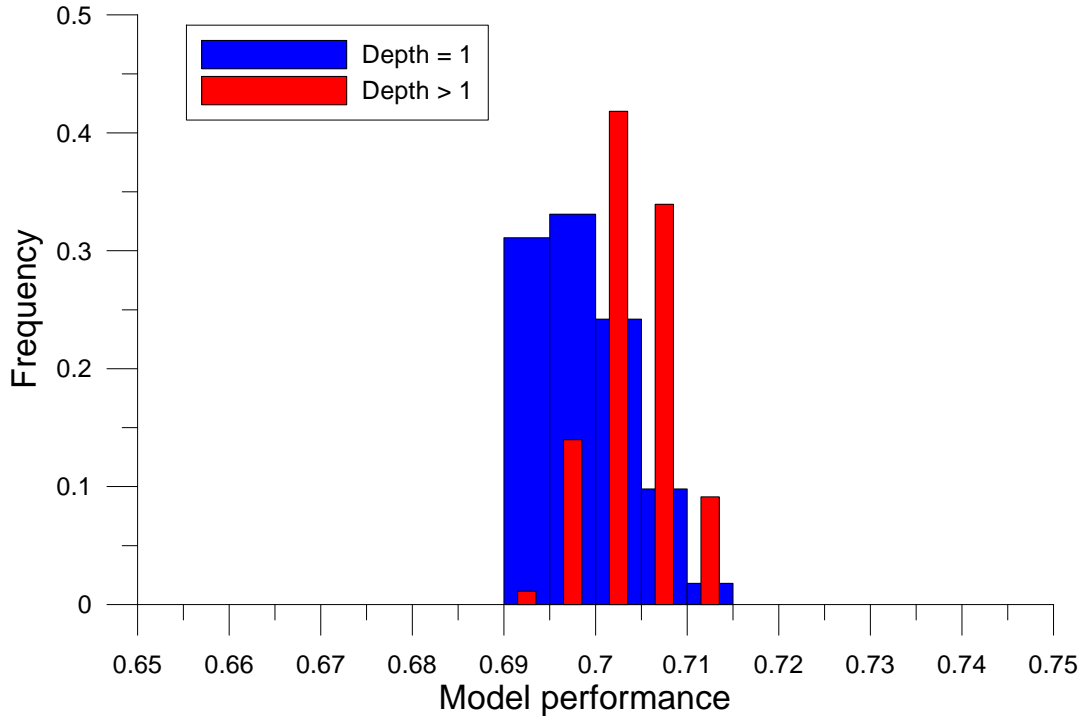


**Figure 5.2:** *The performance of the model using different depth*

The model performance was calculated for each time period. The set of good parameter vectors was identified for each time period separately and the depth of each parameter with respect to this set was calculated. In this way, three depth values were assigned to each parameter vector.

Subcatchment	Rottweil (Neckar)		Tübingen (Steinlach)		Süssen (Fils)	
Time period	Annual Precipitation ( <i>mm</i> )	Annual Discharge ( <i>mm</i> )	Annual Precipitation ( <i>mm</i> )	Annual Discharge ( <i>mm</i> )	Annual Precipitation ( <i>mm</i> )	Annual Discharge ( <i>mm</i> )
1961-1970	997.53	375.26	851.84	400.36	1007.94	575.55
1971-1980	908.48	309.36	808.14	366.62	960.02	512.62
1981-1990	997.21	385.66	888.84	404.86	1041.72	541.81

**Table 5.5:** *Runoff characteristics for different time periods*

The sets with the 50 and 150 deepest parameter vectors were identified for each time period. The intersection of the convex sets corresponding to the 50 deepest points consisted of 36 for the 150 point set 84 points indicating that depth is stable over all time periods. Note that a parameter vector was considered to be in the intersection if it had positive depth with respect the sets considered. As a set of 10000 points were considered, an independent selection of two sets with 150 points would have led with

### 5.3 Geometrical Structure of the Good Parameter Set

high probability to there being no points in the intersection. This means that parameters with large depth are robust with respect to the selected time period.

As a second test, the parameters with greater depth for one time period were used for another time period and their performance was calculated. In Table 5.6, the results of the transferred model quality with respect to the depth corresponding to the time period 1961-1970 are shown. Note that the subset of the boundary points was selected by choosing only points for which the performance exceeds a given threshold. This way we obtained two sets with the same mean performance. Note that for the interior points, the performance in the other time periods is significantly better than those of the boundary points. The standard deviations of the performance for the validation time periods are smaller for the interior points. This indicates that the transfer of these parameters is more reasonable for the parameter vectors from the interior.

Time period	Boundary points				Points with depth > 5			
	Mean	Std	Min	Max	Mean	Std	Min	Max
1961-1970	0.682	0.010	0.667	0.711	0.682	0.015	0.647	0.705
1971-1980	0.630	0.043	0.488	0.714	0.673	0.019	0.634	0.726
1981-1990	0.751	0.029	0.641	0.798	0.776	0.017	0.715	0.804

**Table 5.6:** Model performance for parameter vectors according to their depth corresponding to the time period 1961-1970

#### 5.3.3 Sensitivity

The sensitivity is not investigated in the usual way in order to see how the model reacts to changes of individual parameters. Instead, the parameter vectors are considered sensitive if a small change of the whole vector leads to a big change (usually drop) in the performance of the model. The sensitivity of the boundary points and inside points was compared. For this purpose parameter vectors were altered from the boundary ( $D(\theta_1) = 1$ ) and from the inside ( $D(\theta_2) > 1$ ) of the set. A specific vector  $\eta$  was added and subtracted from the selected parameter vectors. This way the vectors  $\theta_1$  and  $\theta_2$  were altered to the same extent. Four new parameter vectors

$$C_1 = \theta_1 - \eta$$

$$C_2 = \theta_1 + \eta$$

$$C_3 = \theta_2 - \eta$$

$$C_4 = \theta_2 + \eta$$

are created. We select

$$\eta = \frac{\theta_1 - \theta_2}{2}$$

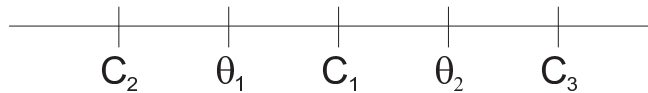
(monotonic decrease toward outside) thus  $C_2 = C_4$ . Due to the properties of the depth  $D(C_1) \geq 1$  while  $D(C_2) \leq 1$ . For  $C_3$  one cannot make any statements on the depth.

Figure 5.3 explains the construction of the three points in one dimension.

The above construction of parameter vectors  $C_1, C_2$  and  $C_3$  was carried out for a large number of randomly selected pairs  $\theta_1$  and  $\theta_2$ . The  $\theta_1$  and  $\theta_2$  were selected in such a manner that their mean performance was the same. Table 5.7 shows the statistics of the Nash-Sutcliffe coefficients for the sets corresponding to  $C_1, C_2$  and  $C_3$ . One can see that the inside points all have good performance and the standard deviation is small. Points at  $C_2$  (outside points) have the worst performance while  $C_3$  is better than  $C_2$  but worse than  $C_1$ . The skewness of the performance is nearly zero for the inside set  $C_3$ , while in other cases, the strong negative skew indicates that in some cases the performance loss due to the shift outside of the set is extremely high. The same alteration of the parameters leads to less performance loss for deep points than for shallow points. Further, there is no loss if the parameter vector remains in the convex set of deep parameters. This again highlights the advantage of deep parameter vectors.

Variable	Mean NS	Standard deviation	Skewness	Max NS	Min NS
$C_1$	0.692	0.005	0.30	0.710	0.677
$C_2$	0.576	0.101	-6.95	0.658	-0.491
$C_3$	0.686	0.024	-5.58	0.713	0.363

**Table 5.7:** Model performance for the inner and the shifted boundary and deep points



**Figure 5.3:** Construction of the points  $C_1, C_2$  and  $C_3$  in one dimension for sensitivity analysis of parameters

## 5.4 Robust Parameter Estimation (ROPE)

In section 5.3.1 of this Chapter, it was shown that parameters in the interior (expressed through data depth) of the set of good points are themselves good, transferable and not very sensitive. A possible explanation for this is that these parameters can be regarded as a kind of compromise solution - where none of the processes represented by the parameters is over-emphasized.

#### 5.4 Robust Parameter Estimation (**ROPE**)

For modeling purposes one might be interested in finding the set of good parameters and also the identification of the deep parameter vectors for robust modeling. For this purpose the following procedure is suggested:

1. The limits for the  $d$  selected parameters are identified
2.  $N$  random parameter vectors forming the set  $X_N$  are generated in the  $d$  dimensional rectangle bounded by the limits defined in 1
3. The hydrological model is run for each parameter vector in  $X_N$  and the corresponding model performances are calculated
4. The subset  $X_N^*$  of the best performing parameters is identified. This might be for example the best 10 % of  $X_N$
5.  $M$  random parameter sets forming the set  $Y_M$  are generated, such that for each parameter vector  $\theta \in Y_M$ ,  $D(\theta) \geq L$  (with  $L \geq 1$ ) where the depth is calculated with respect to the set  $X_N^*$
6. The set  $Y_M$  is relabeled as  $X_N$  and steps 3-6 are repeated until the performance corresponding to  $X_N$  and  $Y_M$  does not differ more than what one would expect from the observation errors

Figure 5.4 contains a pictorial explanation of the ROPE algorithm. First, from the maximum and the minimum range of parameters, a large set of parameters (containing say, 10000 uniformly distributed parameters) is generated as shown in Figure 5.4(a). Now, the model is run for all the parameters and the best 10 percent of the parameters are selected as produced in Figure 5.4(b). After removing the parameters outside the boundary, as shown in Figure 5.4(c), another set of the same number of parameters is generated such that it has higher depth and the parameters are within the boundary space (Figure 5.4(d)). Again the model is allowed to run; performance is calculated and the best 10 percent parameters are selected. The cycle of iteration is continued until the pre-determined number of iterations is over or the variation in performance is within a selected range. In this way, we go deeper and deeper into a data cloud which gives a better and more structured combination of parameters.

Note that the **ROPE** algorithm can be easily modified to obtain a general multivariate optimization procedure. The algorithm was used for three selected subcatchments (Rottweil, Tübingen, Süssen). Four iterations were enough to find a *good* set of parameters for all the catchments. The performance of the model during calibration periods is summarized in figure 5.5 for the Süssen catchment. As one can see, the subsequent iterations of the algorithm deliver better sets. The mean NS for the iterations increased from 0.767 (iteration 2) through 0.773 (iteration 3) to 0.775 (iteration 4). The improvement in the last iteration is very small and less than what one would expect to be caused by measurement errors. Therefore the algorithm stopped after this iteration.

Figure 5.6 shows the dotted plots of the selected model parameters for Süssen catchment. The performance corresponding to the parameters of iteration 4 are better than those

5 Robust Estimation of Hydrological Model Parameters

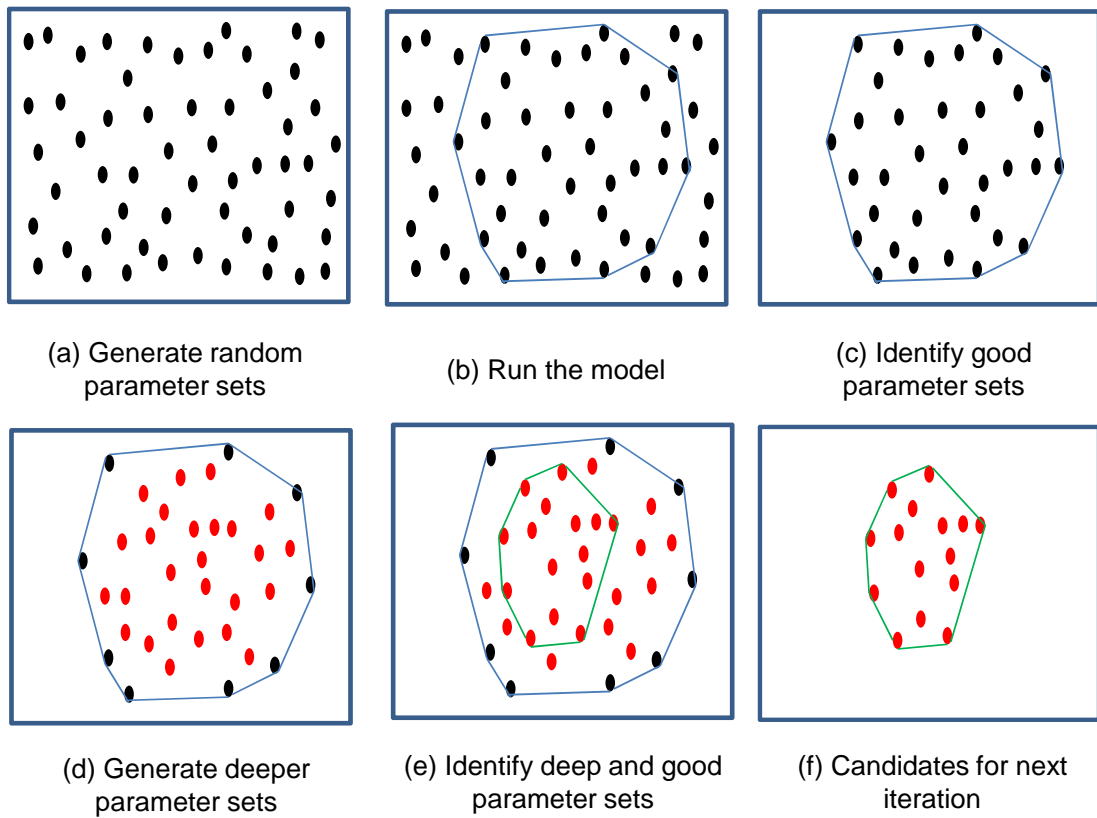


Figure 5.4: Systematic representation of the ROPE algorithm

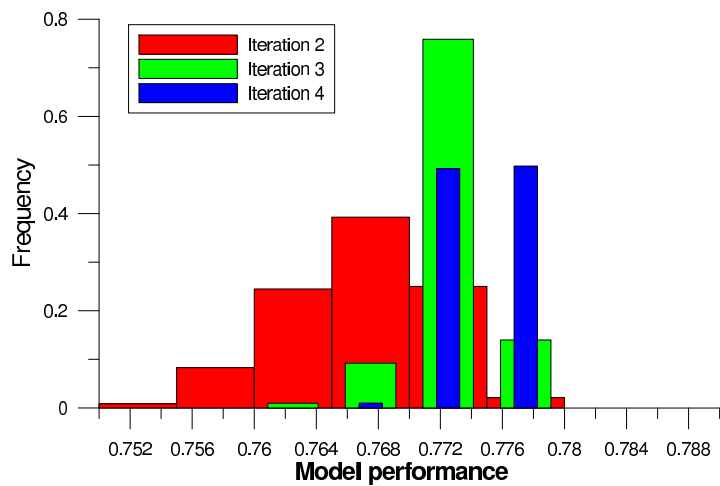
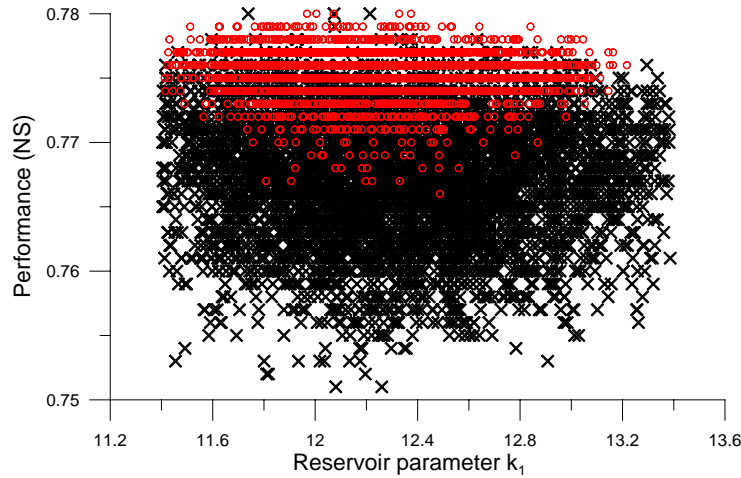


Figure 5.5: Histograms of the model performances for the different iterations of the algorithm for the Süssen catchment



corresponding to iteration 2 but the parameter range remains the same. Figure 5.7 shows the two dimensional scatter plot for the two model parameters for iterations 2 and 4 obtained for the Tübingen catchment. One has the impression that these parameters can take a wide range of values, and that there is no difference between the the two sets. The ranges of the parameters for the Rottweil catchment for iteration 1 and 4 are listed in Table 5.3. Even if the ranges are very similar for many parameters one has to bear in mind that these are two dimensional projections of 9 dimensional sets. The sets themselves are very different; the ratio of their 9 dimensional volumes is approximately 0.01 (calculated as Monte Carlo integral).



**Figure 5.6:** *Parameter value vs. model performance for the sets obtained in iteration 2 (crosses) and iteration 4 (circles) for the Süssen catchment*

Figure 5.8 shows the sensitivity of the calculated discharge with respect to two sets of parameter vectors with different depth. 1000 parameter vectors from the boundary (depth = 1) and from the interior (depth > 1) were taken and the corresponding hydrographs were calculated. The 95 % and the 5 % lines show that the interior parameter vectors lead to smaller differences in calculated discharge. The differences between the 95 % and the 5 % values are plotted separately in Figure 5.9, showing that taking interior parameter vectors leads to an approximately 20 % reduction.

In the case study presented here, all parameters in the final set  $Y_M$  performed well. In the case of other models, or other performance measures, this may not necessarily be the case. However, the set  $Y_M$  always contains a large portion of good parameters and possible transformations (i.e. taking the logarithm of some parameters) might fix this problem.

5 Robust Estimation of Hydrological Model Parameters

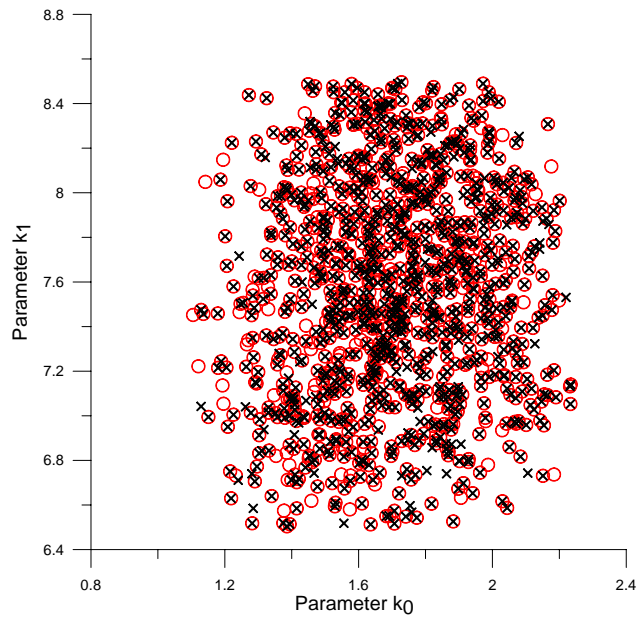


Figure 5.7: Parameter value for the sets obtained in iteration 2 (crosses) and iteration 4 (circles) for the Tübingen catchment

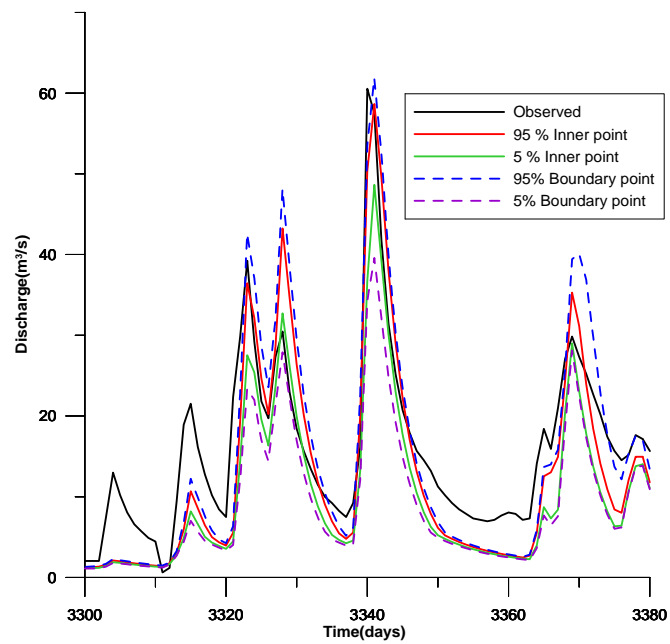
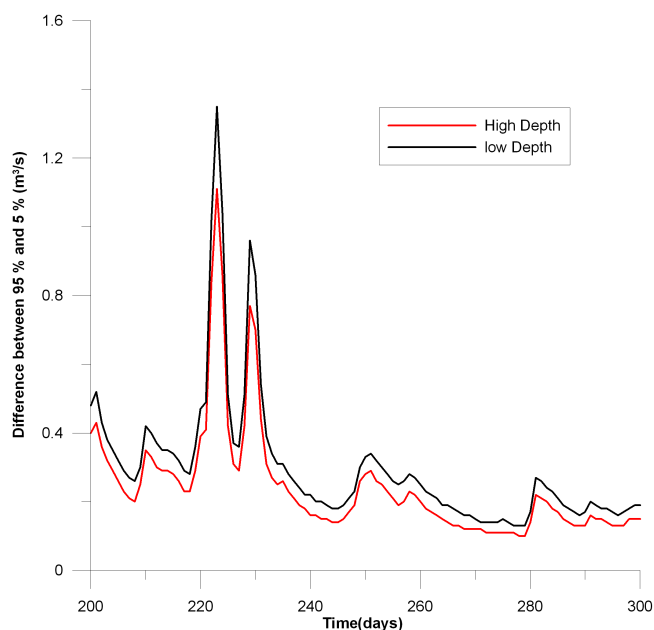


Figure 5.8: Hydrograph with confidence interval for boundary points and inner points

## 5.5 Application of the ROPE Algorithm to Different Models and Different Catchments



**Figure 5.9:** Confidence band width of high depth Vs confidence band width of low depth

## 5.5 Application of the ROPE Algorithm to Different Models and Different Catchments

To test further the robustness and to generalize, the ROPE algorithm was tested on different catchments and different models.

### 5.5.1 Result from HYMOD

As very similar to HBV, the ROPE algorithm was tested on another conceptual hydrological model, HYMOD. The description of the HYMOD model is given in Chapter 4. The results from two different catchments is given below.

#### Upper Neckar Catchments

The description of the catchments is given in Chapter 4. The HYMOD model was calibrated for the time period 1961-70 and validated for other time periods. Table 5.8 shows the calibration and validation results. It can be seen from Table 5.8 that this model also performs very similar to HBV. The parameter vector obtained by the ROPE calibration is very well transferable to other time periods.

## 5 Robust Estimation of Hydrological Model Parameters

Period	Mean NS	Max NS	Min NS	std
1961-1970	0.6944	0.7014	0.6921	0.00175
1971-1980	0.6241	0.6435	0.5860	0.00909
1981-1990	0.7465	0.7607	0.7251	0.00617
1991-2000	0.6777	0.6960	0.6493	0.00864

**Table 5.8:** Model performance for calibration time period 1961-1970 and validation for other time period for Rottweil

### Catchments in England and Wales

The description of the catchments is given in Chapter 4. The HYMOD model was calibrated for the time period 1981-85 and validated for other time period. Table 5.9 shows the calibration and validation result for catchment 27. It can be seen from Table 5.9 that the ROPE algorithm can be used to calibrate HYMOD conceptual model on catchments other than those where it was developed. The parameters obtained by calibration are good for transferring to other time periods. The result from the other catchments shows a very similar trend.

Period	Mean NS	Max NS	Min NS	std
1981-1985	0.880	0.882	0.877	0.00089
1986-1990	0.843	0.848	0.8367	0.00229

**Table 5.9:** Model performance (NS) for calibration time period 1981-1985 and validation for the other time period for catchment 27 in the UK

### 5.5.2 Result from three reservoirs model

#### Indian catchments

Some properties of Indian watersheds are quite different than their European counterparts. Topographic slopes, particularly in headwater regions are steeper in India, rivers are much wider with uncontrolled widths, rainfall intensities are higher and so is the input solar radiation/temperature. Temporal distribution of rainfall is highly skewed in India. Some rivers, particularly on the Indian peninsular are non-perennial and due to this, stream gauging is usually limited to the monsoon season only. Typical catchment sizes that are considered for management of water and associated resources are larger in India than in Europe. Data measurement networks are comparatively weak in India; typical lengths of time series data are shorter and data quality is poorer, also. The details of the Indian catchments is also given in Chapter 4.

With the above background, the ROPE algorithm was tested on the data of Indian watersheds using a three reservoir conceptual model to test the performance of the ROPE algorithm under situations that are dramatically different than those for which it was developed.

### Model calibration and validation

The data for the period 1983-86 was chosen for model calibration. The length of computational time step was one day. First, a few model runs were taken to have some idea about the range of the parameters. Maximum and minimum values of the model parameters are presented in Table 5.10. Next, a large number of uniformly distributed parameters sets were generated within the identified range and the model runs were taken with each set of parameters. The Nash-Sutcliffe coefficient (Nash and Sutcliffe, 1970) was used as the objective function for the model evaluation. Based on this index, the best 10 percent parameter sets were chosen and again the maximum and minimum values of the parameters were determined.

Parameters	Maximum	Minimum	Unit
$S_{max}$	500	5	mm
$C_{max}$	1500	15	mm
$F_C$	0.90	0.1	-
$F_{inf}$	0.99	0.001	-
$C_{int}$	0.99	0.001	-

**Table 5.10:** Range of model parameters

After getting a proper range of parameters, the model was calibrated using the ROPE algorithm. Figure 5.10 shows the model and the observed hydrograph for the calibration period. It can be seen that during the calibration runs, the catchment dynamics has been captured well at low peaks but the model has not given good results for very high peaks. This could be due to data limitations.

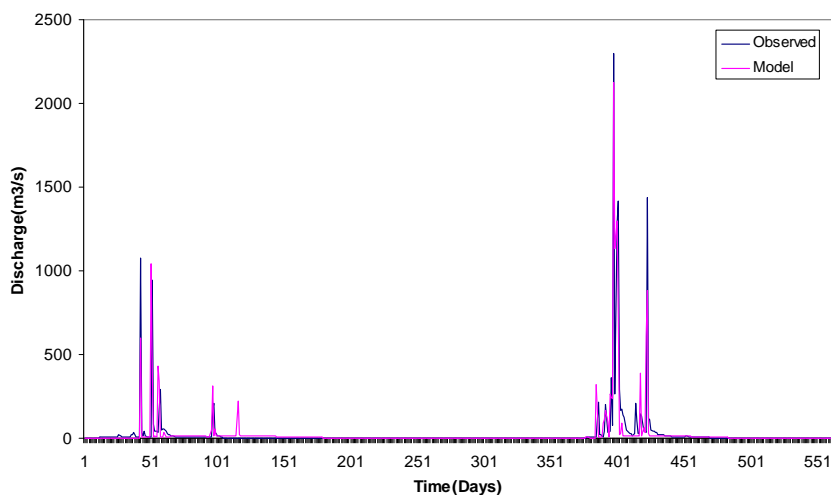


**Figure 5.10:** Observed and model hydrograph for calibration run

During calibration, a very wide range of model parameters has been considered to avoid

## 5 Robust Estimation of Hydrological Model Parameters

local minima. The ROPE algorithm has a feature that it does not give a single value of parameters after calibration; instead, it gives a vector of parameter set. After the calibration, the range of parameters has been considerably narrowed down and the final range is given in Table 5.11. It can be seen that some the parameters like  $C_{max}$  have the maximum reduction in the range. The final range of the parameters is still very wide but they perform equally well. Please note that not all parameters in this range are good since it is not a uniform space.

Parameters	Maximum	Minimum	Unit
$S_{max}$	95.093	95.093	mm
$C_{max}$	921.545	167.429	mm
$F_C$	0.888	0.481	-
$F_{inf}$	0.917	0.233	-
$C_{int}$	0.931	0.104	-

**Table 5.11:** Range of model parameters after calibration

It can be seen here that some parameters have a large range and some small. This happens because of different sensitivities of the parameters. The model was validated using the data for the period 1987-88. Robustness of the calibrated parameters can be seen in Table 5.12 in which the statistics of 1000 parameter sets is given. It is very clear from Table 5.12 that parameters obtained by the ROPE algorithm are well transferable to some other time period. The value of NS index is poor because of the quality of the data. Figure 5.11 shows the observed and simulated hydrographs for the validation period. It may be noted that in the previous study by Jain (1993), on the same basin and using the same model, similar results were obtained. The result of the ROPE calibration was better as compared to the previous study due to its robustness in transferability of parameters in time. Further, instead of single value of each parameter, the ROPE calibration gives a space of good parameter sets.

	Mean NS	Max NS	Min NS	Std
Calibration	0.612	0.622	0.609	0.00289
Validation	0.639	0.691	0.603	0.02875

**Table 5.12:** Performance for calibration and validation

The ROPE algorithm was tested on Indian watershed data using a conceptual model to examine its performance under situations that are diametrically different than those for which it was developed. It has been found that the algorithm is effective in estimating parameters of a conceptual model in a typical Indian watershed. There were limitations regarding spatial coverage of raingauge stations as well as the quality of data, as mentioned earlier. Further, the potential evaporation data for the catchments was also not representative since the station was away from the basin. The performance of the model and the ROPE algorithm is encouraging in light of the above constraints on data availability.

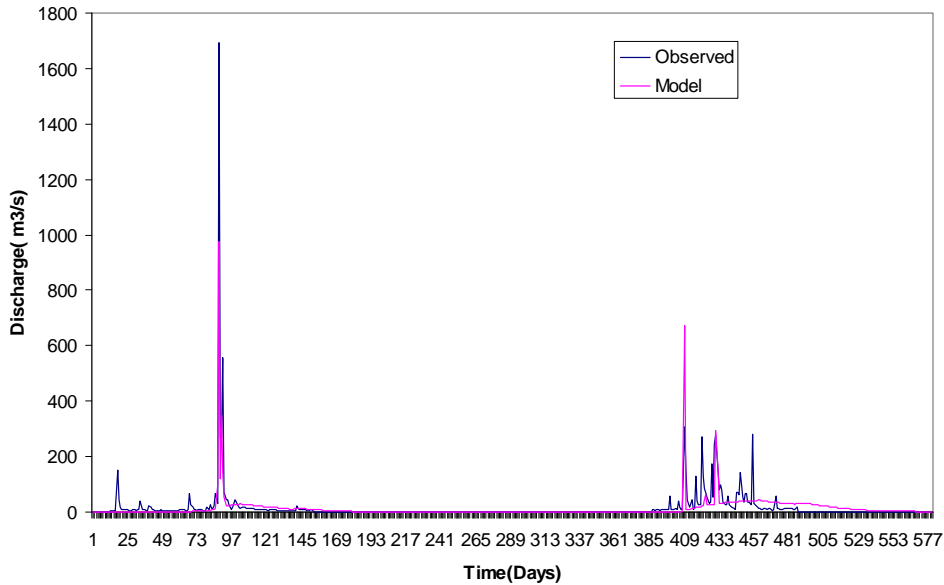


Figure 5.11: Observed and model hydrograph for validation

## 5.6 Modification of the ROPE Algorithm

### 5.6.1 Sequential replacement of weak parameters (SRWP)

The ROPE algorithm was further modified and improved by sequential replacements of weak parameter vector with another deeper and good parameter vector. A Monte Carlo simulation was made and upper N percentage good performing parameters were taken to form a boundary/domain of parameter space. A new parameter was generated in the defined domain such that the depth of the parameter vector is greater than zero in that domain. The performance of this generated parameter set was calculated. If the performance of this newly generated parameter set is better than the minimum performance in the predefined domain then the minimum performance parameters of the predefined domain is replace with newly generated parameter set. This step-wise procedure is repeated until difference between the maximum and minimum performance in the domain of parameter space is acceptable. A general description of SRWP method is given below. Also, the the methodology is Illustrated in Figure 5.12.

1. Generate N parameter vector from uniform distribution in the feasible parameter space.
2. Compute the criterion value at each parameter set.

1

## 5 Robust Estimation of Hydrological Model Parameters

3. Sort the parameters set in order of increasing or decreasing criterion based on the goal (minimize or maximize)
4. Select best parameter vectors  $Y$  and make a convex hull of  $Y$ .
5. Generate a new parameter set such that its depth  $> 0$  in  $Y$  and compute criterion value for this parameter set.
6. If the criterion value is better than worst criterion in  $Y$ , replace the corresponding parameter set with newly generated parameter set.
7. Continue repeating the steps 5 and 6 until there is no change in volume of the convex hull ( $Y$ ) or minimum performance is satisfied.

This algorithm does not converge to a single *best* parameter vector, instead it gives a convex hull of parameter where all the parameters are almost equally good. This algorithm can be applied for any performance measure or objective function. The methodology was demonstrated using the HYMOD conceptual model on the Upper Neckar catchments of South-West Germany (Chapter 4).

## 5.7 Case Study

The SRWP algorithm can be considered as an optimization procedure.

### 5.7.1 Application of the SRWP algorithm on test functions

The methodology was tested on some of the well know simple to complex test functions. Details about the test functions and their properties is given below. For all the seven test functions given in below, SRWP algorithm was used to obtained the theoretical optima. SRWP method succeeded in all case. In all these cases, SRWP methods has converged to an optimal value. The beauty of this SRWP method is that, it does not converge to a single value, instead giving region or space where optimal parameters can lye. Figure 5.13 to 5.26 show the contour map of the test function and optimal region mapped by SRWP method. It can be seen from figures that the SRWP method has successfully mapped the optimal region in different levels of function complexity.

#### McCormick Function

$$f(x) = \sin(x_1 + x_2) + (x_1 - x_2)^2 - 1.5x_1 + 2.5x_2 + 1 \quad (5.3)$$

Search domain  $x_1 \in [-1.5, 4], x_2 \in [-3, 4]$  and  $f_{min}(-0.54719, -1.54719) = -1.9133$

#### Levy Function

$$f(x) = \sin^2(3\pi x_1) + (x_1 - 1)^2 [1 + \sin^2(3\pi x_2)] + (x_2 - 1)^2 [1 + \sin^2(2\pi x_2)] \quad (5.4)$$

Search domain  $x_1 \in [-10, 10], x_2 \in [-10, 10]$  and  $f_{min}(1, 1) = 0$



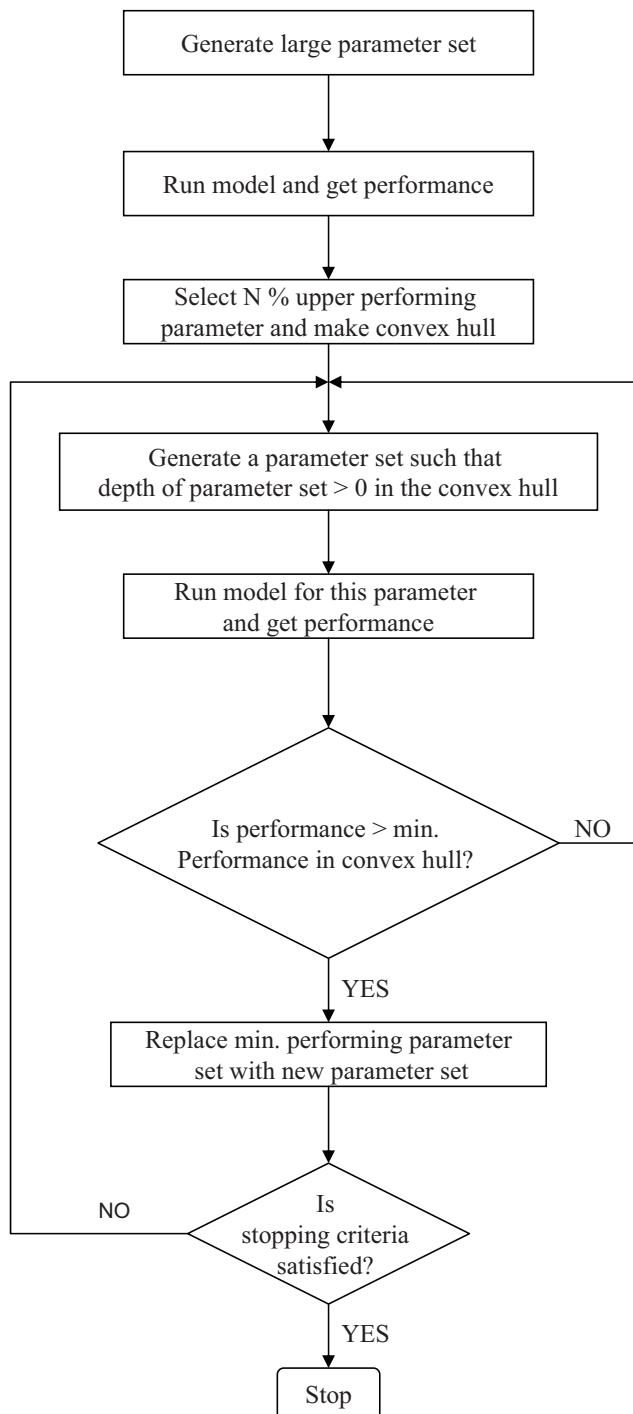


**Figure 5.12:** Schematic explanation of the sequential replacement of weak parameters algorithm

**Styblinski-Tang Function**

$$f(x) = \frac{1}{2} \sum (x_i^4 - 16x_i^2 + 5x_i) \quad (5.5)$$

Search domain  $x_1 \in [-5, 5], x_2 \in [-5, 5]$  and  $f_{min}(-2.903534, -2.903534) = -78.332$

**Leon Function**

$$f(x) = 100(x_2 - x_1^2)^2 + (1 - x_1)^2 \quad (5.6)$$

Search domain  $x_1 \in [-1.2, 1.2], x_2 \in [-1.2, 1.2]$  and  $f_{min}(1, 1) = 0$

**Giunta Function**

$$f(x) = 0.6 + \sum \left[ \sin\left(\frac{16}{15}x_i - 1\right) + \sin^2\left(\frac{16}{15}x_i - 1\right) + \frac{1}{50}\sin\left(4\left(\frac{16}{15}x_i - 1\right)\right) \right] \quad (5.7)$$

Search domain  $x_1 \in [-1, 1], x_2 \in [-1, 1]$  and  $f_{min}(0.45834282, 0.45834282) = 0.0602472184$

**Rastrigin Function**

$$f(x) = 2 + x_1^2 + x_2^2 - \cos(18x_1) - \cos(18x_2) \quad (5.8)$$

Search domain  $x_1 \in [-1, 1], x_2 \in [-1, 1]$  and  $f_{min}(0, 0) = 0$

**Six-Hump Camelback Function**

$$f(x) = 1.036285 + 4x_1^2 - 2.1x_1^4 + \left(\frac{1}{3}\right)x_1^6 + x_1x_2 - 4x_2^2 + 4x_2^4 \quad (5.9)$$

Search domain  $x_1 \in [-2, 2], x_2 \in [-1, 1]$  and  $f_{min}(0.08983, -0.7126)$   
 $and(-0.08983, 0.7126) = 0$

## 5.8 Case Study Result from SRWP Algorithm

SRWP algorithm has consistently performed well for all simple to complex test functions. So, it was further tested for a practical hydrological model. The HYMOD model was calibrated for time period 1961-70 by the above mentioned method and validated for other time periods. Figure 5.27 shows the improvement of the performance due to sequential replacement of weak parameters with deeper parameters. It can be seen from figure 5.27 that the mean Nash Sutcliff coefficient (NS) has improved from 0.64 to 0.69 (from first convex hull to final) and there is gradual improvement in maximum NS as well. It could have improved further if we had allowed more iterations. It can be seen from same figure how the difference of maximum and minimum decreases and at a certain point of time the difference between maximum and minimum is very low and acceptable. This result shows that after certain number of replacement of parameters we can not get much improvement, so we can stop searching for better parameters. The rate of acceptance of parameter vector for replacement with weak parameter set decreases

5.8 Case Study Result from SRWP Algorithm

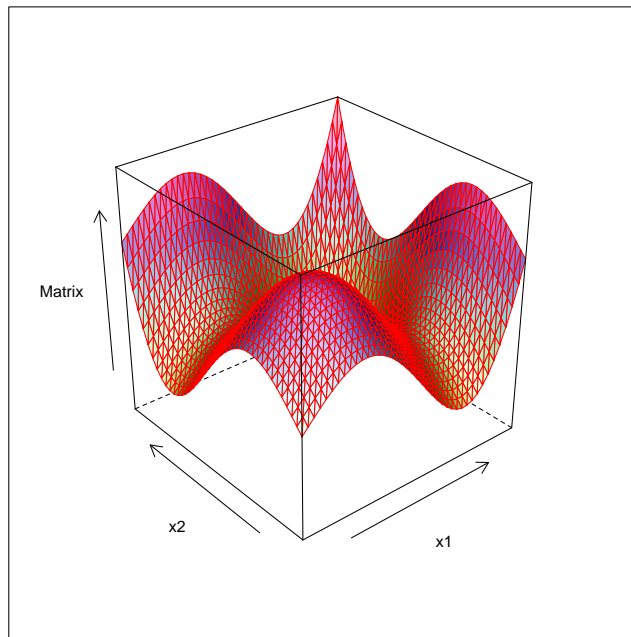


Figure 5.13: *Giunta function*

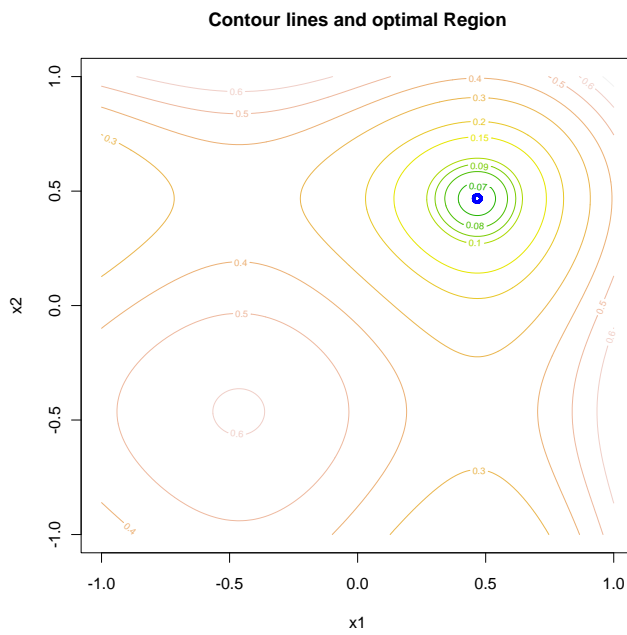


Figure 5.14: *Contour Map for Giunta function and optimal region*

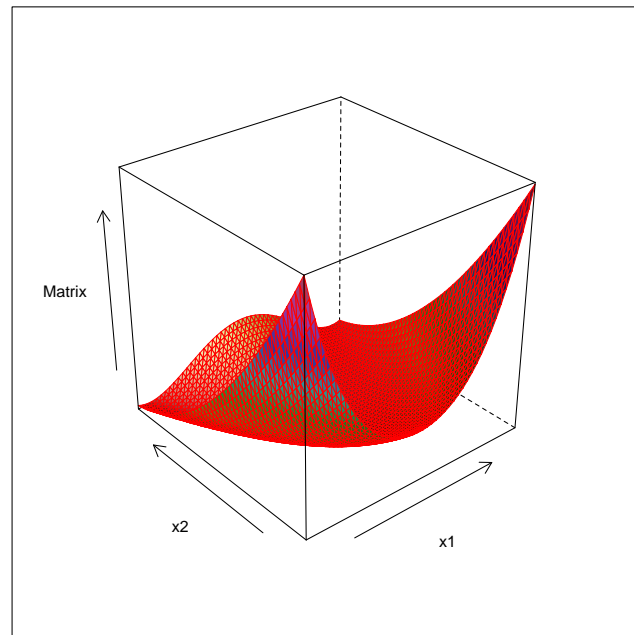


Figure 5.15: Leon function

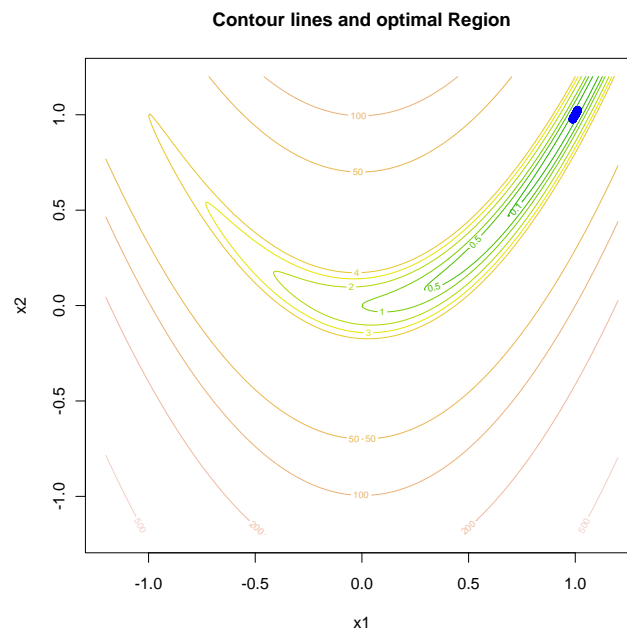


Figure 5.16: Contour Map for Leon function and optimal region

5.8 Case Study Result from SRWP Algorithm

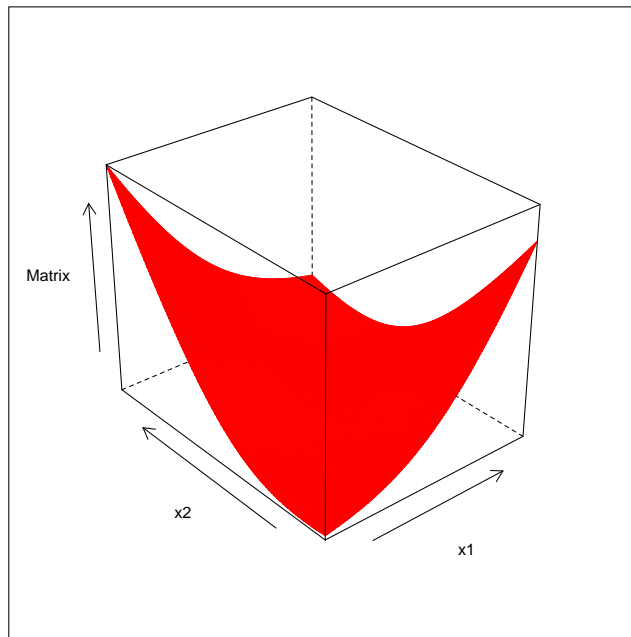


Figure 5.17: *McCormick function*

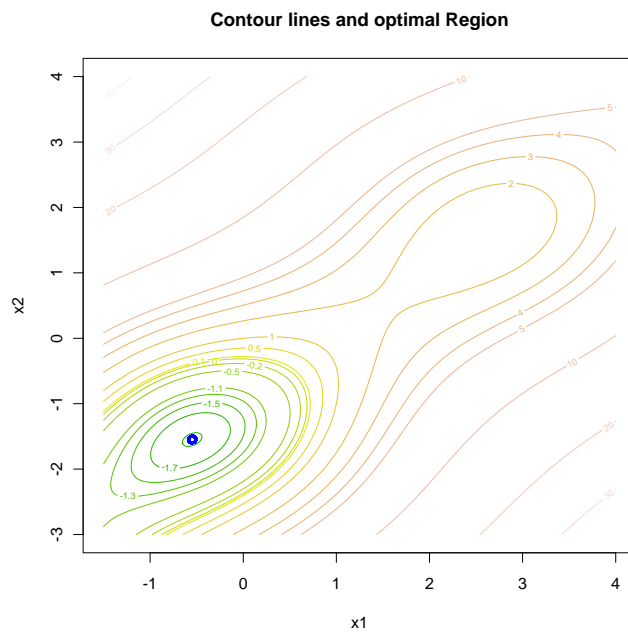
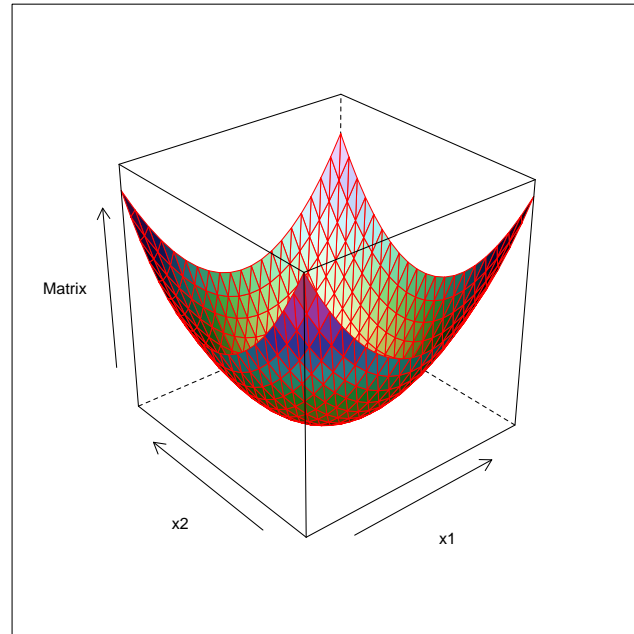
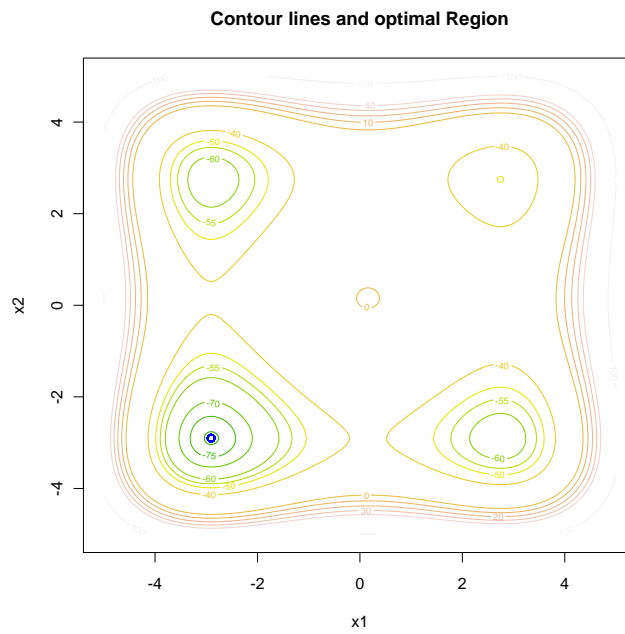


Figure 5.18: *Contour Map for McCormick function and optimal region*



**Figure 5.19:** *Styblinski-Tang function*



**Figure 5.20:** *Contour Map for Styblinski-Tang function and optimal region*

5.8 Case Study Result from SRWP Algorithm

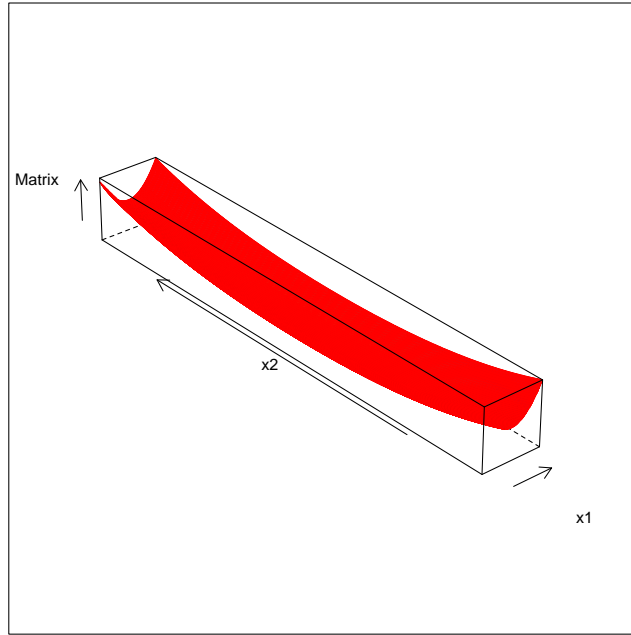


Figure 5.21: *Levy function*

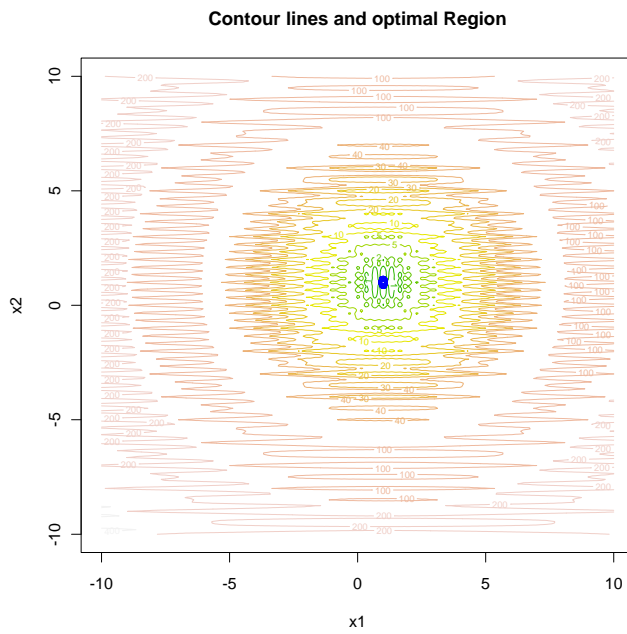


Figure 5.22: *Contour Map for Levy and optimal region*

5 Robust Estimation of Hydrological Model Parameters

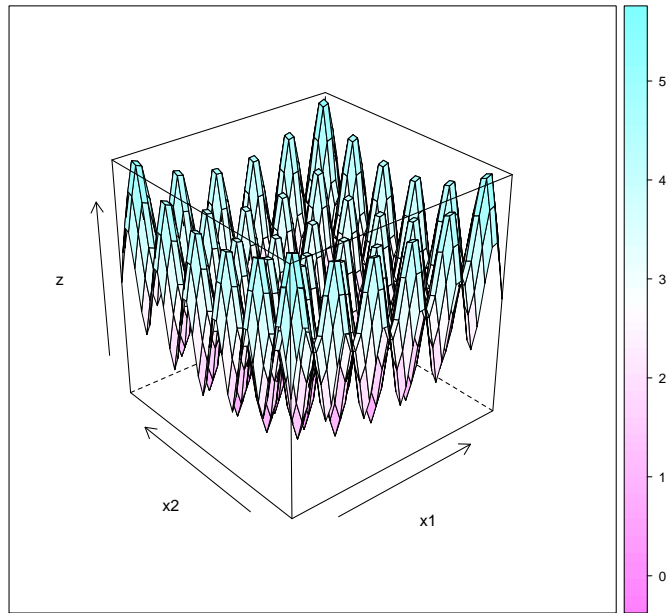


Figure 5.23: Rastrigin function

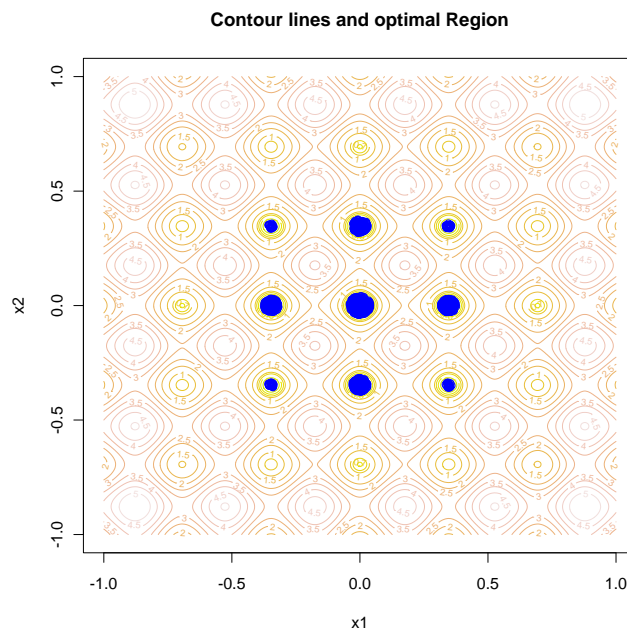


Figure 5.24: Contour Map for Rastrigin function and optimal region



5.8 Case Study Result from SRWP Algorithm

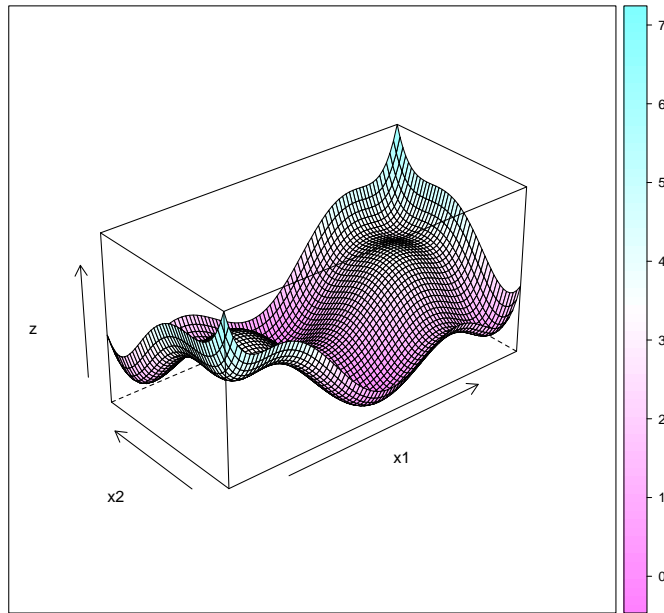


Figure 5.25: Six-Hump Camelback function

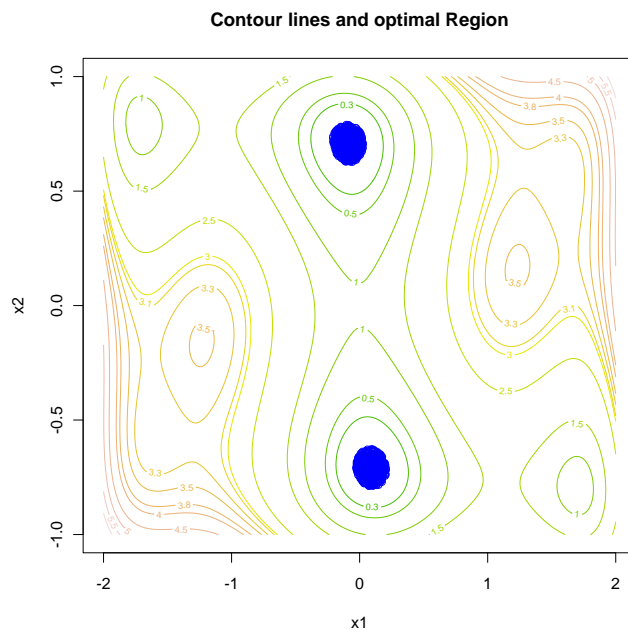
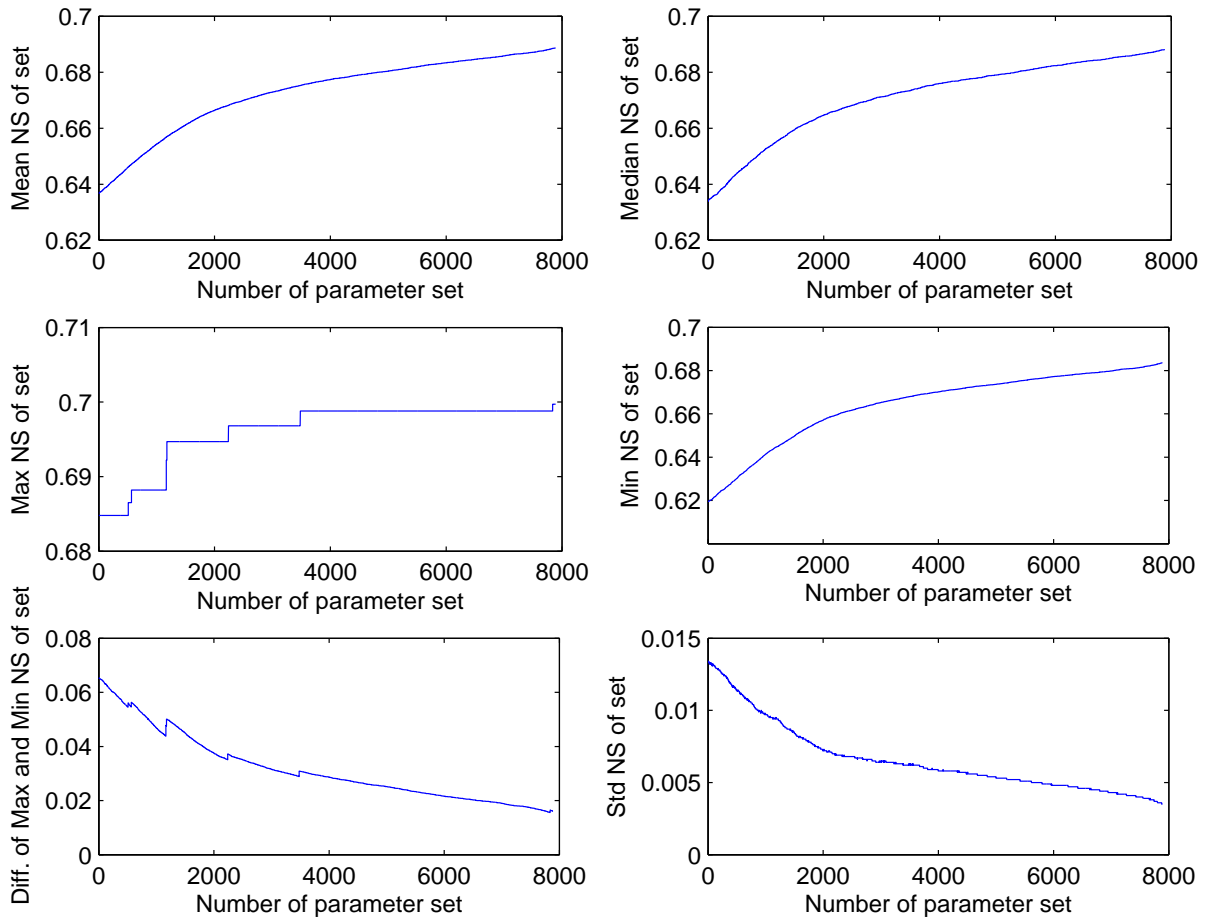


Figure 5.26: Contour Map for Six-Hump Camelback function and optimal region

## 5 Robust Estimation of Hydrological Model Parameters

as the number of iteration increases. This is because the volume of parameter space shrinks so much that there is very little scope to improve the model parameters. It is very obvious that for smaller difference of maximum and minimum we need a larger number of iterations and there will be, consequently, more rejection. Table 5.13 shows the transferability of the parameter to the other time periods. It is very clear that the parameters have performed well for all three time periods.



**Figure 5.27:** Improvement of performance by SRWP algorithm

Table 5.14 shows the initial and final range of parameters of the model. It is clear from table that we have a wide range of the parameters after calibration. Even the volume of the parameters has reduced though range of the parameters is not very narrow. Figure

### 5.8 Case Study Result from SRWP Algorithm

Period	Mean NS	Max NS	Min NS	std
1961-1970	0.69	0.70	0.68	0.0035
1971-1980	0.62	0.65	0.56	0.0135
1981-1990	0.75	0.76	0.71	0.0082
1991-2000	0.68	0.70	0.64	0.0104

**Table 5.13:** Model performance for calibration time period 1961-1970 and validation for other time period for Rottweil

5.28 shows the spread of the parameters range at initial N percentage to final parameters sets. It can be seen from figure that at N percentage we have a wide range of parameters which have narrowed down as the number of iterations increased. As we can not plot an eight dimensional figure, a plot matrix is made for clear visualization. Figure 5.29 shows the plot matrix of the initial N percentage parameters. Here it is clear that there is no clear structure of any parameters. However, from the final plot matrix of the parameters (fig. 5.30) we can see that the parameter vector is less scattered and more structured.

Parameters		Initial	Sequential calibration
Cmax	Max	600.000	564.0294
	Min	150.000	230.1859
Beta	Max	8.000	7.3445
	Min	3.000	3.3579
Alpha	Max	0.800	0.5503
	Min	0.200	0.3751
$R_S$	Max	0.200	0.0200
	Min	0.010	0.0102
$R_Q$	Max	0.700	0.6897
	Min	0.300	0.5933
Th	Max	1.500	1.4008
	Min	-1.000	0.1912
DD	Max	3.000	2.9030
	Min	1.000	1.1726
Dew	Max	2.000	0.8976
	Min	0.000	0.0847

**Table 5.14:** Initial and final parameter range

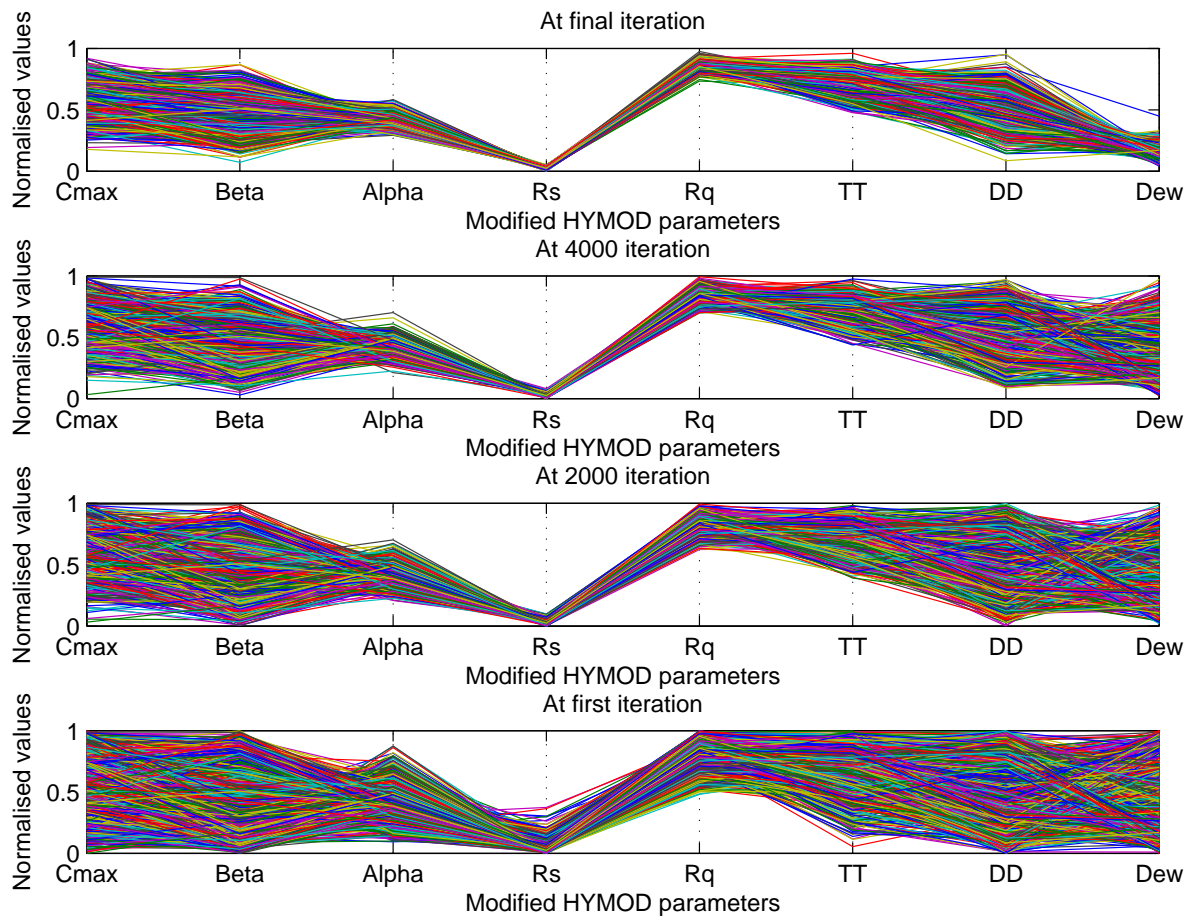


Figure 5.28: Different parameter at different iteration

5.8 Case Study Result from SRWP Algorithm

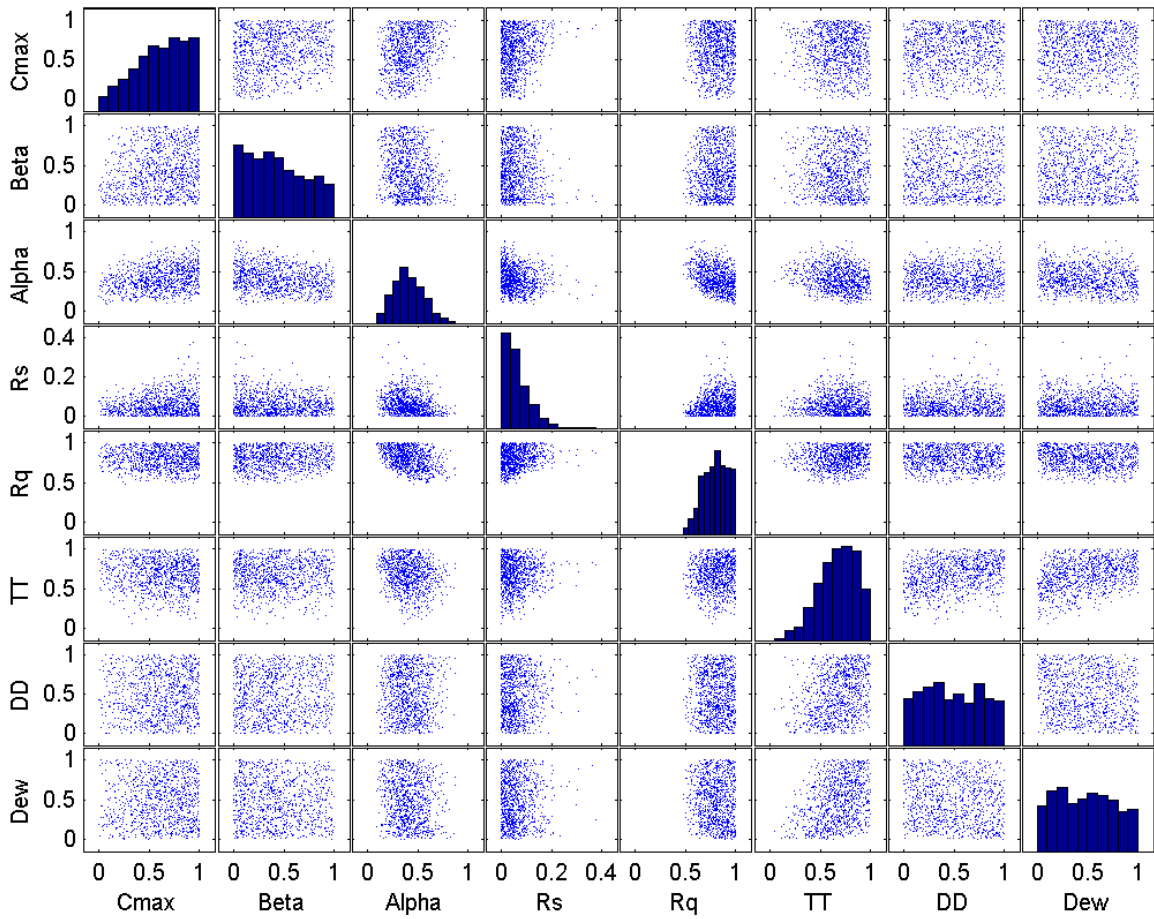


Figure 5.29: Plot matrix of parameter at initial iteration

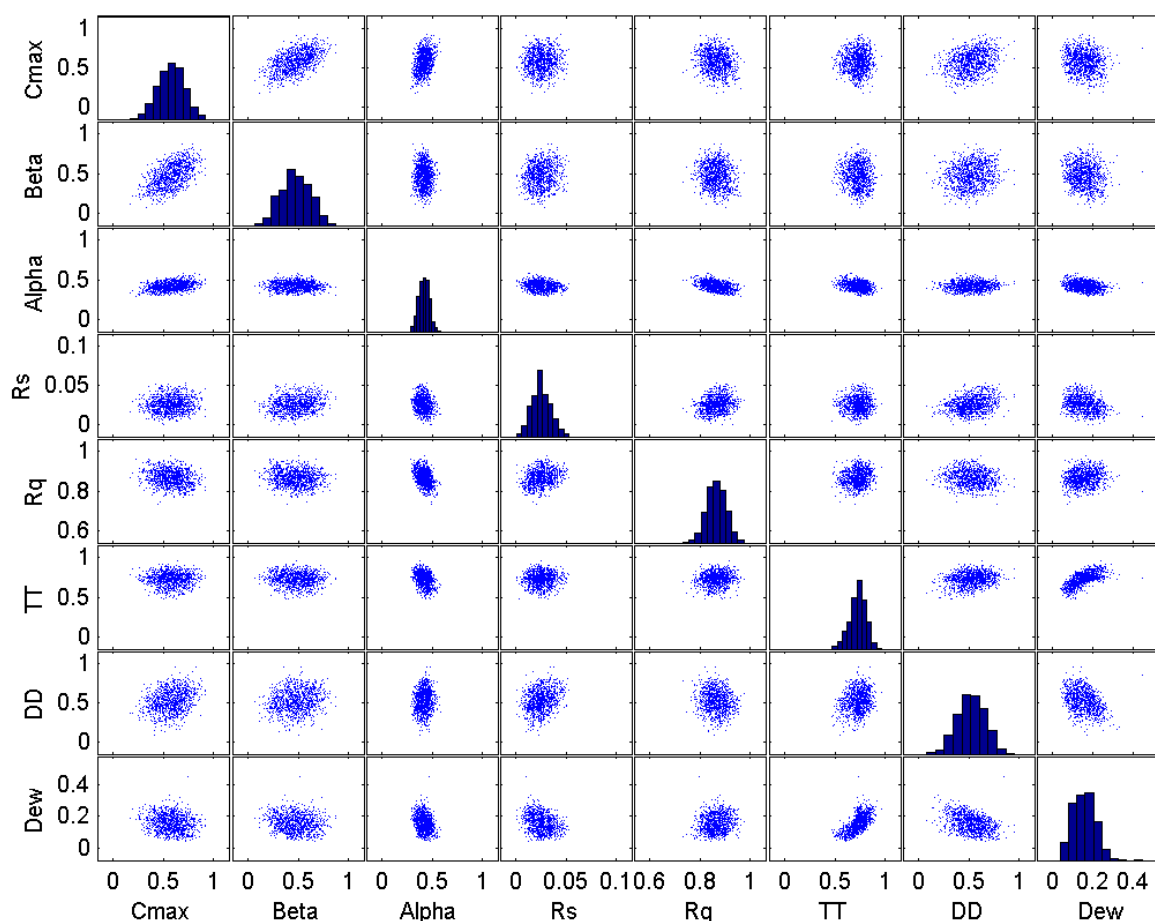


Figure 5.30: Plot matrix of parameter at final iteration

### 5.8.1 Comparison with existing methods

The result given in table 5.13 were compared to the previous study by [Bárdossy and Singh \(2008\)](#) on same study area using ROPE algorithm. It has been found that performance by both methods is very similar in term of calibration time period and validation time periods but with fewer number of iterations. The robustness of ROPE algorithm is still maintained by the sequential calibration method. For further comparison, the HYMOD model was calibrated using commonly used global optimization algorithm shuffled complex evolution (SCE-UA) ([Duan et al., 1993](#)). Table 5.15 shows the calibration and validation performance of SCE-UA. It can be seen clearly from table 5.13 and 5.15 that

### 5.8 Case Study Result from SRWP Algorithm

calibration of the model using the methodology developed in this chapter give a very similar result as obtained by global optimization. The final parameters obtained by SCE-UA optimization is given in table 5.16. The result of the sequential calibration method was better as compared to the previous study due to its robustness in transferability of parameters in time. Also the convergence is faster then SCE-UA. It does not depend much on the initial values too. The advantage of the sequential calibration method over global optimization lies in its final parameters. In sequential calibration method we get a parameter space instead of a single value of parameters. this helps address somehow the equifinality problem. Small changes in parameters does not change the performance. Hence, the results of the sequential calibration method is more robust.

	1961-1970	1971-1980	1981-1990	1991-2000
	NS	NS	NS	NS
SCE-UA	0.70	0.64	0.74	0.69

**Table 5.15:** Model performance for calibration time period 1961-1970 and validation for other time period for Rottweil using SCE-UA

Parameters		Initial	SCE-UA
Cmax	Max	600.000	258.5820
	min	150.000	
Beta	Max	8.000	6.0050
	min	3.000	
Alpha	Max	0.800	0.5360
	min	0.200	
$R_S$	Max	0.200	0.0200
	min	0.010	
$R_Q$	Max	0.700	0.6550
	min	0.300	
Th	Max	1.500	0.7860
	min	-1.000	
DD	Max	3.000	2.2770
	min	1.000	
Dew	Max	2.000	0.2250
	min	0.000	

**Table 5.16:** Initial and final Parameter Range in SA and SCE-UA

## 5.9 Conclusions

- In this chapter, the effect of observation uncertainty on the parameter estimation was investigated. It could be shown that observation errors can lead to very different optimal model parameters if the uniqueness of the parameters is assumed and the parameters corresponding to the optimum of the performance function are identified.
- Observational uncertainty of the input and the discharge leads to variability of the model performance. This variability has to be considered in model parameter estimation. All model parameters which do not differ more in their performance than what can be caused by measurement errors could themselves be the best parameters.
- Data depth is a useful tool to identify particular and robust parameter sets. Parameters with low data depth are near the boundary and are sensitive to small changes and do transfer to other time periods less well as well as high depth ones.
- From the examples discussed in this chapter, one could see that equally performing parameters are not necessarily equally transferable or equally sensitive. Data depth can help to find domains with robust and transferable parameters.
- A stepwise algorithm to find a convex set containing good model parameters was developed.
- In this chapter, model performance was measured by the traditional Nash-Sutcliffe coefficient. Other measures can be treated similarly - but might lead to different parameter sets.
- The ROPE algorithm was tested on different model like HYMOD and Three reservoir, in different catchments such as the England and Indian catchments, where catchments characteristic differed substantially and had different data availability. The result shows ROPE has performed well on these catchments and models. This makes ROPE algorithm a more general purpose tool for model calibration.
- In a further extension to the ROPE algorithm, a very simple and effective optimization algorithm called Sequential Replacement of Weak Parameter (SRWP), was introduced for the automatic calibration of hydrological model. In SRWP algorithm weak parameter set is sequentially replaced with another deeper and good parameter sets.
- SRWP easily overcomes the local minima and converges to optimal region. SRWP does not converges to a single optima, instead it gives a convex hull of optimal region.



# 6 Impact of Objective Function on Mapping of Model Parameters During Calibration

This chapter describes the analysis of the parameter space mapped by different objective functions during the calibration of a hydrological model by the ROPE algorithm.

## 6.1 Introduction

The hydrological model is used for different purposes. Hence, the same model can have different goals; this leads us to having different objective functions for model calibration. There are several objective functions, though not a single objective function can describe all the components of a hydrograph. Different objective function give emphasis to different types of simulated and observed behaviors of hydrograph. There is no universal objective function that exists which can give simultaneously importance to all parts of the hydrograph. There are significant trade off exist between the different objective function. It is nearly impossible to have a unique set of parameters which can satisfy all the objective simultaneously (Moussa and Chahinian, 2009; Krause et al., 2005; Madsen, 2000). The selection of objective function depends on the very basic purpose of the model use and the modeler. Generally, a single objective function may not be viable for all the case. Single objective function is often inadequate to measure accurately the simulation of all the important characteristics of the system that are reflected in the observation series (Madsen, 2000; Madsen et al., 2002). Hence, the multi-objective calibration appear to be the basic solution of the above mentioned problem. Ever so, it is very important to know which objective function map parameters in which space. What are their intersection in space? What is the volume of the space and to what extent does the volume of parameter space shrink during calibration? Answers to these very basic question will lead us to a better calibration strategy.

## 6.2 Methodology

The HYMOD, a conceptual hydrological model was calibrated on a different objective function using the ROPE algorithm for the Upper Neckar catchments. The details of the ROPE algorithm is given in Chapter 5. For details about the model and catchments please refer to Chapter 4.

### 6.2.1 Objective functions

The objective functions used for this research are the Nash-Sutcliffe coefficient (Nash and Sutcliffe, 1970), root mean square, volume error and peak error. The following equations (6.1 to 6.4) describe the mathematical form of objective functions. To normalize the effect of the extreme value, a logarithm of above mention objective function was defined. To calculate the logarithm objective function, discharge was replaced with logarithm of discharge.

$$NS = 1 - \sum_{i=1}^N \frac{(Q_o(i) - Q_m(i))^2}{(Q_o(i) - \widehat{Q}_o)^2} \quad (6.1)$$

$$RMSE = \left[ \frac{\sum_{i=1}^N (Q_o(i) - Q_m(i))^2}{N} \right]^{1/2} \quad (6.2)$$

$$VE = \frac{1}{N} \sum_{i=1}^N \left| \frac{(Q_m(i) - Q_o(i))}{Q_o(i)} \right| \quad (6.3)$$

$$PE = \frac{1}{N} \sum_{i=1}^N \left| \frac{(Q_{m(peak)}(i) - Q_{o(peak)}(i))}{Q_{o(peak)}(i)} \right| \quad (6.4)$$

Where, NS is Nash-Sutcliffe coefficient,  $Q_o$  is the observed discharge,  $Q_m$  is model discharge. RMSE is root mean square, N is the simulation length. VE is volume error, PE is peak error,  $Q_{m(peak)}$  is peak model discharge,  $Q_{o(peak)}$  is observed peak discharge. The peak discharge was defined based on a threshold value. Each catchments can have different threshold value. The case study presented in this chapter has used 20  $m^3/s$  as threshold. Notation used for each objective function, which is used in rest of this chapter is given in table 6.1.

Notation	Objective function
OF1	Nash Sutcliffe coefficient
OF2	Root mean square error
OF3	Volume error
OF4	Peak error
OF5	Log Nash Sutcliffe coefficient
OF6	Log Root mean square error
OF7	Log Volume error
OF8	Log Peak error

**Table 6.1:** Different objective functions and their notations

The ROPE algorithm was used for calibrating HYMOD model on Upper Neckar catchment for the period 1961-70, based on all the eight objective function mentioned above. The parameters obtained by each objective functions after calibration of HYMOD model

are compared with the initial values, given in the Tables 6.2 and 6.3. From these tables, it is very clear that the shrinkage in range of parameters are varying from one objective function to the others. Range also varies from parameter to parameter within an objective function. All the eight objective functions have different parameter ranges when compared to the initial range of parameters. For example, parameter  $C_{max}$  have very wide range in OF3 and OF7 compared to others. The search domains vary from one objective function to the other. This shows that the each objective function gives importance to a different part of the hydrograph. Consequently, a proper choice of objective function is very important. Hence, a proper diagnosis of these parameter space is given in following sections.

Parameters		Initial	OF1	OF2	OF3	OF4
$C_{max}$	Max	600.000	573.670	418.517	500.158	180.932
	min	150.000	294.680	278.057	403.468	151.032
Beta	Max	8.000	6.905	6.815	4.994	7.944
	min	3.000	3.727	3.428	3.043	5.564
Alpha	Max	0.800	0.525	0.519	0.564	0.552
	min	0.200	0.383	0.385	0.477	0.311
$R_S$	Max	0.200	0.023	0.022	0.012	0.042
	min	0.010	0.010	0.010	0.010	0.013
$R_Q$	Max	0.700	0.679	0.676	0.572	0.668
	min	0.300	0.592	0.591	0.455	0.531
Th	Max	1.500	1.100	1.124	1.324	0.845
	min	-1.000	0.281	0.264	0.324	-0.007
DD	Max	3.000	2.865	2.812	2.677	2.558
	min	1.000	1.388	1.320	1.132	1.171
Dew	Max	2.000	1.684	1.608	1.685	1.786
	min	0.000	0.093	0.088	0.136	0.015

**Table 6.2:** Parameter range obtained by different objective functions after calibration

### 6.2.2 Parameter space for model calibration

Due to the higher dimensionality and complex interaction of model parameters, it is quite difficult to visualize the parameter space of hydrological model, during calibration process. ROPE algorithm gives a space of good parameters after calibration, instead of a single parameter set. Hence, figure 6.1 represents the parameters obtained by the each objective function. The X axis shows all the eight parameters of HYMOD and Y axis shows the normalized value of calibrated 1000 best parameters. It is very clear from the figure that the parameters mapped by Nash-Sutcliff coefficient and root mean square error are very similar in nature in comparison, volume error and peak error have very different parameter range and region. Similarly, the parameters obtained by taking the

6 Impact of Objective Function on Mapping of Model Parameters During Calibration

Parameters		Initial	OF5	OF6	OF7	OF8
$C_{max}$	Max	600.000	594.365	587.927	590.246	205.170
	min	150.000	460.161	460.325	502.045	170.493
Beta	Max	8.000	6.779	6.637	5.009	7.871
	min	3.000	4.987	4.959	3.727	7.052
Alpha	Max	0.800	0.536	0.537	0.549	0.623
	min	0.200	0.491	0.491	0.482	0.513
$R_S$	Max	0.200	0.013	0.013	0.013	0.062
	min	0.010	0.011	0.011	0.011	0.037
$R_Q$	Max	0.700	0.607	0.603	0.605	0.647
	min	0.300	0.549	0.552	0.522	0.592
Th	Max	1.500	1.140	1.134	1.392	0.974
	min	-1.000	0.707	0.714	0.833	0.578
DD	Max	3.000	2.764	2.756	2.786	2.818
	min	1.000	1.893	1.870	1.957	1.978
Dew	Max	2.000	1.781	1.894	1.668	1.735
	min	0.000	0.632	0.635	1.047	0.919

**Table 6.3:** Parameter range obtained by different log objective functions after calibration

logarithm of selected objective functions is given in figure 6.2. It is important to bear in mind that the parameters from logarithm of objective function are entirely different than the parameters obtained by the simple objective functions. This proves that any change to the objective functions mean different search space. They all search optimal parameters in a different way and there is no common space which is shared for all the objective functions, this is investigated in next section. The volume of parameter space obtained by different objective functions was calculated by the help of Monte Carlo integration. It has been found that the volume of the space is very different in different objective functions. In figure 6.3, it is show how the volume of the parameter space changes in each objective functions at each iteration of ROPE algorithm. The X axis represent normalized volume and Y axis represents, the number of iteration in ROPE algorithm. The volume of space decreases as the number of iteration increases. Apart from the peak error, the volume reduction of space is similar for Nash-Sutcliff coefficient, root mean square error, and volume error. It is clear from figure that the shrinkage of parameters space volume is not the same for different objective functions. This implies that we reach optimal parameters at different rate. So it is very important to set different termination criteria for different objective function in our optimization algorithm. To visualize the shrinkage of volume during each iteration of ROPE algorithm by different objective functions, diffusion space was used. The diffusion space gives visualization of higher dimension space in lower dimension. Figure 6.4 to 6.7 shows the diffusion space of eight dimension parameter space of HYMOD model, in three dimensions for each objective function and at each iteration of ROPE algorithm. Figure 6.4 gives initial

parameter space, where we can see good performance (red points) is scattered all over the space. Please bear in mind, in diffusion space, some of the sensitive and important parameter may dominate the space. However, this will not effect the visualization of shrinkage of the volume and rate of shrinkage. We can clearly see that, at initial iteration of ROPE algorithm, for all the objective function, good parameters are widely scattered in space. As iterations increase in ROPE algorithm, these good parameters shrink toward a specific region in each objective functions. It is very noticeable that, in all objective functions, optimal parameters are not at the same region. Only OF1 and OF2 have given similar region, which strengthen previous result as discuss above. From these diffusion space figures one can see that, the rate of shrinkage of parameters space is very much faster for OF4 than for OF1, OF2 and OF3. This also confirms the similar result, what we obtained during volume calculation by Mote Carlo integration. Hence, it can be conclude that each objective function has a different shrinkage rate for parameter space in calibration.

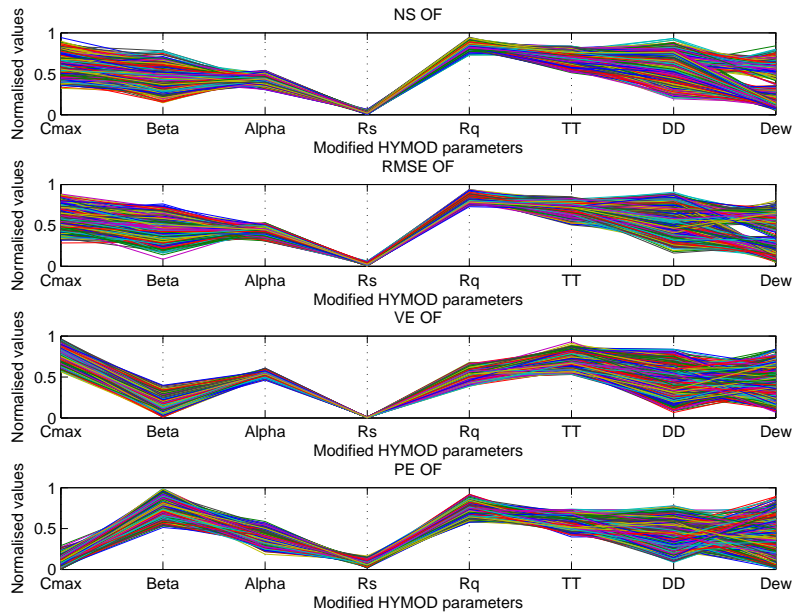


**Figure 6.1:** *Parameter values for different objective functions*

## 6 Impact of Objective Function on Mapping of Model Parameters During Calibration

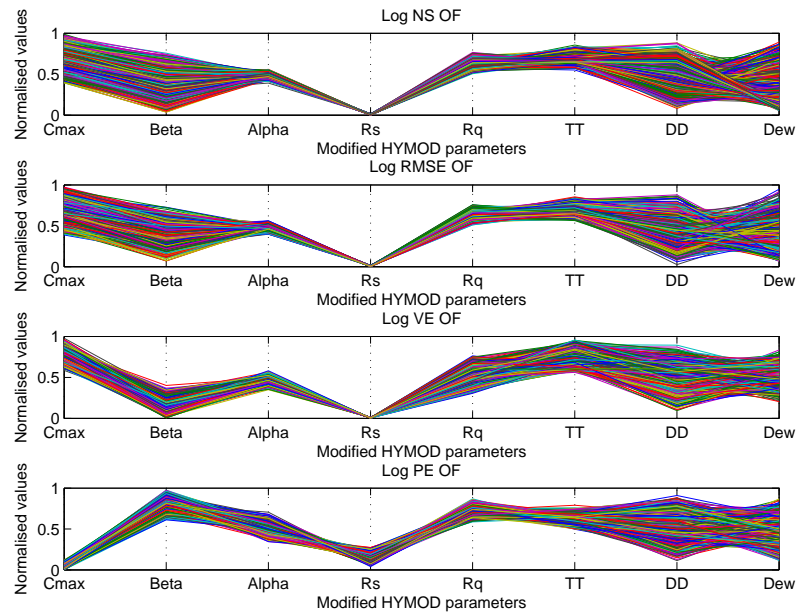


**Figure 6.2:** Parameter values for the different Logarithmic objective functions

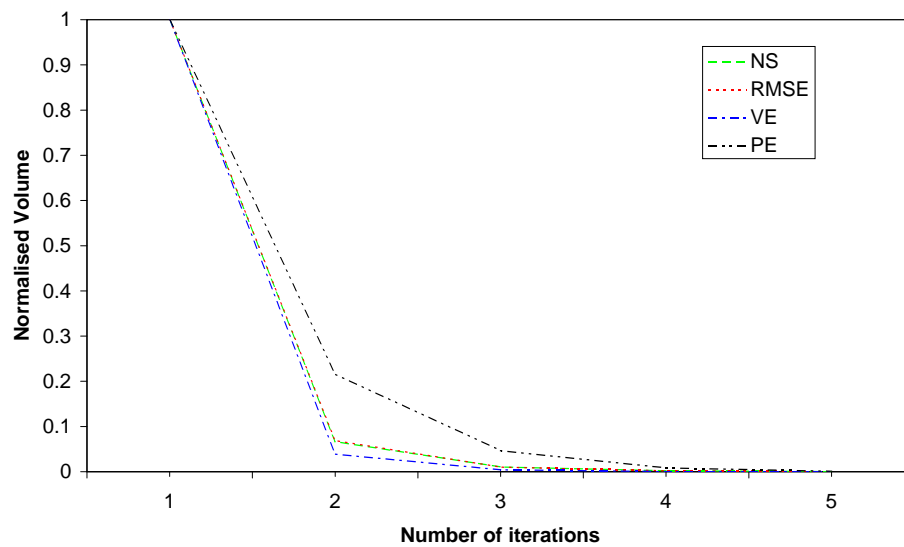


**Figure 6.3:** Decrease in volume of space by each objective functions

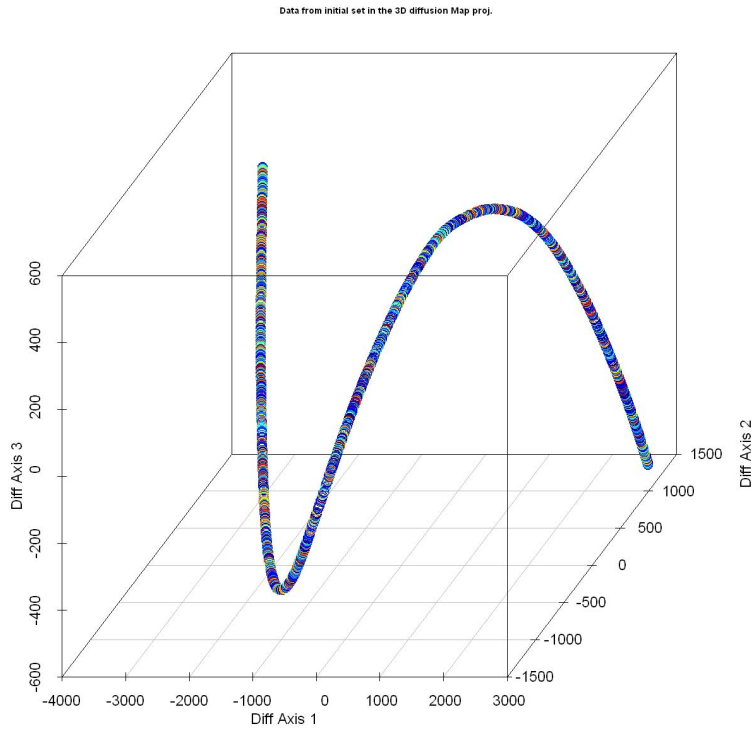


**Figure 6.4:** *Initial parameters in the diffusion space (red colour represents higher performance)*

### 6.2.3 Intersection of parameter space

It would be very ideal case, if there is a set in the parameter space which satisfies all the objective functions. To see this, it is very important to know if there is any intersection of parameter set exists when the model is calibrated by different objective functions. The intersection of parameter space was investigated by the help of the depth function. We calculate how deep the parameter vector is in other parameter vectors. i.e. if there is intersection of parameter space, then depth will be greater than zero. The number of parameter sets having depth greater than 1 gives the strength of intersection. The intersection of parameter vectors at different iteration of ROPE algorithm, obtained by different objective functions, is given in figure 6.8. The number marked inside the circle represents the strength of intersection relative to 1000 (i.e. 1000 means 100 % intersection). It can be seen that there is only intersection between parameter vectors obtained by the Nash-Sutcliffe coefficient and root mean square error. It shows that the Nash-Sutcliffe coefficient and root mean square error are of similar nature and they map the parameters in a similar fashion. They give emphasis to nearly same behavior of hydrograph. This is because the formulations of root mean square error and Nash-Sutcliffe coefficient are very similar. At the initial iteration, all the objective function

## 6 Impact of Objective Function on Mapping of Model Parameters During Calibration

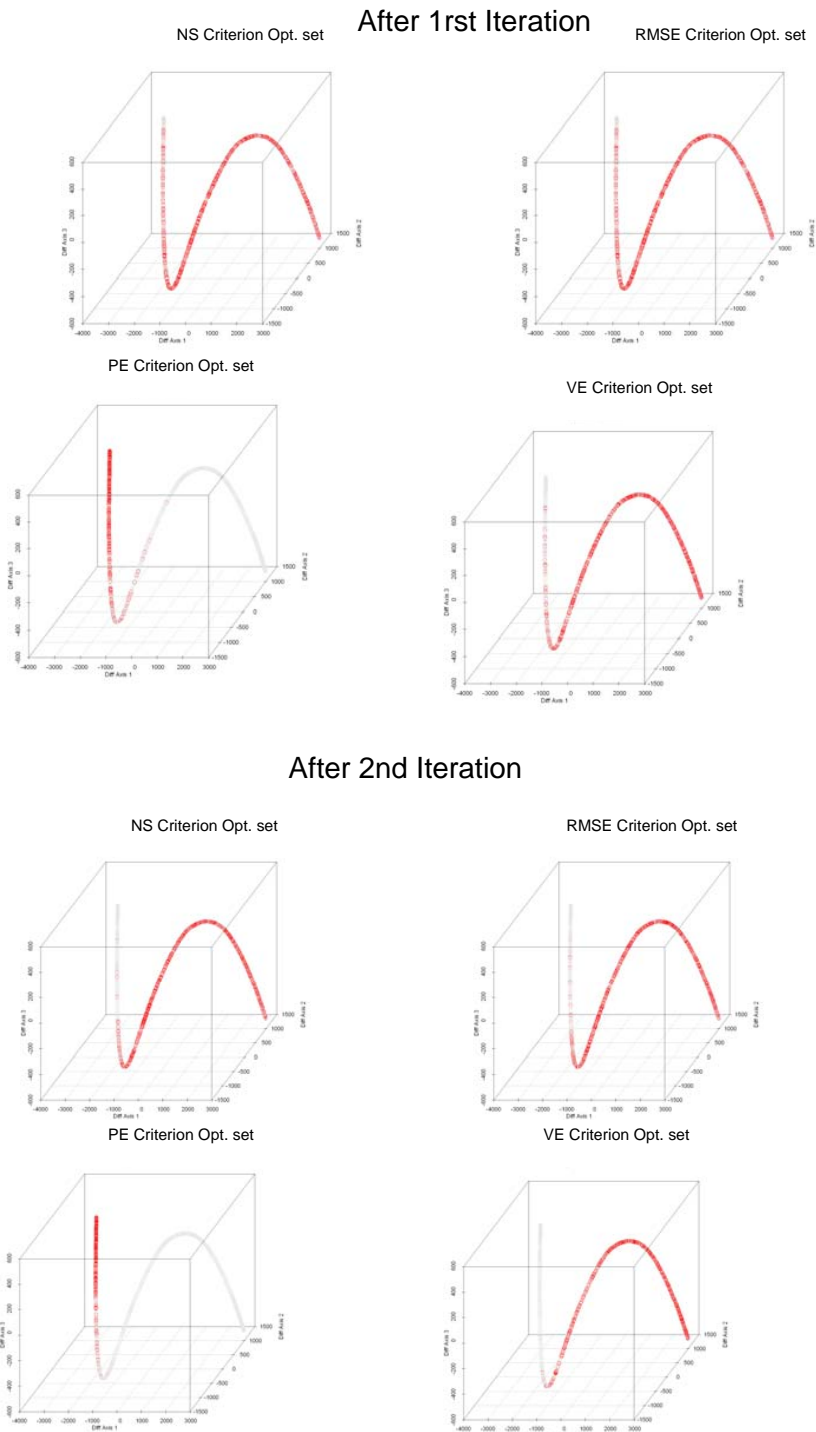
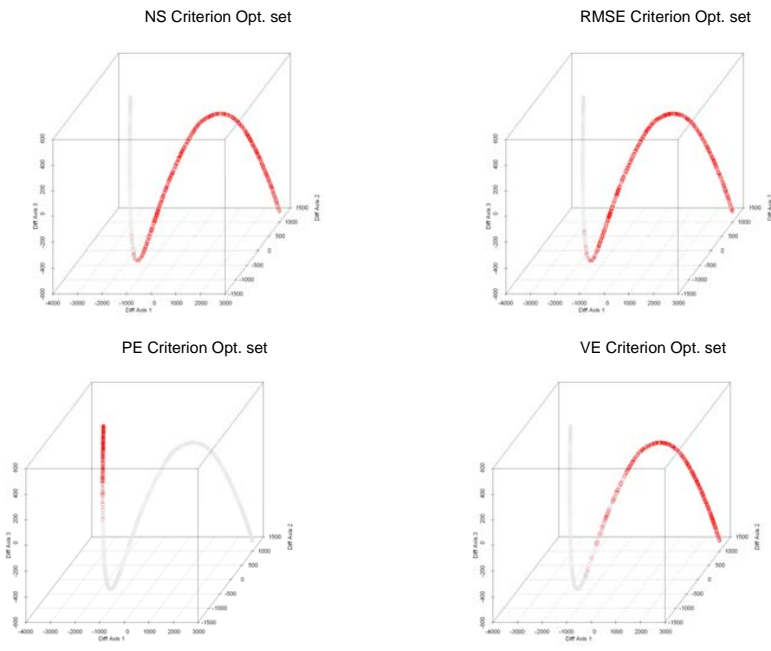


**Figure 6.5:** Decrease in volume of space after third and fourth iteration of ROPE algorithm by different objective functions in diffusion space



After 3rd Iteration



After 4th Iteration

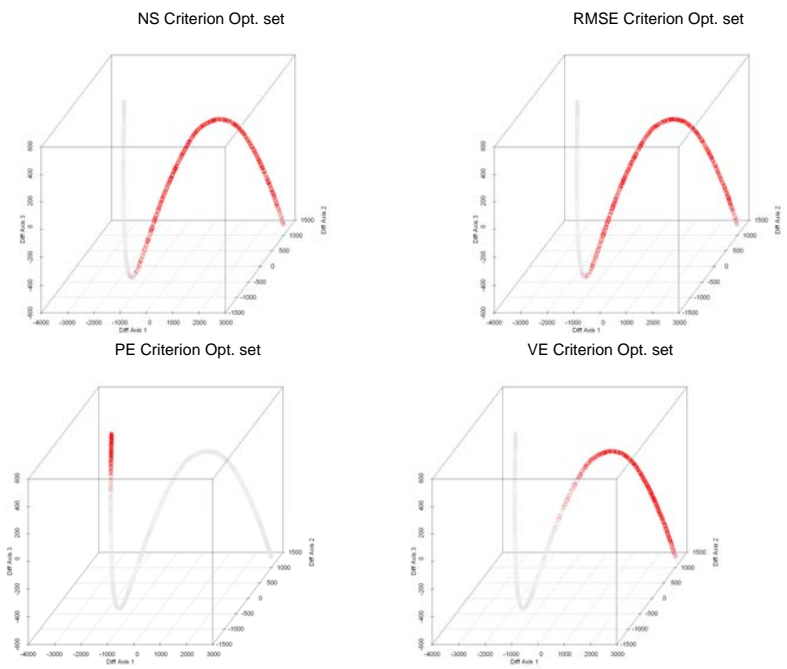


Figure 6.6: Decrease in volume of space after first and second iteration of ROPE algorithm by different objective functions in diffusion space

## 6 Impact of Objective Function on Mapping of Model Parameters During Calibration

After 5th Iteration

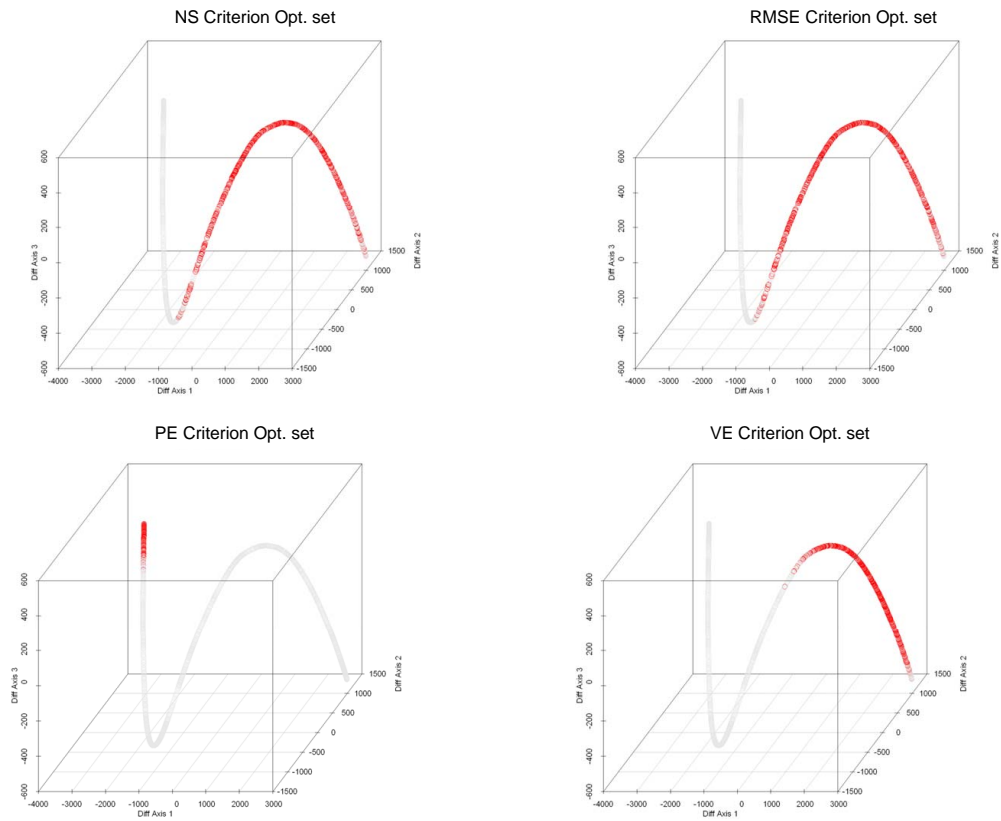


Figure 6.7: Decrease in volume of space after fifth iteration of ROPE algorithm by different objective functions in diffusion space

do have intersection space, and is common to all. However, as iteration increases, this intersecting space, becomes weaker and weaker. As we can see from iteration four, there is no intersection for OF1, OF3 and OF4, same as in iteration five. This shows that these objective function search their parameters in different space. To make a good trade-off between all the objective functions, such that they give equal emphasis to all behavioral aspects of the hydrograph, we tried to get intersection of parameter vectors obtained by different objective function at lower iteration of ROPE algorithm. This can be represented mathematically as:

$$P_1 = P_{NS} \cap P_{RMSE} \cap P_{VE} \cap P_{PE} \quad (6.5)$$

$$P_2 = (P_{NS} \cap P_{RMSE}) \cup (P_{NS} \cap P_{VE}) \cup (P_{NS} \cap P_{PE}) \quad (6.6)$$

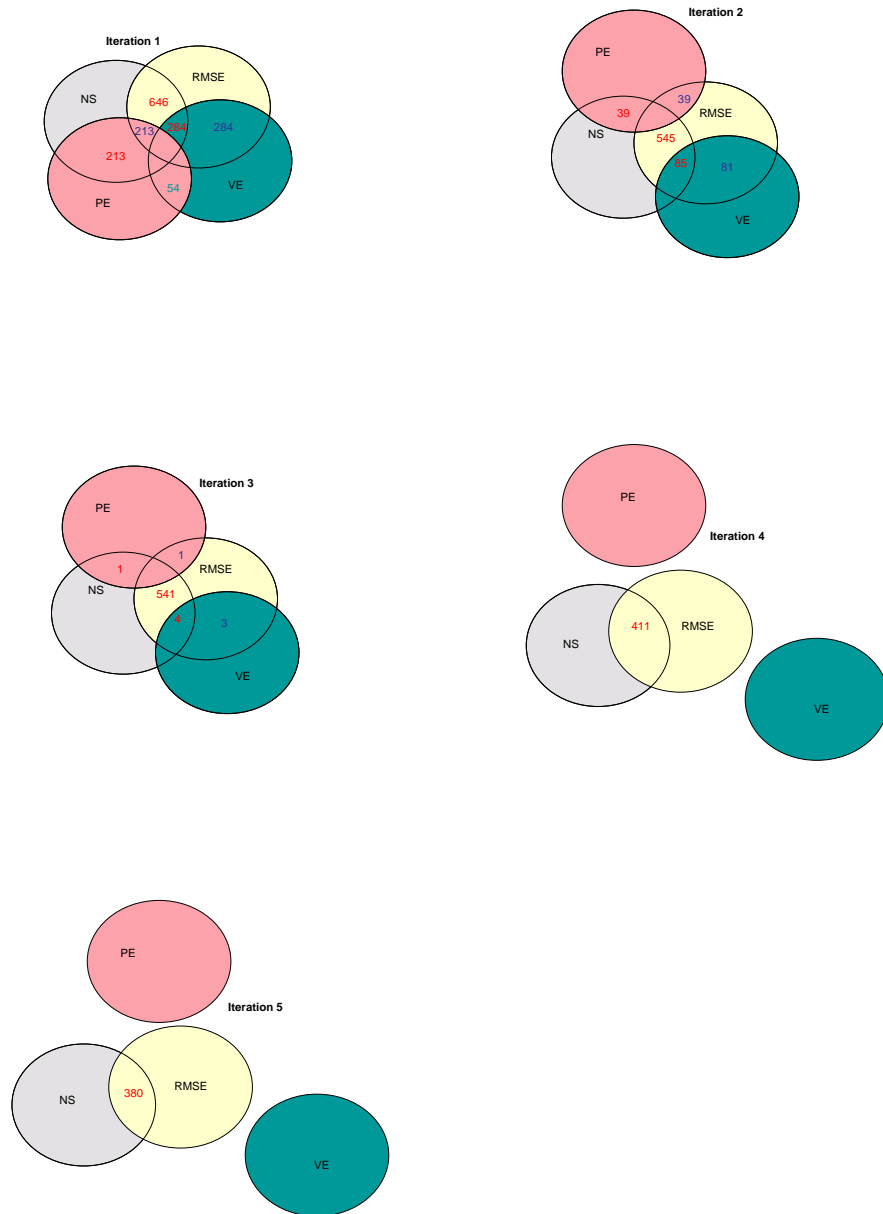
Where,  $P_1$  is parameter space, which is intersection of all the parameter space obtained by each objective functions.  $P_{NS}$  is parameter space obtained by calibration using OF1 as objective function. Similarly,  $P_{RMSE}$ ,  $P_{VE}$ ,  $P_{PE}$  are the parameter space obtained as OF2, OF3 and OF4 used for calibration.  $P_2$  is the parameter space of union of pairwise intersection of parameter space, obtained during calibration based on different objective functions.  $P_1$  and  $P_2$  was obtained for all iterations of ROPE algorithm and it was found that at higher iteration  $P_1$  marked dark in figure 6.9 is void set. It was also found that at higher iteration  $P_2$  is also a void set, but at lower iteration they are not. So, we have to take parameter space at lower iteration, since this space satisfied all the behavior of the hydrograph. Now if we calibrate using any of the objective functions we may expect better parameters, as we have chosen the parameter from restricted space which can describe the hydrograph better. However, the space  $P_1$  and  $P_2$  is very small and it existing at lower iteration only. Therefore, we can not expect a very good model calibration performance because we get  $P_1$  at the initial iteration of the ROPE algorithm. Figure 6.10 shows the histogram of performance and compares the result obtained when calibrated from space  $P_1$  with other space. It can clearly be seen from the figure that performance is not as good as when calibrated with whole space. This is because the volume of  $P_1$  is very small. We could increase the space by taking  $P_2$  but in this space the performance is also poor; the reason is the same as mentioned above for parameter space  $P_1$ .

The proper explanation for the poor performance, when calibrated using space  $P_1$  and  $P_2$  space is given by figure 6.8. It can be seen clearly that as iteration in ROPE algorithm, increases  $P_1$  and  $P_2$  decrease. At higher iteration,  $P_1$  is a void set and  $P_2$  has very small space. This proves that different objective functions emphasise different behavior of the hydrograph and there is no space available that can satisfy all the objective function. This also highlights sensitivity of ROPE algorithm with respect to objective functions.

#### 6.2.4 Hierarchical optimization

It is very clear from above diagnosis of parameters space for different objective functions that there is no space that can precisely simulate all the important characteristics of

6 Impact of Objective Function on Mapping of Model Parameters During Calibration



1

**Figure 6.8:** Intersection of parameter space for different objective functions at different iterations of ROPE algorithm (the numbers specify the strength of intersection)

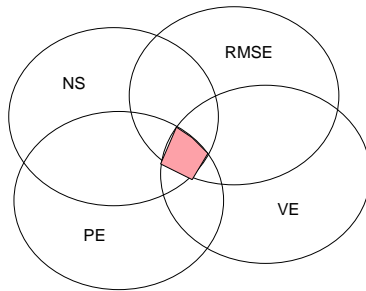


**Figure 6.9:** *An ideal intersection of parameter space for different objective functions*

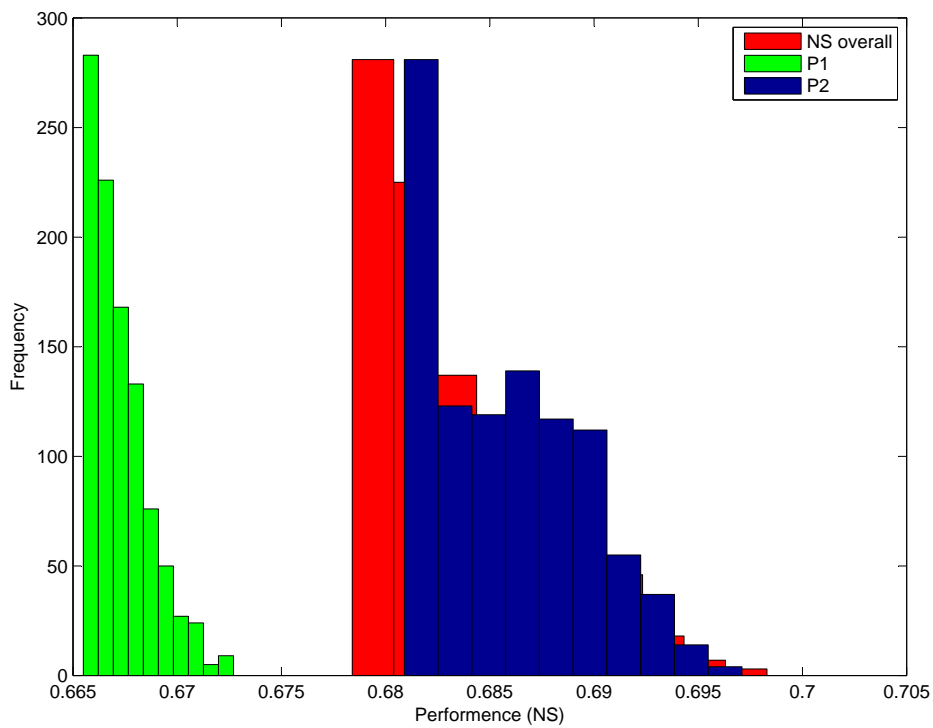


**Figure 6.10:** *Comparison of the performance from space  $P_1$ ,  $P_2$  over all space*

hydrograph. Furthermore, different objective functions achieve optimal parameters at different rates. From the literature we can see that many authors have questioned the credibility of using single objective function (Gupta et al., 1998; Yapo et al., 1998; Vrugt et al., 2003; Tang et al., 2006; Khu and Madsen, 2005) and many more. To overcome the problem of single objective function a hierarchical optimization algorithm was proposed. The algorithm for hierarchical optimization (HOP) can be summarized as:

1. Constrain the search domain of ROPE algorithm using one objective function which is universal in nature and give importance to over all characteristics of hydrograph.
2. Further constrain the space using another objective function
3. Repeat steps 1 and 2 until we fulfill our requirement to represent the dynamics of the hydrograph.

In this method, it is advisable that the first objective function should be such that it should be good enough to represent overall characteristics of the hydrograph and good for transferability to another time period.

### 6.3 Application and Results

The HYMOD model was calibrated using ROPE algorithm on the Upper Neckar catchment for time period 1961-70 in two ways. Firstly, model was calibrated separately on all the eight objective functions mentioned above. The performance of the model by each objective function is given in tables 6.4 and 6.5, where different performance criteria is calculated for each objective function. The logarithm of objective functions have outperformed the general objective functions. This is because the logarithm of objective functions gives equal weight to extreme and low-flow. We can see from table that OF1 and OF2 have very similar all the performance criteria, whereas OF3 and OF4, volume error and peak error are better, as they have been calibrated on this as an objective function. Nonetheless, they have low Nash Sutcliff coefficient and high RMSE. Figure 6.11 and 6.12 shows hydrograph and difference of 95 and 5 percentage of discharge of different hydrographs contained by different objective functions. We can see that the Nash-Sutcliff coefficient and root mean square error have captured a very similar dynamic. This is because they have very similar parameter search space. OF4 has given more importance to peaks and has been reflected in the hydrograph, as they have better dynamic at peaks. The difference of 95 and 5 percentage is lower for volume error and highest for peak error. This may be due to not having a proper overall balance. Both peak error and volume error objective functions give importance to only particular parts of the hydrograph.

Secondly, the model was calibrated on HOP algorithm and comparison was made from above mention result. Logarithmic Nash Sutcliff coefficient is a general purpose objective function. Hence, it was used firstly to get initial parameter space in HOP algorithm. Subsequently log RMSE, log volume error, and log peak error, was used as objective

Diff. OF		NS	RMSE ( $m^3/s$ )	Volume Error	Peak Error
OF1	Mean	0.683	3.879	0.360	0.332
	Max	0.698	3.910	0.408	0.350
	Min	0.678	3.787	0.331	0.309
	Std.	0.0041	0.0252	0.0138	0.0076
OF2	Mean	0.684	3.876	0.362	0.331
	max	0.697	3.908	0.421	0.348
	Min	0.679	3.795	0.333	0.311
	Std.	0.0042	0.0261	0.0145	0.0073
OF3	Mean	0.627	4.211	0.315	0.382
	Max	0.663	4.434	0.316	0.430
	Min	0.586	4.000	0.310	0.346
	Std.	0.0145	0.0818	0.0011	0.0154
OF4	Mean	0.581	4.460	0.621	0.294
	max	0.666	4.847	0.703	0.297
	Min	0.506	3.986	0.451	0.285
	Std.	0.0257	0.1374	0.0392	0.0022

**Table 6.4:** *Optimized at different objective functions but all the performance criteria is calculated for each objective function*

function in subsequent iteration of ROPE algorithm. This means, at each iteration of ROPE we used different objective function. This gives a parameter space at end of calibration, which may be good for all the objective function, as all objective function was used in defining boundary of parameter space. Table 6.6 shows the performance obtained by hierarchical optimization using log objective functions. The performance obtained is very similar to individual logarithm of objective functions. For example, Nash Sutcliff coefficient of 0.78, RMSE of  $0.397 m^3/s$ , volume error of 0.609 and peak error of 0.093 is obtained when they are calibrated on these objective function (table 6.5), whereas Nash Sutcliff coefficient of 0.779, RMSE of  $0.397 m^3/s$ , volume error of 0.648 and peak error of 0.133 is obtained when they are calibrated based on HOP algorithm (table 6.6), which is practically the same. Hence, we can say that, the HOP can be used as multi-objective calibration. The beauty of hierarchical objective function is that we can search our parameters in all the domain. This has been reflected in lower standard deviation of the performance in final optimal parameter space obtained by hierarchical calibration (table 6.6). The final parameters are such that they fulfill all the criteria of different objective functions.

Hierarchical calibration may lead us to space which will be more robust for all objective functions. As we have seen from the diagnosis of parameter space, each different objective function search parameters in a different way and has an entirely different range of final parameters and different distribution (fig. 6.13). Hence, if our purpose of the model is for flood forecasting and instead of choosing Nash-Sutcliff coefficient or peak error

## 6 Impact of Objective Function on Mapping of Model Parameters During Calibration

Diff. OF		NS	RMSE ( $m^3/s$ )	Volume Error	Peak Error
OF5	Mean	0.780	0.397	0.671	0.138
	Max	0.786	0.399	0.727	0.158
	Min	0.778	0.391	0.628	0.122
	Std.	0.0017	0.0015	0.0181	0.0066
OF6	Mean	0.780	0.397	0.669	0.138
	Max	0.787	0.398	0.718	0.156
	Min	0.778	0.391	0.628	0.122
	Std.	0.0016	0.0014	0.0168	0.0064
OF7	Mean	0.758	0.416	0.609	0.164
	Max	0.776	0.445	0.612	0.217
	Min	0.724	0.401	0.600	0.132
	Std.	0.0083	0.0071	0.0024	0.0153
OF8	Mean	0.540	0.573	1.287	0.093
	Max	0.632	0.677	1.623	0.094
	Min	0.360	0.513	1.097	0.090
	Std.	0.0465	0.0285	0.0994	0.0005

**Table 6.5:** Optimized by logarithm of different objective functions but all the performance criteria is calculated for each objective function

	NS	RMSE ( $m^3/s$ )	Volume Error	Peak Error
Mean	0.779	0.397	0.648	0.133
Max	0.784	0.400	0.654	0.134
Min	0.776	0.393	0.640	0.130
Std	0.0015	0.0013	0.0024	0.0007

**Table 6.6:** Result from hierarchical calibration



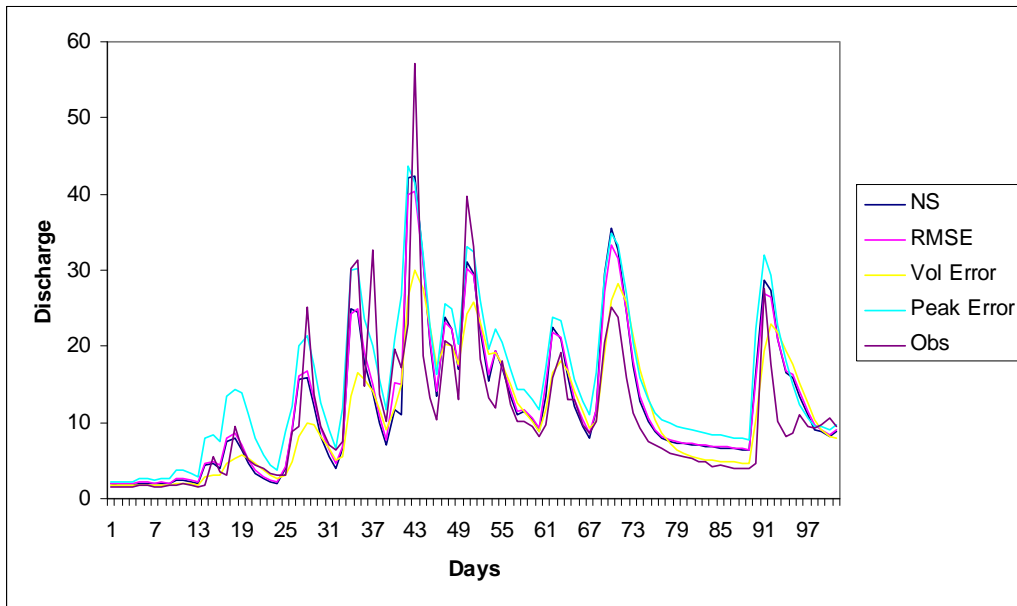


Figure 6.11: Hydrograph from different objective functions

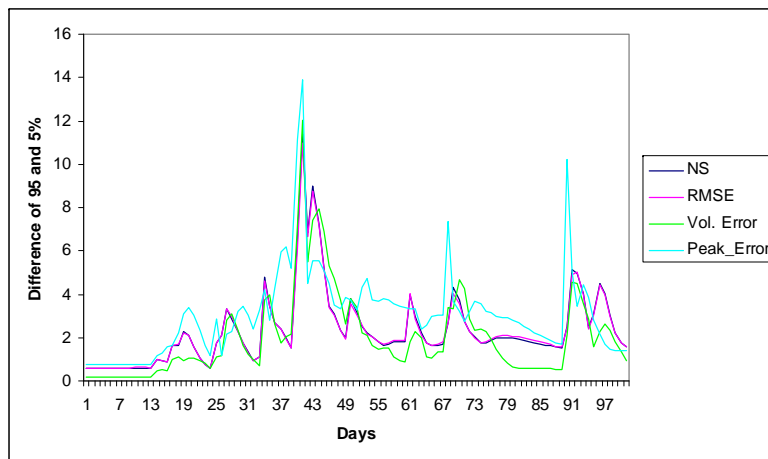


Figure 6.12: Difference of 95 and 5 percent from different objective functions

as objective function for calibration, we choose volume error as objective function, this will lead to false and uncertain prediction. So it is very important to chose a proper objective function and provide an large enough number of iterations to reach optimal parameters.

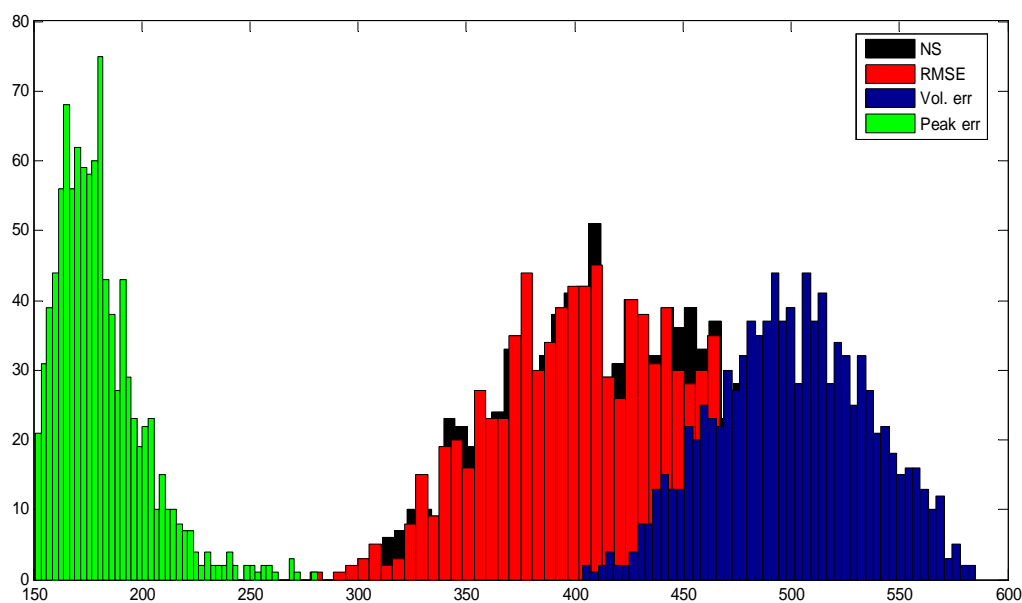


Figure 6.13: Distribution of parameter ( $C_{max}$ ) obtained by different objective functions

## 6.4 Conclusions

- In this chapter parameter space mapped by different objective functions were investigated. It could be shown that each objective function lead to very different optimal parameter space. This is because each objective functions give emphasise on different part of hydrograph.
- Optimal parameter space searched by each objective function are different. Hence, no parameter space exists, that may be good for all the objective functions simultaneously in order to fit or describe completely and accurately the characteristics of the hydrograph.
- From the examples discussed in this chapter, one can see that a proper choice of a particular objective function is important for reducing uncertainty in prediction. This is simply because-if we need to give importance to the peak of the hydrograph

and choose volume error as an objective function-we may lead to wrong parameter space.

- Based on the objective functions, a large enough number of iterations should be provided in order to reach optimal parameter sets. This is because the volume reduction of the parameter space for each objective function is different.
- A Hierarchical calibration strategy, which make use of different objective function simultaneously was developed. The Hierarchical calibration may be a good alternative to single and multi-objective calibration, because it ensure robust parameter space for all objective function.

## 7 Calibration of Hydrological Models on Hydrologically Unusual Events

The study of the use of data depth has provided an insight into the robustness in selection of a region in a space which may contain more information. The length of the observation period used for model calibration has a great influence on the identification of the parameters. So in this chapter, data depth has been used to select information rich segments from a series and to calibrate the model using this information to improve the efficiency of the model calibration.

### 7.1 Introduction

The available past observations of discharge and weather (temperature, precipitation, etc.) are used for calibration purposes. The observation period might contain floods, droughts and a normal flow period. It can be assumed that the calibration can only be successful if the observation period is representative of the hydrological behavior of the catchment. The information contained in the observations with respect to the parameters is not uniformly distributed along the series. Certain time periods might be useful for the identification of specific parameters while others might be useless. For example, summer observations are of no use to identify snow melt related parameters. In a study, [Wagener et al. \(2003\)](#) show that information contained in a data series is non homogeneous. Only certain time period of the observation series truly represent the hydrological behavior of a catchment.

The length and information content of a time series play a vital role in the parameter identification of a model. Several authors have investigated the subject of data requirement for the identification of stable parameters ([Gupta and Sorooshian, 1985](#); [Harlin, 1991](#); [Yapo et al., 1996](#); [Xia et al., 2004](#); [Perrin et al., 2007](#); [Seibert and Beven, 2009](#)). Even so it is very difficult to say precisely what length of data is enough to perfectly identify the model parameters. Other investigators had reported a data length of one year to 8 years as being sufficient to obtain robust parameters. However, it can not be generalized because different models have different levels of complexity. Moreover, the information content of data is generally not known. For this reason we always use whole data series so that the model can get correct information to identify its parameters. There are several cases where the time series are not complete. There is a need, therefore, for some method which can identify the critical time period in a given time series and which contains most of the information to identify the model parameters.

The proper choice of calibration data may play a great role in identifying parameters for

the hydrological model. However, it still remains difficult to say which data and what length of data is sufficient for the proper choice of calibration data for the ideal identification of model parameters. The data which contains lots of hydrological variability may be the best choice for calibration data because they contain most of information for parameter identification (Gupta and Sorooshian, 1985). In this chapter, a similar hypothesis was tested, assuming unusual events in a given series may represent most of hydrological variability. These unusual events are termed as critical events since they contain most of the information which can help us in the identification of proper model parameters.

The objective of this chapter is to develop a simple and reliable technique for the identification of those time periods (events) that can best be used for the model calibration. It is assumed that if a model works well in critical time periods it may work well in general. Critical events correspond to unusual circumstances such as the appearance of unusual rainfall amounts or increases of discharge or long dry periods. These events can be identified from the observations with the help of the statistical depth function.

## 7.2 Methodology

For illustrating the methodology, an example of linear regression was selected as a theoretical problem. Simple regression fits a straight line  $y = ax + b$  to a data set  $Z_n = (x_i, y_i); i = 1, \dots, n \in \mathbb{R}^2$ . This fit can be described with  $\theta = (a, b)$  where  $a$  and  $b$  are slope and intercept, respectively. Three cases were defined for detail study.

1. Case 1: All the  $n$  points
2. Case 2: Only selected  $n^*$  critical points
3. Case 3: Only selected  $n^*$  (same number as in case 2) random points

A regression line was fitted using  $n$  ( $n = 100$ ) points in two dimension space. For second case  $n^*$  ( $n^* = 10$ ) points were carefully selected from upper and lower spread of data. In case 3  $n^*$  points were selected randomly and regression line was fitted. The process of fitting the line for all three cases was done 1000 times. Repeated trial leads to the histogram. Figure 7.1 shows the histogram of the slope of the line estimated by all three cases. From this figure it is clear that case 1 and case 2 have very similar distribution, whereas for case 3 it is not. This shows that carefully selection of points may produce a result that compares to when using the whole of the data. At first glance, this may appear to challenge the widely repeated concept that we can fit better regression if we use more data. However, to fit a straight, line two points are enough and inbetween points do not bring much information. This can be seen from case 2, where both extremes of data were taken for regression. So from this example, we can see only about 10 percentage of data can give regression nearly equally good if we select carefully. The concept of this theoretical example can be further extended for real hydrological modeling.

A short series of discharges or precipitations may have a great number of sequences which look very similar and can be regarded as a kind of repetition of previous events. Some,

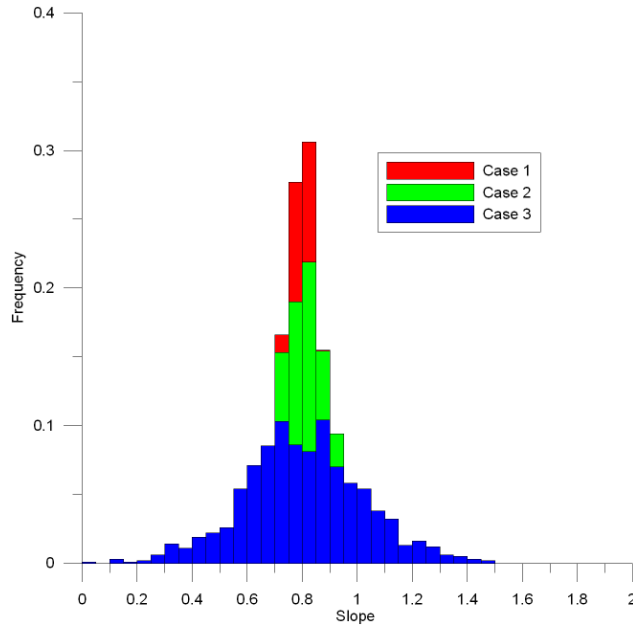


Figure 7.1: Histogram for slopes in all the three cases

however, for example maxima and minima, differ from previous observations. In order to identify unusual hydrological events the statistical concept of data depth is used.

### 7.2.1 Identification of critical time period using data depth function

The information content of the data can enhance the reliability of hydrological prediction. Hence, if we can select only those data which are hydrologically reliable and from a critical time period having more variability then we may improve our calibration process (Gupta and Sorooshian, 1985). To identify the critical time period that contains enough information for identifying the model parameters, unusual sequences in the series of discharges and precipitation are to be identified. The intermittent property of precipitation makes a direct identification of unusual events only for high precipitation amounts possible. However, for hydrological modeling, droughts might be of equal importance. Thus instead of the precipitation  $P(t)$  the series of antecedent precipitation indices is used. The antecedent precipitation index  $API$  is defined as:

$$API(t+1) = \alpha API(t) + P(t+1) \quad (7.1)$$

Where  $0 < \alpha < 1$  is a constant. The higher  $\alpha$  the more influence is assigned to past precipitation. The other possibility to identify unusual hydrological events is to use the observed discharge series  $Q(t)$ . For simplicity, denote the selected series (API or discharge) as  $X(t)$ . Unusual events are defined as a sequence of  $X$  values. For this

purpose the  $d$ -dimensional set of subsequent  $X$  values is defined as:

$$\mathbf{X}_d = \{(X(t-d+1), X(t-d+2), \dots, X(t)) \mid t = d, \dots, T\} \quad (7.2)$$

Where  $T$  is the number of observation time steps available. Again, for simplicity, denote  $X_d(t) = (X(t-d+1), X(t-d+2), \dots, X(t))$ . For each  $t$ , the statistical depth  $X_d(t)$  with respect to the set  $\mathbf{X}_d$  is calculated and denoted by  $D(t)$ . The statistical depth is invariant to affine transformations, however non-linear transformations might have an effect on the depth. Depth can be calculated using untransformed observations, their logarithms or their ranks. Time steps  $t$  with  $D(t) < D_0$  are considered to be unusual. In this chapter, critical events are defined around the unusual (low depth) days. A time  $t$  is part of a critical event if there is an unusual time  $t^*$  in its neighborhood, defined as  $|t - t^*| < \delta_t$ . An example of events which were selected by using discharge and API is given in Figure 7.2. It is important to see that critical events selected by API and discharge are almost at the same time period in a series. This shows that we can use either API or discharge for critical event selections. One can have the impression that only the high magnitude API and discharge can be unusual in nature. This is not true, however: The low API and discharge can also be critical events, though this is not shown in figure 7.2.

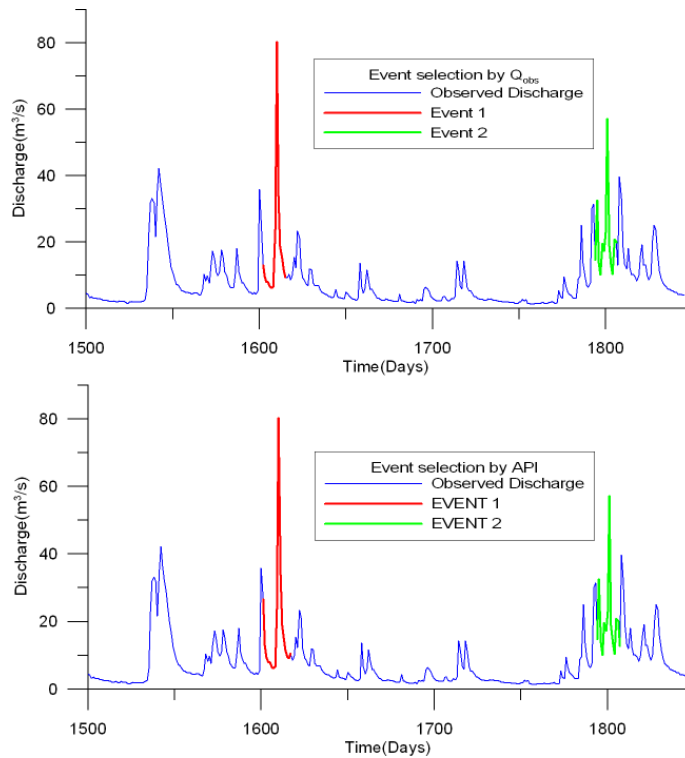


**Figure 7.2:** Example of event selection from Neckar Catchment (Rottwiel)

### 7.2.2 Identification of Critical Events (ICE algorithm)

For practical purpose one might be interested in finding critical events for model calibration. For this purpose the following procedure is suggested.

- Select a discharge or precipitation series
- Calculate API from precipitation series (using equation 7.1)
- Create a multivariate data set of API or discharge series (denoted by  $X_d$  as given by equation 7.2)
- Calculate for each day  $t$  the statistical depth  $D(t)$  of  $X_d(t)$  with respect to the set  $\mathbf{X}_d$ .
- For day  $t$ ,  $D(t) < D_0$  is treated as critical depth and a window of  $n$  day is taken around it as a events.
- Define an objective function, where the objective function is calculated only for the critical events.
- Minimize or maximize the objective function for only those critical events using ROPE algorithm (Bárdossy and Singh, 2008).

## 7.3 Application and Results

To demonstrate the methodology in practical case, two conceptual hydrological model HBV and HYMOD were used on the Upper Neckar catchment.

Unusual event were select using discharge and API for different time period, by applying above mentioned ICE algorithm. Both the model HYMOD and HBV were calibrated using ROPE algorithm on the three cases given below.

1. Case 1 Using whole series for given time period
2. Case 2 Using only selected critical events for given time period
  - Case 2(a) Critical event selection based on discharge series
  - Case 2(b) Critical event selection based on precipitation (API) series
3. Case 3 Using only selected (same number as in case 2) random events for given time period

The mean Nash-Sutcliff coefficient (NS) of parameter vectors obtained by model calibration based on the critical events and randomly selected events were compared with the mean Nash-Sutcliff coefficient of parameters vector obtained by using whole time series. Model calibration is slightly worse than using all data, if one uses the selected critical time period only. Table 7.1 and table 7.2 show the calibration result by HYMOD and



HBV respectively for the time period 1961-70. From the tables it is clear that the performance of the model calibration based on critical time period is comparable with model calibration on whole data series. Cases 2(a) and 2(b) have nearly equal Nash-Sutclif coefficient in calibration for both models. This shows that event selection can be done either using API or discharge give similar parameters in calibration of a model. Both the HBV and HYMOD model have behaved very similar in the calibration period. The most noticeable point is that only six percentage of data is enough to calibrate equally good as when using the whole data provided that the events are selected properly. When the events were selected randomly the calibration performance was poor as compared to events selected with the help of depth function. This is because data depth selects only those events which are unusual and contain more information. It is not a big surprise to get equally good results in calibration when carefully selected data is taken for calibration. Further, its robustness should be reflect in prediction time period. Tables 7.3 to 7.4 show that the model is calibrated on unusual events (selected based on discharge or API) is as good transferable as when whole data series is used for calibration. The transferability was tested for three different time periods (1971-80, 1981-90, 1991-2000). In all the time periods both models behaved similarly well and the transferability was as good as if we had used whole data series. At the same time, when the parameter obtained by calibrated on randomly selected events was transferred to other time period was poor. This shows that a careful selection of events is necessary for proper identification of model parameters. It is also important to note that event selected based on discharge or API give similar results in validation. Hence, it can be conclude that a information contained event can be selected either based on discharge or API.

	mean NS	max NS	min NS	std	days	percentage
Case 1	0.6944	0.7014	0.6921	0.00175	3652	100
Case 2(a)	0.6771	0.6993	0.6282	0.01313	238	6.51
Case 2(b)	0.6810	0.6986	0.6428	0.01002	237	6.48
Case 3	0.6414	0.6654	0.6135	0.00850	242	6.62

**Table 7.1:** Calibration of HYMOD model at Rottweil over period 1961-70

	mean NS	max NS	min NS	std	days	percentage
Case 1	0.6994	0.7140	0.6980	0.00135	3652	100
Case 2(a)	0.6967	0.7090	0.6820	0.00613	238	6.51
Case 2(b)	0.6897	0.7110	0.6800	0.00484	237	6.48
Case 3	0.6571	0.6720	0.6240	0.00703	242	6.62

**Table 7.2:** Calibration of HBV model at Rottweil over period 1961-70

In some of the previous studies (Harlin, 1991; Yapo et al., 1996; Xia et al., 2004; Perrin et al., 2007; Seibert and Beven, 2009) the selection of events was part of continuous series or random selection of events. Here, the random section can not be a good solution for event selection because it will depend on a person's individual expertises. Critical time

## 7 Calibration of Hydrological Models on Hydrologically Unusual Events

	mean NS	max NS	min NS	std
Case 1	0.6241	0.6435	0.5860	0.00909
Case 2(a)	0.6268	0.6474	0.5793	0.01273
Case 2(b)	0.6254	0.6485	0.5973	0.01029
Case 3	0.5214	0.5705	0.4787	0.01856

**Table 7.3:** Validation of HYMOD model at Rottweil over period 1971-80

	mean NS	max NS	min NS	std
Case 1	0.7076	0.7300	0.6820	0.01014
Case 2(a)	0.6995	0.7110	0.6840	0.00545
Case 2(b)	0.6989	0.7230	0.6660	0.01201
Case 3	0.6304	0.6500	0.5930	0.01038

**Table 7.4:** Validation of HBV model at Rottweil over period 1971-80.

identification by data depth function is more robust, since it is using robust properties of data depth function to identify the hydrological variability in a series. The result of this study also demonstrated the fact that when events was selected randomly, it is not good in transferability. This is basically due to the fact that the random selection of events can not select a desired hydrological variability, which can be use for identification of model parameters.

To see the effect of length of the data on the model calibration, the HYMOD model was calibrated on the first year using critical events and subsequently one year of data was added for calibration, thus each calibration has one parameter sets (e.g calibration using 1971 data has one parameter set; second calibration is 1971-72, therefore, two years of data have another parameter set and so on). This procedure was also repeated for randomly selected events. Figures 7.3 and 7.4 show model performance of each parameter set obtained by each calibration, which was validated over ten year periods (1961-70, 1981-90). The X axis shows the number of years used for calibration and Y axis shows the performance over ten years. From figure 7.3, it can be seen that when only one year of data was used for calibration, the validation over 1971-80, Nash Sutcliff coefficient is 0.65, whereas for randomly selected events it was just 0.51. When the first two year of data was used for calibration, the validation performance for 1961-70 has decreased; in comparison randomly selected events performance has increased. This can only be possible by chance (because it may have selected good events from fist year). The addition of a second year brought down the performance; this may be due to insufficient amount of data taken for calibration. In general, it can be seen from figure that performance increases as the number of year increases, but after some period of time, there is no further improvement in the performance. The performance for the critical event selected by ICE algorithm was always better then randomly selected events. On average, seven to eight years of data (critical events) seem to be moderate for model calibration.

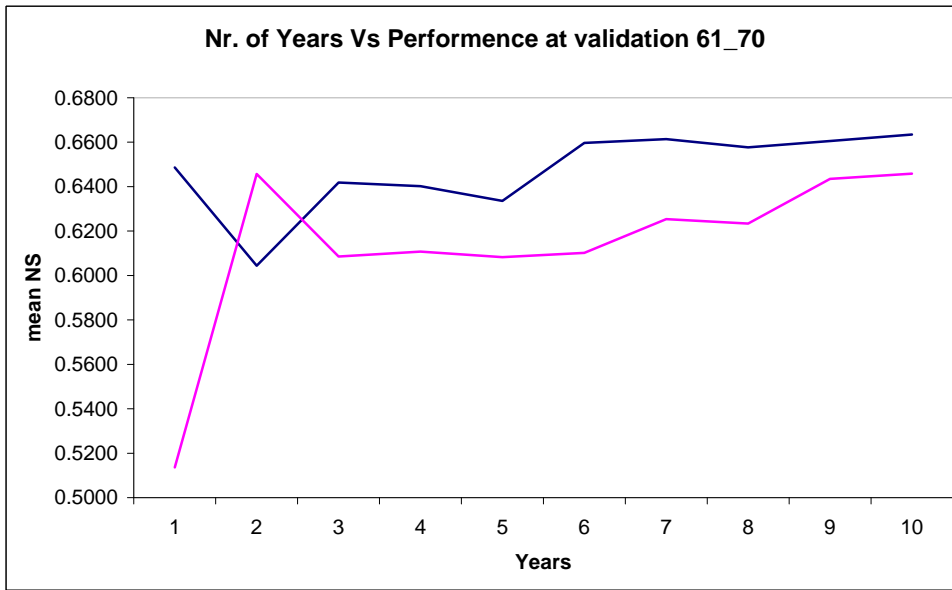


Figure 7.3: The sequential addition of years to the calibration of HYMOD and validated over 10 years (1961-70)

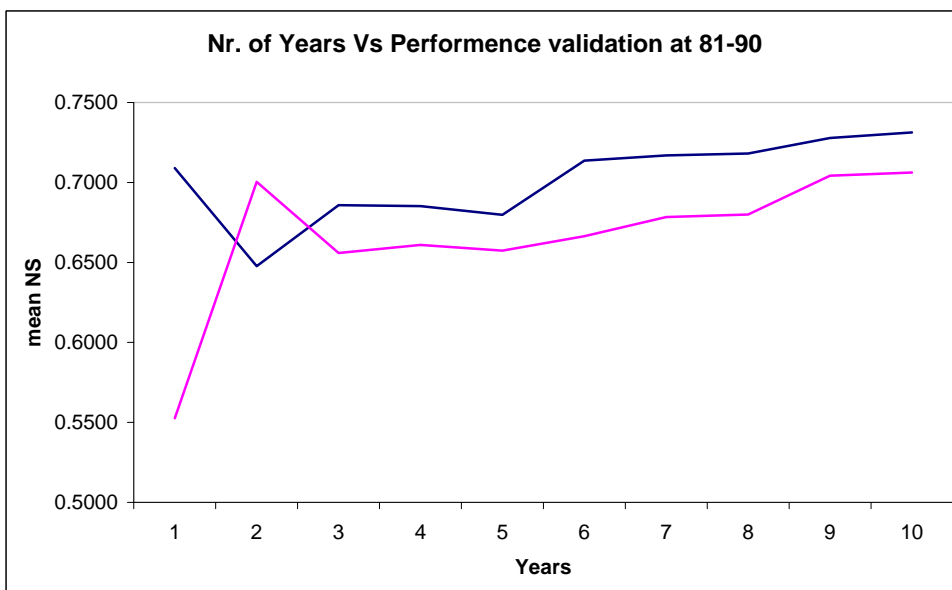


Figure 7.4: The sequential addition of years to the calibration of HYMOD and validated over 10 years (1981-90)

## 7.4 Extension to Ungauged Catchments

In catchments with available discharge data, hydrological model parameters can be estimated using critical events as discussed in section 7.2. But the biggest question remains for ungauged catchments. For ungauged catchments parameters can only be identified using knowledge and availability of hydrological, meteorological and geographical information. The results of the ICE algorithm show that smartly selected and measured events are sufficient to identify the parameters of the model. Indeed, the prediction is as good as that arising from the calibration using the whole time period. Hence, this same concept can be extended in ungauged catchments provided we start measuring unusual events. The possibility of days becoming unusual can be defined by the help of predicted precipitation. With the help of the ICE algorithm we can decide whether the predicted precipitation will lead to critical events or not. If it is a critical event, we can measure the discharge and if it is not a critical then it is not important for the identification of the model parameters. This way, from data scarce regions, we can measure hydrological critical events and the model can be calibrated on these events. For this the strategy adopted in this chapter is given in following section.

### 7.4.1 Practical application: start measuring important events

For measuring important events, a Conditional Depth with Precipitation curve was prepared. This curve can be used based on predicted precipitation. If a given days precipitation makes its statistical depth zero for that day, then it is important to measure the discharge. Which may be useful for model calibration. Figure 7.5 shows a Conditional Depth with Precipitation curve for four different days. It can seen from figure 7.5(a) that if predicted precipitation is more than 10 mm, it will end up being an unusual events; if precipitation is less than that, then it is not important to measure. Similarly, we can see from figure 7.5(c-d) that different amounts of precipitation is making the events unusual. This way form an ungauged catchment we can measure few selected critical events, which may be give more robust result then making some kind of functional or regressional relationship with catchments properties and model parameters.

To illustrate the concept, precipitation for time period 1991-2000 from the Upper Neckar catchment is taken as predicted precipitation. As this is predicted precipitation, the API is calculated in forward ways. Practically, API was calculated step-wise using next days precipitation. This means the series is growing based on predicted precipitation. The ICE algorithm was then used to decide the event is critical or not. In this case, depth was calculated with respect to previous multivariate data set created from the past and this series changes each time as new predicted precipitation come in. The event was selected for the above mentioned time period using the ICE algorithm. This process was repeated for random selection. Hence three cases can be formulated as follows:

1. Case 1 Using whole series for given time period, API is based on known precipitation

## 7.4 Extension to Ungauged Catchments

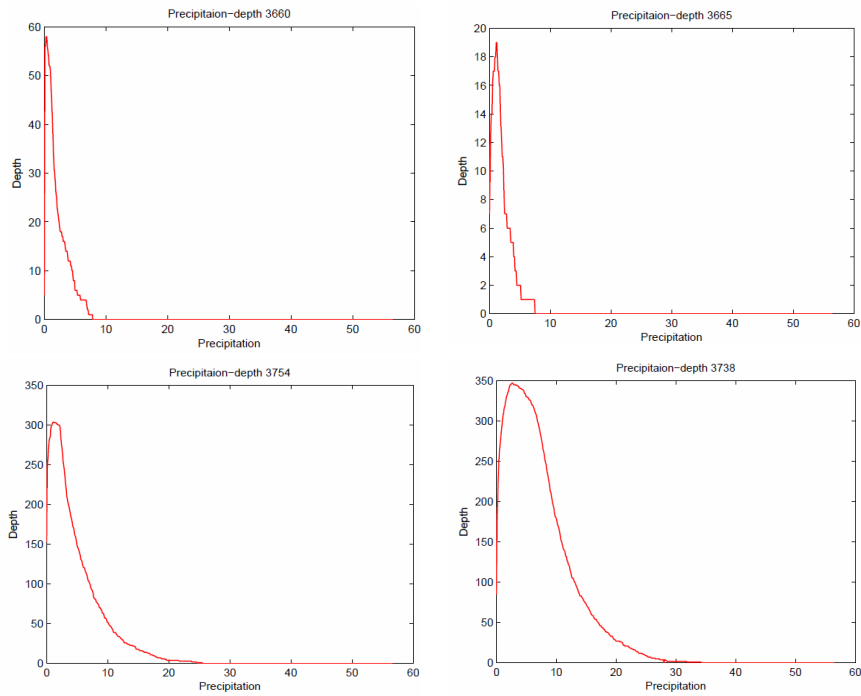


**Figure 7.5:** *Conditional depth with precipitation curve for measuring events*

2. Case 2 Using only selected critical events for given time period, API is based on predicted precipitation
3. Case 3 Using only selected (same number as in case 2) random events for given time period, API is based on predicted precipitation

The HYMOD model was calibrated on all the three cases as mentioned above. Table 7.5 shows that the result of model calibration when the events were selected using predicted precipitation and non-predicted precipitation. The results also show that the calibration from predicted API event selection is slightly worse than when calibrated using whole time period for known precipitation. For the calibration, case 3 is as good as case 2. Table 7.6 shows the transferability to other time periods for all three cases. It is very clear from the table that, for case 2, the performance is as good as case 1; however, case 3 has not shown the same trend in performance for the calibration. This clearly shows that we can use predicted precipitation to decide the unusuality of an event. So this can be easily used for ungauged catchment to measure some critical events. This highlights also the ability of the ICE algorithm to be extended to ungauged catchments and for practical application in deciding which event to be measured.

## 7 Calibration of Hydrological Models on Hydrologically Unusual Events

	mean NS	max NS	min NS	std
Case 1	0.620	0.640	0.613	0.0054
Case 2	0.615	0.645	0.536	0.0193
Case 3	0.615	0.646	0.559	0.0186

**Table 7.5:** Calibration of HYMOD for Rottweil for time period 1991-00; event selection is based on predicted precipitation and known precipitation

	mean NS	max NS	min NS	std
Case 1	0.734	0.759	0.708	0.0100
Case 2	0.731	0.758	0.672	0.0140
Case 3	0.713	0.749	0.615	0.0183

**Table 7.6:** Validation of HYMOD for Rottweil for time period 1981-90; event selection is based on predicted precipitation and known precipitation

Hence, it is advisable to prepare a Conditional Depth with Precipitation curve for ungauged catchments of interest. Based on this curve and given actual precipitation, one can decide to measure the event or not. Once we have certain number of events we can calibrate our model for that ungauged catchment. This will be more reliable than any other method for prediction in ungauged basins.

## 7.5 Applications of the ICE Algorithm

To test further the robustness and to generalize, the ICE algorithm was tested on different models and different catchments

### 7.5.1 Result from physically based model

The ICE algorithm was developed using conceptual model. To make more general purpose, it was used in a complex physically based model like WaSim-ETH. A brief explanation of the application of the ICE algorithm for WaSim-ETH is given in this section; for more details please refer to combine work with [Liang \(2010\)](#). For details about the WaSim-ETH model refer to Chapter 4. The study area chosen for this work is located in the Rems catchment (for more details, refer to chapter 4). The data for the period 1992-1993 was chosen for the model calibration. Year 1992 was used for model warm up. A events were selected based on discharge using ICE algorithm. An example of event selected from calibration period is given in figure 7.6. It is very noticeable here that low flow can also be chosen as a critical event. The TOPMODEL approach of WaSim-ETH model was used in this chapter. The nine most sensitive parameters of soil modules were calibrated using the ROPE algorithm for two cases:

- Case 1 Using whole data set
- Case 2 Using carefully selected events

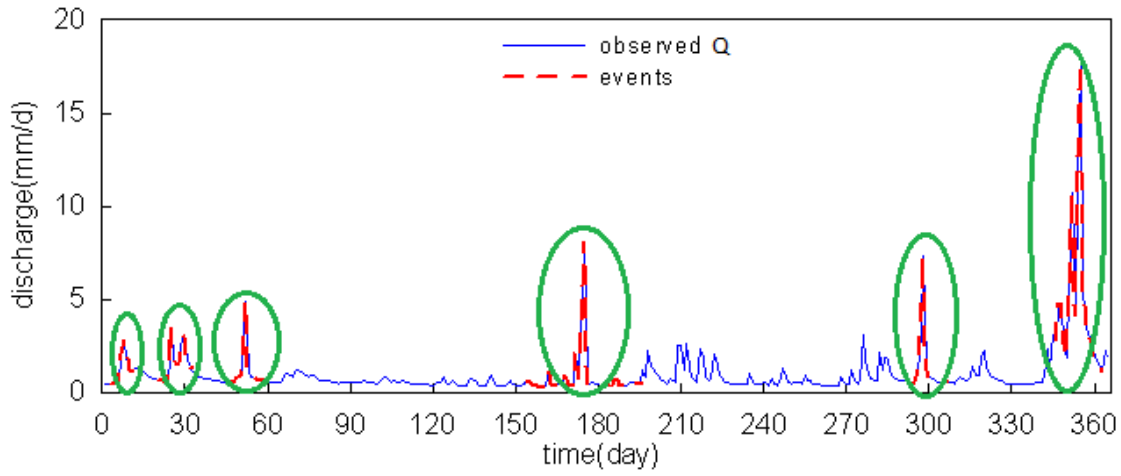


**Figure 7.6:** Critical events selected from year 1993 from Rems catchments

Para.		initial	min	max	mean	std.
$m$	case 1	0.0001-0.2	0.006	0.080	0.035	0.022
	case 2		0.0004	0.086	0.040	0.022
$T_{kor}$	case 1	0.1-500	6.71	52.4	29.5	11.3
	case 2		7.29	78.8	44.5	20.1
$K_{kor}$	case 1	0-5000	38.7	922.7	455.9	205.1
	case 2		80.7	946.9	476.0	212.2
$k_D$	case 1	0-500	31.6	53.2	42.7	4.25
	case 2		39.6	61.3	49.4	2.49
$sh_{max}$	case 1	0-100	3.66	57.0	32.5	13.2
	case 2		9.71	85.7	46.3	21.8
$k_H$	case 1	0-1000	29.9	254.1	141.1	53.9
	case 2		41.3	454.7	228.5	99.8
$P_{grz}$	case 1	0-100	1.520	23.4	13.2	5.50
	case 2		0.806	43.3	21.7	9.66
$r_k$	case 1	0-1.0	0.211	0.846	0.546	0.174
	case 2		0.112	0.944	0.536	0.212
$cmlt$	case 1	0-1.0	0.217	0.943	0.551	0.172
	case 2		0.060	0.878	0.487	0.209

**Table 7.7:** Statistics of the best 10 % parameter sets of WaSim-ETH, calibrated by ROPE algorithm

Table 7.7 shows the statistical result of the best 10 % calibrated parameter set. It is very clear from table that model parameters obtained using both cases (as mentioned above) is very different. In order to see the difference of parameter properties obtained during calibration for both cases, the distribution of each parameter value is plotted (fig 7.7). Here, one can see that, parameter distribution for each case is different. Some of the parameters, like  $K_d$ , the surface flow recession constant, are more structured in case 2 than case 1. This shows that this parameter is more identifiable in case 2. When we look carefully at the model structure, this parameter is active during peak flows, and event selected by ICE algorithm were related to peaks. So it is obvious that these parameter get a better chance to adjust during calibration in case 2. Very similar features can be seen in other parameters. To compare the structure of the distribution of parameter obtained in both the cases, the statistical entropy was introduced. Smaller entropy means more structure in distribution. Statistical entropy is given by:

$$S = - \sum p_i \ln p_i \quad (7.3)$$

where  $i$  is the class of discretization and  $p_i$  is the corresponding probability of occurrence in that class. Statistical entropy for all the parameters of WaSim-ETH model is given in table 7.8. The entropy values for parameters  $m$ ,  $r_k$  and  $cmlt$  calibrated using case 1 are smaller, which implies that these parameters are more concentrated in one or two certain classes, while those calibrated using case 2 are more scattered. On the other hand, parameters  $T_{kor}$ ,  $k_D$ ,  $sh_{mx}$ ,  $k_H$  and  $P_{grz}$  have a lower statistical entropy values in case 2. This shows that these parameters as more structured in this case where we selected events by the ICE algorithm. This gives more identifiability to these parameters. For  $K_{kor}$ , the entropy values in both cases are more or less the same, which means the identifiability of this parameter on certain values doesn't change much. However, it doesn't mean these certain values will be the same since entropy only represents the scattering degree of a sample, but not why at which point of the sample is scattered.

Para.	$m$	$T_{kor}$	$K_{kor}$	$k_D$	$sh_{mx}$	$k_H$	$P_{grz}$	$r_k$	$cmlt$
case 1	1.74	1.97	2.04	1.05	2.12	1.98	1.99	1.80	1.91
case 2	2.04	1.76	2.07	0.52	1.77	1.72	1.81	2.03	2.09

**Table 7.8:** Statistical entropy for different parameters of WaSim-ETH

The calibrated WaSim-ETH model was validated for another time period (1994-1996). Table 7.9 shows the calibration and validation results. The comparison for both the cases were made based on several objective functions as given in table. For different objective functions, the performance of the parameter sets obtained by case 1 is slightly better than those by case 2 in calibration period. However, if we look for the validation period, the result obtained by both the cases is nearly the same. The mean Nash Suttcliff coefficient for year 1994, 1995, 1996 is 0.93, 0.78 and 0.88, respectively, in case 1 and is very similar in case 2. Calibration using both the cases is therefore, nearly the same. To aid the visual appraisal of the results, the hydrograph for the calibration and validation period is plotted in figure 7.8. ROPE calibration does not give single parameter set,



## 7.5 Applications of the ICE Algorithm

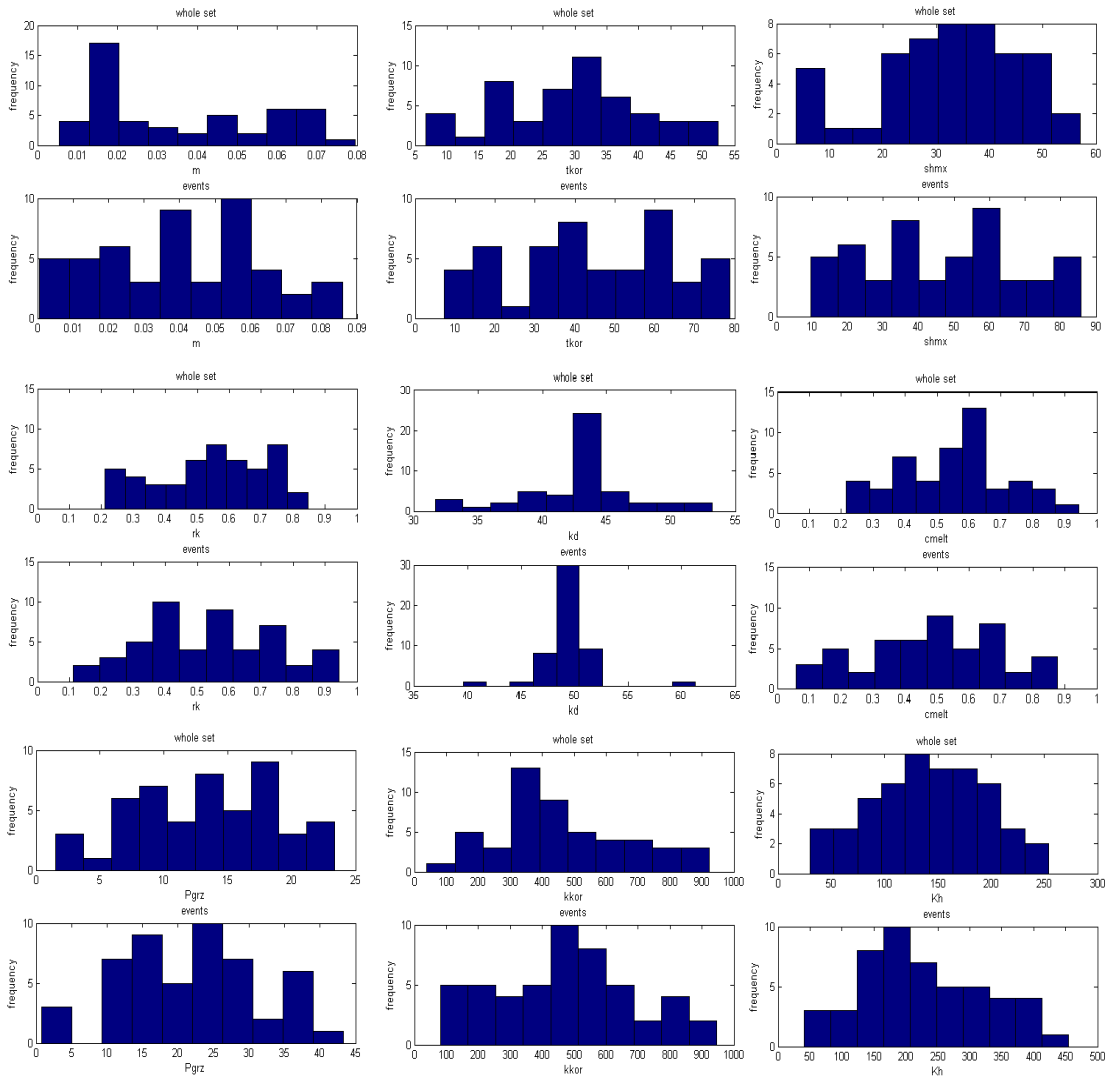


Figure 7.7: Distributions of parameters calibrated in both cases

instead giving parameter space, hence confidence bound for hydrograph is plotted in figure 7.8. As we can see from figure, in both the cases, dynamic of hydrograph is same in calibration period except at certain peaks (e.g. at days around 330 to 360). During validation for year 1994 to 1996, the result in case 1 and case 2 is nearly equal. This clearly indicates that the event selected by ICE algorithm is also suitable for calibrating a very complex physically based model.

Obj. func.		calib93		valid94		valid95		valid96	
		case 1	case 2	case 1	case 2	case 1	case 2	case 1	case 2
NS	min	0.833	0.833	0.924	0.924	0.738	0.779	0.869	0.868
	max	0.851	0.841	0.951	0.947	0.816	0.816	0.913	0.914
	mean	0.837	0.834	0.932	0.925	0.786	0.781	0.884	0.871
	stdv	0.006	0.001	0.010	0.004	0.012	0.006	0.016	0.008
logNS	min	0.761	0.761	0.709	0.709	0.723	0.736	0.594	0.612
	max	0.808	0.789	0.775	0.768	0.792	0.785	0.672	0.664
	mean	0.774	0.762	0.734	0.712	0.754	0.739	0.631	0.615
	stdv	0.018	0.005	0.028	0.012	0.020	0.010	0.022	0.010
RMSE	min	0.573	0.593	0.397	0.411	0.405	0.404	0.218	0.217
	max	0.606	0.606	0.493	0.494	0.483	0.443	0.267	0.268
	mean	0.600	0.606	0.464	0.490	0.435	0.441	0.251	0.265
	stdv	0.010	0.003	0.035	0.015	0.013	0.006	0.017	0.009
logRMSE	min	0.292	0.306	0.316	0.321	0.285	0.289	0.310	0.313
	max	0.326	0.326	0.360	0.360	0.328	0.320	0.344	0.337
	mean	0.316	0.325	0.344	0.358	0.309	0.319	0.328	0.335
	stdv	0.013	0.004	0.018	0.008	0.013	0.006	0.010	0.005

**Table 7.9:** Statistics for calibration and validation of WaSim-ETH (best 10 % performance)

## 7.5.2 Result from data driven model

The ICE algorithm was also applied in improving the training of Artificial Neural Networks (data driven model for fitting), an application that relies on information-rich data. As the name suggests, data driven models (DDM) try to infer the behavior of a given system from the data presented for model training/calibration. Hence, the input data used for training should cover the entire range of inputs that the system is likely to experience and data of all the relevant variables should be used. Some modellers (Maier and Dandy, 2000; Bowden et al., 2002; Anctil et al., 2004; Bowden et al., 2005; Leahy et al., 2008) feel that the DDMs have the ability to determine which model inputs are critical and so a large amount of input data is given to the models, at times without any pre-processing. This approach has many disadvantages: more time and effort is needed to train the model and frequently one may end up at a locally optimal solution.

A number of studies have been carried out in the past to determine the inputs to the data driven models (Gaweda et al., 2001; Bowden et al., 2002; Anctil et al., 2004; Bowden

## 7.5 Applications of the ICE Algorithm

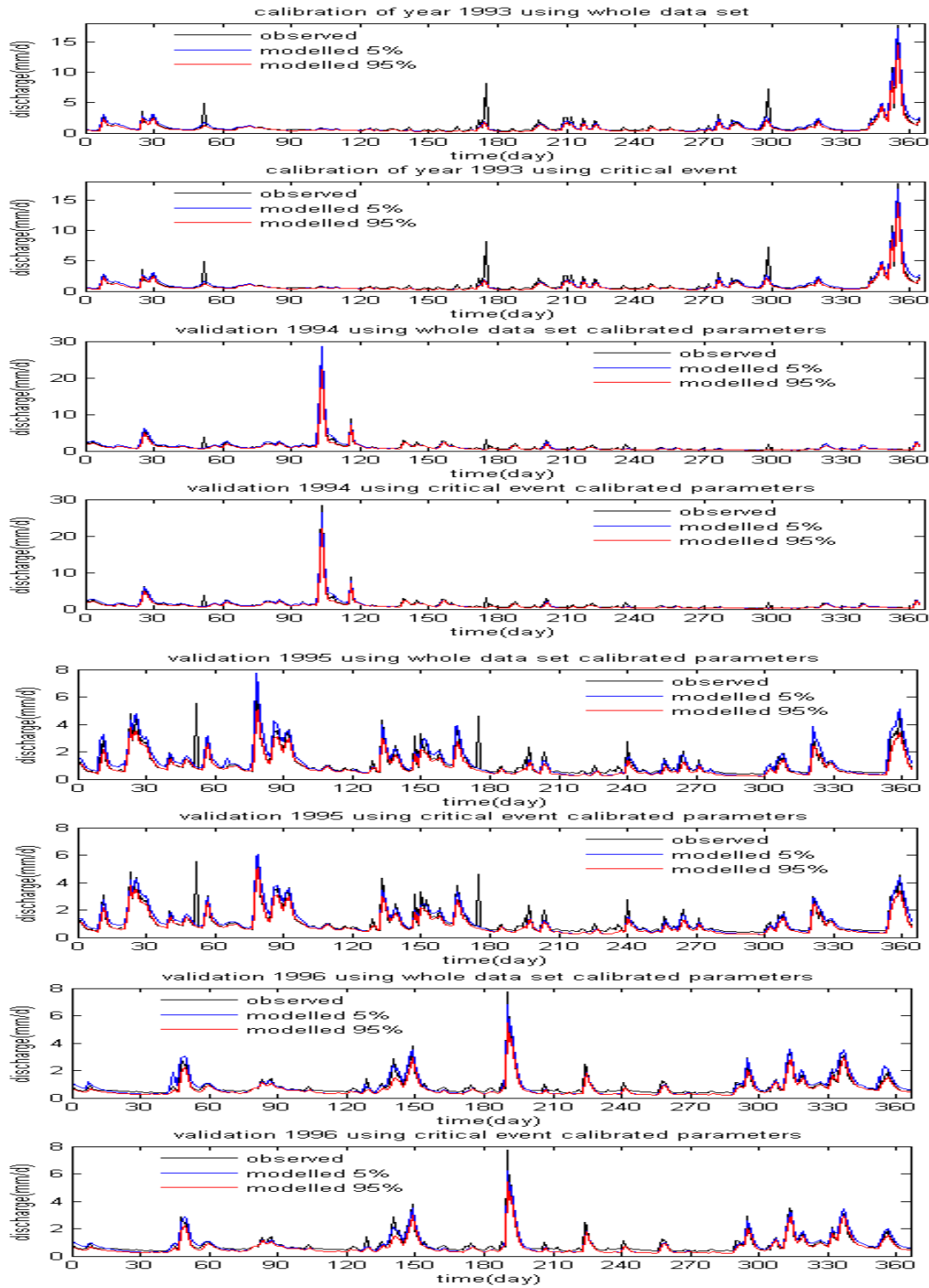


Figure 7.8: Calibration and validation with 90 % confidence

et al., 2005; May et al., 2008; Fernando et al., 2009). In data driven modeling (Fuzzy, ANN) there is no rigorous criteria that exists for input selection (Gaweda et al., 2001). Commonly used methods involve taking a time series model to determine the inputs for a DDM. A review of relevant studies was provided by Maier and Dandy (2000). Regarding the length of the data series, a common assumption is that the use of a longer time series of data will result in better training. This is because a longer series may contain different kinds of events and this may improve the training of DDMs. However, experience shows that a longer time series does not necessarily mean more information because there can be many repetitions of similar type of information (Wagener et al., 2003). In such cases, one may not necessarily get a better trained model despite wasting a lot of computational time and may over-fit the series (Fernando et al., 2009; Gaweda et al., 2001).

From the above discussion, it is can be concluded that the training of a DDM could be improved if the data of the events that are “rich” in information are used. Here the term “rich” denotes the data with very high information content. Use of this term is based on the fact that some data epochs contain more information about the system than others. Available input data can be pre-processed to leave out the data which does not contain any new information. This is important in training a DDM because these critical events mainly influence the training process and the calculation of weights.

In this study, geometrical properties of data were used to identify critical events from the long time series of data. Identification of critical events (ICE) algorithm was used to identify the critical events from the data series. An artificial neural network (ANN), which is a DDM approach, was trained on the critical events identified by the identification of critical events (ICE) algorithm. To test the robustness of the ICE algorithm for identification of critical events, random selection of events was performed and ANN was also trained on randomly selected events. The result was compared with the ANN trained on whole data.

## 7.6 Case Study

The methodology presented in the previous section will be demonstrated on a ANN to fit a discharge and sediments rating curve. This is useful because, for the design and management of a water resources project, it is very much essential to know the volume of sediments transported by river. It is possible to measure directly how much sediment is transported by river but not continuously. Consequently, a sediment rating curve is generally used instead. These curves can be constructed by several methods. In this regard, ANNs seem to be nice tools for fitting the relationship between river discharge and sediment.

### 7.6.1 Artificial neural networks

Artificial neural networks derive their central theme from highly simplified mathematical models of biological neural networks. ANNs have the ability to learn and generalize from

examples to produce meaningful solutions to problems even when the input data contains errors or is incomplete. They can also process information rapidly. ANNs are capable of adapting their complexity to model systems that are non-linear and multi-variate, and whose variables involve complex inter-relationships. Furthermore, ANNs are capable of extracting the relation between the input and output of a process without any knowledge of the underlying principles. Because of the generalizing capabilities of the activation function, one need not make any assumption about the relationship (i.e. linear or non-linear) between input and output.

Since the theory of ANNs has been described in numerous papers and books, the same is described here in brief. A typical ANN consists of a number of layers and neurons; the most commonly used neural network in hydrology being a three-layered feed-forward network. The flow of data in this network takes place from input layer to hidden layer and then to the output layer.

Input layer is the first layer of the network whose role is to pass the input variables onto the next layer of the network. The last layer gives the output of the network and is appropriately called as output layer. The layer(s) in between the input and output layer are called hidden layer(s). The processing elements in each layer are called neurons or nodes. The number of nodes in input and output layers depends on the problem to be addressed and are decided before commencing the training. The number of hidden layers and the number of nodes in each hidden layer depend on the problem and the data and are usually determined by a trial and error procedure. A synaptic weight is assigned to each link to represent the relative connection strength of two nodes at both ends in predicting the input-output relationship. The output of any node  $j$ ,  $y_j$ , is given as:

$$y_j = f \left( \sum W_i \cdot X_i + b_j \right) \quad (7.4)$$

where  $X_i$  is the input received at node  $j$ ,  $W_i$  is the input connection pathway weights,  $m$  is the total numbers of inputs to node  $j$ , and  $b_j$  is the node threshold. Function  $f$  is an activation function which determines the response of a node to the total input signal that is received. Sigmoid function is the commonly used activation function which is bounded above and below, is monotonically increasing, and is continuous and differentiable everywhere.

The error back propagation algorithm is the most popular algorithm used for the training of the feed forward ANNs (ASCE, 2000a). In this process, each input pattern of the training data set is passed through the network from the input layer to output layer. The network output is compared with the desired target output, and an error is computed as

$$E = \sum \sum (y_i - t_i)^2 \quad (7.5)$$

where  $t_i$  is a component of the desired output  $T$ ,  $y_i$  is the corresponding ANN output,  $p$  is the number of output nodes;  $P$  is the number of training patterns. This error is propagated backward through the network to each node and, correspondingly, the connection weights are adjusted.

Due to the boundation of the sigmoid function between 0 and 1, all input values should

be normalized to fall in the range between 0 and 1 before being feed into a neural network (Smith and Eli, 1995). The output from the ANN should be denormalized to original domain before interpreting the results. ASCE (2000a,b) contains a detailed review of the theory and applications of ANNs in water resources. Maier and Dandy (2000) have also reviewed modeling issues and applications of ANNs for the prediction and forecasting of hydrological variables. Maier et al. (2010) have provided a state-of-the-art review of ANN applications to river systems.

Govindaraju and Rao (2000) have described many applications of ANNs to water resources. ANNs have been applied in the area of hydrology include rainfall-runoff modeling (Cigizoglu, 2003; Wilby et al., 2003; Lin and Chen, 2004), river stage forecasting (Imrie et al., 2000; Lekkas et al., 2001; Shrestha et al., 2005; Campolo et al., 2003), reservoir operation (Jain et al., 1999), describing soil water retention curves (Jain et al., 2004) and optimization or control problems (Bhattacharya et al., 2003). Other studies have also shown that ANNs are more accurate than conventional methods in flow forecasting and drainage design (Zealand et al., 1999).

Furthermore, the ANN method was used extensively for the prediction of various variables (streamflow, precipitation, suspended sediment etc.) in the water resources field (Tokar and Johnson, 1999; Cigizoglu, 2003, 2004; Jain et al., 2004; Sudheer and Jain, 2004; Kumar et al., 2005; Cigizoglu and Kisi, 2005, 2006; Cigizoglu and Alp, 2006; Alp and Cigizoglu, 2007; Solomatine and Ostfeld, 2008; Shamseldin, 2010). Kumar et al. (2002) found that an ANN model can be trained to predict lysimeter ET<sub>0</sub> values better than the standard PM method. Sudheer et al. (2002) and Keskin and Terzi (2006) tried to compute pan evaporation using temperature data with the help of ANN. Sudheer and Jain (2003) employed a radial-basis function ANN to compute the daily values of ET for rice crops. Trajkovic et al. (2003) examined the performance of radial basis neural networks in evapotranspiration estimation. Kisi (2007) studied the modeling of ET from climatic data using a neural computing technique which was found to be superior to the conventional empirical models such as Penman, and Hargreaves. Modelling of ET with the help of ANN was also attempted by Kisi (2006); Kisi and Öztürk (2007); Jain et al. (2008).

### 7.6.2 Data used in the study

The data used in this study was the same as used by Jain (2001). For more details about study area and data please refer to Jain (2001). The sufficiently long time series to obtain stable parameter from two gauging stations on the Mississippi River were available. Both stations are in Illinois and operated by the U.S. Geological Survey (USGS). These stations are located near Chester (USGS Station No. 07020500) and Thebes (USGS Station No. 07022000). The drainage areas at these sites are 1,835,276 km<sup>2</sup> (708,600 mi<sup>2</sup>) for Chester and 1,847,190 km<sup>2</sup> (713,200 mi<sup>2</sup>) at Thebes. For these stations, daily time series of river discharge and sediment concentration were downloaded from the web server of the USGS and the river stage data were provided by USGS personnel. River discharge and sediment concentration were continuously measured at these sites for estimating the suspended-sediment discharge. For more details about the measurement, please refer

to Porterfield (1972) and <http://co.water.usgs.gov/sediment/introduction.html>. After examining the data and noting the periods in which there were gaps in one or more of the three variables, the periods for calibration and validation were chosen. For the Chester station, the data of December 25, 1985 to August 31, 1986 were chosen for calibration, and the data from September 1, 1986 to January 31, 1987 were chosen for validation. For the Thebes station, the data from January 1, 1990 to September 30, 1990 were used for calibration, and data from January 15, 1991 to August 10, 1991 were used for validation. It may be noted that the periods from which calibration and validation data were chosen for the Thebes site span approximately the same temporal seasons (January-September and January-August). The data for the Chester site, however, covers different months (i.e. December-August and September-January).

### 7.6.3 Different cases for the training of ANN

#### Rating Curves and Input to ANN

The records of stage can be transferred into record of discharge using rating curve. Normally, a rating curve has the form

$$Q = a.H^b \quad (7.6)$$

Where, Q is discharge ( $m^3/s$ ), H is river stage (m); a and b are constant. The establishment of a rating curve is a non-linear problem. In a study, Jain and Chalisgaonkar (2000) showed that ANN can represent stage and discharge relation better than conventional ways.

A sediment rating curve has very similar non-linear form as discharge rating curve. Usually, the relationship is given by

$$S = c.Q^d \quad (7.7)$$

Where, S is suspended sediment concentration ( $mg/l$ ), Q is discharge ( $m^3/s$ ); c and d are constant. Please note that, establishing a sediment rating curve is two step process. The measured stage data are used to estimate discharge and then discharge is used to established the sediment rating curve. So, river stage, discharge, and sediment concentration is main component for analysis.

The input to the ANN was river stage at the current and previous times. The other input was water discharge and sediment concentration at previous times. Hence, there are two output nodes, one corresponding to discharge and the other for sediment.

For each data set, ANN model was trained and tested for three cases:

- Case 1: Using the entire time series of data available
- Case 2: Using the data pertaining to critical events only (selected by depth function), and

- Case 3: Using the data pertaining to randomly selected events (same number of events as in Case 2). Here, a number of runs were taken by randomly selecting the events and the results reflect the average of ten repetitions.

Programs were developed in Matlab 6.5 software using the neural network toolbox to pre-process the data, train the ANN and test it.

An integrated three-layer, ANN as described by Jain (2001), was trained using the calibration period data pertaining to river stage, discharge, and sediment concentration (Fig.7.9). The number of nodes in the hidden layer that gave the best sum of square error (SSE) and correlation coefficient (CC) was determined by trial and error. Using the weights obtained in the training phase for each case, the performance of the ANN was checked by using the testing period data.

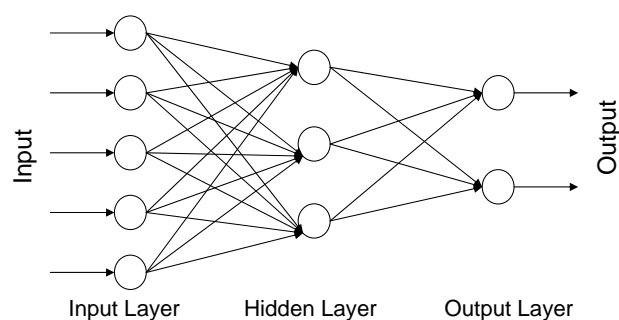


Figure 7.9: Three-Layer, Feed Forward ANN structure

#### 7.6.4 Results from rating curve analysis

Stage discharge and sediment rating relations were determined for both sites using the ANN by following the same procedure as used by Jain (2001). Tables 7.10 and 7.11 give the root mean square error (RMSE), SSE and correlation for each case for the Chester site for training and testing period, respectively. It can be seen from Table 7.10 that for discharge, the CC and RMSE are nearly the same for Case 1 and 2; CC and RMSE for Case 3 are somewhat inferior. For the sediment concentration data, CC and RMSE was slightly inferior for Case 3. Validation results given in Table 7.11 show that for the discharge data, CC is very high and is nearly the same for Case 1 and 2 whereas it is “bit smaller” for Case 3; RMSE is bit higher for Case 3. For the sediment data, CC is very high for Case 2 and is lower and nearly the same for Case 1 and 3; RMSE is the best for Case 2 followed by Case 1 and worst for Case 3.



Case	Discharge			Sediments			% data used
	Correlation	RMSE	SSE	Correlation	RMSE	SSE	
1	9.977e-01	1.330e-02	7.296e+06	9.537e-01	6.116e-02	4.913e+06	100
2	9.979e-01	1.503e-02	4.931e+06	9.502e-01	7.823e-02	4.254e+06	53
3	9.954e-01	2.309e-02	5.486e+06	9.212e-01	7.908e-02	2.051e+06	53

**Table 7.10:** *RMSE, SSE and correlation coefficient from the ANN model for the training period of Chester site*

Case	Discharge			Sediments		
	Correlation	RMSE	SSE	Correlation	RMSE	SSE
1	9.928e-01	6.557e-02	1.130e+08	8.695e-01	7.874e-02	5.192e+06
2	9.904e-01	6.914e-02	1.257e+08	9.049e-01	6.859e-02	3.939e+06
3	9.670e-01	2.129e-01	5.664e+08	8.444e-01	1.225e-01	5.979e+06

**Table 7.11:** *RMSE, SSE and correlation coefficient from the ANN model for the validation period of Chester site*

To aid the visual appraisal of the results, time series graphs were prepared. Figure 7.10 presents observed and computed discharge for various cases for the Chester station for the validation period. The match is very good except for the first and the major peak. Overall, the match is the best for Case 1 followed by Case 2 and Case 3, the difference between Case 1 and 2 being minor. Figure 7.11 presents the time series plot for the sediment data. Here for some peaks and troughs, the graph for Case 1 is closer to the observed while for some others, the graph for Case 2 is closer. The graph for Case 3 appears to be consistently underperforming. These figures affirm the interpretation of results from Tables 7.10 and 7.11 that the ANN estimates by using the whole data and ANN trained on critical events, show a similar match with the observed curve whereas training by random selection of events is inferior.

Tables 7.12 and 7.13 give the RMSE, SSE and CC for the three cases for the Thebes site for training and testing period, respectively. Results in Table 7.12 show that for discharge, the CC is very high and nearly the same for Case 1 and 2 while it is bit smaller for the Case 3. The same can be said for RMSE which is nearly twice for the Case 3 compared to Case 2. Both CC and RMSE are inferior for Case 3. For sediment concentration data, CC is highest for Case 1, followed by Case 2 and then Case 3. RMSE was very small for Case 1 and was almost the same for the remaining two cases.

Cases	Discharge			Sediments			% data used
	Correlation	RMSE	SSE	Correlation	RMSE	SSE	
Case 1	9.946e-01	2.137e-02	4.431e+07	9.045e-01	5.636e-02	7.005e+06	100
Case 2	9.929e-01	3.273e-02	2.968e+07	8.296e-01	1.023e-01	6.769e+06	29
Case 3	9.723e-01	6.034e-02	3.706e+07	7.425e-01	9.816e-02	1.339e+06	29

**Table 7.12:** *RMSE, SSE and correlation coefficient of the ANN model for training period of Thebes site*

7 Calibration of Hydrological Models on Hydrologically Unusual Events

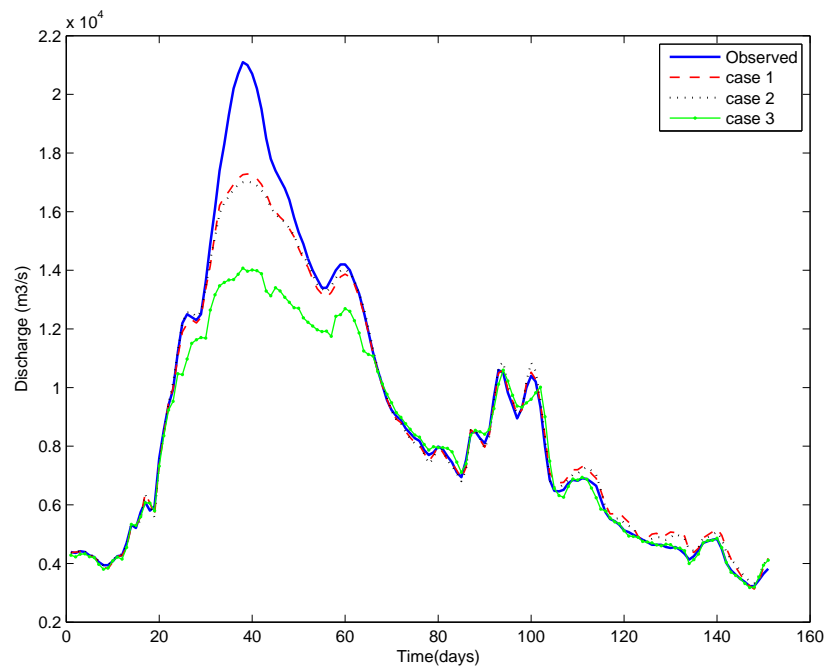


Figure 7.10: Observed and computed discharge by different cases for the Chester validation period

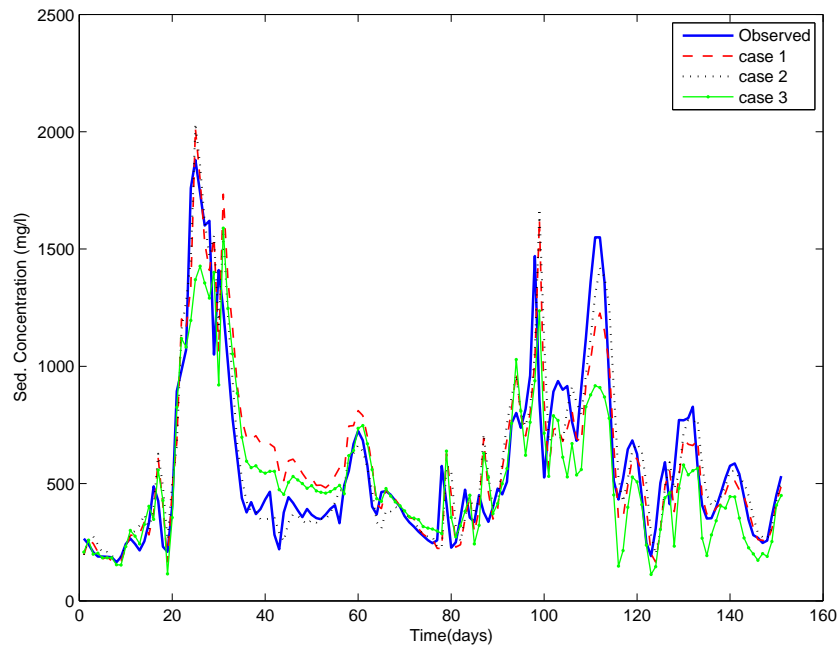


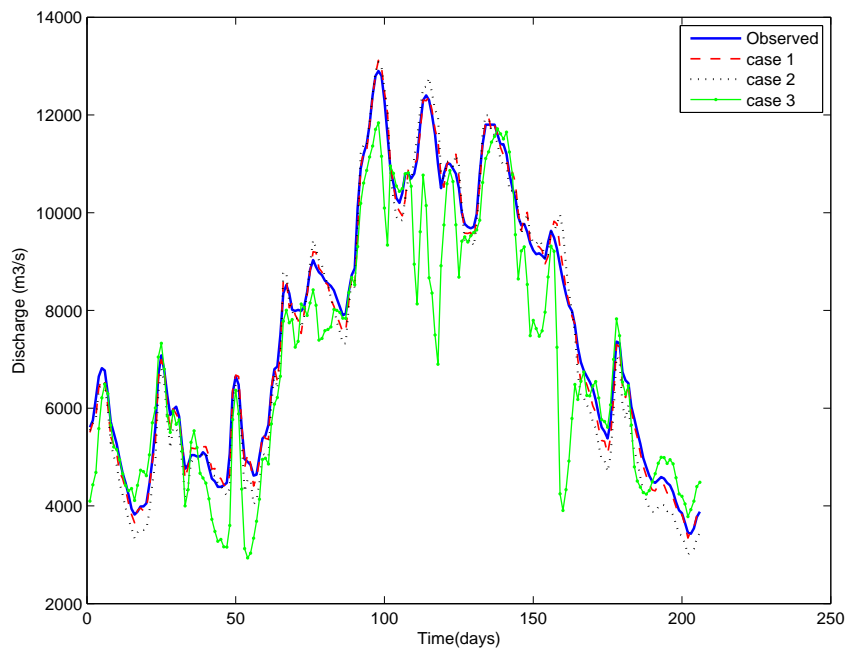
Figure 7.11: Observed and computed sediment concentration for each case for the Chester validation period

Cases	Discharge			Sediments		
	Correlation	RMSE	SSE	Correlation	RMSE	SSE
Case 1	9.975e-01	1.085e-02	8.700e+06	9.439e-01	3.987e-02	2.671e+06
Case 2	9.949e-01	2.226e-02	3.571e+07	9.440e-01	4.049e-02	2.755e+06
Case 3	9.273e-01	1.017e-01	2.773e+08	8.984e-01	1.510e-01	8.350e+06

**Table 7.13:** *RMSE, SSE and correlation coefficient of the ANN model for validation period of Thebes site*

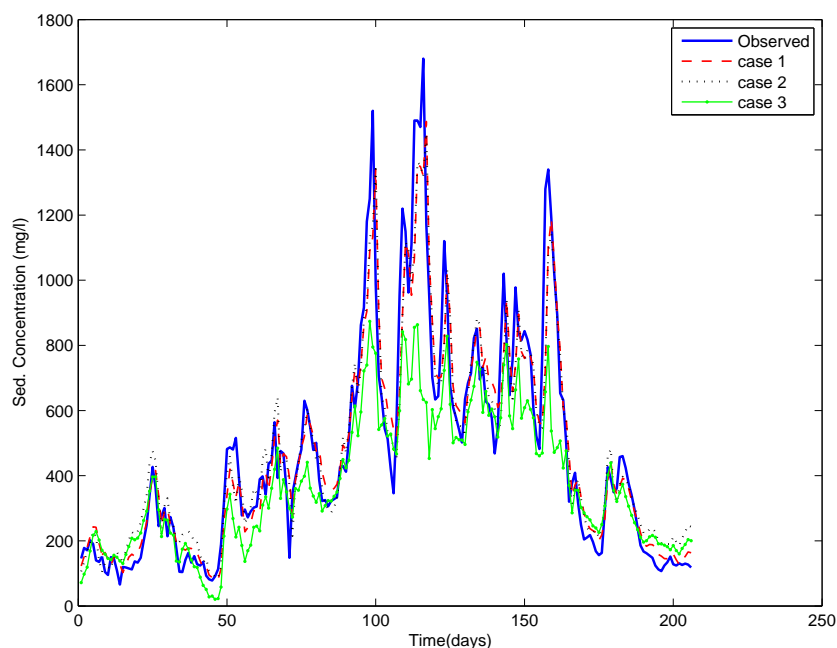
Validation results given in Table 7.13 show that for discharge, CC is very high and is nearly the same for Case 1 and 2; it was smaller for Case 3. RMSE was quite high for Case 3 as compared to the two other cases. For the sediment data, the performance indices had similar behavior - CC was much less and RMSE was much high for Case 3 compared to the other two cases.

Figure 7.12 shows the temporal variation of observed discharge and the estimates for all the above three cases using ANN for calibration period for the Thebes site. It can be appreciated from this figure that the graphs pertaining to Case 1 and 2 are very close to the observed discharge curve, whereas the data for random events has been unable to train the ANN properly. A poorly trained ANN fails in the test runs as evidenced in figure 7.13. Based on these results, it can be stated that the performance of



**Figure 7.12:** *Observed and computed discharge by different cases for the Thebes validation period*

ANN trained using “data-rich” events is as good as that using the whole data set. At



**Figure 7.13:** Observed and computed sediment concentration by different cases for the Thebes validation period

a first glance, this statement may appear to challenge the widely repeated concept that an ANN becomes wiser as more data are used to train it. However, on closer scrutiny this concept supports the fact that if the data has multiple events which contain similar information about the natural system then the ANN is not going to learn much despite spending a prolonged time in training.

Training of any neural network is considered to be successful if the trained network works well on the testing data set. The analysis of results and discussion presented above clearly shows that the ANN trained on critical events has performed equally well for the tested data set. A model trained using a particular data set is likely to perform well on a test data set if both the data sets are representative of the system and have similar features. A question arises as how to judge whether that these data sets are similar or not.

To test this we did a split sampling and divided the data in two sets, namely training and testing. We located the critical events as mentioned above and the ANN was trained on the training data set. We validated the trained ANN on the testing set and calculated the depth of each data point of the testing set in the convex hull of the training set. Thus we can locate which points of the testing set are in the convex hull of the training set. This means, in practice, that we can determine how similar the testing set with respect to the training set. In a recent study [Bárdossy and Singh \(2010\)](#) have used a similar concept in selection of a appropriate explaining variables for regionalization. For

visual appraisal of the concept, please refer to the figure 7.14. The space where depth is greater than zero means, it has very similar properties as the training set. Figure 7.15 shows that residuals in model and observed discharge. In this figure calculated depth is normalized and plotted along the residual as to indicate depth equal to zero or higher. It can be appreciated from this figure that period where depth is zero, residual is very high and period where depth is higher residual is lower. This is indicated in the figure with dark and dotted circles, respectively. Similar results can be seen in the case of sediment data as shown in figure 7.16. This illustrates that the points which are inside the convex hull of training set are the points where we can expect low errors. Practically it also indicates that testing points which are in the convex hull of training set are similar to the training set. Thus without running the model, we can predict the performance of the model *a priori* by looking at geometry of the training and testing data.

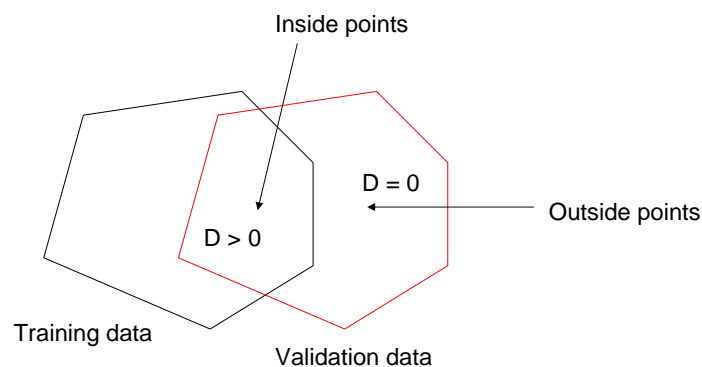


**Figure 7.14:** Convex hull of the training and testing set

## 7.7 Conclusions

- In this chapter, information contained in a time series was investigated and found that smartly selected events are sufficient to identify the parameters of the model. Indeed, the prediction is as good as that arising from the calibration using the whole time period.
- The comparison of event selection using precipitation and discharge series shows that, event selection by both ways locate almost the same time period in a discharge series. Hence, event can be selected based on discharge or precipitation series.

7 Calibration of Hydrological Models on Hydrologically Unusual Events

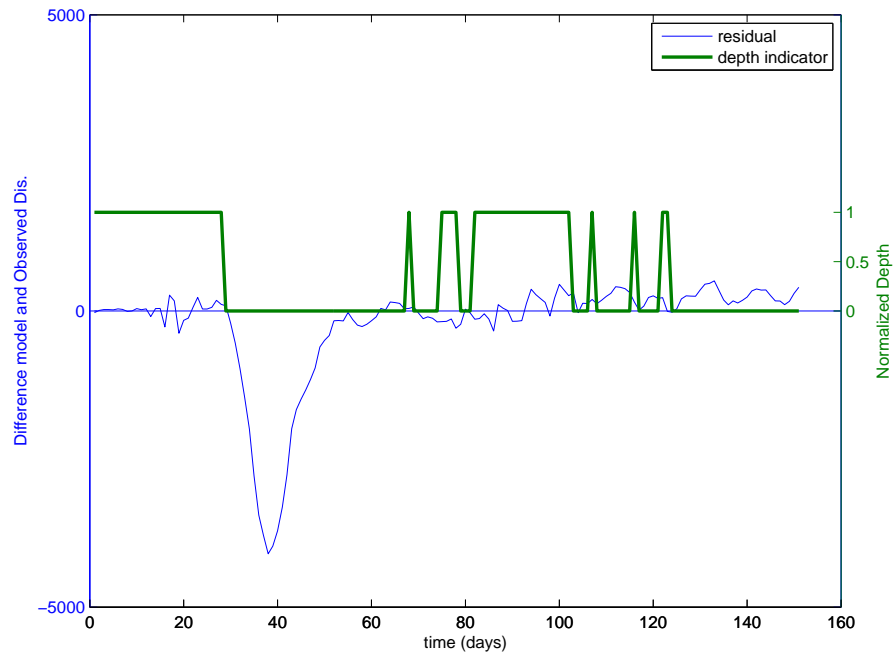


Figure 7.15: Residuals of the observed and computed discharge at each validation period for the Chester site

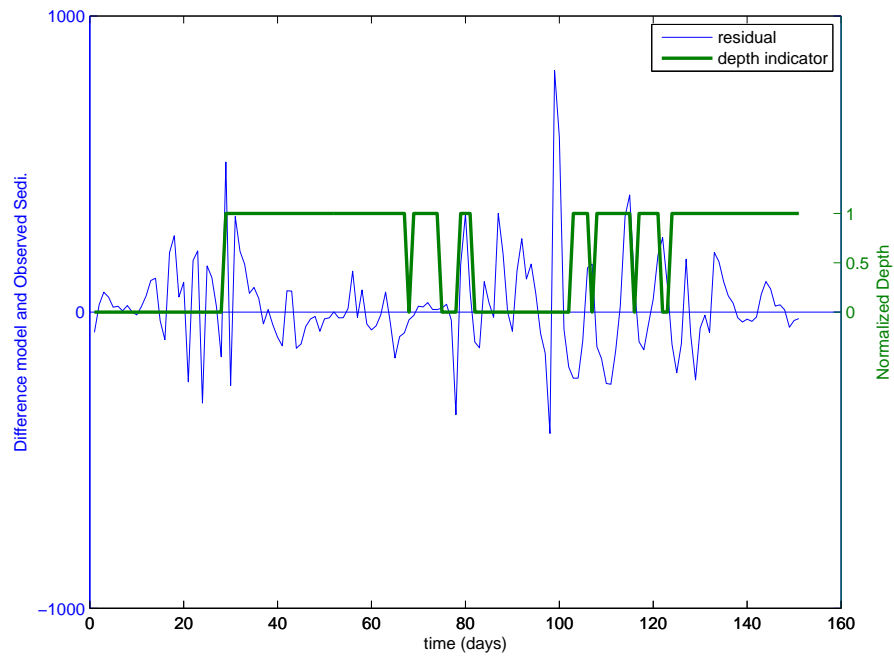


Figure 7.16: Residuals of the observed and computed sediment concentration at each validation period for the Chester site

- A novel algorithm (ICE) for identification of critical events was developed.
- Data depth is a useful tool to identify critical events. Data points with low data depth are critical for model calibration.
- Models can be calibrated with carefully selected unusual events but not with random selection of the events.
- The unusual events are a small portion of the whole period (approx 6 percent in this case study).
- Based on future precipitation prediction and appearance of new events, ICE algorithm can help to decide when to recalibrate a forecasting model.
- Concept of this chapter can be used for prediction in ungauged basin. ICE algorithm help to decide which events to be measure and hence it can be extend to ungauged catchments prediction problem.
- The concept of ICE algorithm is not a model dependent. ICE algorithm can also be used for physically complex model like WaSim-ETH and can reduce simulation time and complexity.
- The ICE algorithm can also applied in improving the training of Artificial Neural Networks (data driven model for fitting), an application that relies on information-rich data. ANN trained using the data of critical events or information rich data gave similar result as the ANN trained using the complete data set.
- If the testing data set is in the convex hull of training data set, it implies testing data set is similar to training data set. So we can expect low error. The concept developed in this chapter can be used to guess the performance of the testing set without running the model.

# 8 Robust Dynamic Parameter Estimation for Hydrological Models

Usually the parameters of the models are assumed to be time independent. However some of the catchment properties are not stationary. Hence some of the model parameters corresponding to a certain natural process may vary with time. The purpose of this chapter is to develop a methodology which can investigate dynamic nature of parameters in a model.

## 8.1 Introduction

Generally hydrological models are calibrated by seeking one optimal or best parameter set that represent the catchments in space and time. Problems with non-uniqueness of the solutions for the parameter estimation problem have been reported by many authors. An aspect that has been investigated in less detail is the issue that optimal parameter estimates often vary with the time period chosen for calibration. Some of the basic reason may be, that some system dynamics might not be well represented or missing due to model structural error such as errors in the model states, e.g. due to errors in the model input. Characteristics of the system, which are assumed static, are actually changing, e.g. the vegetation cover. Others, e.g. different causal rainfall events, are assumed similar in a lumped model etc. The main problem is how can we estimate whether parameters are time-varying and, if they do, at what time-scale?

A study done by [Wagener et al. \(2003\)](#) shows that parameter of hydrological model uses information from some specific period of time series. Generally, parameters of hydrological models are assumed to be time independent. But it may possible that some of the behavior of catchment may change in time. Hence, the parameter should also be change in time so that it can utilize the maximum information.

Present hydrological models are not perfect due to several reason like short and erroneous observation series and incomplete knowledge of the processes. Therefore, it cannot become perfect even with longer observation series because we have limited ability to learn a process. We only can play with the parameters of hydrological models, though the uniqueness of the parameters will remains not well defined. The models are consequent in reproducing themselves under the similar conditions but nature is less consequent. Two events look very similar but the responses from them can be entirely different.

Lack of identifiability of parameters of hydrological model, leads to uncertainty in model and may limit significantly the use of models for purposes such as parameter regionalization or the investigation of land-use or climate change scenarios ([Wagener et al.](#),



2001). We are lacking model diagnostic tools that help us estimate parameter variability and guide our efforts to understand the reasons for the variability. The idea that the parameters in hydrological models may vary with time and space is the key to solving the problem of model structure identification (Lin and Beck, 2007). When model parameters varying with time, the model will have more flexibility to describe time varying behavior of nature. This may lead to more realistic and better model prediction.

Beck (1987) studied the role of uncertainty in the identification of mathematical models of water quality and in prediction. The Problems they reviewed were the uncertainty about model structure, uncertainty in the estimated model parameter values, the propagation of prediction errors, the consequence of lack of proper model identifiability are the difficulty in the interpretation and explanation of past observed system behavior. Liu et al. (2008) investigated how model improvement can be possible, if we can identify where and how its behavior is inconsistent with the underlying assumption and data. Conventionally, the model parameters are considered to be constant in time: as long as no physical changes that would alter the hydrological responses, e.g. land use or geomorphological modification. The model failed to simulate different system behavior with a single, constant parameter set, suggesting inadequacies in the functionality of the model. Time varying parameter may compensate for partial errors constrained in the underlying model structure. Model parameters are linked with assumption of certain system component or process, and time varying parameters can constitute useful information in detecting where the adequacies exit and how to rectify. Over parameterization and equifinality may lead the model parameter non-identifiable and can make model diagnostics difficult in dynamic parameter analysis.

Lin and Beck (2007) modified RPE(Recursive Prediction Error) algorithm for estimating time varying nature of model parameters for identify model structure. Wagener et al. (2003) studied the major sources of uncertainty in current modeling procedures is a lack of understanding to evaluate model structures and the inability of calibration procedures to distinguish between the suitability of different parameter sets. The evaluation of model structure can be examined with respect to the failure of individual components, and periods of high information content for specific parameters can be identified. In a study of identifiability of hydrological model parameters, Vrugt et al. (2002) concluded that some set of measurements data contained a very substantial amount of information for the identification of specific model parameters. Reichert and Mieleitner (2009) used the concept of time dependent parameters in hydrological model. They concluded that the concept of time dependent parameters is useful for mechanistic models in which internal variables have a direct physical meaning. In a very recent study Abebe et al. (2010) concluded that the time varying nature of parameters is due to inadequacies in the model structure or unsteady hydrodynamic and hydroclimatic conditions.

The purpose of this chapter is to to develop a robust estimation approach for dynamic parameterization of hydrological model. The concept of dynamic parameters will be illustrated with examples from the Upper Neckar catchment. The hydrological model chosen is a modified version of the HBV model concept. A description of the catchment and the model is provided in Chapter 4.

## 8.2 Concept of Time Varying Parameters

Conventionally temporal invariance of parameters are assumed in hydrological modeling. However, certain catchment properties are not stationary in time and space. Soil properties like macropores shows high variability in space and time. System theoretic modeling idea do not often attempt to represent nonlinear dynamic inherent in rainfall to runoff process and it does not perform always well over long period of time when the catchment storage and soil wetness is changing over wide range (Young, 2005). Göttinger and Bárdossy (2008) found that hydrological model perform better in summer than winter due to reduced complexity in summer, when fewer processes are active and soil is mostly dry. This indicates that if we calibrate our model for whole period, the parameter are getting compensates at the cost in a reduction of the over all performance. One can not represent time varying process perfectly with time invariance parameters of the model. Hence it is very important to make parameters of our hydrological model as time varying in nature.

There are certain processes in the hydrological cycle which are not static hence parameters representing these process must be dynamic. Some process are very fast and some not. So a window type of approach can be applied to consider the uncertainty and noise in dynamic variability of parameters. The different size of window can be chosen for variability of parameters. A typical window size is given as  $2n + 1$ , where  $n$  is number of time step.

### 8.2.1 Robust dynamic parameter estimation (RDPE) algorithm

From the forthcoming discussion it is very clear that, if we allow our time variability in our model parameters, we may better represent non-linear behavior of hydrological process in a watershed. Hence, in this research a similar hypothesis is used and a new RDPE algorithm is developed. The RDPE algorithm is schematically summarized in figure 8.1. RDPE algorithm has three section. The first section defines the range of the parameters and the scale of variation of the parameters. For example, keeping all the parameters constant, except one, the ROPE algorithm was used for getting parameter space and its performance. One such example for parameter beta is given in figure 8.2. The X axis represents the range of the parameter beta, while the Y axis represents the performance (NS). From this figure, one can see that, the model performance increases as the model parameter beta increases, but after certain value performance again decreases. So it is clear that the variation of this parameter should be fixed between a range of 1.2 to 2.5, instead of keeping it 1 to 6. One point to be noted from this figure is that when parameter beta was taken from boundary points (low depth points), their performance is poorer then higher depth points. Hence, for fixing the range of variation, higher depth should be taken. Thus we can restrict the range of parameters for variation. In a similar manner, we can restrict the range of other parameters of the model. It has been found that range of certain parameters does not vary much, however, from initial range. i.e. for a wide range of these parameters performance is good. After getting the range of parameters, for a particular window size, the parameters of the model is optimized

using simulated annealing. A window size of  $2n + 1$  was defined around each time period for optimize parameters at that particular time period. During the process of the optimization for each window size, we obtained a time series of parameters. This time series of parameters can be used for two further purposes, namely for model structure analysis and for model prediction improvement. The model structure diagnosis can be done to define sensitive and insensitive periods for parameters. At the same time we can investigate reason for time varying nature of parameters. Further, time series of parameters can be use to build predictive model of parameters. This model can be use for future prediction, which will then become more realistic.

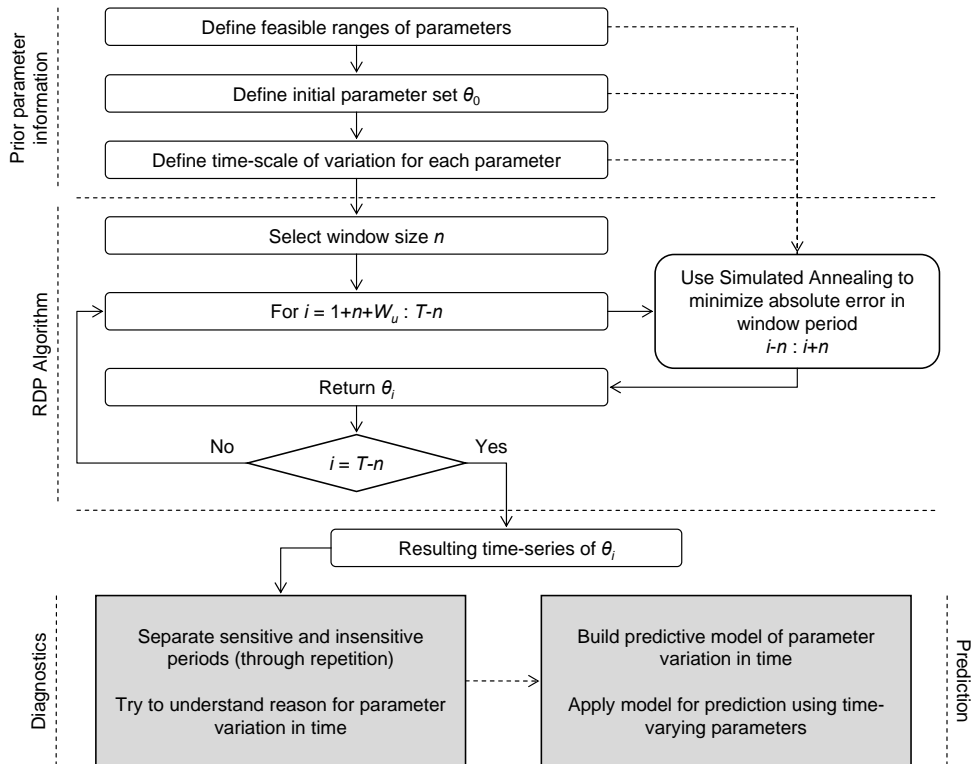
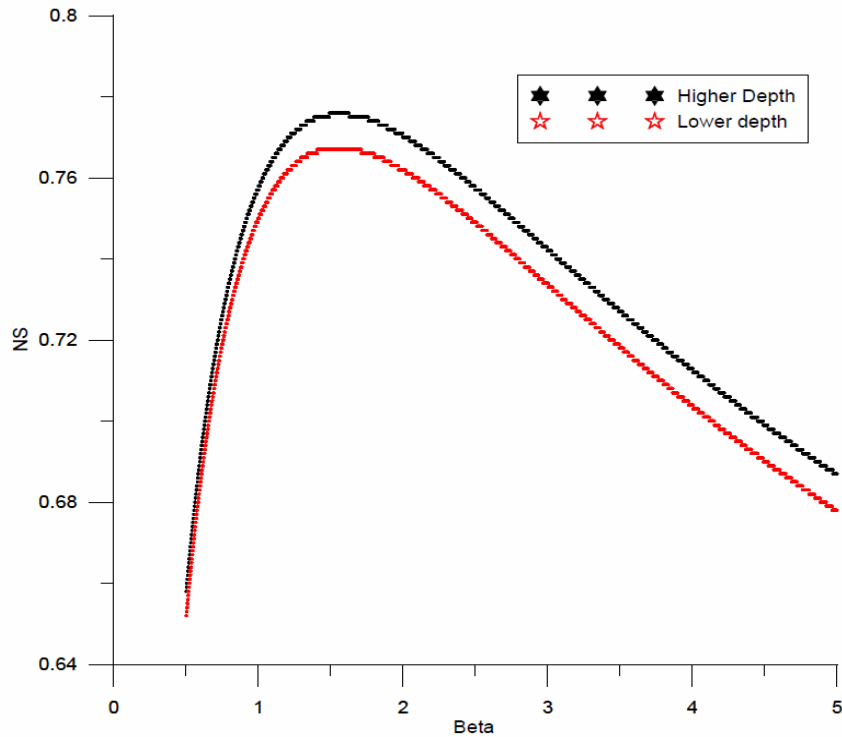


Figure 8.1: Schematic outline of RDPE algorithm

### 8.2.2 Diagnosis of model

The HBV model was calibrated in the frame work of RDPE algorithm. The various window size was used for each model parameters. For example,  $n = 5, 10, 20, \dots$  has been used to define the window size. It has been found that  $n = 5$  is more suitable to consider the uncertainty and noise in dynamic variability of model parameters, for



**Figure 8.2:** Parameter Beta and Performance (NS) at low depth and at high depth

models like HBV. Data from 1961 to 1965 are used for calibration on daily time step. The time series of model parameters was obtained by RPDE algorithm after the calibration. The typical time series of parameter beta is given in figure 8.3, where y axis is the normalized value of parameter beta. From time series of model parameters an active and inactive period for the different models can be identified. For example, figure 8.4 shows time series of parameter beta with y axis normalized; we can clearly see that this parameter is active only during wet periods and inactive during dry periods. If we look at model structure of HBV, it is clear that parameter beta is very important parameter in calculation of effective precipitation and it has influence on wet and dry periods. A very similar trend can be seen from the other parameters of the model. An example from other parameter is given in figure 8.5 where time series of degree day parameter is shown. It can be seen from figure that this parameter is important only after snow period. It is an obvious fact that snow parameter should be active only when there is snow. So it can be concluded that all the parameters have different times for being active or inactive. Some of the parameters are active during winter season, while others during dry periods. During investigation of different parameters of the HBV model, it has been found that some of the parameters have more variation over time, while others

## 8.2 Concept of Time Varying Parameters

less. So, for example, parameters ,  $K_1$ ,  $K_2$ ,  $DD$ ,  $Dew$  etc have wide variation over time (fig. 8.6), while parameters  $L$ ,  $MAXBAS$ ,  $K_{per}$ ,  $FC$ ,  $PWP$  are very less (fig. 8.7). If we look into the model structure of the HBV model, it is clear that those parameters with wide variation over time have direct relation to the actual process in nature, where process are changing constantly. This diagnosis can be useful for building a parameter model, which will reduce computational time, since parameters will be calculated only when they should be active. This may lead to improvement in model prediction. We can see from table 8.1 that using time varying parameter there is improvement in model calibration interns of Nash Sutcliff coefficient 0.81 to 0.87. This may be because of the flexibility of the parameters to adjust for better fit and are thus able to describe process in a more realistic way.

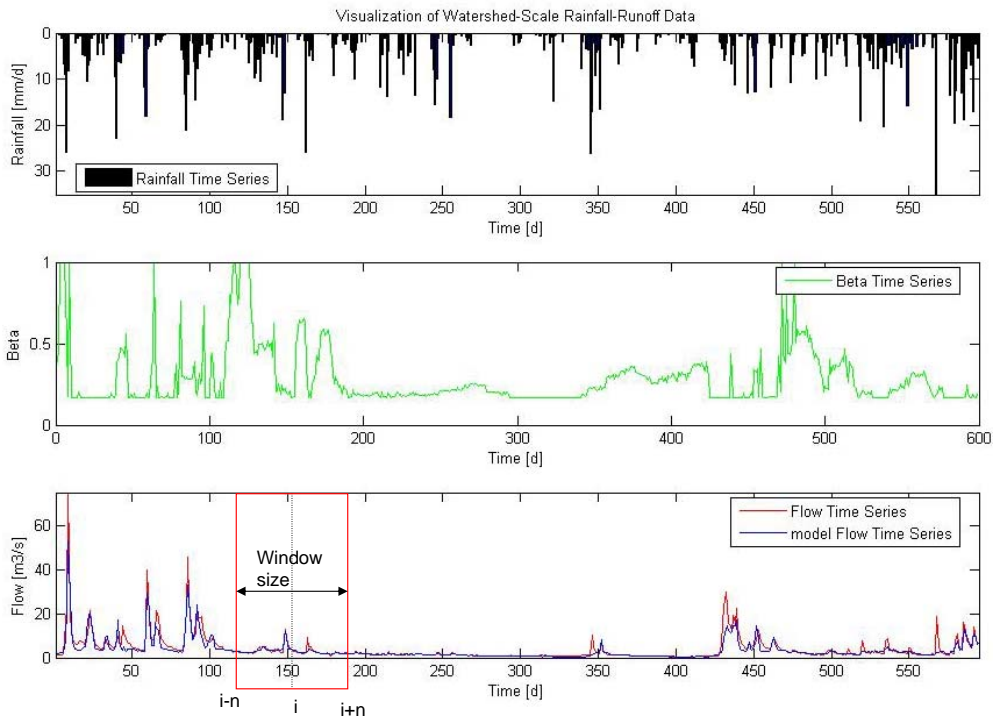


**Figure 8.3:** Typical time series of beta with window size

Time period	Simple time invariant calibration (NS)	RDP calibration ( NS)
1961-1966	0.81	0.87

**Table 8.1:** Calibration of model by time invariant and with RPDE method

## 8 Robust Dynamic Parameter Estimation for Hydrological Models

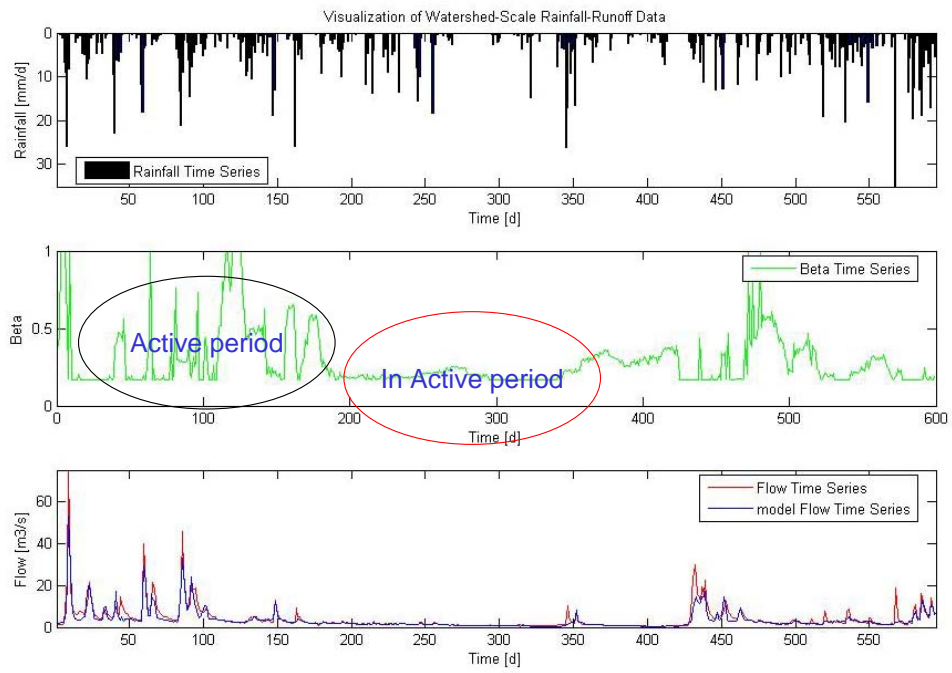


Figure 8.4: Active and inactive period for parameter  $\beta$

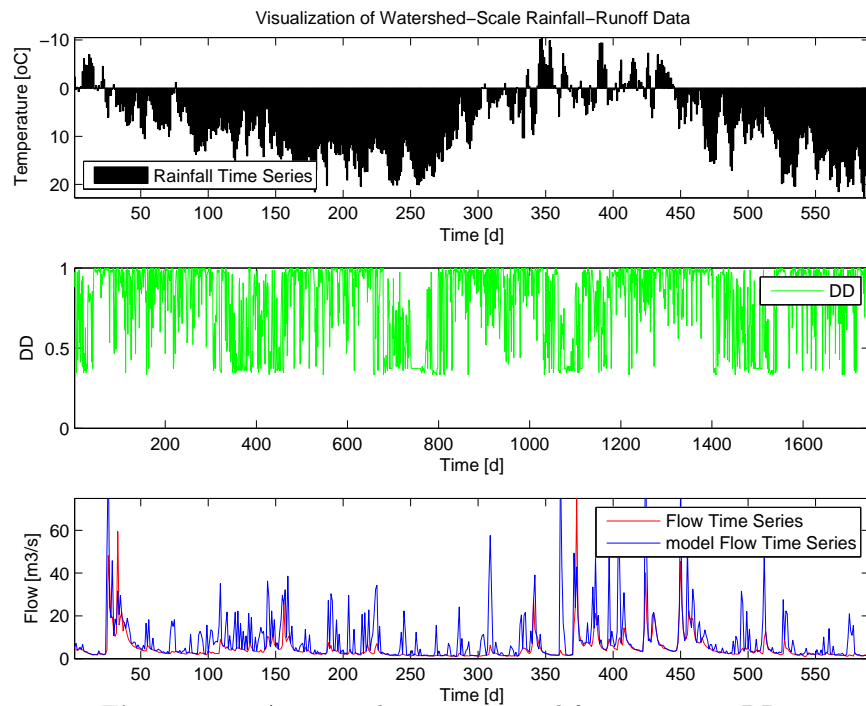
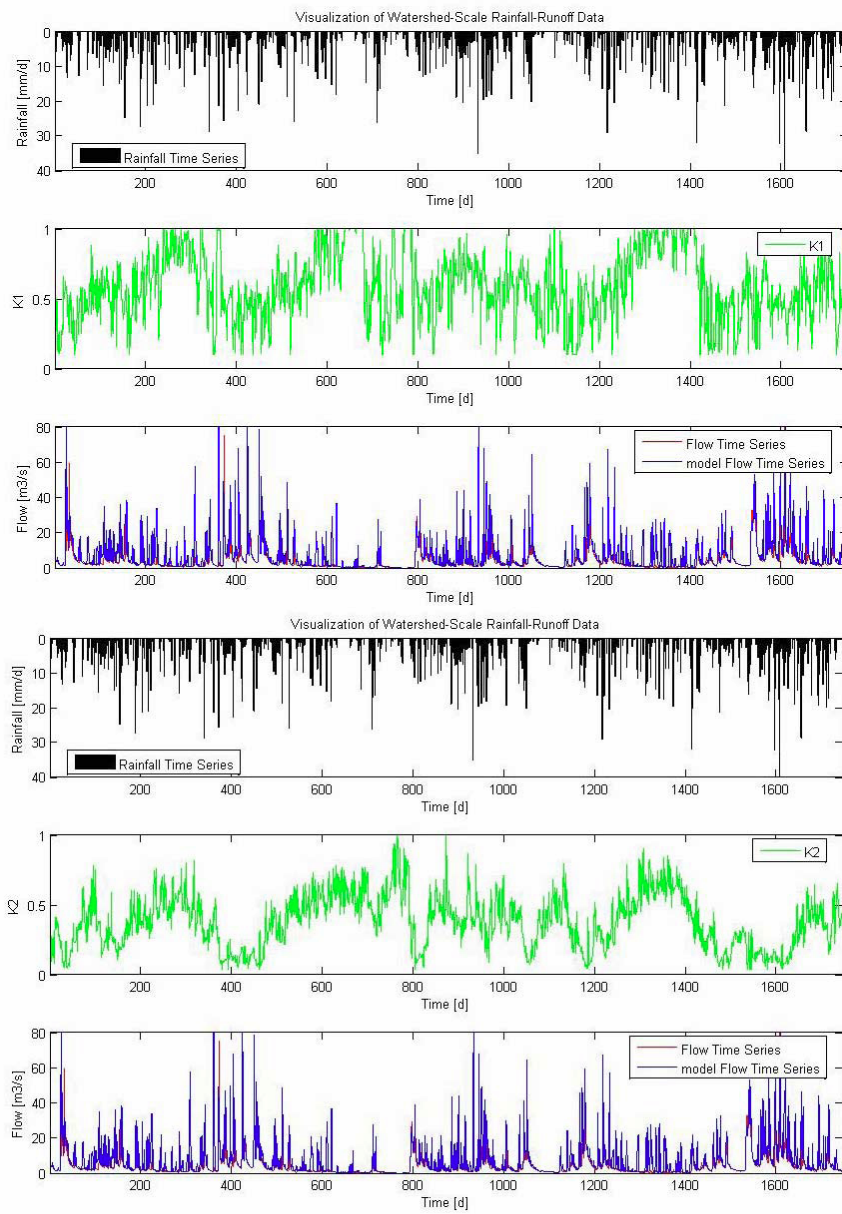


Figure 8.5: Active and inactive period for parameter  $DD$

## 8.2 Concept of Time Varying Parameters



**Figure 8.6:** Example of parameters, which has more variation over time

## 8 Robust Dynamic Parameter Estimation for Hydrological Models

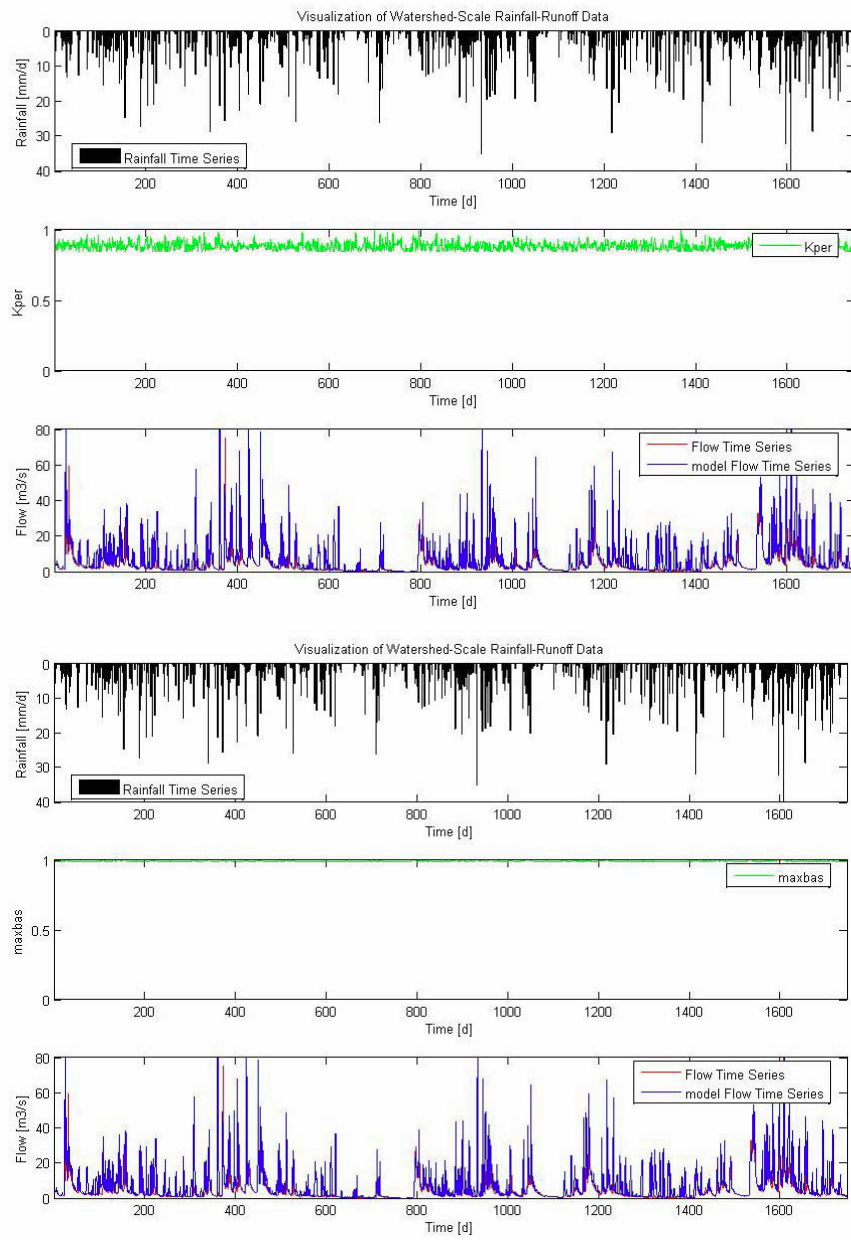


Figure 8.7: Example of parameters, which has less variation over time



To compare the structure of the parameter distribution, obtained during calibration, the statistical entropy was calculated. Smaller entropy employs more structure in distribution. A brief overview of statistical entropy is given in Chapter 7. Statistical entropy for few parameters of HBV model is given in table 8.2. It can be seen from table that parameter beta has lowest entropy, followed by the threshold temperature and degree day factor. If we look definition of the parameters in the model structure, we can see these parameters are very important for conceptualization of the model. The lower statistical entropy practically means more identifiability of the model parameter. Hence, from calculated entropy, we can conclude that parameter beta is more identifiable than threshold temperature ( $TT$ ) followed by degree day factor ( $DD$ ) and so on.

$Beta$	$DD$	$TT$	$FC$	$PWP$	$K_0$	$K_1$	$K_2$
1.2921	1.7687	1.6841	1.8877	1.8877	1.7937	1.7924	1.8643

**Table 8.2:** Statistical entropy for different parameters of HBV model

### 8.2.3 Hydrological model prediction

From the above section, we have seen that all the parameters are not active all the time. Using this diagnosis result we can build a model of parameters, where parameters will get importance only when they are active.

The previous section showed that more number of parameters, means, more flexibility to the model and lead to have a better performance in calibration. The major problem in calibrating a model with time varying parameter is that it does not have a single parameter set. We can obtain distribution of parameter using time varying parameterization. The major problem is how do we use this for the future? So, in this research, two methodologies are proposed for prediction as follow:

- Method 1: Random sampling, i.e. ensemble using distribution of parameter time series obtained by RDPE algorithm
- Method 2: Parameter model, i.e. making use of parameter time series obtained in RDPE calibration and input time series of precipitation.

#### Method 1: Random sampling

In this prediction, the basic assumption is, that the distribution of parameter time series will not change in the future. So, the proposed procedure is the following:

1. Use the calibrated model until an event begins (here events means when precipitation start)
2. If an event begins choose parameter randomly from distribution.
3. Calculate the model with selected parameter until end of the event

4. Continue from 1. until the time is over
5. Repeat this procedure N times

### Method 2: Parameter model

The second way for model prediction is to make parameter model by relating time series of parameter and meteorological data. In this research, the rainfall was related with parameter and a relationship was established. For example,

$$Y = A \cdot X + B \quad (8.1)$$

Where  $Y$  is model parameter time series, obtained during RDPE calibration and  $X$  is rainfall time series during calibration.  $A$  and  $B$  are regression coefficient. As we have time series of model parameters obtained during RDPE calibration and rainfall time series for calibration time period, we can fit a simple regression and  $A$  and  $B$  can be estimated for each parameters. Once  $A$  and  $B$  is estimated for each parameters, we can use prediction time period rainfall time series in equation 8.1 to get time series of parameters for prediction time period. Thus, we are able to preserve the dynamic variability of the model parameters for future predictions.

### Results and application

The HBV model was calibrated on Upper Neckar catchments for time period of 1961-65 based on RDPE algorithm. This calibrated model was used to predict for different time periods. The two methods of prediction, mentioned above were compared with the prediction, where the parameters were obtained by calibration assuming time invariant model parameters. Table 8.3 shows the validation result for different time periods using three prediction methods. Here, the random sampling result is a mean of 100 samples. From table 8.3 one can be see that the prediction done by parameter model method 2 is superior than random sampling as well as than from time invariant case. It is very clear that a very simple regression model for the parameter is very consistence in prediction for different time periods. For time period 1971-1975, it has a slightly poorer performance than simple the calibration; this may be due to fact that the parameter is related to precipitation by the regression coefficient and hence the precipitation data for that period is may be not good. One can see this as a limitation of this method of prediction. Even so, it is very important to note that, method 2 of prediction keep the dynamic variability of parameters for prediction, which intern give flexibility to the model to adjust and represent hydrological processes, which can give better prediction. This has clearly reflected by better prediction of this method as compare to other methods of prediction in all the time periods. Hence, hypothesis of time varying nature of model parameters can use for improving model prediction.

Time period	Simple time invariant (NS)	Random sampling (mean NS)	Parameter model (NS)
1966-1970	0.67	0.72	0.72
1971-1975	0.75	0.74	0.74
1975-1980	0.78	0.79	0.80
1981-1985	0.64	0.70	0.71

**Table 8.3:** *Validation using different parameter by each method for different time periods*

### 8.3 Conclusions

- By including parameters of dynamic nature it was not only possible for us to improve the model calibration but prediction also. This clearly indicate that our concept of applying the time varying parameters to a hydrological model is reasonable due to physical reason.
- In this chapter, the RDPE algorithm was developed and used to identify the dynamic nature of hydrological model parameters.
- It was also possible to apply the RDPE algorithm to the model diagnosis in order to detect deficiency in the model structure.

## 9 Regionalization of the Hydrological Model Parameters Using Data Depth

The process of parameter estimation for hydrological model is complex and tedious for ungauged catchments. The unavailability of observed discharge series increases the difficulties involved. Regionalisation of model parameters is the only possibility that gives a solution to this problem. After the successfully development of a robust methodology for parameter estimation in gauged catchments, this research continued to developed a robust and user friendly parameter estimation technique for ungauged catchments.

### 9.1 Introduction

The application of hydrological models is limited due to several reasons. One important limitation is the data availability. Discharges are only measured at a few selected river cross sections, leading to a small number of catchments for which the runoff calculated from the models might be verified. Further, the high spatial and temporal variability of the meteorological input (such as precipitation, temperature or wind) cannot fully be captured by the usually small number of meteorological stations. Radar measurement of precipitation can provide a more detailed space-time information on precipitation, but unfortunately, the reliability of the data is, at present, still low. Other influencing factors, such as soil properties, also vary considerably in space and even to some extent in time (e.g. macropores in soils). These problems among others make models based on physical principles unsuitable for many practical applications. Models, which to some extent use analogous concepts, can partly smoothen out the effects of variability and thus, can often be successfully used for practical purposes. The limitation of these models is that some of their parameters are not directly related to physically measurable quantities. Therefore, those have to be estimated from observations using calibration techniques. For this purpose, observed discharge series are needed. In order to use partly conceptual models for catchments without discharge observations, the model parameters have to be regionalized since they cannot be calibrated. In hydrology, regionalization is applied widely and successfully. One such example is the assessment of possible extremes floods ([Burn et al., 2007](#)) and low flows ([Ouarda et al., 2008](#)). Catchment properties are used as a basis in these procedures. The regionalization of hydrological model parameters is only possible if they can be related to catchment characteristics. The link between model parameters and catchment properties has to be identified and quantified. This task is further complicated by the fact that model parameters are not measured quantities. These have to be identified for example by using an inverse procedure that maximizes

some selected quality measures, such as the frequently used Nash-Sutcliffe coefficients (Nash and Sutcliffe, 1970), which are based on the reproduction of the observed discharge series.

Hundecha and Bárdossy (2004) studied a regionalization method based on *a priori* defined transfer function. They found that a reasonable relationship between the model parameters and the catchment properties can be established by calibrating the parameters of the transfer function instead of the model parameters. In a similar study by Göttinger and Bárdossy (2007), the relationship between the model and the catchment parameters was established by imposing different conditions on the regionalization function. Furthermore, Merz and Blöschl (2004) examined eight regionalization methodologies in 308 catchments in Austria. They found that the best regionalization methods are those that make use of the average parameters of immediate upstream and downstream neighbors followed by regionalization by kriging. In a similar study, Parajka et al. (2005) found that the kriging and similarity based approaches performed best. An overview of regionalization methodologies and different approaches can be found in Wagener et al. (2004).

The purpose of this chapter is to develop a methodology for regionalization based on the geometry of the catchment property vectors. We concentrate on catchments which do not differ too much from the observed catchments. Instead of choosing the risky way of extrapolating results, it has been decided to restrict regionalisation to catchments whose properties are inside the domain (formally in the convex hull) of the properties corresponding to the observed catchments. However the suggested procedure makes it possible for not only a single parameter vector, but a whole set of parameters can be derived for these catchments. This method does not allow for extrapolation. Nonetheless, it has been shown that the corresponding methodology for the selection of the catchment properties can be used for other regionalization approaches too. A case study with a number of small to medium size British catchments, modelled using HYMOD, illustrates the methodology. The effect of relaxing the convexity assumption is discussed; the study shows that both the traditional linear regression approach and the suggested weighting fail similarly in extrapolation cases.

## 9.2 Methodology

The steps needed to regionalize the hydrological model parameters are:

1. The identification of the model parameters for the donor catchments (gauged catchments)
2. The identification of the catchment properties to be used for the transfer of model parameters
3. The assessment of the procedure to transfer model parameters to the ungauged catchments

## 9 Regionalization of the Hydrological Model Parameters Using Data Depth

The first step is usually done by model calibration by using a numerical optimization procedure. For the regionalization of model parameters, one of the major problems is that there is a large number of parameter vectors which perform nearly equally well. It is difficult to decide which of these should be taken for regionalization. Dotty plots, showing model performances as a function of individual parameters, show that a wide range of parameter values can lead to good model performance.

After performing step 1, classical multivariate regression take care of steps 2 and 3 using a stepwise procedure as demonstrated in (Samaniego and Bárdossy, 2006). The most significant variable is selected first and the corresponding linear regression is calculated. Then, stepwise, new variables enter the system until no significant improvement can be achieved. This procedure can be used to regionalize certain discharge characteristics such as annual discharge or extremes.

More sophisticated procedures combine all the three steps mention above, for example, in Hundscha and Bárdossy (2004); Götzinger and Bárdossy (2007) the transfer function parameters are estimated simultaneously with the model parameters. In Lamb and Kay (2004), a procedure for the stepwise estimation of the parameters is suggested, where the regionalization of a parameter is followed by a recalibration of the other parameters. Another important step, although seldomly considered is the decision, whether the regionalization for the ungauged catchment can be performed on the basis of the gauged (donor) catchments or not. For ungauged catchments whose properties are very different from those of the donor catchments, a regionalization might be unreasonable. In order to make regionalization reasonable, one might allow the procedure to work for catchments whose properties are comparable range to the donor catchments. A further measure is to restrict the regionalization to ungauged catchments whose relevant properties for the regionalization are inbetween the properties of the donor catchments in a geometrical sense - *i.e.* they are in the convex hull of the property vectors of donor catchments. Figure 9.1 schematically explains the concept. The triangle represent the convex hull of properties of the observed catchments. The point marked with \* (star) is representing a catchment with properties inside the convex hull, for which a regionalization is “safe”. The point marked with circle, correspond to a catchment for which extrapolation is required. This point is outside of the convex hull.

Formally a vector  $\mathbf{v} = (v_1, \dots, v_k)$  is in the convex hull of the vectors  $\mathbf{u}^i = (u_1^i, \dots, u_k^i)$  for  $i = 1, \dots, m$  if and only if

$$v_j = \sum_{i=1}^m \lambda_i u_j^i$$

for all  $j = 1, \dots, k$  with  $\lambda_i \geq 0$  and  $\sum_{i=1}^m \lambda_i = 1$ .

If this is the case, then step 3 of the procedure might become unnecessary for linear regionalization. To see this let us assume that  $(b_1^*, \dots, b_j^*)$ , denotes the parameters of the hydrological model for catchment \*. Assuming a linear function can be used to regionalize the model parameters, this would mean that any selected model parameter  $b_j^k$  for catchment  $k$  can be calculated as a linear function of the catchment characteristics

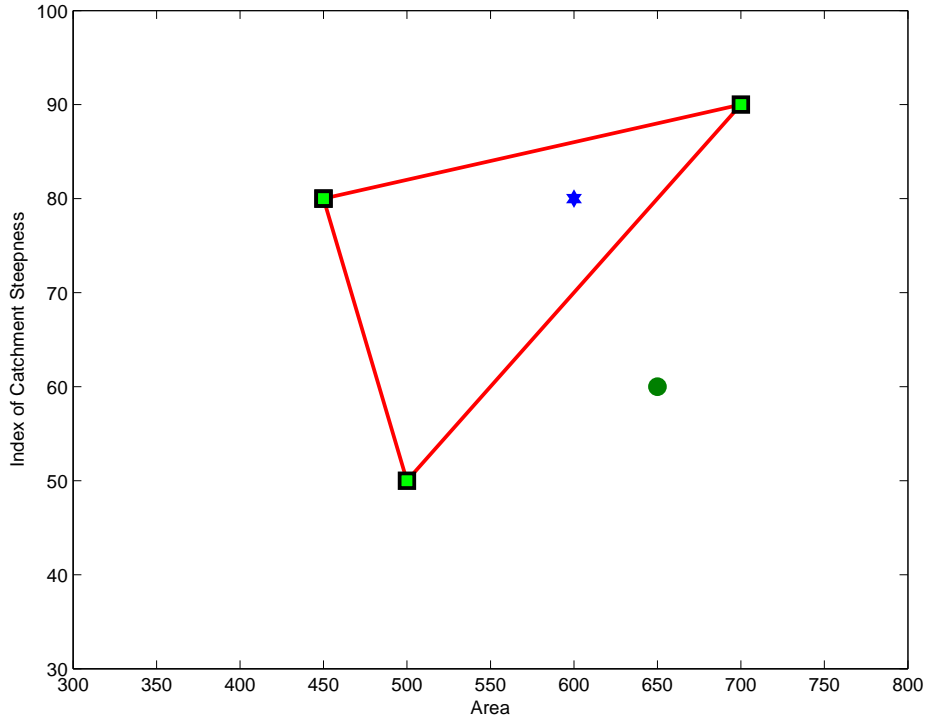


**Figure 9.1:** Schematic representation of inside catchment (blue star) and case of extrapolation (green circle)

$c_i^k$ :

$$b_j^k = a_{0,j} + \sum_{i=1}^I a_{i,j} \cdot c_i^k \quad (9.1)$$

If one restricts regionalization to catchments whose properties are not outside the ranges of the catchments with observations, or even restricting them to their convex hull, then all selected properties of a catchment  $k$  in the convex hull can be written as a linear combination of the properties of catchments. After this, one has:

$$c_i^k = \sum_{l=1}^L \lambda_l \cdot c_i^l \quad i = 1, \dots, I \quad (9.2)$$

Further  $\lambda_l \geq 0$  and  $\sum \lambda_l = 1$ . (Note that the weights are the same for each property.) Combining equations (9.1) and (9.2) leads to:

$$b_j^k = a_{0,j} + \sum_{i=1}^I a_{i,j} \cdot \sum_{l=1}^L \lambda_l \cdot c_i^l \quad (9.3)$$

exchanging the summations gives:

$$b_j^k = a_{0,j} + \sum_{l=1}^L \lambda_l \cdot \left( \sum a_{i,j} \cdot c_i^l \right) \quad (9.4)$$

Assuming that  $\sum_{l=1}^L \lambda_l = 1$  leads to the equation:

$$b_j^k = \sum \lambda_l \cdot b_j^l \quad (9.5)$$

This equation says that in the case of a linear regionalization function the model parameters can be calculated directly using the weights  $\lambda_l$  without the explicit calculation of the coefficients  $a_{i,j}$ . A weighted combination of the model parameters was suggested in Kay et al. (2006). However, their weights are based on catchment similarity indices, while here weights can directly be identified from the catchment properties.

Note that for a given catchment, weights  $\lambda_l$  are either non-existent (for catchments with property vectors outside the convex hull), or are in general non-unique (for catchments inside the convex hull) leading to a set of parameter vectors. The estimator obtained under the mentioned constraints will be called the *convex estimator* in the rest of this chapter.

Of course, a perfect regionalization is not possible, thus one can assume a random error  $\varepsilon_j^k$

$$b_j^k = a_{0,j} + \sum_{i=1}^I a_{i,j} \cdot c_i^k + \varepsilon_j^k \quad (9.6)$$

This modifies equation 9.5 to

$$b_j^k = \sum_{l=1}^L \lambda_l \cdot b_j^l + \sum_{l=1}^L \lambda_l \varepsilon_j^l \quad (9.7)$$

Thus assuming that the errors are independent (which is the assumption for multiple linear regression)

$$\text{Var} \left[ b_j^k - \sum_{l=1}^L \lambda_l \cdot b_j^l \right] = \sum_{l=1}^L \lambda_l^2 \left( \varepsilon_j^l \right)^2 \quad (9.8)$$

Equation 9.8 shows that the estimation error variance depends on the weights  $\lambda_l$ . Combining  $\lambda_l \geq 0$  with  $\sum_{l=1}^L \lambda_l = 1$  implies that

$$\sum_{l=1}^L \lambda_l^2 \leq 1$$

thus the estimator defined in equation (9.5) is at least as good as the linear estimation defined in (9.1).

However, for the estimator 9.5 note that one only needs the geometrical properties of the catchment characteristics (relevant for regionalization) and, consequently, no fit of the



regression parameters  $a_{i,j}$  is required. This means that a regionalization on the basis of a few catchments becomes possible, in contrast to the multiple linear regression approach where a small number of samples makes the parameter estimation very uncertain. The eventual non-uniqueness of the weights  $\lambda$  leads to a set of model parameters, even if only one parameter vector is used for each catchment with observations. On the other hand, the convex estimator can only be used for catchments which are in the convex hull of the catchments with observations (in the sense of relevant catchment properties).

A weighted sum estimator could also be used outside the convex hull (which is extrapolation case) without considering the  $\lambda_l > 0$  condition; however, in this case, the squared sum of the  $\lambda$ 's has to be restricted. Furthermore, due to the extrapolation, the estimator may become unreliable. This problem is demonstrated and discussed in the application section.

Another problem, namely, that the model parameters cannot be identified as unique parameters for the catchments with observations (equifinality), remains and leads to the problem of deciding on which model parameters  $b$  to combine in (9.5). This problem is discussed in following sections.

### 9.2.1 Choice of catchment properties

The selection of appropriate catchment properties is a central problem for regionalization. Usually a great number of candidates are used and sequentially the most important ones are selected. For the above proposed regionalization, the method is restricted to the convex hull of the donor catchment property vectors. As more properties are selected, the number of catchments which remain in convex hull, becomes smaller. Thus it is essential to keep the number of relevant catchment properties as small as possible. For this purpose, we develop a procedure to investigate whether, for a choice of relevant catchment properties the regionalization could be performed using the convex combination (9.1) for all catchments with observations.

This problem can be treated from a geometrical viewpoint. In [Bárdossy and Singh \(2008\)](#), it is shown that good performing parameters (e.g. parameters with which the model has an Nash-Sutcliffe coefficient (NS) above a given threshold, or the root mean squared error below a threshold) of a model (denoted as  $B^*$  and for a given catchment  $*$ ) can be effectively embedded in a convex set in the  $J$  ( $J =$  number of model parameters) dimensional space of model parameters. In fact, for several models, the convex set can be selected such that all parameter vectors of this set are good (meaning that  $B^*$  is itself convex). The relevant catchment properties are well selected if there is a linear function of these properties which provides well performing parameters for each catchment. This means that this linear function intersects with each  $B^*$ .

In order to select the catchment characteristics, the sets  $B^*$  of the observed catchments are investigated. The goal is to find out whether for a selected set of catchment properties there is a linear function (9.1) such that this function intersects with all sets of good performing model parameters. If a set of properties is selected then for a catchment with observations for which the regionalization on the basis of the other catchments can be performed using (9.5) serves as control. For this, one can try all possible parameters

of the donor catchments for the regionalization. If none of the combinations work well for the selected catchment, then the regionalization using these properties will fail - and other properties have to be selected.

The formal description of this procedure is as follows. Assume the regionalization procedure should be checked for a catchment with a vector of characteristics  $(c_1^*, \dots, c_I^*)$ . If this vector is in the convex hull of the parameter vectors corresponding to the other catchments then

$$C = \left\{ (c_1^l, \dots, c_I^l); l = 1, \dots, L \right\}$$

(which means  $c_i^* = \sum_{l=1}^L \lambda_l \cdot c_i^l$  with  $\sum_{l=1}^L \lambda_l = 1$  and  $\lambda_l \geq 0$ ). If the catchment properties are such that a regionalization using them is reasonable, equation (9.7) should lead to good model parameters for the catchment indicated by \*.

For each catchment \*, whose selected catchment properties are in the convex hull of the other catchments properties and which have discharge observations, one can check whether the selected catchment properties would allow a regionalization for it. This also means that there are good parameters for \* in the convex hull of the parameter sets  $B^l$ . If, on other hand,

$$B^* \cap \text{conv} (B^1, \dots, B^L) = \emptyset \quad (9.9)$$

then this property is not fulfilled. Consequently, any regionalization using the selected catchment properties cannot provide good parameters. The advantage of the formulation (9.9) is that it provides a purely geometrical condition which can be checked without performing the regionalization explicitly. This can be used to select an appropriate set of explaining variables for the regionalization. The corresponding selection of appropriate variables (**SAV**) algorithm is as follows:

1. Take all catchments with the set of possible catchment characteristics
2. Identify the sets of good parameters  $B^l$  for each catchment  $l = 1, \dots, L$  using the ROPE algorithm described in [Bárdossy and Singh \(2008\)](#)
3. Select a catchment property  $c_{i_1}$ ; set  $m = 1$  and define a set of selected indices  $S_m = \{i_1\}$
4. Select a catchment  $l = 1$
5. Select an  $m+1$  catchments with observations which do not include  $l$  ( $\{l_1, \dots, l_{m+1}\} \subset \{1, \dots, L\} - \{l\}$ ); check if the vector of selected catchment properties  $(c_{i_1}^l, \dots, c_{i_m}^l)$  is in the convex hull of the vectors corresponding to the above chosen  $m + 1$  catchments  $((c_{i_1}^{l_1}, \dots, c_{i_m}^{l_1}), \dots, (c_{i_1}^{l_{m+1}}, \dots, c_{i_m}^{l_{m+1}}))$ . If yes then regionalization can be checked for this combination - the convex combination should perform for the selected catchment  $l$  as target and the  $m + 1$  catchments as donors.
6. If the above condition holds, check if

$$B^l \cap \text{conv} (B^{l_1}, \dots, B^{l_{m+1}}) \neq \emptyset$$

holds. This means all convex combinations of all good parameters for the donor catchments are considered. If none of them gives good parameters for the target then the regionalization cannot be performed.

7. If the above condition does not hold, then the set of selected catchment properties is not sufficient to perform the regionalization. In this case, an additional property  $c_{i_{m+1}}$  has to be selected. The new  $S_{m+1} = S_m \cup \{i_{m+1}\}$  is defined and  $m = m + 1$ . The algorithm continues with step 4.
8. Repeat steps 5 to 7 until all  $m + 1$  element subsets of the set  $\{1, \dots, L\} - \{l\}$  are visited
9. Repeat steps 5 to 8 until all catchments  $l$  are considered
10. The resulting set  $S_m$  consists of the indices of catchment properties which are good candidates for linear regionalization

The above algorithm might have two singular outcomes:

- No set of the catchment properties fulfills the above conditions. In this case, one has to select additional properties and might weaken the conditions defining the good sets  $B^l$ .
- The catchment properties lead to a case where condition 5 of the above algorithm is never fulfilled. In this event, the selected properties make all catchments singular and the regionalization using (9.7) cannot be performed.

Note that the increase in the selected catchment properties in step 7 leads to a decrease in the number of intersections to be checked in step 6. The selection of the catchment property in steps 3 and 7 should be based on hydrological understanding - the purpose of the algorithm is to decide whether a selection is reasonable or not.

Once a set of catchment properties is selected, a method for the selection of the appropriate model parameter vectors has to be done.

The calculation of the intersection in step 6 is done by the Monte Carlo simulation that generates elements in  $B^l$  and checks if they belong to the convex hull of the union of the sets corresponding to the other catchments.

Figures 9.2 and 9.3 schematically explain the algorithm for the case of two model parameters and one and two catchment properties, respectively. In the first case, a single catchment property is taken for all the catchments available. The two extreme catchments are identified from the catchment property under consideration and shown by circles (red and black) in figure 9.2(a). Figure 9.2(b) illustrates the good parameters  $B$  in the model parameter space corresponding to these two extreme catchments. Using these two extreme catchments good model parameters ( $B^l$ ), one can construct their convex hull as shown in figure 9.2(c). Now in order to check the feasibility of the regionalization we need to take a catchment whose catchment property lies within the properties corresponding to the two extreme catchments; this is then marked by a circle

(blue point) and shown in figure 9.2(d). If this (blue) catchment can be regionalized using the selected property, then in the parameter space of the set of good parameters corresponding to the (blue) catchment (in the blue rectangle) should have an intersection with the convex hull of the parameters of the catchment corresponding to the two extreme catchments (black and red points). This can be verified in figure 9.2(e) where in our case the intersection is empty. In this case no linear function of the selected catchment property using the black and red catchments would lead to good performing model parameters for the blue catchment. Thus at least one more catchment property has to be taken into account. This is explained in figure 9.3, where the catchment property space is two dimensional (two properties). The three catchments corresponding to the corners of the triangle in the property space possess good parameters in the convex sets (denoted by the same colors). For an inside catchment (green point), the corresponding good set intersects with the convex hull corresponding to the three corners. Therefore the condition of step 7 is fulfilled. To see if this condition is fulfilled throughout, it should be checked for all catchments to decide whether two properties are enough to perform regionalization. If not, an additional catchment property has to be considered.

Note that the above algorithm can also be used to identify the properties for a regionalization with a non-linear function, which is monotonic in each of its variables. The reason for this is that monotonic functions are able to map the interior of a set to the interior of the image set.

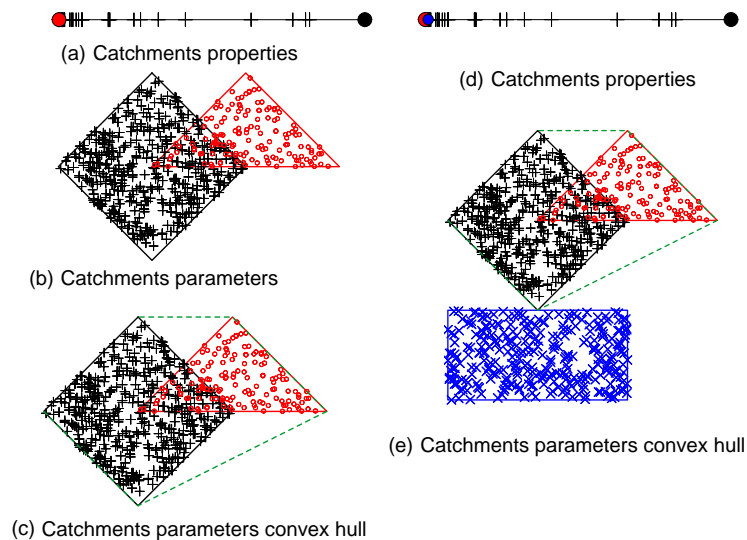


**Figure 9.2:** The condition of step 7 of the algorithm for the case of one catchment property (red and black are two extreme catchments and blue is inbetween catchment)

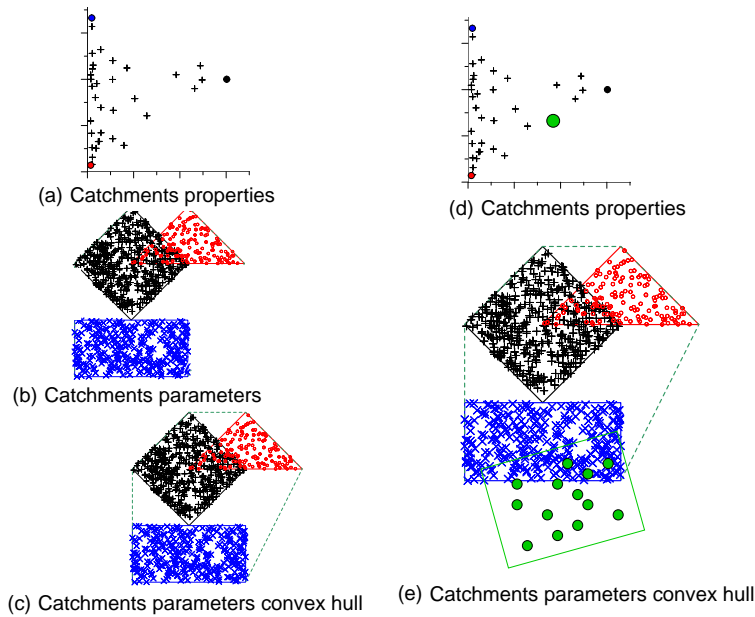


**Figure 9.3:** *The condition of step 7 of the algorithm for the case of two catchment properties (red, black and blue are the extreme catchments and green is inbetween catchment)*

## 9.2.2 How to perform regionalization

It would be ideal if all good model parameters of the catchments could be combined to good parameters of the catchment of interest using (9.5). Unfortunately, this is unlikely to ever be the case. In [Bárdossy and Singh \(2008\)](#), we showed that for a catchment the deepest parameter vectors are robust and transferable to other time periods. In light of this, a reasonable choice of model parameters for (9.5) is to take the deepest points of the good sets  $B^l$ . The definition of data depth can be found in the Chapter 3. Another possibility is to perform an explicit multiple linear regression according to (9.1) using the deepest parameters for the observed catchments. Alternatively, an implicit multiple regression, as described in [Hundecha and Bárdossy \(2004\)](#), can be used where model parameters are restricted to the sets  $B^l$ .

## 9.3 Case Study

The concept of the regionalization will be illustrated with examples from British catchments. The hydrological model chosen for this research is the HYMOD. A short overview of the study area and model concept description is provided in Chapter 4.

## 9.4 Application and Results

### 9.4.1 Choice of catchment properties

Nine possible catchment properties were selected to be considered for regionalization and are listed in table 9.1. In order to check the quality of the regionalization, the good set of parameters was identified for each catchment using the ROPE algorithm. As for the model performance measure  $NS_p$ , a combination of the Nash-Sutcliffe coefficient for the whole time period ( $N_a$ ) and the Nash-Sutcliffe coefficient calculated for each year  $t$  ( $N_y$ )  $y = 1, \dots, NY$  ( $NY$  being the number of years) was selected:

$$NS_p = N_a + \min(N_1, \dots, N_{NY}) \quad (9.10)$$

This performance measure restricts the possible parameters set by taking only those which are nearly equally good for all years.

Characteristic	Unit	Description
AREA	km <sup>2</sup>	Watershed drainage area
BFIHOST		Base-flow index derived using HOST classification
DPSBAR	m/km	Index of watershed steepness
APSBAR		Index representing the dominant aspect of watershed slopes
APSVAR		Index representing the invariability of aspect of watershed slopes
RMED-1H	mm	Median annual maximum 1-hour precipitation
MED PERM		Percentage soil within watershed with medium/mixed permeability
LOW PERM		Percentage soil within watershed with low permeability

**Table 9.1:** *The catchments properties to be considered for regionalization (Yadav et al. (2007))*

The selection of appropriate variables (SAV) algorithm described in Section 9.2.1 was applied to the selected catchments with the list of properties defined in table 9.2. The intersection of the sets was calculated using the Monte Carlo simulation. This means that the points in the possible parameter domain were simulated uniformly (after rescaling). Then each simulated point was checked to see if the point belonged to the set corresponding to the catchment. In the case when a single catchment property was selected, there were always cases with empty intersections. A step-wise increase of the catchment property led to non-empty intersections, if three catchment properties were selected. In this case, the selected catchment properties were: AREA (catchment area), BFIHOST (base flow index), DPSBAR (index of catchment steepness).

### 9.4.2 Regionalization

The transfer of parameters to unobserved catchments was tested using the classical linear regionalization approach (9.1), using multiple linear regression and with the convex combinations (9.5). In the first step, regionalization was restricted to catchments whose selected properties were in the convex combination of those of the other catchments.

## 9.4 Application and Results

Cat. Nr.	AREA	BFIHOST	DPSBAR	APSBAR	APSVAR	RMED-1H	MOD PERM	LOW PERM
1	569.8	0.49	112.10	109.8	0.19	9.1	16.4	26.2
2	269.4	0.46	32.83	93.2	0.25	0.4	0.0	0.0
3	321.9	0.33	125.70	12.3	0.20	10.7	0.0	0.0
4	74.9	0.46	109.67	94.7	0.34	10.0	0.0	0.0
5	196.3	0.43	75.96	300.6	0.24	10.1	0.0	87.4
6	86.1	0.21	67.67	55.6	0.31	10.7	0.0	0.0
7	282.3	0.37	101.84	169.8	0.13	10.5	28.3	1.1
8	59.2	0.60	147.69	173.7	0.24	10.1	0.0	46.7
9	83.0	0.78	144.58	185.4	0.09	10.2	21.0	0.0
10	55.2	0.90	61.13	69.3	0.24	10.6	0.0	0.0
11	68.9	0.51	62.65	108.6	0.17	12.2	0.0	71.1
12	194.0	0.55	40.79	97.0	0.16	12.6	0.0	44.5
13	98.8	0.86	13.50	203.0	0.18	11.1	0.0	7.7
14	238.2	0.53	30.98	121.3	0.15	11.0	0.0	73.3
15	106.7	0.94	78.39	147.7	0.18	10.6	0.0	12.4
16	1040.0	0.90	50.10	176.0	0.15	10.6	0.1	3.1
17	220.6	0.81	80.13	125.0	0.15	10.9	25.5	13.2
18	202.5	0.54	85.00	195.0	0.11	11.4	31.7	40.6
19	112.7	0.39	91.19	227.2	0.17	12.0	0.0	100.0
20	87.0	0.69	80.74	242.4	0.15	11.8	0.0	76.9
21	826.2	0.42	106.94	219.9	0.07	11.9	2.3	95.4
22	135.2	0.47	72.51	218.3	0.17	10.7	12.8	44.3
23	47.9	0.46	64.00	270.1	0.24	10.8	4.3	84.1
24	259.0	0.61	22.76	119.3	0.11	9.4	0.0	73.2
25	203.3	0.67	161.66	122.8	0.19	9.8	0.0	83.7
26	1090.4	0.48	157.20	214.0	0.09	11.3	0.1	99.2
27	893.6	0.53	112.35	285.7	0.10	11.0	0.0	100.0
28	53.9	0.27	152.19	89.3	0.17	11.2	0.0	100.0

**Table 9.2:** *The numerical values of the considered catchment properties*

## 9 Regionalization of the Hydrological Model Parameters Using Data Depth

Thus two groups were obtained. The first group contained the so called *boundary* catchments; whose properties cannot be obtained as a convex combinations of the others. The second group contained the *inside* catchments whose properties are in the convex hull of the properties of the boundary catchments. Table 9.3 lists the *boundary* and the *inside* catchments. Regionalization was performed and checked for each inside catchment. As an illustration of the methodology, Table 9.4 shows a set of possible boundary catchments and the corresponding weights for the target inside catchment 20. The linear parameter estimation was carried out by using the deepest parameters for the catchments in the boundary set. For comparison, a set of randomly selected good parameters were also used.

Boundary	Inside
2	1
3	4
6	5
8	7
9	12
10	17
11	18
13	19
14	20
15	22
16	
21	
23	
24	
25	
26	
27	
28	

**Table 9.3:** List of the boundary and the inside catchments

Inside Catchment	Boundary Catchment	Weights	AREA	BFIHOST	DPSBAR
20	2	0.127761	269.4	0.46	32.83
	6	0.109825	86.1	0.21	67.67
	8	0.260020	59.2	0.60	147.69
	10	0.502394	55.2	0.90	61.13
				87.0	0.69

**Table 9.4:** A set of possible boundary catchments for catchment 20 and the corresponding weights



The convex combinations were also applied both for the deepest parameters and randomly selected good ones too. As it often is inside catchments, the catchment properties can be expressed as a large number of convex combinations of the boundary catchments. Some of the special cases were selected.

The performance of the explicit multiple linear regression (9.1) using the deepest and randomly selected parameter vectors for the estimation of the regression coefficients, and the corresponding results using the convex estimator (9.5) is shown in table 9.5. As one can see, the performances of the two estimators are similar. The deepest parameter vectors lead to the best estimations for both cases. The performance of the models using the regionalized parameters is comparable to the performance which was obtained using calibration. Note that one cannot expect a better performance for the target catchment than the performance of the model parameters on the catchments which were used for regionalization. Figure 9.4 shows the observed and the simulated hydrographs for catchment 17 using the convex estimator (using 4 boundary catchments only) and multiple linear regression with the deepest point. Figure 9.5 shows the same in the case of an extrapolation.

Inside Cat	Opt	Weighted Combination					Multiple Regression				
		Deep	Random				Deep	Random			
			Mean	Max	Min	Std		Mean	Max	Min	Std
1	1.16	1.13	1.12	1.13	1.12	0.0026	1.14	1.14	1.14	1.12	0.0044
4	0.94	0.85	0.85	0.86	0.82	0.0071	0.87	0.87	0.88	0.85	0.0065
5	1.20	1.11	1.11	1.12	1.09	0.0059	1.12	1.12	1.13	1.11	0.0034
7	1.67	1.65	1.65	1.65	1.64	0.0030	1.64	1.63	1.64	1.62	0.0042
12	1.33	1.20	1.22	1.25	1.17	0.0168	1.25	1.25	1.26	1.24	0.0053
17	1.63	1.37	1.36	1.42	1.31	0.0242	1.43	1.42	1.50	1.34	0.0341
18	1.41	1.00	1.02	1.06	0.98	0.0181	1.02	1.02	1.05	0.98	0.0137
19	1.69	1.63	1.63	1.64	1.63	0.0025	1.60	1.60	1.61	1.59	0.0033
20	1.70	1.45	1.45	1.49	1.39	0.0176	1.52	1.51	1.53	1.47	0.0135
22	1.47	1.26	1.26	1.28	1.23	0.0117	1.26	1.26	1.28	1.24	0.0064

**Table 9.5:** The performance ( $NS_p$ ) of the convex estimation (9.5) and the explicit multiple linear regression using the deepest and randomly selected parameter vectors for inside catchments

Equations as mentioned above, could also be used for extrapolation if negative weights  $\lambda < 0$  are allowed. Unfortunately in this case, all possible parameter vectors could be obtained in the form of (9.5). Thus, for extrapolation with (9.5) another criterion is needed, for example a 'best' estimator minimizing the estimation variance can be used. This means that  $\sum_{l=1}^L \lambda_l^2$  is minimized under the conditions imposed by the catchment properties and  $\sum_{l=1}^L \lambda_l = 1$ .

This estimator can be used both for inside and boundary catchments. The  $\lambda_l$  weights

9 Regionalization of the Hydrological Model Parameters Using Data Depth

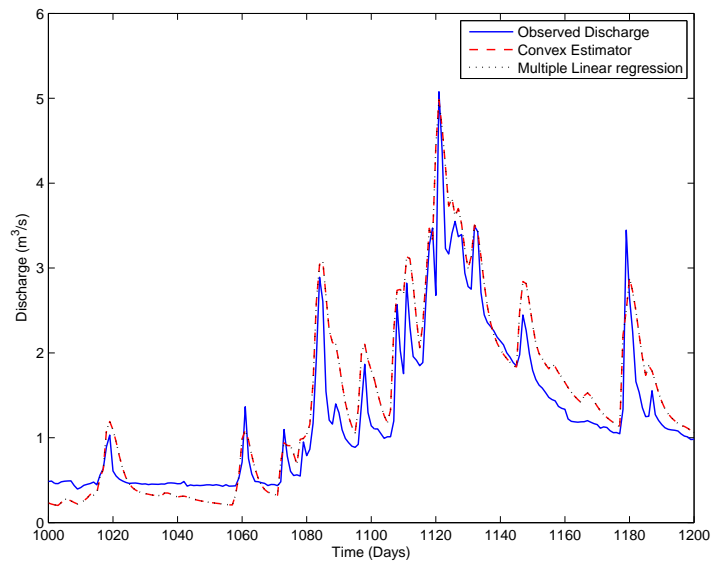


**Figure 9.4:** Observed and simulated hydrographs for catchment 17 using the convex estimator (using 4 boundary catchments only) and multiple linear regression with the deepest point

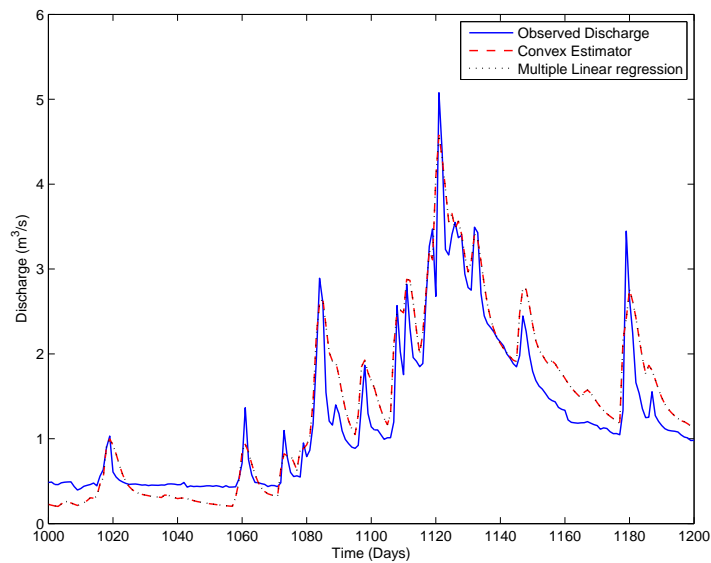


**Figure 9.5:** Observed and simulated hydrographs for catchment 17 using the convex estimator and multiple linear regression with the deepest point in case of extrapolation (negative weights allowed)

are determined by solving the minimization problem:

$$\sum_{l=1}^L \lambda_l^2 \rightarrow \min$$

under the constraints:

$$c_i^* = \sum_{l=1}^L \lambda_l \cdot c_i^l \quad i = 1, \dots, I \quad (9.11)$$

and

$$\sum_{l=1}^L \lambda_l = 1$$

For this regionalization, which is not restricted to the convex hull (allowing negative weights), a cross validation was performed. The corresponding results are listed in table 9.6. One can see that for extrapolation, both multiple linear regression and the weighted sum have failed for catchment 16, which is a boundary catchment. Its properties differ strongly from those of the other catchments, meaning that the parameter estimation for this catchment could be risky. The corresponding sum of the squared weights is the largest for this catchment, indicating the highest uncertainty of the estimation. One could assume that the bad performance is due to hydrologically different behavior of this catchment. This is not the case, however, as will be shown in the next paragraphs. To test the effectiveness of the method with fewer boundary catchments, all  $J + 1$  element subsets of the catchment property vectors corresponding to the boundary set, which contained the property vector of the target catchment in their convex hull, were identified. For our case, this means that for each inside catchment as a target, all sets of the 4 boundary catchments whose properties contained those of the target catchment in their convex hull were obtained. Table 9.7 shows the number of all possible four catchment combinations of boundary catchments for describing the inside catchments. For any  $J + 1$  selected catchments, the weights  $\lambda_l$  are unique (due to the constraint that  $\sum \lambda_l = 1$ ). The estimation was carried out using these weights and the performance of the resulting parameter set was calculated. Figure 9.6 shows the performance of the estimator for selected target catchments using the deepest and randomly selected parameters. The x-axis shows the minimal performance corresponding to the selected boundary catchments; while on the y-axis, one can read the performance of the model for the target catchment using the convex estimator (9.5) for the selected combination. One cannot expect a better performance for the target catchments than for the catchments used for the regionalization, thus, the points above the main diagonal are obtained more or less by chance. Note also that a large number of combinations can be formed. All regionalizations which used the deepest parameter vectors performed well. On the other hand, the quality from the randomly selected (i.e. less deep) ones was less, showing larger scattering. This may consequently lead to lower performances.

In order to check whether catchment 16 behaves irregularly compared to the others, as one might assume based on the cross validation results for multiple linear regression

9 Regionalization of the Hydrological Model Parameters Using Data Depth

Cat Nr.	Opt	Weighted Combination					Multiple Regression				
		Deep	Random				Deep	Random			
			Mean	Max	Min	Std		Mean	Max	Min	Std
1	1.16	1.13	1.13	1.14	1.12	0.0031	1.14	1.14	1.15	1.12	0.0068
2	1.18	1.15	1.15	1.16	1.14	0.0042	1.13	1.13	1.15	1.12	0.0050
3	1.34	1.25	1.25	1.27	1.24	0.0069	1.26	1.25	1.27	1.24	0.0059
4	0.94	0.87	0.87	0.89	0.85	0.0089	0.88	0.87	0.89	0.85	0.0062
5	1.20	1.13	1.13	1.14	1.12	0.0038	1.12	1.13	1.14	1.12	0.0044
6	1.02	1.02	1.02	1.03	1.01	0.0046	0.99	1.09	1.04	0.98	0.0164
7	1.67	1.65	1.65	1.66	1.64	0.0028	1.64	1.64	1.65	1.63	0.0032
8	1.04	0.93	0.93	0.95	0.91	0.0071	0.95	0.95	0.97	0.91	0.0111
9	1.55	1.23	1.22	1.28	1.16	0.0230	1.31	1.23	1.39	1.06	0.0871
10	1.25	1.03	1.03	1.11	0.98	0.0217	1.03	1.03	1.11	0.999	0.0211
11	1.10	0.96	0.96	0.97	0.95	0.0048	0.98	0.97	0.99	0.94	0.0112
12	1.33	1.26	1.25	1.27	1.24	0.0063	1.24	1.24	1.25	1.23	0.0043
13	1.69	1.65	1.63	1.67	1.55	0.0247	1.64	1.65	1.68	1.55	0.0233
14	1.11	0.99	0.99	0.99	0.98	0.0023	0.98	0.98	0.98	0.97	0.0026
15	1.29	1.26	1.25	1.31	1.17	0.0280	1.18	1.17	1.26	1.04	0.0543
16	1.59	-4.22	-4.08	-1.30	-7.456	1.4227	-3.81	-5.15	-0.51	-13.80	4.1568
17	1.63	1.48	1.47	1.52	1.43	0.0171	1.44	1.44	1.51	1.36	0.0341
18	1.41	1.08	1.07	1.11	1.04	0.0127	1.07	1.07	1.19	1.04	0.0129
19	1.69	1.64	1.63	1.64	1.63	0.0036	1.62	1.68	1.64	1.61	0.0087
20	1.70	1.50	1.49	1.51	1.48	0.0060	1.52	1.50	1.53	1.47	0.0173
21	1.54	1.45	1.45	1.48	1.43	0.0091	1.42	1.43	1.46	1.40	0.0186
22	1.47	1.30	1.30	1.31	1.29	0.0042	1.27	1.28	1.30	1.26	0.0088
23	1.40	1.38	1.38	1.39	1.37	0.0030	1.36	1.37	1.38	1.36	0.0077
24	1.35	1.08	1.08	1.11	1.04	0.0158	1.15	1.14	1.16	1.07	0.0098
25	1.43	1.06	1.05	1.15	0.93	0.0410	1.09	1.06	1.13	0.96	0.0391
26	1.55	1.37	1.37	1.42	1.34	0.0173	1.29	1.30	1.37	1.23	0.0352
27	1.73	1.54	1.54	1.57	1.51	0.0111	1.62	1.60	1.64	1.52	0.0341
28	1.36	1.38	1.38	1.42	1.34	0.0181	1.31	1.34	1.38	1.29	0.0267

**Table 9.6:** Cross validated performance ( $NS_p$ ) of the relaxed convex combination (negative weights allowed) and multiple linear regression using the deepest and randomly selected parameter vectors

Inside catchment Nr.	Total number of possible combinations (4 catchments combinations)
1	359
4	183
5	249
7	151
12	211
17	256
18	470
19	168
20	256
22	323

**Table 9.7:** Number of possible combinations for the choice of 4 boundary catchments which include the properties of the given inside catchments

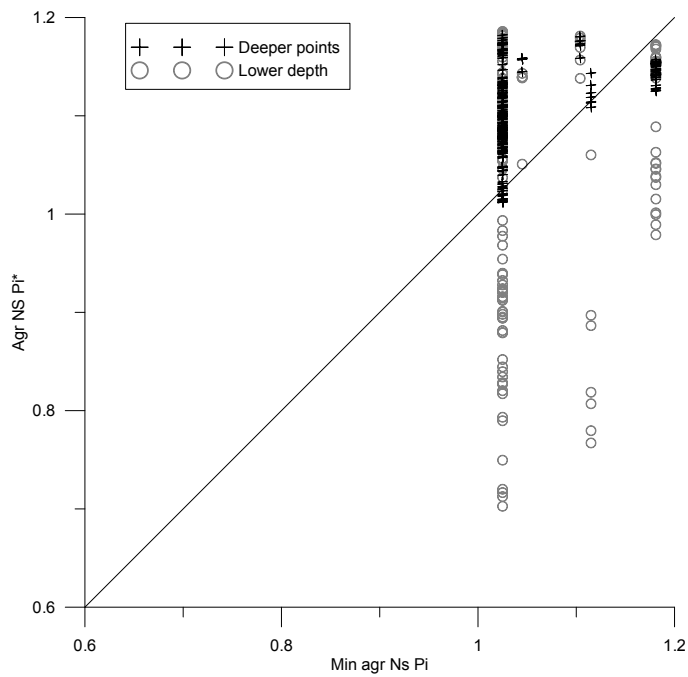


**Figure 9.6:** The performance ( $NS_p$ ) of the convex estimator for target catchment 5 using the possible 4 catchment combinations with the deepest (red crosses) and randomly selected parameters (black stars)

## 9 Regionalization of the Hydrological Model Parameters Using Data Depth

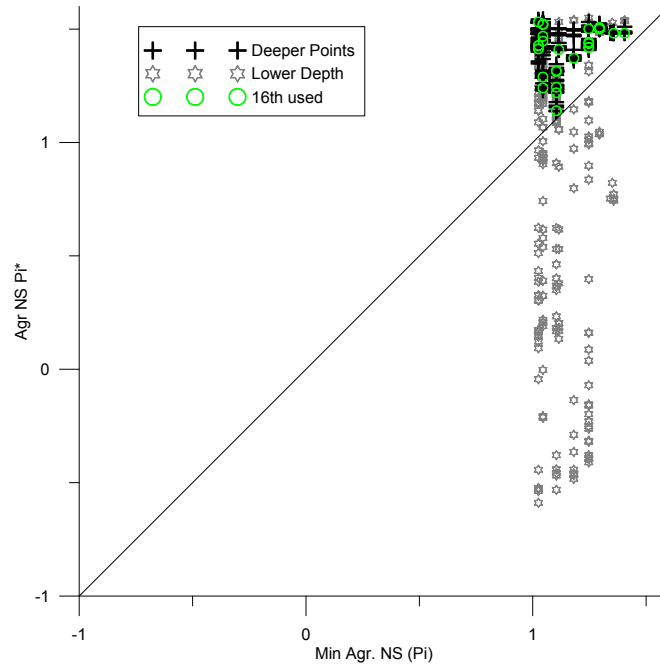


**Figure 9.7:** The performance ( $NS_p$ ) of the convex estimators for catchment number 20 using the deepest (red crosses) and lower depth (black stars). The estimators using the deepest parameter vectors including catchment 16 are marked with a green cross

estimation, all combinations for which this catchment were used for regionalization were selected. If catchment 16 would be an irregularly behaving catchment, then the combinations where catchment 16 is used should not perform well. However, this is not the case. Figure 9.7 shows that all combinations which include catchment 16 perform as good as the other combinations. The impossibility of the regionalization for catchment 16 is mainly caused by the inability to estimate the overall slope of the linear function from the other catchments.

## 9.5 Conclusions

- In this chapter the possibilities to regionalize a conceptual model parameters using explicit and implicit methods were discussed. It was shown that for a catchment whose property vector is in the convex hull of the property vector of observed catchments, a linear regionalization can be replaced by a convex combination for which an explicit estimation of the coefficients of the regionalization function was not required.
- The idea of convex combinations could be used to check whether a set of properties should be used for regionalization. Selection of appropriate variables (SAV) algorithm was developed for this purpose.

- After selection of the catchment properties, regionalization can be carried out using either the classical linear regression approach or using the convex combinations.
- The developed methodology was applied to a set of 28 British catchments using the HYMOD model. For the case study, three catchment properties were identified as necessary for the regionalization of the five model parameters.
- Data depth is a useful tool to identify unique parameter vectors for regionalization. If parameter vectors with a low data depth (which are near the boundary of the good parameter set) are used for regionalization the performance for the target catchment varies strongly. The deepest parameter sets lead to good regionalizations both for the linear regression and the convex combination methods.
- The performance of the model using regionalized parameters is comparable to the performance of the model on the catchments used for regionalization.
- The restriction of the estimator (9.5) to convex combinations (with non-negative weights) allows regionalization toward the *inside* of the observed set. This restriction is reasonable, since the transfer of parameters to catchments which differ strongly from the observed ones is always risky.
- As the methodology does not require the estimation of transfer function parameters, it can be used in the case of a small number of catchments too. This was demonstrated for the selected British catchments. Depending on the number of boundary catchments, the convex combination became non-unique, but even using the minimum number of catchments, the estimation quality did not decrease.
- Formally, the non-negativity condition can be relaxed but this leads to an increase of the squared sum of the weights and thus the estimation variance also increases. Further, this allows extrapolation which, as stated above, might be problematic.
- In the case study region, one catchment was identified whose properties are on the boundary of the property vector set and for which regionalization using other catchments failed. However, this catchment could be applied well to the regionalization of the inside catchments. This result showed that extrapolation might lead to problems even for reasonably behaving catchments.

# 10 Summary and Outlook

## 10.1 Summary

This research work was aimed at developing an efficient, practical and robust methodology for parameter estimation for a reliable hydrological modeling at gauged and ungauged basins.

The estimation of hydrological model parameters is a challenging task. With increasing capacity of computational power several complex optimization algorithms have emerged, although none of the algorithms gives a unique and *very best* parameter vector. This may be due to several reasons, like process understanding, computational power, error in model structure and so on. Moreover, the parameters of fitted hydrological models depend upon the input data. The quality of input data cannot be assured as there may be measurement errors for both input and state variables. So it is obvious that when input is erroneous than we can not expect output to be perfect. In this research in order to see the effect of observational error on parameters, stochastically generated synthetic measurement errors were applied to observed discharge and temperature data. A multiplicative and additive error were applied to discharge and temperature, respectively. With this modified data, the model was calibrated and the effect of measurement errors on parameters was analysed. It was found that the measurement errors have a significant effect on the best performing parameter vector. The erroneous data led to very different optimal parameter vectors. To overcome this problem, and to find a set of robust parameter vectors, a geometrical approach based on Tukey's half-space depth was used. Data depth is nothing but a quantitative measurement of how central a point is with respect to a multivariate data cloud or a distribution. This gives us the central outward ordering of a data points in a multivariate sample. One advantage of Tukey's half-space depth is that it is invariant to affine transformations of space. This means that the different ranges of the parameters have no influence on their depth. This makes it suitable to use the depth function for different applications in hydrological science. This could be specifically, be for identifying parameter space of any hydrological model, because each parameter of the hydrological model has different scale and range. Hence, this properties was utilized in this research work. The depth of the set of  $N$  randomly generated parameters was calculated with respect to the set with the best model performance (Nash-Sutcliffe efficiency was used for this research) for each parameter vector. Based on the depth of parameter vectors, one can find a set of robust parameter vectors. Furthermore, depth of a parameter set can give clues about the performance of the parameter set. For example, low depth parameters are unusual combination of parameters. They may perform poor, whereas high depth parameter sets are more robust



combinations of parameters and may give better performance. The results from this research also show that the parameters chosen according to the above criteria have low sensitivity and perform well when transferred to a different time period. The method was firstly demonstrated on the Upper Neckar catchment in Germany. The conceptual HBV model was used to develop the methodology. The algorithm developed based on the data depth function is termed as robust parameter estimation (ROPE) algorithm. The ROPE algorithm is an iterative algorithm to find a convex set containing a good model parameters. The ROPE algorithm can give us a convex set containing good parameter set instead of a single parameter set as we obtained in other optimization algorithms. To make general purpose, the ROPE algorithm was tested on different models like HYMOD and the Three reservoir, in different catchments in England and India catchments, where catchments exhibit very contrasting characteristics and have different data availability. The result shows that the ROPE algorithm has performed well on these catchments and models consequently, we can state that the ROPE algorithm is a general purpose tool for model calibration. In further extension to ROPE algorithm, a very simple and effective optimization algorithm called Sequential Replacement of Weak Parameter (SRWP) was introduced for automatic calibration of hydrological model. In SRWP algorithm the weak parameter set is sequentially replaced with another deeper and good parameter set. The SRWP was tested on several test functions as well as with hydrological models. The SRWP result was compared with the generally used global optimization shuffled complex evolution (SCE-UA) algorithm. The results showed that SRWP easily overcomes the local minima and converges to optimal region. The SRWP does not converges to a single optima, giving instead a convex hull of optimal region. The biggest advantage however, is it converges faster and we can use any kind of criteria or objective function. This algorithm also gives a convex set of a good parameter set instead of a single parameter set. The applicability of SRWP was demonstrated using the HYMOD conceptual model on Upper Neckar catchments of South-West Germany. The results show that the parameters estimated by this stepwise calibration are robust and it is comparable to commonly used global optimization technique.

Hydrological models are used for different purposes. Any particular model can have different goals, which leads us to having different objective functions for model calibration. There are several objective functions, but not a single objective function can describe all the components of a hydrograph. So in this research an attempt was made taken to analysis the parameter space mapped by different objective functions during calibration of a hydrological model by ROPE algorithm. A conceptual hydrological model HYMOD was calibrated using ROPE algorithm with different objective functions, namely, the Nash-Sutcliff coefficient, root mean square error, volume error and peak error. Also with the logarithm Nash-Sutcliff coefficient, logarithm root mean square error, logarithm volume error and logarithm peak error was considered. In this research, only these objective functions were chosen, as these are the ones that we most commonly used. Other function can also be tested in similar ways. It was found that the different objective function have mapped different parameter spaces. Interestingly, perhaps, the Nash-Sutcliff coefficient and root mean square error have very similar parameter distributions. This is

because formulation of both the objective function is very similar. There is no common intersection of parameter space obtained by different objective functions. This shows that objective functions have great influence on optimal parameters of a model. These requires that proper choice is necessary to fulfill the specific purpose of the modeling. The volume shrinkage of parameter space by different objective functions was also different. This indicates that optimal parameters obtained by different objective functions proceeded at different rates. So we should be very careful in choosing the number of iterations for different objective functions. The diagnosis of parameter space has lead us to develop a hierarchical calibration technique. In this, we calibrated our model using one of the objective functions and after getting a convex boundary we can use another objective function and so on. Through this we can overcome the problem of the single and multi-objective function. The results of this research should be very helpful for the robust parameterization of hydrological models.

Usually it is a question of great concern that how much data should be used for model calibration. The length of the observation period used for model calibration has a great influence on the identification of the parameters. Information contained in a time series is not distributed uniformly. We can assume time periods that covers unusual behavior may contain more information for model calibration. So, in this contribution, model parameters are estimated from so-called unusual time periods. These unusual time periods (critical time periods) were identified from discharge or precipitation observations series using the statistical concept of data depth. Depth functions was used to identify unusual events from four days lagged discharge or API (antecedent precipitation index) series. Data with low half-space depth are considered as unusual. Data with low half-space depth are considered as unusual. The critical event selected by API and discharge are almost at the same time period in a series. Model calibration was only slightly worse than using all data if one uses the selected critical periods only. The transferability of the parameters for different time periods is for the rank based depth significantly better than when using all data. Two different models (HBV and HYMOD) were used to demonstrate the methodology for the Neckar catchment in South-West Germany. The developed algorithm, based on data depth for identification of critical time periods is termed as ICE (Identification of Critical Events) algorithm. Using ICE algorithm, we can make precipitation and data depth curve, which can be useful tool for prediction in ungauged basin. To test further the robustness and to generalize, the ICE algorithm was tested on different models and different catchments. It has been used for physically based hydrological models, like the WaSim-ETH on the Rems catchments. The results showed that the complex models like WaSim-ETH can successfully calibrate using critical events selected by ICE algorithm. The ICE algorithm can be very helpful in data driven modeling. So to test the ability of ICE algorithm a study on Artificial Neural Networks (ANNs) was conducted.

Artificial Neural Networks (ANNs) are classified as a data driven technique which implies that their learning improves as more and more training data are presented. This observation is based on the premise that longer time series of training samples will contain more events of different types and hence the generalization ability of the ANN will

improve. However, longer time series of training samples need not necessarily contain more information. If there is considerable repetition of the same type of information, the ANN may not become 'wiser' and one may be just wasting computational efforts and time. This research assumes that there are segments in a long time series which contain large quantum of information. If an ANN is trained using these segments rather than the whole series, the training would be the same or better. Here, data depth function was used as tool for identification of critical segments in a time series. Different ANN architectures were trained using the whole time series data and using the data of only critical segments. A comparison of the results shows that the performance of the ANNs is only slightly worse than using all data if one uses the selected critical periods only.

Due to the simplification of the complex natural processes and the limited availability of observations the parameters of these models cannot be identified perfectly. Usually the parameters of the models are assumed to be time independent. However some of the catchment properties are not stationary. Hence, some of the model parameters corresponding to a certain natural process may vary with time. The purpose of this research was to develop a methodology which can investigate dynamic nature of parameters in a model. In this study a robust dynamic parameter (*RDPE*) estimation algorithm was developed. The *RDPE* can be used for diagnosis of hydrological model as well as for improvement of model prediction using time varying nature of parameters. After identifying the range of time varying parameters using *ROPE* algorithm, moving window approach and simulated annealing was used to optimize the parameters of HBV model for the each window size. The resulting time series of parameters was used for defining sensitive and insensitive periods in parameter time series. It was also used for understanding the reason for parameter variation in time. To improve the prediction, from time series of parameters, a predictive parameter model was developed and applied in future predictions. The methodology has been demonstrated on mezo-scale catchments in the Neckar basin in South-West Germany using the HBV model. Further, it is shown that the new methodology leads to more realistic confidence intervals for model simulations and model structure identification. This *RDPE* algorithm can be used as tool to improve process understanding and can improve model structure.

The parameter estimation in ungauged basins is more difficult than gauged catchments. The parameters of hydrological models with no or short discharge records can only be estimated using regional information. One can assume that catchments with similar characteristics show a similar hydrological behavior. Therefore a regionalization of hydrological model parameters on the basis of catchment characteristics is plausible. However, due to the non-uniqueness of the rainfall/runoff model parameters (equifinality), a procedure of a regional parameter estimation by model calibration and a subsequent fit of a regional function is not appropriate. In this research a different procedure based on the depth function and convex combinations of model parameters was introduced. Catchment characteristics to be used for regionalization can be identified by the same procedure. This is very useful as we can immediately decide if our available catchments characteristics are enough to be regionalized or not. Regionalization is then performed using different approaches: multiple linear regression using the deepest parameter sets

and convex combinations. The results of this research work are more robust as we are not fitting any kind of function. Moreover the results showed that regionalization based on the depth function and convex combinations of model parameters was reasonable. The algorithm developed, based on convex combination, was termed as selection of appropriate variable (SAV). An example of 28 British catchments was used to illustrate the methodology. The HYMOD model was used for this purpose work. The results of this research showed that, the SAV algorithm was very useful for robust regionalization. In this research, several algorithms, for example, ROPE algorithm, SRWP algorithm, HOP algorithm, ICE algorithm, RDPE algorithm and SAV algorithm were developed to answer the basic questions raised in the objectives of this research. These algorithms were very useful for the robust and reliable hydrological modeling in gauged and ungauged basins.

## 10.2 Outlook

Based on the observations and the experiences gained during the course of this study, following suggestions may be pointed out for the further possible studies in the similar direction:

- ROPE algorithm give a parameter vectors for a hydrological model after calibration. It also give idea about boundary and deeper parameters, so it might be very useful to use deeper parameters for regionalization and could contribute to a better prediction in ungaged basins.
- The ROPE methodology can be extended for uncertainty analysis by relating the likelihood of the parameter sets to their depth.
- SRWP algorithm can be tested on different hydrological model. SRWP algorithm can be further improved by including hyperplane at different optimal space and searching optimal parameter sets separately in this region.
- Modeling water quality is very complex due to complicated measuring process. So ICE algorithm may be useful tool for selecting some rare events.
- Generally a number of input series may available for data driven model. Combination of several series may lead to similar output. Hence, if we can select a proper combination of input series for data driven model, we may save time and can improve efficiency. ICE algorithm can be extended for choosing proper input to data driven model. Those combination of input series have larger number of higher depth may be better input to data driven model.
- From this study, it is clear that critical time period in a series can be use for parameter identification of hydrological model. Similar ways ICE algorithm can be extend to study influence of spatial variability in hydrological modeling. ICE algorithm can be useful for reclassify grid based on catchments properties. Similar class get similar parameters. This may reduce complexity in distributed model.

- Physically based hydrological model are directly related with catchments conditions and characteristics. There is variability in time and space in a catchments. Hence, RDPE algorithm can be useful tool for study model structure problem for physically based model.
- Regionalization methodology (SAV) developed in this research can tested one different model and catchments to make more generalization of the concept.



## Bibliography

- Abebe, N., Ogden, F., and Pradhan, N.: Sensitivity and Uncertainty Analysis of the Conceptual HBV Rainfall-Runoff Model: Implications for Parameter Estimation, *Journal of Hydrology*, 389, 301–310, 2010.
- Ahmed, S. and de Marsily, G.: Comparison of geostatistical methods for estimating transmissivity using data transmissivity and specific capacity, *Water Resources Research*, 23, 1717–1737, 1987.
- Alp, M. and Cigizoglu, H. K.: Suspended sediment estimation by feed forward back propagation method using hydro meteorological data, *Environmental Modelling and Software*, 22 (1), 2–13, 2007.
- Anctil, F., Perrin, C., and Andréassian, V.: Impact of the length of observed records on the performance of ANN and of conceptual parsimonious rainfall-runoff forecasting models, *Environmental Modelling & Software*, 19, 357–368, 2004.
- Andréassian, V., Perrin, C., Michel, C., Usart-Sanchez, I., and Lavabre, J.: Impact of imperfect rainfall knowledge on the efficiency and the parameters of watershed models, *Journal of Hydrology*, 250, 206–223, 2001.
- ASCE: ASCE Task Committee on Application of Artificial Neural Networks in Hydrology. Artificial Neural Networks in hydrology, I: Preliminary Concepts, *Journal of Hydrologic Engineering*, 5(2), 115–123, 2000a.
- ASCE: ASCE Task Committee on Application of Artificial Neural Networks in Hydrology. Artificial Neural Networks in hydrology, II: Hydrological Applications, *Journal of Hydrologic Engineering*, 5(2), 124–137, 2000b.
- Bárdossy, A.: Calibration of hydrological model parameters for ungauged catchments, *Hydrol. Earth Syst. Sci.*, 11, 703–710, 2007.
- Bárdossy, A. and Singh, S. K.: Robust estimation of hydrological model parameters, *Hydrology and Earth System Sciences*, 12, 1273–1283, <http://www.hydrol-earth-syst-sci.net/12/1273/2008/>, 2008.
- Bárdossy, A. and Singh, S. K.: Regionalization of hydrological model parameters using data depth, *Hydrology Research*, under review, 2010.
- Bárdossy, A., Pegram, G. S., and Samaniego, L.: Modeling data relationships with a local variance reducing technique: Applications in hydrology, *Water Resources Research*, 41(W08404), doi:10.1029/2004WR003851, 2005.

## *Bibliography*

- Barnett, V.: The ordering of multivariate data, *Journal of the Royal Statistical Society*, 139, 318 – 355, 1976.
- Beck, M. B.: Water Quality Modeling: A Review of the Analysis of Uncertainty, *Water Resources Research*, 23 (8), 1393–1442, 1987.
- Bergström, S.: The HBV model. In: *Computer Models of Watershed Hydrology*, Water Resources Publications, Littleton, Colorado, USA, 1995.
- Bergström, S. and Graham, L.: On the scale problem in hydrological modelling, *Journal of Hydrology*, 211, 253–265, 1998.
- Beven, K.: *Rainfall-Runoff Modelling: The Primer*, Wiley, 2000.
- Beven, K.: A manifesto for the equifinality thesis, *Journal of Hydrology*, 320, 18–36, 2006.
- Beven, K. and Binley, A. M.: The future of distributed models: model calibration and uncertainty prediction, *Hydrological Processes*, 6, 279–298, 1992.
- Beven, K. and Freer, J.: Equifinality, data assimilation, and data uncertainty estimation in mechanistic modelling of complex environmental systems using the GLUE methodology, *Journal of Hydrology*, 249, 11–29, 2001.
- Beven, K. J. and Kirkby, M.: A physically based, variable contributing area model of basin hydrology, *Hydrological Science Bulletin*, 24, 43–69, 1979.
- Bhattacharya, B., Lobbrecht, A. H., and Solomatine, D. P.: Neural networks and reinforcement learning in control of water systems, *Journal of Water Resources Planning and Management*, ASCE, 129 (6), 458–465, 2003.
- Blasone, R. S.: Parameter estimation and uncertainty assessment in hydrological modelling, Ph.D. dissertation, Technical University of Denmark, 2007.
- Blöschl, G. and Sivapalan, M.: Scale issues in hydrological modelling: a review, *Hydrological processes*, 9, 251–290, 1995.
- Bowden, G. J., Maier, H. R., and Dandy, G. C.: Optimal division of data for neural network models in water resources applications, *Water Resources Research*, 38, 1010, 2002.
- Bowden, G. J., Dandy, G. C., and Maier, H. R.: Input determination for neural network models in water resources applications. Part 1 - background and methodology, *Journal of Hydrology*, 301, 75–92, 2005.
- Boyle, D. P., Gupta, H. V., Sorooshian, S., Koren, V., Zhang, Z., and Smith, M.: Toward Improved Streamflow Forecasts: Value of Semidistributed Modeling, *Water Resources Research*, 37 (11), 2749–2759, 2001.



- Burn, D. H., Ouarda, T. B. M. J., and Shu, C.: Estimation of extreme flow quantiles and quantile uncertainty for ungauged catchments, IAHS-AISH Publication, 313, 417–424, 2007.
- Campolo, M., Soldati, A., and Andreussi, P.: Artificial neural network approach to flood forecasting in the River Arno, *Hydrological Sciences Journal*, 48 (3), 381–398, 2003.
- Chebana, F. and Ouarda, T. B. M. J.: Depth and homogeneity in regional flood frequency analysis, *Water Resources Research*, doi:10.1029/2007WR006771, 2008.
- Cheng, A. Y., Liu, R. Y., and Luxh ej, J. T.: Monitoring multivariate aviation safety data by data depth: control charts and threshold systems, *IIE Transactions*, 32, 861–872, 2000.
- Cigizoglu, H. K.: Estimation, forecasting and extrapolation of river flows by artificial neural networks, *Hydrological Sciences Journal*, 48 (3), 349–361, 2003.
- Cigizoglu, H. K.: Estimation and forecasting of daily suspended sediment data by multi layer perceptrons, *Advances in Water Resources*, 27, 185–195, 2004.
- Cigizoglu, H. K. and Alp, M.: Generalized Regression Neural Network in modelling river sediment yield, *Advances in Engineering Software*, 372, 63–68, 2006.
- Cigizoglu, H. K. and Kisi, O.: Flow prediction by three back propagation techniques using k-fold partitioning of neural network training data, *Nordic Hydrology*, 361, 1–16, 2005.
- Cigizoglu, H. K. and Kisi, O.: Methods to improve the neural network performance in suspended sediment estimation, *Journal of Hydrology*, 317(3-4), 221–238, 2006.
- Das, T.: The Impact of Spatial Variability of Precipitation on the Predictive Uncertainty of Hydrological Models, Ph.D. dissertation No. 154, University of Stuttgart, 2006.
- Donoho, D. L. and Gasko, M.: Breakdown properties of location estimates based on halfspace depth and projected outlyingness, *The Annals of Statistics*, 20(4), 1808–1827, 1992.
- Duan, Q., Gupta, V., and Sorooshian, S.: Shuffled complex evolution approach for effective and efficient global minimization, *Journal of Optimization Theory and Applications*, 76, 501–521, 1993.
- Fernandez, W., Vogel, R., and Sankarasubramanian, A.: Regional calibration of a watershed model, *Hydrological Sciences Journal*, 45(5), 689–707, 2000.
- Fernando, T. M. K. G., Maier, H. R., and Dandy, G. C.: Selection of input variables for data driven models: An average shifted histogram partial mutual information estimator approach, *Journal of Hydrology*, 367, 165 – 176, 2009.

## Bibliography

- Gaweda, A. E., Zurada, J. M., and Setiono, R.: Input selection in data-driven fuzzy modeling, Proceedings of the 10th IEEE International Conference of Fuzzy Systems FUZZ-IEEE, 1, 2–5, 2001.
- Götzinger, J. and Bárdossy, A.: Comparison of four regionalisation methods for a distributed hydrological model, *Journal of Hydrology*, 333, 374–384, 2007.
- Götzinger, J. and Bárdossy, A.: Generic error model for calibration and uncertainty estimation of hydrological models, *Water Resources Research*, 44, [doi:10.1029/2007WR006691](https://doi.org/10.1029/2007WR006691), 2008.
- Govindaraju, R. S. and Rao, A.: *Artificial Neural Networks in Hydrology*, Kluwer Academic Publishers, Dordrecht, 2000.
- Gupta, H., Sorooshian, S., and Yapo, P.: Toward improved calibration of hydrologic models: Multiple and noncommensurable measures of information, *Water Resources Research*, 34 (4), 751–763, 1998.
- Gupta, H., Sorooshian, S., Hogue, T. S., and Boyle, D. P.: Advances in Calibration of Watershed Models, *Calibration of Watershed Models*. AGU Monograph Series. Water Science and Application 6, pp. 9–28, 2003.
- Gupta, V. K. and Sorooshian, S.: The relationship between data and the precision of parameter estimates of hydrologic models, *Journal of Hydrology*, 81, 57–77, 1985.
- Hamurkaroğlu, C., Mert, M., and Saykan, Y.: Nonparametric control charts based on mahalanobis depth, *Journal of Mathematics and Statistics*, 33, 57–67, 2004.
- Harlin, J.: Development of a process oriented calibration scheme for the HBV hydrological model, *Nordic Hydrol*, 22, 15–36, 1991.
- Hartmann, G. M.: Investigation of evapotranspiration concept in hydrological modelling for climate change impact assessment, Ph.D. dissertation No. 161, University of Stuttgart, 2007.
- Hendrickson, J. D., Sorooshian, S., and Brazil, L. E.: Comparison of Newton-Type and Direct Search Algorithms for Calibration of Conceptual Rainfall-Runoff Models, *Water Resources Research*, 24 (5), 691–700, 1988.
- Hugg, J., Rafalin, E., Seyboth, K., and Souvaine, D.: An experimental study of old and new depth measures, *ALENEX06*, Springer-Verlag Lect. Notes Comp. Sci., 8, 5164, 2006.
- Hundecha, Y. and Bárdossy, A.: Modeling of the effect of land use changes on the runoff generation of a river basin through parameter regionalization of a watershed model, *Journal of Hydrology*, 292, 281–295, 2004.
- Ibbitt, R. P.: Effects of random data errors on the parameter values for a conceptual model, *Water Resources Research*, 8 (1), 70–78, 1972.

- Imrie, C. E., Durucan, S., and Korre, A.: River flow prediction using artificial neural networks: generalization beyond the calibration range, *Journal of Hydrology*, 233, 138–153, 2000.
- Jackson, D. R. and Aron, G.: Parameter estimation in hydrology: the state of the art, *Water Resources Bulletin*, 7, 457–472, 1971.
- Jain, S. K.: Application of SHE Model to Kolar Subbasin of Narmada., Report No. CS-33, National Institute of Hydrology, Roorkee, 1990.
- Jain, S. K.: Calibration of conceptual models for rainfall-runoff simulation, *Hydrological Sciences Journal*, 38(5), 431–441, 1993.
- Jain, S. K.: Development of integrated sediment rating curves using ANNS, *Journal of Hydraulic Engineering*, 127(1), 30–37, 2001.
- Jain, S. K. and Chalisgaonkar, D.: Setting up stage-discharge relations using ANN, *Journal of Hydrologic Engineering*, 5, 428, 2000.
- Jain, S. K., Das, A., and Srivastava, D. K.: Application of ANN for reservoir inflow prediction and operation, *Journal of Water Resources Planning and Management*, ASCE, 125(5), 263–271, 1999.
- Jain, S. K., Singh, V. P., and van Genuchten, M.: Application of ANN for reservoir inflow prediction and operation, *Journal of Water Resources Planning and Management*, ASCE, 9(5), 415–420, 2004.
- Jain, S. K., Nayak, P. C., and Sudheer, K. P.: Models for estimating evapotranspiration using artificial neural networks, and their physical interpretation, *Hydrological Processes*, 22, 2225–2234, 2008.
- Jakeman, A. J. and Hornberger, G. M.: How much complexity is warranted in a rainfall-runoff model?, *Water Resources Research*, 29, 2637–2650, 1993.
- Kavetski, D., Kuczera, G., and Franks, S.: Calibration of conceptual hydrological models revisited: 2. Improving optimisation and analysis, *Journal of Hydrology*, 320, 187–201, 2006a.
- Kavetski, D., Kuczera, G., and Franks, S. W.: Calibration of conceptual hydrological models revisited: 1. Overcoming numerical artefacts, *Journal of Hydrology*, 320, 173–186, 2006b.
- Kay, A. L., Jones, D. A., Crooks, S. M., Calver, A., and Reynard, N. S.: A comparison of three approaches to spatial generalization of rainfall-runoff models, *Hydrological Processes*, 20, 3953–3973, 2006.
- Keskin, M. E. and Terzi, O.: Artificial Neural Network models of daily pan evaporation, *Journal of Hydrologic Engineering*, 11(1), 65–70, 2006.

## *Bibliography*

- Khu, S. and Madsen, H.: Multiobjective calibration with Pareto preference ordering: An application to rainfall-runoff model calibration, *Water Resources Research*, 41, W03004, 2005.
- Kisi, O.: Generalized regression neural networks for evapotranspiration modeling, *Journal of Hydrological Sciences*, 51(6), 1092–1105, 2006.
- Kisi, O.: Evapotranspiration modeling from climatic data using a neural computing technique, *Hydrological Processes*, 21, 1925–1934, 2007.
- Kisi, O. and Öztürk, O.: Adaptive neurofuzzy computing technique for evapotranspiration estimation, *Journal of Irrigation and Drainage Engineering*, 133, 368, 2007.
- Krause, P., Boyle, D. P., and Bäse, F.: Comparison of different efficiency criteria for hydrological model assessment, *Advances in Geosciences*, 5, 89–97, 2005.
- Kuczera, G.: Improved Parameter Inference in Catchment Models 1. Evaluating Parameter Uncertainty, *Water Resources Research*, 19(5), 1151–1162, 1983a.
- Kuczera, G.: Improved Parameter Inference in Catchment Models 2. Combining Different Kinds of Hydrologic Data and Testing Their Compatibility, *Water Resources Research*, 19(5), 1163–1172, 1983b.
- Kuczera, G.: Efficient subspace probabilistic parameter optimization for catchment model, *Water Resources Research*, 33 (1), 177–185, 1997.
- Kumar, A. R. S., Sudheer, K. P., and Jain, S. K.: Rainfall-runoff modeling using artificial neural networks: comparison of network types, *Hydrological Processes*, 19(6), 1277–1291, 2005.
- Kumar, M., Raghuwanshi, N. S., Singh, R., Wallender, W. W., and Pruitt, W. O.: Estimating Evapotranspiration using Artificial Neural Network, *Journal of Irrigation and Drainage Engineering*, ASCE, 128(4), 224–233, 2002.
- Lamb, R. and Kay, A. L.: Confidence intervals for a spatially generalized, continuous simulation flood frequency model for Great Britain, *Water Resources Research*, 40, W07501, 2004.
- Leahy, P., Kiely, G., and Corcoran, G.: Structural optimisation and input selection of an artificial neural network for river level prediction, *Journal of Hydrology*, 355, 192–201, 2008.
- Lekkas, D. F., Imrie, C. E., and Lees, M. J.: Improved non-linear transfer function and neural network methods of flow routing for real-time forecasting, *Journal of Hydroinformatics*, 3(3), 153–164, 2001.
- Liang, J.: Improving Calibration Strategy of Physically Based Model WaSiM-ETH Using Critical Events, M.Sc. Thesis, University of Stuttgart, 2010.

- Liang, J., Sing, S. K., and Bárdossy, A.: Calibration of physically based model on critical events, WATER 2010 SYMPOSIUM, Quebec City, 2010.
- Lin, G. F. and Chen, L. H.: A non-linear rainfall-runoff model using radial basis function network, *Journal of Hydrology*, 289, 1–8, 2004.
- Lin, L. and Chen, M.: Robust estimating equation based on statistical depth, *Statistical Papers*, 47, 263–278, 2006.
- Lin, Z. and Beck, M. B.: On the identification of model structure in hydrological and environmental systems, *Water Resources Research*, 43 (W02402), doi:10.1029/2005WR004796, 2007.
- Liu, R. Y.: On a notion of data depth based on random simplices, *The Annals of Statistics*, 18, 405–414, 1990.
- Liu, R. Y.: Control charts for multivariate processes, *American Statistical Association*, 90, 1380–1387, 1995.
- Liu, R. Y. and Singh, K.: A Quality Index Based on Data Depth and Multivariate Rank Tests, *Journal of the American Statistical Association*, 88, 252–260, 1993.
- Liu, R. Y., Parelius, J. M., and Singh, K.: Multivariate analysis by data depth: descriptive statistics, graphics and inference, *The Annals of Statistics*, 27(3), 783–858, 1999.
- Liu, Y., Wagener, T., and Young, P. C.: Dynamic parameter analysis for hydrological and environmental model diagnostics and improvement, Working Paper, 2008.
- Madsen, H.: Automatic calibration of a conceptual rainfall–runoff model using multiple objectives, *Journal of Hydrology*, 235, 276–288, 2000.
- Madsen, H., Wilson, G., and Ammentorp, H.: Comparison of different automated strategies for calibration of rainfall-runoff models, *Journal of Hydrology*, 261, 48–59, 2002.
- Mahlanobis, P. C.: On the generalized distance in statistics, *Proceeding of Natural Academic Science India*, 12, 49 – 55, 1936.
- Maier, H. R. and Dandy, G. C.: Neural networks for the prediction and forecasting of water resources variables: a review of modelling issues and applications, *Environmental Modelling and Software*, 15, 101–124, 2000.
- May, R. J., Maier, H. R., Dandy, G. C., and Fernando, T. M. K.: Non-linear variable selection for artificial neural networks using partial mutual information, *Environmental Modelling & Software*, 23, 1312–1326, 2008.
- Merz, R. and Blöschl, G.: Regionalisation of catchment model parameters, *Journal of Hydrology*, 287, 95–123, 2004.

## *Bibliography*

- Michaud, J. and Sorooshian, S.: Comparison of simple versus complex distributed runoff models on a midsized semiarid watershed, *Water Resources Research*, 30, 593–605, 1994.
- Miller, K., Ramaswami, S., Rousseeuw, P., Sellares, T., Souvaine, D., Streinu, I., and Struyf, A.: Efficient computation of depth contours by methods of computational geometry, *Statistics and Computing*, 13, 153–162, 2003.
- Moore, R. J.: The probability-distributed principle and runoff production at point and basin scales, *Hydrological Sciences Journal*, 30(2), 273–297, 1985.
- Moradkhani, H., Sorooshian, S., Gupta, H. V., and Houser, P. R.: Dual state-parameter estimation of hydrological models using ensemble Kalman filter, *Advances in Water Resources*, 28, 135 – 147, 2005.
- Moussa, R. and Chahinian, N.: Comparison of different multi-objective calibration criteria using a conceptual rainfall-runoff model of flood events, *Hydrology and Earth System Sciences*, 13, 519–535, 2009.
- Nash, J. and Sutcliffe, J.: River flow forecasting through conceptual models. 1. A discussion of principles, *Journal of Hydrology*, 10, 282–290, 1970.
- Oja, H.: Descriptive statistics for multivariate distributions, *Statistics and Probability Letters*, 1, 327–332, 1983.
- Ouarda, T., Charron, C., and St-Hilaire, A.: Statistical models and the estimation of low flows, *Canadian Water Resources Journal*, 33, 195–206, 2008.
- Oudin, L., Perrin, C., Mathevet, T., Andréassian, V., and Michel, C.: Impact of biased and randomly corrupted inputs on the efficiency and the parameters of watershed models, *Journal of Hydrology*, 320, 62–83, 2006.
- Parajka, J., Merz, R., and Blöschl, G.: A comparison of regionalisation methods for catchment model parameters, *Hydrology and Earth System Sciences*, 9, 157–171, 2005.
- Patil, S. R.: Regionalization of an event based nash cascade model for flood prediction in ungauged basins, Ph.D. dissertation No. 175, University of Stuttgart, 2008.
- Paturel, J. E., Servat, E., and Vassiliadis, A.: Sensitivity of conceptual rainfall-runoff algorithms to errors in input data case of the GR2M model, *Journal of Hydrology*, 168, 111–125, 1995.
- Perrin, C., Michel, C., and Andréassian, V.: Does a large number of parameters enhance model performance? Comparative assessment of common catchment model structures on 429 catchments, *Journal of Hydrology*, 242, 275–301, 2001.
- Perrin, C., Michel, C., and Andréassian, V.: Improvement of a parsimonious model for streamflow simulation, *Journal of Hydrology*, 279, 275–289, 2003.

- Perrin, C., Oudin, L., Andréassian, V., Rojas-Serna, C., Michel, C., and Mathevet, T.: Impact of limited streamflow knowledge on the efficiency and the parameters of rainfall-runoff models, *Hydrological Sciences Journal*, 52, 131–151, 2007.
- Porterfield, G.: Computation of fluvial-sediment discharge., *Techniques of Water-Resources Investigations of the United States Geological Survey*, C3, 1972.
- Refsgaard, J. and Knudsen, J.: Operational validation and intercomparison of different types of hydrological models, *Water Resources Research*, 32, 2189–2202, 1996.
- Reichert, P. and Mieleitner, J.: Analyzing input and structural uncertainty of nonlinear dynamic models with stochastic, time-dependent parameters, *Water Resources Research*, 45, W10 402, 2009.
- Rousseeuw, P. J. and Ruts, I.: Constructing the bivariate Tukey median, *Statistica Sinica*, 8, 827–839, 1998.
- Rousseeuw, P. J. and Struyf, A.: Computing location depth and regression depth in higher dimensions, *Statistics and Computing*, 8, 193–203, 1998.
- Samaniego, L.: Hydrological Consequences of Land Use/ Land Cover Change in Mesoscale Catchments, *Transactions of the institute of hydraulic engineering, University of Stuttgart, Faculty of Civil Engineering, Stuttgart*, Ph.D. dissertation No. 118, 2003.
- Samaniego, L. and Bárdossy, A.: Robust parametric models of runoff characteristics at the mesoscale, *Journal of Hydrology*, 303, 136–151, 2005.
- Samaniego, L. and Bárdossy, A.: Simulation of the Impacts of Land Use/Cover and Climatic Changes on the Runoff Characteristics at the Mesoscale, *Ecological Modelling*, 196, 45–61, 2006.
- Schulla, J. and Jasper, K.: Model description WaSiM-ETH., [http://www.wasim.ch/downloads/doku/wasim/wasim\\_2007\\_en.pdf](http://www.wasim.ch/downloads/doku/wasim/wasim_2007_en.pdf), 2007.
- Seibert, J. and Beven, K. J.: Gauging the ungauged basin: how many discharge measurements are needed?, *Hydrology and Earth System Sciences*, 13, 883–892, <http://www.hydrol-earth-syst-sci.net/13/883/2009/>, 2009.
- Serfling, R.: Generalized Quantile Processes Based on Multivariate Depth Functions, with Applications in Nonparametric Multivariate Analysis, *Journal of Multivariate Analysis*, 83, 232–247, 2002.
- Shamseldin, A.: Artificial neural network model for river flow forecasting in a developing country, *Journal of Hydroinformatics*, 12, 22–35, 2010.
- Shrestha, R. R., Theobald, S., and Nestmann, F.: Simulation of flood flow in a river system using artificial neural networks, *Hydrology and Earth System Sciences*, 9, 313–321, 2005.

## *Bibliography*

- Singh, S. K.: Parameterization of Hydrological Model in Ungauged Catchments: A Regionalization Technique, LAP Lambert Academic Publishing AG & Co KG, Germany, 2010.
- Singh, S. K., Jain, S. K., and Bárdossy, A.: Calibration of a Catchment Model using the ROPE Algorithm, *Hydrology Journal*, p. in review, 2009.
- Singh, V. P. and Woolhiser, D. A.: Mathematical modeling of watershed hydrology, *Journal of Hydrologic Engineering*, 7, 270–292, 2002.
- Sivapalan, M., Takeuchi, K., Franks, S. W., Gupta, V. K., Karambiri, H., Lakshim, V., Liang, X., McDonnell, J. J., Mendiondo, E. M., Connell, O., Oki, T., Pomeroy, J., Schertzer, D., Uhlenbrook, S., and Zehe, E.: IAHS Decade on Predictions in Ungauged Basins (PUB), 2003-2012: Shaping an exciting future for the hydrological sciences, *Hydrological Sciences Journal*, 48 (6), 857–880, 2003.
- Smith, J. and Eli, R. N.: Neural Network models of rainfall-runoff process, *Journal of Water Resources Planning and Management*, 121, 499–508, 1995.
- Solomatine, D. and Ostfeld, A.: Data-driven modelling: some past experiences and new approaches, *Journal of Hydroinformatics*, 10, 3–22, 2008.
- Sorooshian, S., Duan, Q., and Gupta, V. K.: Calibration of rainfall-runoff models: application of global optimization to the Sacramento soil moisture accounting model, *Water Resources Research*, 29, 1185–1194, 1993.
- Sudheer, K. P. and Jain, A.: Explaining the Internal Behaviour of Artificial Neural Network River Flow Models, *Hydrological Processes*, 18(4), 833–844, 2004.
- Sudheer, K. P. and Jain, S. K.: Radial basis function neural networks for modelling rating curves, *Journal of Hydrologic Engineering*, 8(3), 161–164, 2003.
- Sudheer, K. P., Gosain, A. K., Rangan, D. M., and Saheb, S. M.: Modeling evaporation using artificial neural network algorithm, *Hydrological Processes*, 16, 3189–3202, 2002.
- Tang, Y., Reed, P., and Wagener, T.: How effective and efficient are multiobjective evolutionary algorithms at hydrologic model calibration?, *Hydrology and Earth System Sciences*, 10, 289–307, 2006.
- Thapa, P. K.: Physically-based spatially distributed rainfall runoff modelling for soil erosion estimation, Ph.D. dissertation No. 189, University of Stuttgart, 2009.
- Thiemann, M., Trosset, M., Gupta, H., and Sorooshian, S.: Bayesian recursive parameter estimation for hydrologic models, *Water Resources Research*, 37, 2521–2535, 2002.
- Todini, E.: Hydrological catchment modelling: past, present and future, *Hydrology and Earth System Sciences*, 11(1), 468–482, 2007.



- Tokar, A. S. and Johnson, P. A.: Rainfall-runoff modelling using artificial neural networks, *Journal of Hydrologic Engineering*, 4(3), 232–239, 1999.
- Trajkovic, S., Todorovic, B., and Stankovic, M.: Forecasting reference evapotranspiration by artificial neural networks, *Journal of Irrigation Drainage Engineering*, 129, 454–457, 2003.
- Troutman, B. M.: Errors and parameter estimation in precipitation-runoff modeling. 2. Case study, *Water Resources Research*, 21 (8), 1214–1222, 1985.
- Tukey, J.: Mathematics and picturing data, in: *In Proceedings of the 1975 International 17 Congress of Mathematics*, vol. 2, pp. 523–531, 1975.
- Uhlenbrook, S., Seibert, J., Leibundgut, C., and Rodhe, A.: Prediction uncertainty of conceptual rainfall-runoff models caused by problems to identify model parameters and structure, *Hydrol. Sci. J*, 44, 279–299, 1999.
- van der Linden, S. and Woo, M.: Application of hydrological models with increasing complexity to subarctic catchments, *Journal of Hydrology*, 270, 145–157, 2003.
- Vardi, Y. and Zhang, C. H.: The multivariate L1-median and associated data depth, *Proceeding of Natural Academic Science USA*, 97, 1423–1426, 2000.
- Vrugt, J. A., Bouten, W., Gupta, H. V., and Sorooshian, S.: Toward improved identifiability of hydrologic model parameters: The information content of experimental data, *Water Resources Research*, 38(12), 1312, 2002.
- Vrugt, J. A., Gupta, H. V., Bastidas, L. A., Bouten, W., and Sorooshian, S.: Effective and efficient algorithm for multiobjective optimization of hydrologic models, *Water Resources Research*, 39, 1214, 2003.
- Wagener, T., Boyle, D. P., Lees, M. J., Wheater, H. S., Gupta, H. V., and Sorooshian, S.: A framework for development and application of hydrological models, *Hydrology and Earth System Sciences*, 5, 13–26, 2001.
- Wagener, T., McIntyre, N., Lees, M. J., Wheater, H. S., and Gupta, H. V.: Towards reduced uncertainty in conceptual rainfall-runoff modelling: Dynamic identifiability analysis, *Hydrological Processes*, 17(2), 455–476, 2003.
- Wagener, T., Wheater, H. S., and Gupta, H. V.: *Rainfall-Runoff Modelling in Gauged and Ungauged Catchments*, Imperial College Press, London, 2004.
- Wilby, R. L., Abrahart, R. J., and Dawson, C. W.: Detection of conceptual model rainfall-runoff processes inside an artificial neural network, *Hydrological Sciences Journal*, 48(2), 163–181, 2003.
- Xia, Y., Yang, Z.-L., Jackson, C., Stoffa, P. L., and K. Sen, M.: Impacts of data length on optimal parameter and uncertainty estimation of a land surface model, *J. Geophys. Res.*, 109, <http://dx.doi.org/10.1029/2003JD004419>, 2004.

## *Bibliography*

- Yadav, M., Wagener, T., and Gupta, H.: Regionalization of constraints on expected watershed response behavior for improved prediction in ungauged basin, *Advances in Water Resources*, 30, 1756–1774, 2007.
- Yapo, P., Gupta, H., and Sorooshian, S.: Automatic calibration of conceptual rainfall-runoff models: sensitivity to calibration data, *Journal of Hydrology*, 181, 23–48, 1996.
- Yapo, P. O., Gupta, H. V., and Sorooshian, S.: Multi-objective global optimization for hydrologic models, *Journal of Hydrology*, 204, 83–97, 1998.
- Young, P. C.: *Encyclopedia of hydrological sciences*, John Wiley & Sons,, 2005.
- Zealand, C. M., Burn, D. H., and Simonovic, S. P.: Short term streamflow forecasting using artificial neural networks, *Journal of Hydrology*, 214, 32–48, 1999.
- Zuo, Y. and Serfling, R.: General notions of statistical depth function, *The Annals of Statistics*, 28(2), 461–482, 2000.

# Curriculum Vitae

- PERSONAL DATA
- ◇ Family name: **Singh**
  - ◇ Given name: **Shailesh Kumar**
  - ◇ Nationality: **Indian**
  - ◇ Date of birth: **30.09.1981**
  - ◇ Sex: **Male**
  - ◇ Family Status: **Unmarried**
  - ◇ Email: **shaileshiitm@gmail.com**
- EDUCATION
- ◇ **Stuttgart University, Stuttgart, Germany.**  
Ph.D. in Civil Engineering: October 2010 .  
Ph.D Research Title: *Robust parameter estimation for gauged and ungauged catchments.*
  - ◇ **Indian Institute of Technology, Madras, India.**  
M.Tech. in Civil Engineering July 2007.  
Master's project: *Use of upstream and down stream data for calibration of hydrological model.*
  - ◇ **Kerala Agricultural University, Kerala, India.**  
B.Tech in Agricultural Engineering, May 2005.  
Thesis title: *Standardization of vanilla curing Technique.*
- AWARD
- ◇ **IPSWaT-Internationale Aufbaustudien Stipendium des Bundesministeriums für Bildung und Forschung (BMBF) Deutschland zur Promotion unter Internationales Doktorandenprogramm ENWAT (August 2007 – July 2010).**
  - ◇ **DAAD Stipendium des Deutscher Akademischer Austausch Dienst zum Master of Technology Studium M.Tech Thesis (2006–2007).**
  - ◇ **Scholarship from HRD Gov. of India for M.Tech (2005–2006).**
  - ◇ **Gold Medal for Academic Excellence-2005, Kerala Agricultural University, Trichur, India.**
- RESEARCH INTERESTS
- ◇ **Watershed modeling**
  - ◇ **Surface Hydrology**
  - ◇ **Parameter estimation and uncertainty study**
  - ◇ **Prediction in ungauged basin**
  - ◇ **Integrated watershed modeling**

- PUBLICATION ◇ Mathew.M, Raju, R., **Singh, S. K.** and Sudheer, K. P. (2005). Constraints in vanilla cultivation and processing- a survey. XVIIIth National convention of Agricultural Engineers and national seminar on Role of Agricultural Engineers in development of cash crops, held at Agricultural Engineering college and Research Institute, Coimbatore, March 26-27, 2005, p-13.
- CONFERENCE ◇ Mathew M, Sudheer, K. P., **Singh. S. K.**, and Raju, R. (2006). Drying kinetics of vanilla beans during curing process. 40th Annual convention and symposium of Indian Society of Agricultural Engineers, held at Tamilnadu Agricultural University, Agril. Engg College Res. Institute, Coimbatore, January 19-21, 2006.
- ◇ Bárdossy A., **Singh S. K.** (2007). Time varying parameterization of hydrological models, Eos Trans. AGU, 88(52), Fall Meet., San Francisco USA. Suppl., Abstract H14A-01.(Oral presentation).
- ◇ **Singh S. K.**, Bárdossy A. (2008). Influence of time-varying parameterization on hydrological models , Geophysical Research Abstracts Vol. 10, EGU2008-A-02600 EGU General Assembly
- ◇ **Singh S. K.** , Bárdossy A., Wagener T. (2008). Robust dynamic parameter estimation for hydrological models. Eos Trans. AGU, 89(53), Fall Meet., San Francisco USA. Suppl., Abstract H43D-1031.
- ◇ Patil S., Bárdossy A., **Singh S. K.**.(2008). Spatio-Temporal Extrapolation of Unit Hydrograph Parameters Based on Catchment and Event Extrapolators for Predictions in Ungauged Basins. Eos Trans. AGU, 89(53), Fall Meet., San Francisco USA. Suppl., Abstract H23C-0979.
- ◇ **Singh S. K.** , Bárdossy A. (2009). Identification of critical time periods for the efficient calibration of hydrological models, Geophysical Research Abstracts, Vol. 11, EGU2009-5748,EGU General Assembly. (Oral presentation)
- ◇ **Singh S. K.**, Bárdossy A., K. P. Sudheer (2009). Comparison of Regionalization Methods, Geophysical Research Abstract Vol. 11, EGU2009-5769, European Geosciences Union Assembly. (Oral presentation)
- ◇ **Singh S. K.**, Patil S , Bárdossy A.( 2009). Multivariate Logistic Model to estimate Effective Rainfall for an Event, Geophysical Research Abstract Vol. 11, EGU2009-7725,European Geosciences Union Assembly.
- ◇ Kumar V., **Singh S. K.** , Venkataraman G. (2009). Climate change effects on Glacier recession in Himalayas using Multitemporal SAR data and Automatic Weather Station observations, Geophysical Research Abstract Vol. 11, EGU2009-7116-1, European Geosciences Union Assembly.
- ◇ **Singh S. K.**, Bárdossy A.; Wagener T. (2009). Limit to predictability in hydrology due to temporal variability of model parameters, IAHS, Hyderabad (Oral presentation).
- ◇ **Singh S. K.** , Bárdossy A.(2009). Use of data depth function for calibration of hydrological models, IAHS, Hyderabad (Oral presentation).
- ◇ Bárdossy A., **Singh S. K.** (2009). Regionalization of model parameters using data depth function, IAHS, Hyderabad (Oral presentation).
- ◇ **Singh S. K.**, Bárdossy A.(2009). Step wise calibration of hydrological model using unusual events. Eos Trans. AGU, 90(54), Fall Meet., San Francisco USA. Suppl., Abstract H21F-0906.
- ◇ Bárdossy A., **Singh S. K.**(2009). Hydrological modelling in poorly gauged catchments using a constraints. Eos Trans. AGU, 90(54), Fall Meet., San Francisco USA. Suppl., Abstract H24C-04 (Oral presentation).
- ◇ **Singh S. K.**, Bárdossy A. (2010). Effect of observational uncertainty on parameter estimation of hydrological model, Geophysical Research Abstract Vol. 12, EGU2010-3630, European Geosciences Union Assembly.

- ◇ **Singh S. K.**, Sharad K. Jain , Bárdossy A. (2010). Improving Efficiency in Training of Artificial Neural Networks using Information-rich Data, Geophysical Research Abstract Vol. 12, EGU2010-2018, European Geosciences Union Assembly.
- ◇ Bárdossy A. , **Singh S. K.** (2010). Regionalization of hydrologic model parameters vs. regionalization of discharge dependence and statistics, Geophysical Research Abstract Vol. 12, EGU2010-6848, European Geosciences Union Assembly.
- ◇ Ehsan Rabiei,**Singh S. K.**, Bárdossy A. (2010). Improvement in calibration strategy of a conceptual distributed hydrological model using spatial data analysis, Geophysical Research Abstract Vol. 12, EGU2010-2188, European Geosciences Union Assembly. )
- ◇ Elias Tedla Shiferaw, **Singh S. K.**, Bárdossy A. (2010). Evaluating SWAT Predictive Performance Based on Different Spatial Resolution Climatic Data, Geophysical Research Abstract Vol. 12, EGU2010-2166, European Geosciences Union Assembly.
- ◇ Yulizar,**Singh S. K.**, Bárdossy A. (2010). Study of Different Automatic Calibration for Hydrological Modeling, Geophysical Research Abstract Vol. 12, EGU2010-3630, European Geosciences Union Assembly.
- ◇ **Singh S. K.**, Bárdossy A. (2010). A Simple and efficient calibration of hydrological model, Water 2010 Water 2010 Hydrology, Hydraulics and Water Resources in an Uncertain Environment , Quebec City, Canada (July 5-7). (Oral presentation)
- ◇ Bárdossy A.,**Singh S. K.**, (2010). Changes in the frequencies of unusual climatic or hydrological events, Hydraulics and Water Resources in an Uncertain Environment, Quebec City, Canada (July 5-7). (Oral presentation)
- ◇ Jiaying Liang,**Singh S. K.**, Bárdossy A. (2010). Calibration of physically based model on critical events, Hydraulics and Water Resources in an Uncertain Environment, Quebec City, Canada (July 5-7). (Oral presentation)

PUBLICATION ◇ Sudheer, K. P., **Singh. S. K.**, Mathew M, and Raju, R. (2007). Constraints in Production and Post Production Management of Vanilla Crop. Agricultural Engineering Today, Vol. 31(1), PP:37-40.

JOURNAL

Bárdossy A., **Singh S. K.** (2008). Robust estimation of hydrological model parameters., Hydrol. Earth Syst. Sci., 12, 1273-1283.

**Singh S. K.**, S. K. Jain, Bárdossy A.,(2009). Calibration of a Catchment Model using the ROPE Algorithm., Hydrology Journal (in review).

**Singh S. K.**, S. K. Jain, Bárdossy A.,(2010). Improving Efficiency in Training of Artificial Neural Networks using Information-rich Data., Journal of Hydroinformatics. (in review).

Bárdossy A., **Singh S. K.** (2009). Regionalisation of model parameters using data depth function, Hydrology Research (in press).

**Singh S. K.**, Bárdossy A.:(2010). Identification of critical time periods for the efficient calibration of hydrological models (to be submit).

**Singh S. K.**, Bárdossy A., Göttinger J.,(2009). Effect of resolution on regionalization of model parameters (to be submit).

**Singh S. K.**, Bárdossy A., Jim Freer (2009) Study of parameter mapping by different objective function in ROPE algorithm (to be submit).

PUBLICATION ◇ **Singh, S. K.**, Mathew. M, Raju, R. (2010). Standardisation of Vanilla Curing Techniques, BOOK LAP LAMBERT Academic Publishing AG & Co., Germany, ISBN: 978-3-8383-5544-3.

- ◇ **Singh, S. K.** (2010). Parameterization of Hydrological Model in Ungauged Catchments, LAP LAMBERT Academic Publishing AG & Co., Germany, ISBN: 978-3-8383-7558-8.

Curriculum Vitae

- MODELING EXPERIENCE
- ◇ **Conceptual Model:** HBV, HYMOD, ABC model, SIXPAR model, TOPMODEL, Degree day model, EPANET, CROPWAT
  - ◇ **Empirical Model:** Rational Method, Some ET calculation model
  - ◇ **Physical Model:** SWAT, WaSiM-ETH, HEC-RAS, MM5
  - ◇ **Self developed Tools:** ROPE (optimization algorithm), RDPE algorithm (dynamic parameter estimation), ICE algorithm (identification of critical events), Tool for prediction in ungauged basin
- RESEARCH EXPERIENCE
- ◇ **Teaching,** Institute of Hydraulic Engineering (April 2010-till date) lecture for Master student (hydrological modelling)
  - ◇ **August 2007-till date** Research Fellow at Institute of hydraulic engineering, University of Stuttgart.
  - ◇ **Teaching Assistantship,** Institute of Hydraulic Engineering (April 2009-Sep 2009) Exercise and lecture
  - ◇ **HIWI,** Studentische Hilfskraft at ENWAT, Universität Stuttgart (November 2007-till date) Data base managements
  - ◇ **Trainee,** CWRDM, Calicut., (May 2006-Jun 2006) Development of water balance model, lecture for irrigation engineer etc.
  - ◇ **Teaching Assistantship,** IIT Madras (Aug 2005-Sep 2006) Preparation of class notes etc.
  - ◇ **Trainee,** KEMCO, Atahni (Sep 2004-Oct 2004) Assembly of power tiller.
- STUDENT SUPERVISED
- M.Sc Independent Study and Master Thesis
  - Mr. Yulizar**  
Title: Comparison of different optimization algorithm with ROPE  
Master Thesis: Study of Changes in the Frequencies of Unusual Climatic or Hydrological Events
  - Mr. Ehsan Rabiei**  
Title: Calibration of hydrological model on spatially unusual location
  - Miss Liang Jiaying**  
Master Thesis: Improving Calibration Strategy of Physically Based Model WaSiM-ETH Using Critical Events
  - Mr. Elias Tedla Shiferaw**  
Master Thesis: Evaluating SWAT Predictive Performance in Rems Catchment, Southern Germany, Based on Multiple Optimization Algorithms
- JOURNAL EDITING
- ◇ **Reviewer** of Journal of Indian Water Resources Society.
  - ◇ **Reviewer** of Journal of Hydrology.
- PROFESSIONAL MEMBERSHIP
- ◇ **American Geophysical Union (AGU)**
  - ◇ **European Geosciences Union (EGU)**
  - ◇ **International Association of Hydrological Sciences (IAHS)**
  - ◇ **German Water Association (DWA)**
  - ◇ **Indian Water Resources Society (IWRS)**
  - ◇ **Society of Exploration Geophysicists (SEG)**
- MERITS ACHIEVEMENTS
- ◇ **First Rank** in B.Tech, Kerala Agricultural University, Trichur (2005).
  - ◇ **Gold Medal** for Academic Excellence-2005, Kerala Agricultural University, Trichur, India.
  - ◇ **School Topper** in Tenth, Indian School of Learning, Dhanbad.

*Curriculum Vitae*

- ◇ **GATE** Scholarship awarded by Ministry of Human Resource Development, Government of India to pursue M.Tech. at IIT madras
- ◇ **DAAD** Scholarship for M.Tech Theses at Stuttgart University, Germany
- ◇ **IPSWat** Scholarship for Doctoral studies at Institute of Hydraulic Engineering, Stuttgart university, Germany

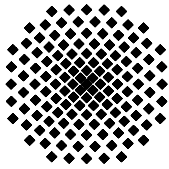
**EXTRA**

**CURRICULAR  
ACTIVITY**

- ◇ **H**as been an active member of National Service Scheme College Unit in UG.
- ◇ **A** member of University football team participated in all south India Inter-University football Tournament.
- ◇ **C**ollege athletics individual champion
- ◇ **D**istrict and university medal winner in athletics.
- ◇ **C**ollege cricket and basketball captain and team member.
- ◇ **H**as been at a post of School Captain
- ◇ **H**as been at a post of College sport club secretary
- ◇ **H**as been at a post of University Union Councilor, KAU
- ◇ **H**as been at a post of President, Student Union of college







## Institut für Wasserbau Universität Stuttgart

Pfaffenwaldring 61  
70569 Stuttgart (Vaihingen)  
Telefon (0711) 685 - 64717/64749/64752/64679  
Telefax (0711) 685 - 67020 o. 64746 o. 64681  
E-Mail: [iws@iws.uni-stuttgart.de](mailto:iws@iws.uni-stuttgart.de)  
<http://www.iws.uni-stuttgart.de>

### Direktoren

Prof. Dr. rer. nat. Dr.-Ing. András Bárdossy  
Prof. Dr.-Ing. Rainer Helmig  
Prof. Dr.-Ing. Silke Wieprecht

### Vorstand (Stand 01.04.2009)

Prof. Dr. rer. nat. Dr.-Ing. A. Bárdossy  
Prof. Dr.-Ing. R. Helmig  
Prof. Dr.-Ing. S. Wieprecht  
Jürgen Braun, PhD  
Dr.-Ing. H. Class  
Dr.-Ing. S. Hartmann  
Dr.-Ing. H.-P. Koschitzky  
PD Dr.-Ing. W. Marx  
Dr. rer. nat. J. Seidel

### Emeriti

Prof. Dr.-Ing. habil. Dr.-Ing. E.h. Jürgen Giesecke  
Prof. Dr.h.c. Dr.-Ing. E.h. Helmut Kobus, PhD

### Lehrstuhl für Wasserbau und Wassermengenwirtschaft

Leiter: Prof. Dr.-Ing. Silke Wieprecht  
Stellv.: PD Dr.-Ing. Walter Marx, AOR

### Versuchsanstalt für Wasserbau

Leiter: Dr.-Ing. Sven Hartmann, AOR

### Lehrstuhl für Hydromechanik und Hydrosystemmodellierung

Leiter: Prof. Dr.-Ing. Rainer Helmig  
Stellv.: Dr.-Ing. Holger Class, AOR

### Lehrstuhl für Hydrologie und Geohydrologie

Leiter: Prof. Dr. rer. nat. Dr.-Ing. András Bárdossy  
Stellv.: Dr. rer. nat. Jochen Seidel

### VEGAS, Versuchseinrichtung zur Grundwasser- und Altlastensanierung

Leitung: Jürgen Braun, PhD  
Dr.-Ing. Hans-Peter Koschitzky, AD

## Verzeichnis der Mitteilungshefte

- 1 Röhnisch, Arthur: *Die Bemühungen um eine Wasserbauliche Versuchsanstalt an der Technischen Hochschule Stuttgart*, und Fattah Abouleid, Abdel: *Beitrag zur Berechnung einer in lockeren Sand gerammten, zweifach verankerten Spundwand*, 1963
- 2 Marotz, Günter: *Beitrag zur Frage der Standfestigkeit von dichten Asphaltbelägen im Großwasserbau*, 1964
- 3 Gurr, Siegfried: *Beitrag zur Berechnung zusammengesetzter ebener Flächen-tragwerke unter besonderer Berücksichtigung ebener Stauwände, mit Hilfe von Randwert- und Lastwertmatrizen*, 1965
- 4 Plica, Peter: *Ein Beitrag zur Anwendung von Schalenkonstruktionen im Stahlwasserbau*, und Petrikat, Kurt: *Möglichkeiten und Grenzen des wasserbaulichen Versuchswesens*, 1966

- 5 Plate, Erich: *Beitrag zur Bestimmung der Windgeschwindigkeitsverteilung in der durch eine Wand gestörten bodennahen Luftschicht, und*  
Röhnisch, Arthur; Marotz, Günter: *Neue Baustoffe und Bauausführungen für den Schutz der Böschungen und der Sohle von Kanälen, Flüssen und Häfen; Gesteungskosten und jeweilige Vorteile, sowie Unny, T.E.: Schwingungsuntersuchungen am Kegelstrahlschieber, 1967*
- 6 Seiler, Erich: *Die Ermittlung des Anlagenwertes der bundeseigenen Binnenschiffahrtsstraßen und Talsperren und des Anteils der Binnenschifffahrt an diesem Wert, 1967*
- 7 *Sonderheft anlässlich des 65. Geburtstages von Prof. Arthur Röhnisch mit Beiträgen von* Benk, Dieter; Breitling, J.; Gurr, Siegfried; Haberhauer, Robert; Honekamp, Hermann; Kuz, Klaus Dieter; Marotz, Günter; Mayer-Vorfelder, Hans-Jörg; Miller, Rudolf; Plate, Erich J.; Radomski, Helge; Schwarz, Helmut; Vollmer, Ernst; Wildenhahn, Eberhard; 1967
- 8 Jumikis, Alfred: *Beitrag zur experimentellen Untersuchung des Wassernachschubs in einem gefrierenden Boden und die Beurteilung der Ergebnisse, 1968*
- 9 Marotz, Günter: *Technische Grundlagen einer Wasserspeicherung im natürlichen Untergrund, 1968*
- 10 Radomski, Helge: *Untersuchungen über den Einfluß der Querschnittsform wellenförmiger Spundwände auf die statischen und rammtechnischen Eigenschaften, 1968*
- 11 Schwarz, Helmut: *Die Grenztragfähigkeit des Baugrundes bei Einwirkung vertikal gezogener Ankerplatten als zweidimensionales Bruchproblem, 1969*
- 12 Erbel, Klaus: *Ein Beitrag zur Untersuchung der Metamorphose von Mittelgebirgsschneedecken unter besonderer Berücksichtigung eines Verfahrens zur Bestimmung der thermischen Schneequalität, 1969*
- 13 Westhaus, Karl-Heinz: *Der Strukturwandel in der Binnenschifffahrt und sein Einfluß auf den Ausbau der Binnenschiffskanäle, 1969*
- 14 Mayer-Vorfelder, Hans-Jörg: *Ein Beitrag zur Berechnung des Erdwiderstandes unter Ansatz der logarithmischen Spirale als Gleitflächenfunktion, 1970*
- 15 Schulz, Manfred: *Berechnung des räumlichen Erddruckes auf die Wandung kreiszylindrischer Körper, 1970*
- 16 Mobasseri, Manoutschehr: *Die Rippenstützmauer. Konstruktion und Grenzen ihrer Standsicherheit, 1970*
- 17 Benk, Dieter: *Ein Beitrag zum Betrieb und zur Bemessung von Hochwasserrückhaltebecken, 1970*

- 18 Gàl, Attila: *Bestimmung der mitschwingenden Wassermasse bei überströmten Fischbauchklappen mit kreiszylindrischem Staublech*, 1971, vergriffen
- 19 Kuz, Klaus Dieter: *Ein Beitrag zur Frage des Einsetzens von Kavitationserscheinungen in einer Düsenströmung bei Berücksichtigung der im Wasser gelösten Gase*, 1971, vergriffen
- 20 Schaak, Hartmut: *Verteilleitungen von Wasserkraftanlagen*, 1971
- 21 *Sonderheft zur Eröffnung der neuen Versuchsanstalt des Instituts für Wasserbau der Universität Stuttgart mit Beiträgen von* Brombach, Hansjörg; Dirksen, Wolfram; Gàl, Attila; Gerlach, Reinhard; Giesecke, Jürgen; Holthoff, Franz-Josef; Kuz, Klaus Dieter; Marotz, Günter; Minor, Hans-Erwin; Petrikat, Kurt; Röhnisch, Arthur; Rueff, Helge; Schwarz, Helmut; Vollmer, Ernst; Wildenhahn, Eberhard; 1972
- 22 Wang, Chung-su: *Ein Beitrag zur Berechnung der Schwingungen an Kegelstrahlschiebern*, 1972
- 23 Mayer-Vorfelder, Hans-Jörg: *Erdwiderstandsbeiwerte nach dem Ohde-Variationsverfahren*, 1972
- 24 Minor, Hans-Erwin: *Beitrag zur Bestimmung der Schwingungsanfachungsfunktionen überströmter Stauklappen*, 1972, vergriffen
- 25 Brombach, Hansjörg: *Untersuchung strömungsmechanischer Elemente (Fluidik) und die Möglichkeit der Anwendung von Wirbelkammerelementen im Wasserbau*, 1972, vergriffen
- 26 Wildenhahn, Eberhard: *Beitrag zur Berechnung von Horizontalfilterbrunnen*, 1972
- 27 Steinlein, Helmut: *Die Eliminierung der Schwebstoffe aus Flußwasser zum Zweck der unterirdischen Wasserspeicherung, gezeigt am Beispiel der Iller*, 1972
- 28 Holthoff, Franz Josef: *Die Überwindung großer Hubhöhen in der Binnenschifffahrt durch Schwimmerhebwerke*, 1973
- 29 Röder, Karl: *Einwirkungen aus Baugrundbewegungen auf trog- und kastenförmige Konstruktionen des Wasser- und Tunnelbaues*, 1973
- 30 Kretschmer, Heinz: *Die Bemessung von Bogenstaumauern in Abhängigkeit von der Talform*, 1973
- 31 Honekamp, Hermann: *Beitrag zur Berechnung der Montage von Unterwasserpipelines*, 1973
- 32 Giesecke, Jürgen: *Die Wirbelkammertriode als neuartiges Steuerorgan im Wasserbau*, und Brombach, Hansjörg: *Entwicklung, Bauformen, Wirkungsweise und Steuereigenschaften von Wirbelkammerverstärkern*, 1974

- 33 Rueff, Helge: *Untersuchung der schwingungserregenden Kräfte an zwei hintereinander angeordneten Tiefschützen unter besonderer Berücksichtigung von Kavitation*, 1974
- 34 Röhnisch, Arthur: *Einpreßversuche mit Zementmörtel für Spannbeton - Vergleich der Ergebnisse von Modellversuchen mit Ausführungen in Hüllwellrohren*, 1975
- 35 *Sonderheft anlässlich des 65. Geburtstages von Prof. Dr.-Ing. Kurt Petrikat mit Beiträgen von:* Brombach, Hansjörg; Erbel, Klaus; Flinspach, Dieter; Fischer jr., Richard; Gál, Attila; Gerlach, Reinhard; Giesecke, Jürgen; Haberhauer, Robert; Hafner Edzard; Hausenblas, Bernhard; Horlacher, Hans-Burkhard; Hutarew, Andreas; Knoll, Manfred; Krummet, Ralph; Marotz, Günter; Merkle, Theodor; Miller, Christoph; Minor, Hans-Erwin; Neumayer, Hans; Rao, Syamala; Rath, Paul; Rueff, Helge; Ruppert, Jürgen; Schwarz, Wolfgang; Topal-Gökceli, Mehmet; Vollmer, Ernst; Wang, Chung-su; Weber, Hans-Georg; 1975
- 36 Berger, Jochum: *Beitrag zur Berechnung des Spannungszustandes in rotations-symmetrisch belasteten Kugelschalen veränderlicher Wandstärke unter Gas- und Flüssigkeitsdruck durch Integration schwach singulärer Differentialgleichungen*, 1975
- 37 Dirksen, Wolfram: *Berechnung instationärer Abflußvorgänge in gestauten Gerinnen mittels Differenzenverfahren und die Anwendung auf Hochwasserrückhaltebecken*, 1976
- 38 Horlacher, Hans-Burkhard: *Berechnung instationärer Temperatur- und Wärmespannungsfelder in langen mehrschichtigen Hohlzylindern*, 1976
- 39 Hafner, Edzard: *Untersuchung der hydrodynamischen Kräfte auf Baukörper im Tiefwasserbereich des Meeres*, 1977, ISBN 3-921694-39-6
- 40 Ruppert, Jürgen: *Über den Axialwirbelkammerverstärker für den Einsatz im Wasserbau*, 1977, ISBN 3-921694-40-X
- 41 Hutarew, Andreas: *Beitrag zur Beeinflußbarkeit des Sauerstoffgehalts in Fließgewässern an Abstürzen und Wehren*, 1977, ISBN 3-921694-41-8, vergriffen
- 42 Miller, Christoph: *Ein Beitrag zur Bestimmung der schwingungserregenden Kräfte an unterströmten Wehren*, 1977, ISBN 3-921694-42-6
- 43 Schwarz, Wolfgang: *Druckstoßberechnung unter Berücksichtigung der Radial- und Längsverschiebungen der Rohrwandung*, 1978, ISBN 3-921694-43-4
- 44 Kinzelbach, Wolfgang: *Numerische Untersuchungen über den optimalen Einsatz variabler Kühlsysteme einer Kraftwerkskette am Beispiel Oberrhein*, 1978, ISBN 3-921694-44-2
- 45 Barczewski, Baldur: *Neue Meßmethoden für Wasser-Luftgemische und deren Anwendung auf zweiphasige Auftriebsstrahlen*, 1979, ISBN 3-921694-45-0

- 46 Neumayer, Hans: *Untersuchung der Strömungsvorgänge in radialen Wirbelkammerverstärkern*, 1979, ISBN 3-921694-46-9
- 47 Elalfy, Youssef-Elhassan: *Untersuchung der Strömungsvorgänge in Wirbelkammerdioden und -drosseln*, 1979, ISBN 3-921694-47-7
- 48 Brombach, Hansjörg: *Automatisierung der Bewirtschaftung von Wasserspeichern*, 1981, ISBN 3-921694-48-5
- 49 Geldner, Peter: *Deterministische und stochastische Methoden zur Bestimmung der Selbstdichtung von Gewässern*, 1981, ISBN 3-921694-49-3, vergriffen
- 50 Mehlhorn, Hans: *Temperaturveränderungen im Grundwasser durch Brauchwassereinleitungen*, 1982, ISBN 3-921694-50-7, vergriffen
- 51 Hafner, Edzard: *Rohrleitungen und Behälter im Meer*, 1983, ISBN 3-921694-51-5
- 52 Rinnert, Bernd: *Hydrodynamische Dispersion in porösen Medien: Einfluß von Dichteunterschieden auf die Vertikalvermischung in horizontaler Strömung*, 1983, ISBN 3-921694-52-3, vergriffen
- 53 Lindner, Wulf: *Steuerung von Grundwasserentnahmen unter Einhaltung ökologischer Kriterien*, 1983, ISBN 3-921694-53-1, vergriffen
- 54 Herr, Michael; Herzer, Jörg; Kinzelbach, Wolfgang; Kobus, Helmut; Rinnert, Bernd: *Methoden zur rechnerischen Erfassung und hydraulischen Sanierung von Grundwasserkontaminationen*, 1983, ISBN 3-921694-54-X
- 55 Schmitt, Paul: *Wege zur Automatisierung der Niederschlagsermittlung*, 1984, ISBN 3-921694-55-8, vergriffen
- 56 Müller, Peter: *Transport und selektive Sedimentation von Schwebstoffen bei gestautem Abfluß*, 1985, ISBN 3-921694-56-6
- 57 El-Qawasmeh, Fuad: *Möglichkeiten und Grenzen der Tropfbewässerung unter besonderer Berücksichtigung der Verstopfungsanfälligkeit der Tropfelemente*, 1985, ISBN 3-921694-57-4, vergriffen
- 58 Kirchenbaur, Klaus: *Mikroprozessorgesteuerte Erfassung instationärer Druckfelder am Beispiel seegangbelasteter Baukörper*, 1985, ISBN 3-921694-58-2
- 59 Kobus, Helmut (Hrsg.): *Modellierung des großräumigen Wärme- und Schadstofftransports im Grundwasser*, Tätigkeitsbericht 1984/85 (DFG-Forschergruppe an den Universitäten Hohenheim, Karlsruhe und Stuttgart), 1985, ISBN 3-921694-59-0, vergriffen
- 60 Spitz, Karlheinz: *Dispersion in porösen Medien: Einfluß von Inhomogenitäten und Dichteunterschieden*, 1985, ISBN 3-921694-60-4, vergriffen
- 61 Kobus, Helmut: *An Introduction to Air-Water Flows in Hydraulics*, 1985, ISBN 3-921694-61-2

- 62 Kaleris, Vassilios: *Erfassung des Austausches von Oberflächen- und Grundwasser in horizontalebene Grundwassermodellen*, 1986, ISBN 3-921694-62-0
- 63 Herr, Michael: *Grundlagen der hydraulischen Sanierung verunreinigter Porengrundwasserleiter*, 1987, ISBN 3-921694-63-9
- 64 Marx, Walter: *Berechnung von Temperatur und Spannung in Massenbeton infolge Hydratation*, 1987, ISBN 3-921694-64-7
- 65 Koschitzky, Hans-Peter: *Dimensionierungskonzept für Sohlbelüfter in Schußbrinnen zur Vermeidung von Kavitationsschäden*, 1987, ISBN 3-921694-65-5
- 66 Kobus, Helmut (Hrsg.): *Modellierung des großräumigen Wärme- und Schadstofftransports im Grundwasser*, Tätigkeitsbericht 1986/87 (DFG-Forschergruppe an den Universitäten Hohenheim, Karlsruhe und Stuttgart) 1987, ISBN 3-921694-66-3
- 67 Söll, Thomas: *Berechnungsverfahren zur Abschätzung anthropogener Temperaturanomalien im Grundwasser*, 1988, ISBN 3-921694-67-1
- 68 Dittrich, Andreas; Westrich, Bernd: *Bodenseeufererosion, Bestandsaufnahme und Bewertung*, 1988, ISBN 3-921694-68-X, vergriffen
- 69 Huwe, Bernd; van der Ploeg, Rienk R.: *Modelle zur Simulation des Stickstoffhaushaltes von Standorten mit unterschiedlicher landwirtschaftlicher Nutzung*, 1988, ISBN 3-921694-69-8, vergriffen
- 70 Stephan, Karl: *Integration elliptischer Funktionen*, 1988, ISBN 3-921694-70-1
- 71 Kobus, Helmut; Zilliox, Lothaire (Hrsg.): *Nitratbelastung des Grundwassers, Auswirkungen der Landwirtschaft auf die Grundwasser- und Rohwasserbeschaffenheit und Maßnahmen zum Schutz des Grundwassers*. Vorträge des deutsch-französischen Kolloquiums am 6. Oktober 1988, Universitäten Stuttgart und Louis Pasteur Strasbourg (Vorträge in deutsch oder französisch, Kurzfassungen zweisprachig), 1988, ISBN 3-921694-71-X
- 72 Soyeaux, Renald: *Unterströmung von Stauanlagen auf klüftigem Untergrund unter Berücksichtigung laminarer und turbulenter Fließzustände*, 1991, ISBN 3-921694-72-8
- 73 Kohane, Roberto: *Berechnungsmethoden für Hochwasserabfluß in Fließgewässern mit überströmten Vorländern*, 1991, ISBN 3-921694-73-6
- 74 Hassinger, Reinhard: *Beitrag zur Hydraulik und Bemessung von Blocksteinrampen in flexibler Bauweise*, 1991, ISBN 3-921694-74-4, vergriffen
- 75 Schäfer, Gerhard: *Einfluß von Schichtenstrukturen und lokalen Einlagerungen auf die Längsdispersion in Porengrundwasserleitern*, 1991, ISBN 3-921694-75-2
- 76 Giesecke, Jürgen: *Vorträge, Wasserwirtschaft in stark besiedelten Regionen; Umweltforschung mit Schwerpunkt Wasserwirtschaft*, 1991, ISBN 3-921694-76-0

- 77 Huwe, Bernd: *Deterministische und stochastische Ansätze zur Modellierung des Stickstoffhaushalts landwirtschaftlich genutzter Flächen auf unterschiedlichem Skalenniveau*, 1992, ISBN 3-921694-77-9, vergriffen
- 78 Rommel, Michael: *Verwendung von Klufdaten zur realitätsnahen Generierung von Klufnetzen mit anschließender laminar-turbulenter Strömungsberechnung*, 1993, ISBN 3-92 1694-78-7
- 79 Marschall, Paul: *Die Ermittlung lokaler Stofffrachten im Grundwasser mit Hilfe von Einbohrloch-Meßverfahren*, 1993, ISBN 3-921694-79-5, vergriffen
- 80 Ptak, Thomas: *Stofftransport in heterogenen Porenaquiferen: Felduntersuchungen und stochastische Modellierung*, 1993, ISBN 3-921694-80-9, vergriffen
- 81 Haakh, Frieder: *Transientes Strömungsverhalten in Wirbelkammern*, 1993, ISBN 3-921694-81-7
- 82 Kobus, Helmut; Cirpka, Olaf; Barczewski, Baldur; Koschitzky, Hans-Peter: *Versuchseinrichtung zur Grundwasser und Altlastensanierung VEGAS, Konzeption und Programmrahmen*, 1993, ISBN 3-921694-82-5
- 83 Zang, Weidong: *Optimaler Echtzeit-Betrieb eines Speichers mit aktueller Abflußregenerierung*, 1994, ISBN 3-921694-83-3, vergriffen
- 84 Franke, Hans-Jörg: *Stochastische Modellierung eines flächenhaften Stoffeintrages und Transports in Grundwasser am Beispiel der Pflanzenschutzmittelproblematik*, 1995, ISBN 3-921694-84-1
- 85 Lang, Ulrich: *Simulation regionaler Strömungs- und Transportvorgänge in Karst-aquiferen mit Hilfe des Doppelkontinuum-Ansatzes: Methodenentwicklung und Parameteridentifikation*, 1995, ISBN 3-921694-85-X, vergriffen
- 86 Helmig, Rainer: *Einführung in die Numerischen Methoden der Hydromechanik*, 1996, ISBN 3-921694-86-8, vergriffen
- 87 Cirpka, Olaf: *CONTRACT: A Numerical Tool for Contaminant Transport and Chemical Transformations - Theory and Program Documentation -*, 1996, ISBN 3-921694-87-6
- 88 Haberlandt, Uwe: *Stochastische Synthese und Regionalisierung des Niederschlages für Schmutzfrachtberechnungen*, 1996, ISBN 3-921694-88-4
- 89 Croisé, Jean: *Extraktion von flüchtigen Chemikalien aus natürlichen Lockergesteinen mittels erzwungener Luftströmung*, 1996, ISBN 3-921694-89-2, vergriffen
- 90 Jorde, Klaus: *Ökologisch begründete, dynamische Mindestwasserregelungen bei Ausleitungskraftwerken*, 1997, ISBN 3-921694-90-6, vergriffen
- 91 Helmig, Rainer: *Gekoppelte Strömungs- und Transportprozesse im Untergrund - Ein Beitrag zur Hydrosystemmodellierung-*, 1998, ISBN 3-921694-91-4, vergriffen

- 92 Emmert, Martin: *Numerische Modellierung nichtisothermer Gas-Wasser Systeme in porösen Medien*, 1997, ISBN 3-921694-92-2
- 93 Kern, Ulrich: *Transport von Schweb- und Schadstoffen in staugeregelten Fließgewässern am Beispiel des Neckars*, 1997, ISBN 3-921694-93-0, vergriffen
- 94 Förster, Georg: *Druckstoßdämpfung durch große Luftblasen in Hochpunkten von Rohrleitungen* 1997, ISBN 3-921694-94-9
- 95 Cirpka, Olaf: *Numerische Methoden zur Simulation des reaktiven Mehrkomponententransports im Grundwasser*, 1997, ISBN 3-921694-95-7, vergriffen
- 96 Färber, Arne: *Wärmetransport in der ungesättigten Bodenzone: Entwicklung einer thermischen In-situ-Sanierungstechnologie*, 1997, ISBN 3-921694-96-5
- 97 Betz, Christoph: *Wasserdampfdestillation von Schadstoffen im porösen Medium: Entwicklung einer thermischen In-situ-Sanierungstechnologie*, 1998, ISBN 3-921694-97-3
- 98 Xu, Yichun: *Numerical Modeling of Suspended Sediment Transport in Rivers*, 1998, ISBN 3-921694-98-1, vergriffen
- 99 Wüst, Wolfgang: *Geochemische Untersuchungen zur Sanierung CKW-kontaminierter Aquifere mit Fe(0)-Reaktionswänden*, 2000, ISBN 3-933761-02-2
- 100 Sheta, Hussam: *Simulation von Mehrphasenvorgängen in porösen Medien unter Einbeziehung von Hysterese-Effekten*, 2000, ISBN 3-933761-03-4
- 101 Ayros, Edwin: *Regionalisierung extremer Abflüsse auf der Grundlage statistischer Verfahren*, 2000, ISBN 3-933761-04-2, vergriffen
- 102 Huber, Ralf: *Compositional Multiphase Flow and Transport in Heterogeneous Porous Media*, 2000, ISBN 3-933761-05-0
- 103 Braun, Christopherus: *Ein Upscaling-Verfahren für Mehrphasenströmungen in porösen Medien*, 2000, ISBN 3-933761-06-9
- 104 Hofmann, Bernd: *Entwicklung eines rechnergestützten Managementsystems zur Beurteilung von Grundwasserschadensfällen*, 2000, ISBN 3-933761-07-7
- 105 Class, Holger: *Theorie und numerische Modellierung nichtisothermer Mehrphasenprozesse in NAPL-kontaminierten porösen Medien*, 2001, ISBN 3-933761-08-5
- 106 Schmidt, Reinhard: *Wasserdampf- und Heißluftinjektion zur thermischen Sanierung kontaminierter Standorte*, 2001, ISBN 3-933761-09-3
- 107 Josef, Reinhold: *Schadstoffextraktion mit hydraulischen Sanierungsverfahren unter Anwendung von grenzflächenaktiven Stoffen*, 2001, ISBN 3-933761-10-7



- 108 Schneider, Matthias: *Habitat- und Abflussmodellierung für Fließgewässer mit unscharfen Berechnungsansätzen*, 2001, ISBN 3-933761-11-5
- 109 Rathgeb, Andreas: *Hydrodynamische Bemessungsgrundlagen für Lockerdeckwerke an überströmbaren Erddämmen*, 2001, ISBN 3-933761-12-3
- 110 Lang, Stefan: *Parallele numerische Simulation instationärer Probleme mit adaptiven Methoden auf unstrukturierten Gittern*, 2001, ISBN 3-933761-13-1
- 111 Appt, Jochen; Stumpp Simone: *Die Bodensee-Messkampagne 2001, IWS/CWR Lake Constance Measurement Program 2001*, 2002, ISBN 3-933761-14-X
- 112 Heimerl, Stephan: *Systematische Beurteilung von Wasserkraftprojekten*, 2002, ISBN 3-933761-15-8
- 113 Iqbal, Amin: *On the Management and Salinity Control of Drip Irrigation*, 2002, ISBN 3-933761-16-6
- 114 Silberhorn-Hemminger, Annette: *Modellierung von Kluftaquifersystemen: Geostatistische Analyse und deterministisch-stochastische Kluftgenerierung*, 2002, ISBN 3-933761-17-4
- 115 Winkler, Angela: *Prozesse des Wärme- und Stofftransports bei der In-situ-Sanierung mit festen Wärmequellen*, 2003, ISBN 3-933761-18-2
- 116 Marx, Walter: *Wasserkraft, Bewässerung, Umwelt - Planungs- und Bewertungsschwerpunkte der Wasserbewirtschaftung*, 2003, ISBN 3-933761-19-0
- 117 Hinkelmann, Reinhard: *Efficient Numerical Methods and Information-Processing Techniques in Environment Water*, 2003, ISBN 3-933761-20-4
- 118 Samaniego-Eguiguren, Luis Eduardo: *Hydrological Consequences of Land Use / Land Cover and Climatic Changes in Mesoscale Catchments*, 2003, ISBN 3-933761-21-2
- 119 Neunhäuserer, Lina: *Diskretisierungsansätze zur Modellierung von Strömungs- und Transportprozessen in geklüftet-porösen Medien*, 2003, ISBN 3-933761-22-0
- 120 Paul, Maren: *Simulation of Two-Phase Flow in Heterogeneous Porous Media with Adaptive Methods*, 2003, ISBN 3-933761-23-9
- 121 Ehret, Uwe: *Rainfall and Flood Nowcasting in Small Catchments using Weather Radar*, 2003, ISBN 3-933761-24-7
- 122 Haag, Ingo: *Der Sauerstoffhaushalt staugeregelter Flüsse am Beispiel des Neckars - Analysen, Experimente, Simulationen -*, 2003, ISBN 3-933761-25-5
- 123 Appt, Jochen: *Analysis of Basin-Scale Internal Waves in Upper Lake Constance*, 2003, ISBN 3-933761-26-3

- 124 Hrsg.: Schrenk, Volker; Batereau, Katrin; Barczewski, Baldur; Weber, Karolin und Koschitzky, Hans-Peter: *Symposium Ressource Fläche und VEGAS - Statuskolloquium 2003, 30. September und 1. Oktober 2003*, 2003, ISBN 3-933761-27-1
- 125 Omar Khalil Ouda: *Optimisation of Agricultural Water Use: A Decision Support System for the Gaza Strip*, 2003, ISBN 3-933761-28-0
- 126 Batereau, Katrin: *Sensorbasierte Bodenluftmessung zur Vor-Ort-Erkundung von Schadensherden im Untergrund*, 2004, ISBN 3-933761-29-8
- 127 Witt, Oliver: *Erosionsstabilität von Gewässersedimenten mit Auswirkung auf den Stofftransport bei Hochwasser am Beispiel ausgewählter Stauhaltungen des Oberrheins*, 2004, ISBN 3-933761-30-1
- 128 Jakobs, Hartmut: *Simulation nicht-isothermer Gas-Wasser-Prozesse in komplexen Kluft-Matrix-Systemen*, 2004, ISBN 3-933761-31-X
- 129 Li, Chen-Chien: *Deterministisch-stochastisches Berechnungskonzept zur Beurteilung der Auswirkungen erosiver Hochwasserereignisse in Flusstauhaltungen*, 2004, ISBN 3-933761-32-8
- 130 Reichenberger, Volker; Helmig, Rainer; Jakobs, Hartmut; Bastian, Peter; Niessner, Jennifer: *Complex Gas-Water Processes in Discrete Fracture-Matrix Systems: Upscaling, Mass-Conservative Discretization and Efficient Multilevel Solution*, 2004, ISBN 3-933761-33-6
- 131 Hrsg.: Barczewski, Baldur; Koschitzky, Hans-Peter; Weber, Karolin; Wege, Ralf: *VEGAS - Statuskolloquium 2004*, Tagungsband zur Veranstaltung am 05. Oktober 2004 an der Universität Stuttgart, Campus Stuttgart-Vaihingen, 2004, ISBN 3-933761-34-4
- 132 Asie, Kemal Jabir: *Finite Volume Models for Multiphase Multicomponent Flow through Porous Media*. 2005, ISBN 3-933761-35-2
- 133 Jacoub, George: *Development of a 2-D Numerical Module for Particulate Contaminant Transport in Flood Retention Reservoirs and Impounded Rivers*, 2004, ISBN 3-933761-36-0
- 134 Nowak, Wolfgang: *Geostatistical Methods for the Identification of Flow and Transport Parameters in the Subsurface*, 2005, ISBN 3-933761-37-9
- 135 Süß, Mia: *Analysis of the influence of structures and boundaries on flow and transport processes in fractured porous media*, 2005, ISBN 3-933761-38-7
- 136 Jose, Surabhin Chackiath: *Experimental Investigations on Longitudinal Dispersive Mixing in Heterogeneous Aquifers*, 2005, ISBN: 3-933761-39-5
- 137 Filiz, Fulya: *Linking Large-Scale Meteorological Conditions to Floods in Mesoscale Catchments*, 2005, ISBN 3-933761-40-9

- 138 Qin, Minghao: *Wirklichkeitsnahe und recheneffiziente Ermittlung von Temperatur und Spannungen bei großen RCC-Staumauern*, 2005, ISBN 3-933761-41-7
- 139 Kobayashi, Kenichiro: *Optimization Methods for Multiphase Systems in the Sub-surface - Application to Methane Migration in Coal Mining Areas*, 2005, ISBN 3-933761-42-5
- 140 Rahman, Md. Arifur: *Experimental Investigations on Transverse Dispersive Mixing in Heterogeneous Porous Media*, 2005, ISBN 3-933761-43-3
- 141 Schrenk, Volker: *Ökobilanzen zur Bewertung von Altlastensanierungsmaßnahmen*, 2005, ISBN 3-933761-44-1
- 142 Hundecha, Hirpa Yeshewatersfa: *Regionalization of Parameters of a Conceptual Rainfall-Runoff Model*, 2005, ISBN: 3-933761-45-X
- 143 Wege, Ralf: *Untersuchungs- und Überwachungsmethoden für die Beurteilung natürlicher Selbstreinigungsprozesse im Grundwasser*, 2005, ISBN 3-933761-46-8
- 144 Breiting, Thomas: *Techniken und Methoden der Hydroinformatik - Modellierung von komplexen Hydrosystemen im Untergrund*, 2006, 3-933761-47-6
- 145 Hrsg.: Braun, Jürgen; Koschitzky, Hans-Peter; Müller, Martin: *Ressource Untergrund: 10 Jahre VEGAS: Forschung und Technologieentwicklung zum Schutz von Grundwasser und Boden*, Tagungsband zur Veranstaltung am 28. und 29. September 2005 an der Universität Stuttgart, Campus Stuttgart-Vaihingen, 2005, ISBN 3-933761-48-4
- 146 Rojanschi, Vlad: *Abflusskonzentration in mesoskaligen Einzugsgebieten unter Berücksichtigung des Sickerraumes*, 2006, ISBN 3-933761-49-2
- 147 Winkler, Nina Simone: *Optimierung der Steuerung von Hochwasserrückhaltebecken-systemen*, 2006, ISBN 3-933761-50-6
- 148 Wolf, Jens: *Räumlich differenzierte Modellierung der Grundwasserströmung alluvialer Aquifere für mesoskalige Einzugsgebiete*, 2006, ISBN: 3-933761-51-4
- 149 Kohler, Beate: *Externe Effekte der Laufwasserkraftnutzung*, 2006, ISBN 3-933761-52-2
- 150 Hrsg.: Braun, Jürgen; Koschitzky, Hans-Peter; Stuhmann, Matthias: *VEGAS-Statuskolloquium 2006*, Tagungsband zur Veranstaltung am 28. September 2006 an der Universität Stuttgart, Campus Stuttgart-Vaihingen, 2006, ISBN 3-933761-53-0
- 151 Niessner, Jennifer: *Multi-Scale Modeling of Multi-Phase - Multi-Component Processes in Heterogeneous Porous Media*, 2006, ISBN 3-933761-54-9
- 152 Fischer, Markus: *Beanspruchung eingeeerdeter Rohrleitungen infolge Austrocknung bindiger Böden*, 2006, ISBN 3-933761-55-7

- 153 Schneck, Alexander: *Optimierung der Grundwasserbewirtschaftung unter Berücksichtigung der Belange der Wasserversorgung, der Landwirtschaft und des Naturschutzes*, 2006, ISBN 3-933761-56-5
- 154 Das, Tapash: *The Impact of Spatial Variability of Precipitation on the Predictive Uncertainty of Hydrological Models*, 2006, ISBN 3-933761-57-3
- 155 Bielinski, Andreas: *Numerical Simulation of CO<sub>2</sub> sequestration in geological formations*, 2007, ISBN 3-933761-58-1
- 156 Mödinger, Jens: *Entwicklung eines Bewertungs- und Entscheidungsunterstützungssystems für eine nachhaltige regionale Grundwasserbewirtschaftung*, 2006, ISBN 3-933761-60-3
- 157 Manthey, Sabine: *Two-phase flow processes with dynamic effects in porous media - parameter estimation and simulation*, 2007, ISBN 3-933761-61-1
- 158 Pozos Estrada, Oscar: *Investigation on the Effects of Entrained Air in Pipelines*, 2007, ISBN 3-933761-62-X
- 159 Ochs, Steffen Oliver: *Steam injection into saturated porous media – process analysis including experimental and numerical investigations*, 2007, ISBN 3-933761-63-8
- 160 Marx, Andreas: *Einsatz gekoppelter Modelle und Wetterradar zur Abschätzung von Niederschlagsintensitäten und zur Abflussvorhersage*, 2007, ISBN 3-933761-64-6
- 161 Hartmann, Gabriele Maria: *Investigation of Evapotranspiration Concepts in Hydrological Modelling for Climate Change Impact Assessment*, 2007, ISBN 3-933761-65-4
- 162 Kebede Gurmessa, Tesfaye: *Numerical Investigation on Flow and Transport Characteristics to Improve Long-Term Simulation of Reservoir Sedimentation*, 2007, ISBN 3-933761-66-2
- 163 Trifković, Aleksandar: *Multi-objective and Risk-based Modelling Methodology for Planning, Design and Operation of Water Supply Systems*, 2007, ISBN 3-933761-67-0
- 164 Götzinger, Jens: *Distributed Conceptual Hydrological Modelling - Simulation of Climate, Land Use Change Impact and Uncertainty Analysis*, 2007, ISBN 3-933761-68-9
- 165 Hrsg.: Braun, Jürgen; Koschitzky, Hans-Peter; Stuhmann, Matthias: *VEGAS – Kolloquium 2007*, Tagungsband zur Veranstaltung am 26. September 2007 an der Universität Stuttgart, Campus Stuttgart-Vaihingen, 2007, ISBN 3-933761-69-7
- 166 Freeman, Beau: *Modernization Criteria Assessment for Water Resources Planning; Klamath Irrigation Project, U.S.*, 2008, ISBN 3-933761-70-0

- 167 Dreher, Thomas: *Selektive Sedimentation von Feinstschwebstoffen in Wechselwirkung mit wandnahen turbulenten Strömungsbedingungen*, 2008, ISBN 3-933761-71-9
- 168 Yang, Wei: *Discrete-Continuous Downscaling Model for Generating Daily Precipitation Time Series*, 2008, ISBN 3-933761-72-7
- 169 Kopecki, Ianina: *Calculational Approach to FST-Hemispheres for Multiparametrical Benthos Habitat Modelling*, 2008, ISBN 3-933761-73-5
- 170 Brommundt, Jürgen: *Stochastische Generierung räumlich zusammenhängender Niederschlagszeitreihen*, 2008, ISBN 3-933761-74-3
- 171 Papafotiou, Alexandros: *Numerical Investigations of the Role of Hysteresis in Heterogeneous Two-Phase Flow Systems*, 2008, ISBN 3-933761-75-1
- 172 He, Yi: *Application of a Non-Parametric Classification Scheme to Catchment Hydrology*, 2008, ISBN 978-3-933761-76-7
- 173 Wagner, Sven: *Water Balance in a Poorly Gauged Basin in West Africa Using Atmospheric Modelling and Remote Sensing Information*, 2008, ISBN 978-3-933761-77-4
- 174 Hrsg.: Braun, Jürgen; Koschitzky, Hans-Peter; Stuhmann, Matthias; Schrenk, Volker: *VEGAS-Kolloquium 2008 Ressource Fläche III*, Tagungsband zur Veranstaltung am 01. Oktober 2008 an der Universität Stuttgart, Campus Stuttgart-Vaihingen, 2008, ISBN 978-3-933761-78-1
- 175 Patil, Sachin: *Regionalization of an Event Based Nash Cascade Model for Flood Predictions in Ungauged Basins*, 2008, ISBN 978-3-933761-79-8
- 176 Assteerawatt, Anongnart: *Flow and Transport Modelling of Fractured Aquifers based on a Geostatistical Approach*, 2008, ISBN 978-3-933761-80-4
- 177 Karnahl, Joachim Alexander: *2D numerische Modellierung von multifraktionalem Schwebstoff- und Schadstofftransport in Flüssen*, 2008, ISBN 978-3-933761-81-1
- 178 Hiester, Uwe: *Technologieentwicklung zur In-situ-Sanierung der ungesättigten Bodenzone mit festen Wärmequellen*, 2009, ISBN 978-3-933761-82-8
- 179 Laux, Patrick: *Statistical Modeling of Precipitation for Agricultural Planning in the Volta Basin of West Africa*, 2009, ISBN 978-3-933761-83-5
- 180 Ehsan, Saqib: *Evaluation of Life Safety Risks Related to Severe Flooding*, 2009, ISBN 978-3-933761-84-2
- 181 Prohaska, Sandra: *Development and Application of a 1D Multi-Strip Fine Sediment Transport Model for Regulated Rivers*, 2009, ISBN 978-3-933761-85-9

- 182 Kopp, Andreas: *Evaluation of CO<sub>2</sub> Injection Processes in Geological Formations for Site Screening*, 2009, ISBN 978-3-933761-86-6
- 183 Ebigo, Anozie: *Modelling of biofilm growth and its influence on CO<sub>2</sub> and water (two-phase) flow in porous media*, 2009, ISBN 978-3-933761-87-3
- 184 Freiboth, Sandra: *A phenomenological model for the numerical simulation of multiphase multicomponent processes considering structural alterations of porous media*, 2009, ISBN 978-3-933761-88-0
- 185 Zöllner, Frank: *Implementierung und Anwendung netzfreier Methoden im Konstruktiven Wasserbau und in der Hydromechanik*, 2009, ISBN 978-3-933761-89-7
- 186 Vasin, Milos: *Influence of the soil structure and property contrast on flow and transport in the unsaturated zone*, 2010, ISBN 978-3-933761-90-3
- 187 Li, Jing: *Application of Copulas as a New Geostatistical Tool*, 2010, ISBN 978-3-933761-91-0
- 188 AghaKouchak, Amir: *Simulation of Remotely Sensed Rainfall Fields Using Copulas*, 2010, ISBN 978-3-933761-92-7
- 189 Thapa, Pawan Kumar: *Physically-based spatially distributed rainfall runoff modeling for soil erosion estimation*, 2010, ISBN 978-3-933761-93-4
- 190 Wurms, Sven: *Numerische Modellierung der Sedimentationsprozesse in Retentionsanlagen zur Steuerung von Stoffströmen bei extremen Hochwasserabflussergebnissen*, 2010, ISBN 978-3-933761-94-1
- 191 Merkel, Uwe: *Unsicherheitsanalyse hydraulischer Einwirkungen auf Hochwasserschutzdeiche und Steigerung der Leistungsfähigkeit durch adaptive Strömungsmodellierung*, 2010, ISBN 978-3-933761-95-8
- 192 Fritz, Jochen: *A Decoupled Model for Compositional Non-Isothermal Multiphase Flow in Porous Media and Multiphysics Approaches for Two-Phase Flow*, 2010, ISBN 978-3-933761-96-5
- 193 Weber, Karolin (Hrsg.): *12. Treffen junger WissenschaftlerInnen an Wasserbauinstituten*, 2010, ISBN 978-3-933761-97-2
- 194 Bliedernicht, Jan-Geert: *Probability Forecasts of Daily Areal Precipitation for Small River Basins*, 2010, ISBN 978-3-933761-98-9
- 195 Hrsg.: Koschitzky, Hans-Peter; Braun, Jürgen: *VEGAS-Kolloquium 2010 In-situ-Sanierung - Stand und Entwicklung Nano und ISCO -*, Tagungsband zur Veranstaltung am 07. Oktober 2010 an der Universität Stuttgart, Campus Stuttgart-Vaihingen, 2010, ISBN 978-3-933761-99-6

- 196 Gafurov, Abror: *Water Balance Modeling Using Remote Sensing Information - Focus on Central Asia*, 2010, ISBN 978-3-942036-00-9
- 197 Mackenberg, Sylvia: *Die Quellstärke in der Sickerwasserprognose: Möglichkeiten und Grenzen von Labor- und Freilanduntersuchungen*, 2010, ISBN 978-3-942036-01-6
- 198 Singh, Shailesh Kumar: *Robust Parameter Estimation in Gauged and Ungauged Basins*, 2010, ISBN 978-3-942036-02-3

Die Mitteilungshefte ab der Nr. 134 (Jg. 2005) stehen als pdf-Datei über die Homepage des Instituts: [www.iws.uni-stuttgart.de](http://www.iws.uni-stuttgart.de) zur Verfügung.

